

1 A genetic and linguistic analysis of the admixture histories of the islands of Cabo Verde

2

3 **Authors:**

4 Romain Laurent¹, Zachary A. Szpiech^{2,3}, Sergio S. da Costa¹, Valentin Thouzeau^{4,5}, Cesar A. Fortes-Lima⁶,
5 Françoise Dessarps-Freichey¹, Laure Lémée⁷, José Utgé¹, Noah A. Rosenberg⁸, Marlyse Baptista^{9,10}, and Paul
6 Verdu^{1,*}.

7

8 **Authors' affiliations :**

9 1. UMR7206 Eco-anthropologie, CNRS-MNHN-Université Paris Cité, Paris, France

10 2. Department of Biology, Pennsylvania State University, University Park, PA 16802, USA

11 3. Institute for Computational and Data Sciences, Pennsylvania State University, University Park, PA 16802,
12 USA

13 4. UMR 7534 Centre de Recherche en Mathématiques de la Décision, CNRS-Université Paris-Dauphine-PSL
14 University, Paris, France

15 5. Département d'Etudes Cognitives, Laboratoire de Sciences Cognitives et Psycholinguistique, ENS-PSL Uni-
16 versity-EHESS-CNRS, Paris, France

17 6. Department of Organismal Biology, Sub-department of Human Evolution, Evolutionary Biology Centre,
18 Uppsala University, Uppsala, Sweden

19 7. Plate-forme Technologique Biomix-Centre de Ressources et Recherches Technologiques (C2RT), Institut
20 Pasteur, Paris, France.

21 8. Department of Biology, Stanford University, Stanford, CA, USA

22 9. Department of Linguistics, University of Michigan, Ann Arbor, MI, USA

23 10. Department of Afroamerican and African Studies, University of Michigan, Ann Arbor, MI, USA

24

25 ***Corresponding author:**

26 Paul Verdu, UMR7206 Eco-anthropologie, CNRS-MNHN-Université Paris Cité, Musée de l'Homme, 17,
27 place du Trocadéro, 75016 Paris, France. Email : paul.verdu@mnhn.fr. Tel : +33 144057317

28

29 **Ethics statement**

30 Research sampling protocols followed the Declaration of Helsinki guidelines and the French laws of scientific
31 research deontology (Loi n° 2016-483 du 20 avril 2016). Research and ethics authorizations were provided by
32 the Ministério da Saúde de Cabo Verde (228/DGS/11), Stanford University IRB (Protocol ID n°23194-IRB
33 n°349), University of Michigan IRB (n°HUM00079335), and the French ethics committees and CNIL (Dec-
34 laration n°1972648). All volunteer participants provided written and video-recorded informed consent.

35

36 **Data availability**

37 The novel genome-wide genotype data, the linguistic utterance counts, and the self-reported anthropological
38 data presented here can be accessed and downloaded via the European Genome-Phenome Archive (EGA)
39 database accession numbers EGAD00001008976, EGAD00001008977, EGAD00001008978, and
40 EGAD00001008979. All datasets can be shared provided that future envisioned studies comply with the in-
41 formed consents provided by the participants, and in agreement with institutional ethics committee's recom-
42 mendations applying to this data.

43

44 **Software availability**

45 *MetHis* is an open source C software available with user manual on GitHub at <https://github.com/romain-laurent/MetHis> (Fortes-Lima et al. 2021).

46

47

48 **Keywords**

49 Admixture; population genetics; historical inference; machine-learning; approximate Bayesian computations;
50 genetic diversity; linguistic diversity; anthropology; slave-trade

51

52

53 **ABSTRACT**

54

55 From the 15th to the 19th century, the Trans-Atlantic Slave-Trade (TAST) influenced the genetic and cultural
56 diversity of numerous populations. We explore genomic and linguistic data from the nine islands of Cabo
57 Verde, the earliest European colony of the era in Africa, a major Slave-Trade platform between the 16th and
58 19th centuries, and a previously uninhabited location ideal for investigating early admixture events between
59 Europeans and Africans. Using local-ancestry inference approaches, we find that genetic admixture in Cabo
60 Verde occurred primarily between Iberian and certain Senegambian populations, although forced and volun-
61 tary migrations to the archipelago involved numerous other populations. Inter-individual genetic and linguistic
62 variation recapitulates the geographic distribution of individuals' birth-places across Cabo Verdean islands,
63 following an isolation-by-distance model with reduced genetic and linguistic effective dispersals within the
64 archipelago, and suggesting that Kriolu language variants have developed together with genetic divergences
65 at very reduced geographical scales. Furthermore, based on approximate bayesian computation inferences of
66 highly complex admixture histories, we find that admixture occurred early on each island, long before the 18th-
67 century massive TAST deportations triggered by the expansion of the plantation economy in Africa and the
68 Americas, and after this era mostly during the abolition of the TAST and of slavery in European colonial
69 empires. Our results illustrate how shifting socio-cultural relationships between enslaved and non-enslaved
70 communities during and after the TAST, shaped enslaved-African descendants' genomic diversity and struc-
71 ture on both sides of the Atlantic.

72

73

74 INTRODUCTION

75 Between the 15th and 19th centuries, European colonization and the Trans-Atlantic Slave-Trade (TAST) put
76 into contact groups of individuals previously isolated genetically and culturally. These forced and voluntary
77 migrations profoundly influenced the descent of numerous European, African, and American populations,
78 creating new cultures, languages, and genetic patterns (1,2).

79 Population geneticists have extensively described genetic admixture patterns in enslaved-African
80 descendants in the Americas, and mapped their genomes for regions of ancestry recently shared with
81 continental Africa and Europe (3,4). This allowed for reconstructing their detailed possible origins, as this
82 knowledge is often intractable with genealogical records alone (1). Furthermore, genetic admixture-mapping
83 methods have been used to identify genetic variation underlying phenotypic variation (5,6), and to identify
84 post-admixture natural selection signatures (7), thus revealing how admixture shaped human populations'
85 recent evolution. Maximum-likelihood approaches based on linkage-disequilibrium (LD) patterns of admixed
86 individuals (8,9) have repeatedly highlighted the diversity of admixture processes experienced by populations
87 historically related to the TAST. In particular, they identified different European, African, and American
88 populations, respectively, at the source of genetic admixture patterns, sometimes consistent with the preferred
89 commercial routes of each European empire (8,10). Furthermore, they identified variable timing of admixture
90 events during and after the TAST, sometimes consistent with major socio-historical events such as the
91 expansion of the plantation economic system or the abolition of slavery (11,12). From a cultural perspective,
92 linguists have shown that novel contact-languages, such as creole languages (13,14), emerged from recurring
93 interactions between socio-economically dominant Europeans with Africans and Americans. Furthermore,
94 they identified the languages of origin of numerous linguistic traits in several creole languages (15–17), and
95 emphasized the complex histories of contacts that shaped language diversity on both sides of the Atlantic.

96 Numerous questions remain unsolved and novel interrogations have emerged concerning the history of
97 admixture during and after the TAST. *i)* While the genetic history of enslaved-African descendants in the
98 Americas has been extensively studied, the influence of the TAST on genetic admixture in Africa remains
99 under-investigated. Studying these questions in Africa would provide invaluable information about the
100 influence of the onset and early stages of the TAST and the subsequent expansion of European empires on
101 genetic admixture patterns on both sides of the Atlantic. *ii)* While admixture-LD inference methods have
102 repeatedly brought novel insights into the admixture processes experienced by enslaved-African descendant
103 populations, they could only explore historical models with one or two pulses of admixture, a methodological
104 limitation (8,9). Complex admixture histories may be expected as a result of the recurring flows of enslaved-
105 Africans forcibly displaced between and within continents, changes of social relationships among enslaved
106 and non-enslaved communities, and variable assimilation of new migrants in pre-existing communities, during
107 and after the TAST (18,19). *iii)* Finally, while the comparison of genetic and linguistic diversities has been the
108 focus of numerous evolutionary anthropology studies at large geographical scales (20,21), it has rarely been
109 endeavored for creole-speaking populations at a local scale in the historical context of the TAST (22–24).

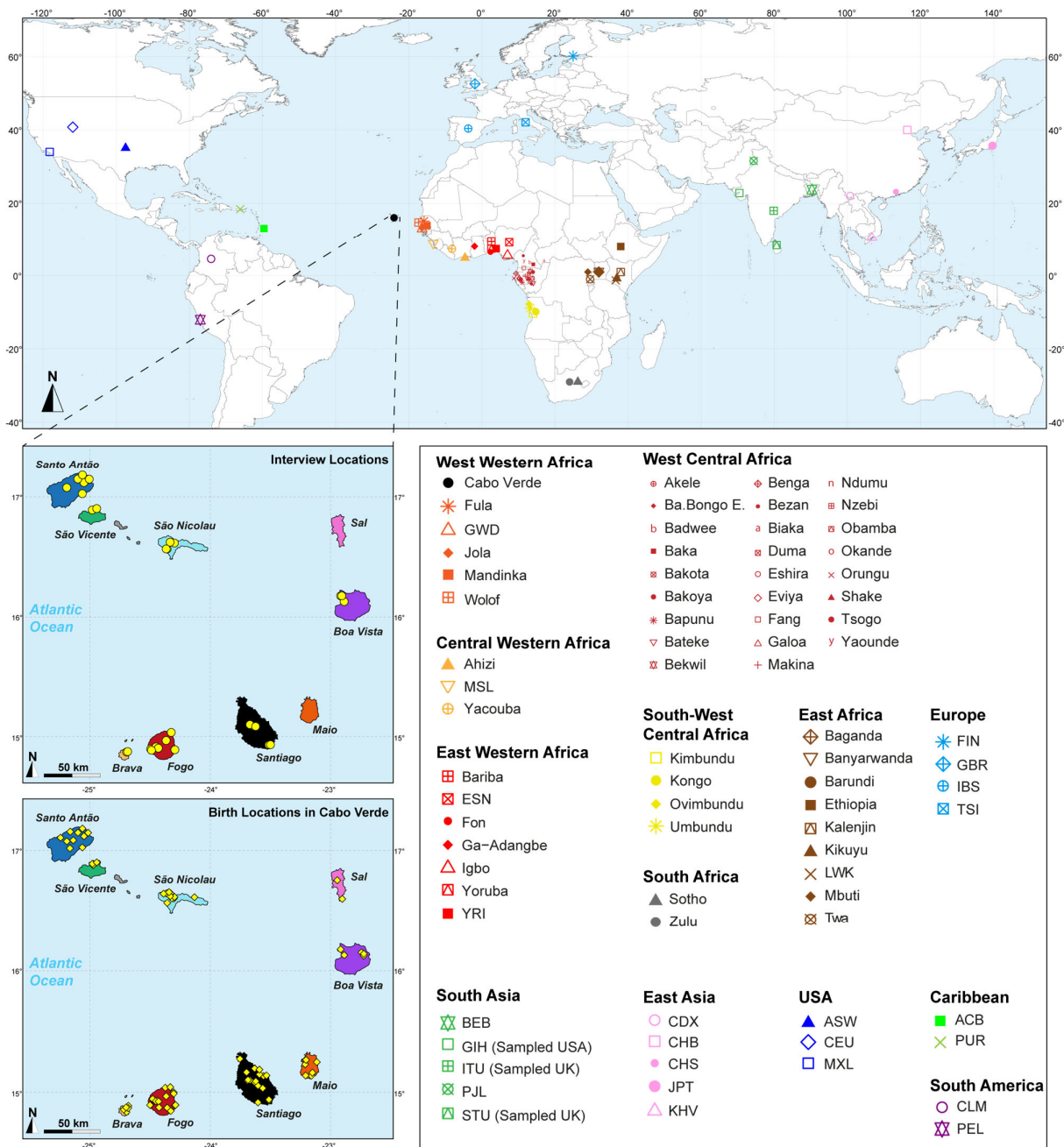
110 Here, we propose to reconstruct the detailed genetic and linguistic admixture histories of Cabo Verde, as
111 this archipelago represents an ideal case to address these three understudied aspects of TAST history. First,
112 Cabo Verde is the first European settlement-colony in Sub-Saharan Africa, located 500 kms West of Senegal
113 in Western Africa (**Figure 1**), and settled in the 1460s by Portuguese immigrants and enslaved-Africans
114 forcibly removed from the continental mainland. After 1492, and in particular after the 17th century expansion
115 of the plantation economy in the Americas, Cabo Verde served as a major slave-trade platform between
116 continents (25). Second, Cabo Verde forms an archipelago of nine inhabited islands that were settled over the
117 course of three centuries due to the changing political, commercial, and migratory contexts (26–28). Therefore,

118 studying the admixture history of Cabo Verde will provide unique insights into the onset of the TAST before
119 1492, and into the history of slavery thereafter. This setting further promises to illustrate, at a micro-
120 geographical scale, island-per-island, the fundamental socio-historical and serial founding migrations
121 mechanisms having influenced genomic patterns in admixed populations throughout the TAST. Finally, Cabo
122 Verdean Kriolu is the first creole language of the TAST, born from contacts between the Portuguese language
123 and a variety of African languages (15,17,29,30). The archipelago thus represents a unique opportunity to
124 investigate, jointly, genetic and linguistic admixture histories and their interactions since the mid-15th century.

125 Previous genetic studies exploring, first, sex-specific genetic diversity, and, then, genome-wide markers
126 from several islands of the archipelago (31–34), attested to the dual, sex-biased, origins of the Cabo Verdean
127 gene-pool, resulting mainly from admixture between African females and European males. Furthermore, these
128 studies described variable admixture patterns between mainland Africa and Europe across islands without
129 distinguishing source populations from different sub-regions within continents. Another, more recent, study
130 investigated which continental mainland European and African populations may have contributed to the Cabo
131 Verde gene-pool without focusing on possible variation across islands (3). Interestingly, adaptive-introgression
132 signals for malaria resistance in Santiago island were recently identified as a result of migrations and genetic
133 admixture during the TAST (35). Finally, while joint analyses of genetic and linguistic diversities from the
134 island of Santiago showed that genetic and linguistic admixture histories possibly occurred in parallel (23),
135 these previous studies did not attempt to formally reconstruct the admixture processes and detailed
136 demographic histories that influenced the observed patterns of genetic or linguistic diversity on the islands of
137 Cabo Verde.

138 Based on these previous studies, we propose to first determine which continental African and European
139 populations in fact contributed to the genetic landscape of each Cabo Verdean island today. Indeed, which
140 enslaved-African populations only briefly transited through the archipelago, and which remained for longer
141 periods is largely debated by historians (25–27); and, while Portuguese influence is clear, further details about
142 which European migrations genetically influenced Cabo Verde remain to be assessed (36). These aspects are
143 often crucial for understanding the genetic history of enslaved-African descendant populations on either side
144 of the Atlantic (1,12,37,38). Second, we propose to further evaluate the possible parallels between genetic and
145 linguistic admixture histories at a micro-geographical scale within each island. We aim at better understanding
146 how contacts shaped cultural variation during the TAST by deciphering the parent-offspring dispersal
147 behaviors within and across islands which shaped the biological and cultural diversity in the archipelago (23).
148 This can be achieved indirectly by exploring the influence of isolation-by-distance mechanisms on the
149 distribution of genetic and linguistic diversity at very reduced geographical scale (~50 km) within a
150 population (39–44). Finally, we reconstruct the detailed history of admixture dynamics in each island since
151 the 15th century, using statistical inference of possible complex admixture histories with Approximate Bayesian
152 Computation (45). Altogether, this highlights the socio-historical mechanisms that shaped the genetic and
153 linguistic diversity of the Cabo Verde population, the first to be born from the TAST.

154
155



156
157
158
159
160
161
162
163
164
165
166
167
168

Figure 1:
Sampling location of 233 unrelated Cabo Verdean individuals, merged with data on 4924 individuals from 77 worldwide populations.
Birth-location of 225 individuals within Cabo Verde are indicated in the bottom map-panel, and birth locations outside Cabo Verde for 6 individuals are indicated in **Figure 1-resource table 1**. Linguistic and familial anthropology interview, and genetic sampling for Cabo Verde participants were conducted during six separate interdisciplinary fieldworks between 2010 and 2018. Further details about populations are provided in **Figure 1-resource table 1**.

Figure 1-resource Table 1: *provided in .xls format*
Population table corresponding to the map in Figure 1 and sample inclusion in all analysis.

169 RESULTS

170 We investigate genetic and linguistic variation in 233 family unrelated Kriolu speakers from the nine Cabo
171 Verdean islands (Brava, Fogo, Santiago, Maio, Sal, Boa Vista, São Nicolau, São Vicente, Santo Antão, **Figure**
172 **1, Figure 1-resource table 1**). With novel genome-wide genotyping autosomal data (**Appendix 1-figure 1**),
173 we first describe genetic differentiation patterns in Cabo Verde and other enslaved-African descendants in the
174 Americas from previous datasets, in particular with respect to continental Africa and Europe. Next, we deploy
175 local-ancestry inferences and determine the best proxy source-populations for admixture patterns in each Cabo
176 Verde island. We then describe runs of homozygosity and genetic isolation-by-distance patterns at reduced
177 geographical scale within Cabo Verde. We also investigate Kriolu linguistic diversity with respect to geogra-
178 phy and socio-cultural co-variates and, then, investigate jointly genetic and linguistic admixture patterns
179 throughout the archipelago. Finally, we infer the detailed genetic admixture history of each island using the
180 machine-learning *MetHis*-Approximate Bayesian Computation (ABC) approach (45).

181

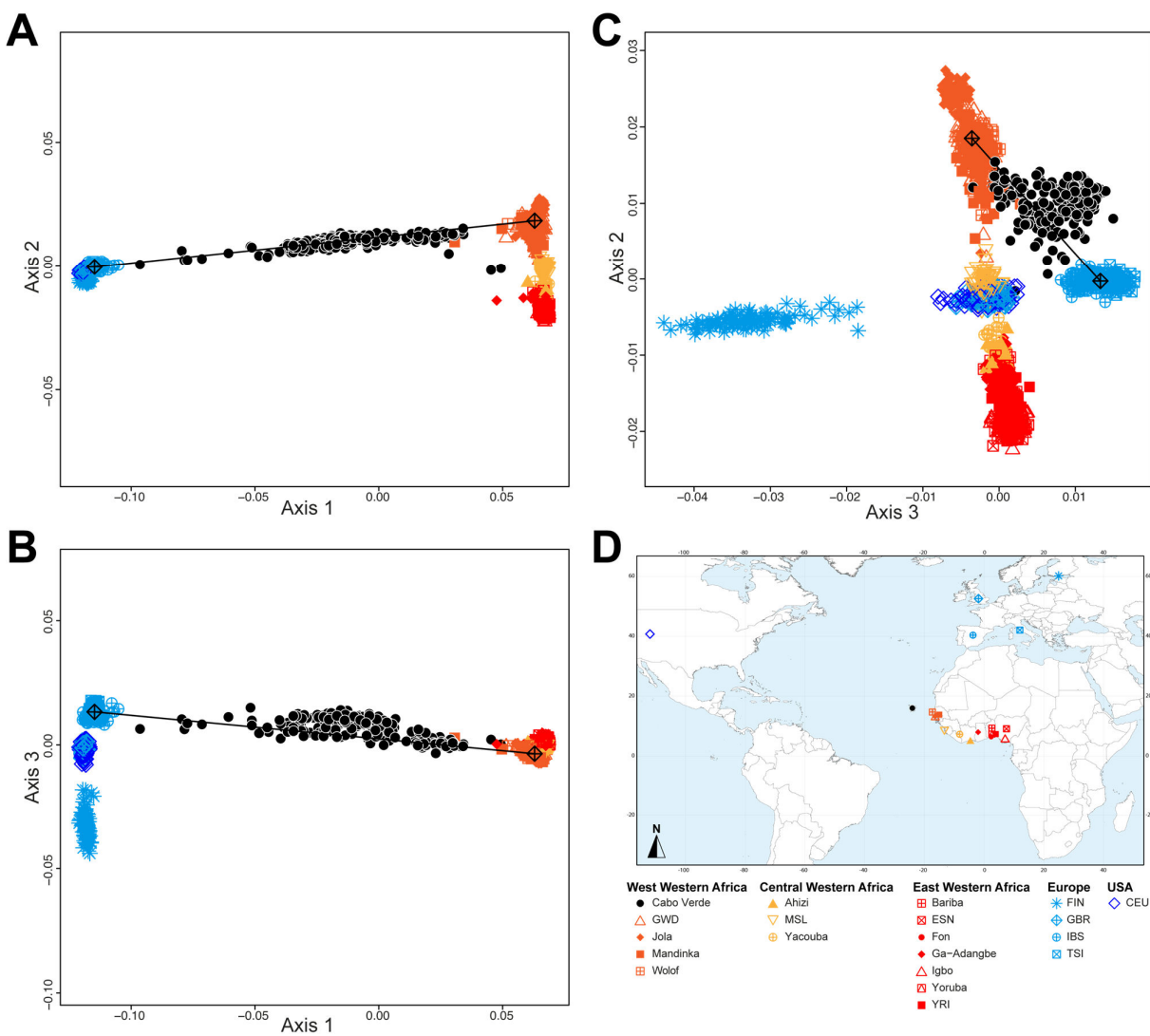
182 **1. Cabo Verde and other TAST-related admixed populations in the worldwide genetic context**

183 We explored genetic diversity patterns captured along the first three axes of the multi-dimensional scaling
184 (MDS) projection of individual pairwise allele sharing dissimilarities (ASD (46)), computed from different
185 individual subsets (**Figure 1-resource table 1**). This ASD-MDS approach is mathematically analogous to
186 PCA based on individual genotypes and therefore captures similar information about individual pairwise ge-
187 netic differentiation (47)^{Chap.-18.5.2}. However, ASD-MDS allows to explore pairwise genetic differentiation for
188 successive individual subsets much more efficiently computationally than classical PCA. Indeed, the individ-
189 ual pairwise ASD matrix only needs to be computed once and then simply subsampled before being projected,
190 and successive subset of individual-pairwise ASD matrices are thus always several orders of magnitude smaller
191 in dimensions than the genotype table to be projected with PCA which comprises, here, 455,705 SNPs in all
192 cases. Detailed ASD-MDS decompositions are provided in **Appendix 2** and **Appendix 2-figure 1-4**. Note that
193 we considered seven geographical regions in Africa shown in **Figure 1**.

194 **Figure 2** shows that the second ASD-MDS axis distinguishes West Western African Senegambian pop-
195 ulations from East Western Africans, while Central Western Africans are at intermediate distances between
196 these two clusters. Moreover, the third MDS axis separates Northern and Southern European populations; the
197 British-GBR and USA-CEU individuals clustering at intermediate distances between the Finnish-FIN, and a
198 cluster represented by Iberian-IBS and Tuscan-TSI Western Mediterranean individuals. Consistently with pre-
199 vious results (3,23), on the first three MDS axes, Cabo Verdean individuals cluster almost exclusively along a
200 trajectory from the Southern European cluster to Senegambia (**Figure 2A-C**), with little traces of affinity with
201 other African or European populations. Instead, the USA African-American ASW (**Figure 2-figure supple-**
202 **ment 1-A-C**) and Barbadian-ACB (**Figure 2-figure supplement 1-D-F**) cluster along a trajectory going from
203 the GBR and CEU cluster to Central and East Western Africa; and Puerto Ricans-PUR cluster along a trajec-
204 tory going from the Southern European cluster to the Central Western African cluster (**Figure 2-figure sup-**
205 **plement 1-G-I**).

206

207



208
 209
 210
 211
 212
 213
 214
 215
 216
 217
 218
 219
 220
 221
 222
 223
 224
 225
 226
 227

Figure 2:
Multidimensional scaling projections of pairwise allele sharing dissimilarities in Cabo Verdeans and continental African and European populations.

A-C) Three-dimensional MDS projection of ASD computed among 233 unrelated Cabo Verdeans and other continental African and European populations using 445,705 autosomal SNPs. Cabo Verdean patterns in panels A-C can be compared to results obtained considering instead the USA African-Americans ASW, the Barbadians-ACB, and the Puerto Ricans-PUR in the same African and European contexts and presented in **Figure 2-figure supplement 1**. We computed the Spearman correlation between the matrix of inter-individual three-dimensional Euclidean distances computed from the first three axes of the MDS projection and the original ASD matrix, to evaluate the precision of the dimensionality reduction. We find significant ($p < 2.2 \times 10^{-16}$) Spearman $\rho = 0.9635$ for the Cabo Verde analysis (A-C). See **Figure 1-resource table 1** for the populations used in these analyses. Sample locations and symbols are provided in panel D.

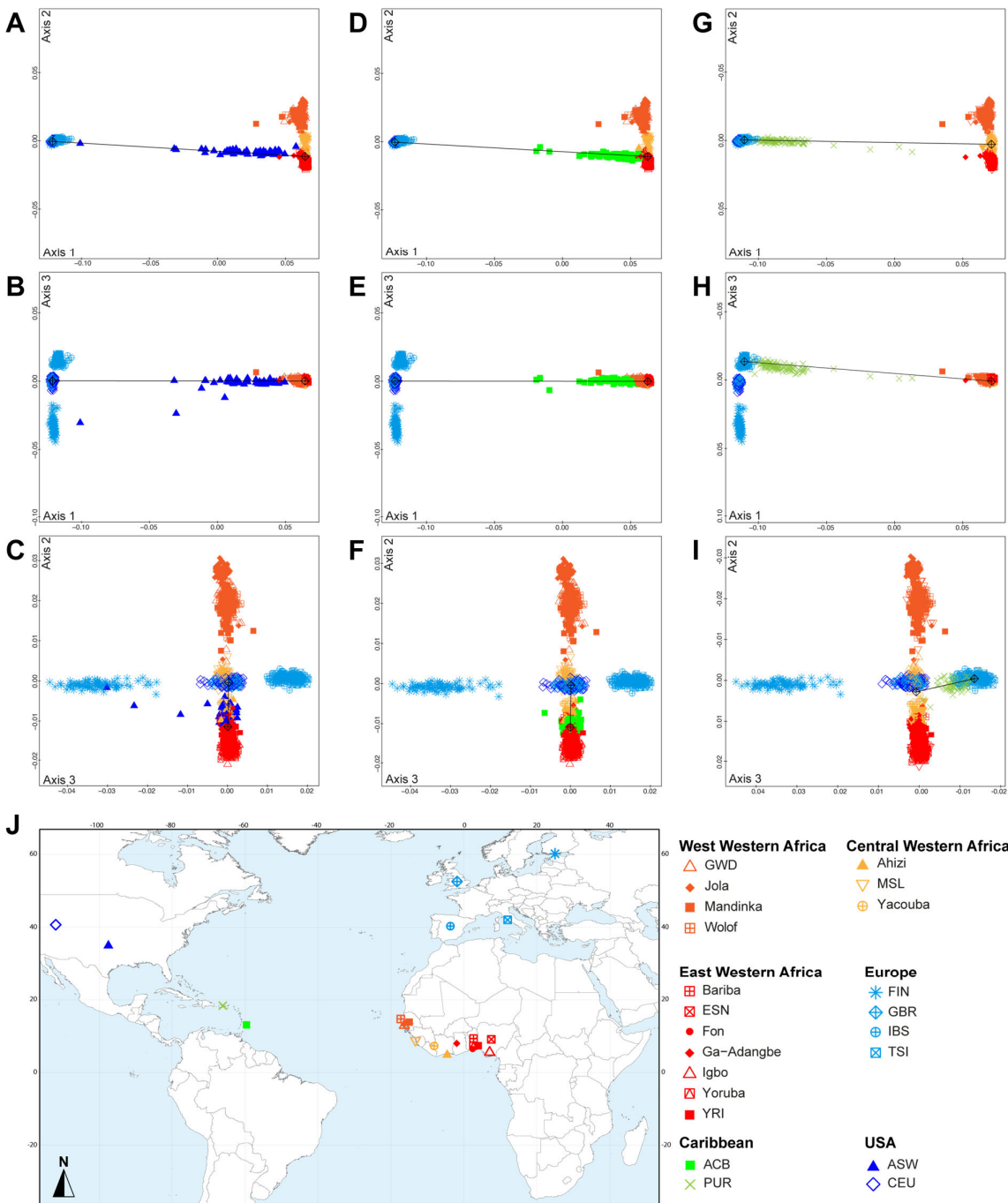
Figure 2-figure supplement 1:
Multidimensional scaling three-dimensional projection of allele sharing pairwise dissimilarities, for the closest subsets of West African and European populations to the African American ASW, Barbadian ACB, and Puerto Rican PUR populations, separately.

228
229
230
231
232
233
234
235
236
237
238
239

Figure 2-figure supplement 1:

Multidimensional scaling three-dimensional projection of allele sharing pairwise dissimilarities, for the closest subsets of West African and European populations to the African American ASW, Barbadian ACB, and Puerto Rican PUR populations, separately.

Three-dimensional MDS projection of ASD computed using 445,705 autosomal SNPs among continental African and European populations and, respectively, the USA African-American ASW (panels A-C), the Barbadians-ACB (panels D-F), or the Puerto Ricans-PUR (panels G-I), in the same European and African contexts as explored in **Figure 2** for Cabo Verdeans in the main text. We computed the Spearman correlation between Euclidean distances on the 3D-MDS projections and the original ASD matrix to evaluate the precision of the dimensionality reduction. We find Spearman $\rho=0.9383$ ($p<2.2\times 10^{-16}$) for the ASW (A-C); 0.9306 ($p<2.2\times 10^{-16}$) for the ACB (D-F); and 0.9437 ($p<2.2\times 10^{-16}$) for the PUR (G-I). Each individual is represented by a single point. Sample locations and symbols are given in **panel J (Figure 1-resource table 1)**.



240
241

242 2. Genetic structure in Cabo Verde and other TAST-related admixed populations

243 Based on these results, we further investigated patterns of individual genetic structure among Cabo Verde-
244 born individuals, ASW, and ACB populations with respect to European and Western, Central, South-Western,
245 and Southern African populations (**Figure 1-resource table 1**), using ADMIXTURE (48). Indeed, ASD-MDS
246 decompositions allow to efficiently identify major genetic pairwise dissimilarities among numerous samples,
247 but exploring multiple combinations of higher order axes remains extremely difficult with this multivariate
248 method. Instead, ADMIXTURE results recapitulate the major axes of genetic variation with increasing values
249 of the number of clusters K , which allows to explore individual pairwise genetic resemblances for numerous
250 major axes of variation at once. Extended descriptions of the results are presented in **Appendix 3**.

251 At $K=2$, the orange genetic-cluster in **Figure 3A** is maximized in African individuals while the blue al-
252 ternative cluster is maximized in Europeans. Cabo Verdean, ASW and ACB individuals exhibit intermediate
253 genotype-membership proportions between the two clusters, consistently with patterns expected for European-
254 African admixed individuals. Among the Cabo Verdean, ASW, and ACB populations, ACB individuals show,
255 on average, the highest membership to the orange “African” cluster (88.23%, SD=7.33%), followed by the
256 ASW (78.00%, SD=10.88%), and Cabo Verdeans (59.01%, SD=11.97%). Membership proportions for this
257 cluster are highly variable across Cabo Verdean islands, with highest average memberships for Santiago-born
258 individuals (71.45%, SD=10.39%) and Maio (70.39%, SD=5.26%), and lowest for Fogo (48.10%, SD=6.89%)
259 and Brava (50.61%, SD=5.80%). Inter-individual membership variation within Cabo Verde islands, captured
260 as F_{st}/F_{st}^{max} values (49), are significantly different across pairs of islands for 32 out of 36 comparisons (Wil-
261 coxon rank-sum test $p < 3.96 \times 10^{-8}$), with variability across islands ranging from a lowest value of 0.010 in
262 individuals from Santo Antão to a highest value of 0.0519 in Santiago (**Figure 3-figure supplement 1**).

263 At $K=5$, the new red cluster is maximized in the YRI, Igbo and ESN populations, distinct from Western
264 and Southern African orange and grey clusters, respectively. Note that the former orange cluster is almost
265 completely replaced with red membership in the ACB and ASW populations, while it remains large for all
266 Cabo Verdean-born individuals. Moreover, Cabo Verde-born individuals’ patterns of membership proportions
267 to the orange, red or grey “African” clusters differ here between individuals born on Santiago, Fogo, Brava,
268 and Maio, and individuals born on Sal, Boa Vista, São Nicolau, São Vicente, and Santo Antão, respectively.
269 The former group of islands exhibit an “African” component resembling patterns of membership proportions
270 found in West Western African individuals, with a majority of membership to the orange cluster and a minority
271 to the red cluster. Instead, the “African” component in individuals born in the latter islands is almost exclu-
272 sively orange. This potentially indicates differences in shared ancestries with different continental African
273 populations across islands in Cabo Verde, which remains to be formally tested (see **Result 3**).

274 At $K=6$, these two groups of islands are now clearly differentiated, as the novel green cluster is maximized
275 in numerous individuals born on Sal, Boa Vista, São Nicolau, São Vicente, and Santo Antão, but represented
276 to a much lesser extent in Santiago, Fogo, and Brava. Instead, individuals in these latter islands retain a ma-
277 jority of membership to the orange “West Western African” cluster, and Maio-born individuals are now found
278 intermediately between the two groups with relatively even memberships to the orange and green clusters
279 respectively. Interestingly, this new green cluster appears to be specific to Cabo Verdean genetic variation, as
280 it is virtually absent from other populations in our dataset except for a small proportion in certain Wolof indi-
281 viduals from West Western Africa.

282 At $K=10$, the light-green cluster is maximized in Cabo Verdean individuals born on Maio, Boa Vista, Sal,
283 and São Nicolau, distinct from the dark green cluster maximized in individuals born on Santo Antão and São
284 Vicente, and hence producing three distinct ADMIXTURE patterns among Cabo Verdean birth-islands. Fur-
285 thermore, an alternative mode at $K=10$ shows (**Appendix 3-figure 1**) that Cabo Verde-born individuals resem-
286 ble more IBS and TSI patterns for their European-like membership than ASW and ACB individuals who,

287 instead, resemble more CEU and GBR patterns, consistently with ASD-MDS results (**Figure 2** and **Figure 2-**
288 **figure supplement 1**).

289 While the modal results comprising the most ADMIXTURE runs for increasing values of K from 11 to
290 13 differentiate novel clustering patterns among continental African and/or European populations (**Figure 3**),
291 alternative, minority, modes here highlight novel possible clustering solutions in turn maximized in different
292 groups of Cabo Verdean islands (**Appendix 3-figure 1**). Ultimately, these alternative ADMIXTURE results
293 are resolved at $K=14$ (**Figure 3**), with the emergence of the new bright yellow cluster maximized in individuals
294 from Boa Vista, and in part in individuals from Maio, while virtually absent from the rest of our data set.

295 Finally, at $K=15$, the novel dark green cluster is maximized in individuals born on Fogo and substantially
296 present in Brava-born individuals' membership proportions, while virtually absent from all other populations
297 in our data set. Note that alternative clustering solutions at $K=15$ disentangle resemblances across other West
298 Central and South-West Central African populations, but do not further propose additional clusters specifically
299 represented by Cabo Verdean variation (**Appendix 3-figure 1**).

300 Therefore, altogether, we identified at least five clustering patterns across Cabo Verdean islands of births
301 nested in increasing values of K , where, respectively, individuals from Fogo and Brava, from Santiago, from
302 Boa Vista, from Sal and São Nicolau, and from Santo Antão and São Vicente resembled more one another
303 than other individuals from elsewhere in Cabo Verde. In this context, note that Maio individuals cluster inter-
304 mediately between the Santiago, Boa Vista and São Vicente clusters.

305 Finally, we aim at describing potential genetic resemblances between the East Asian gene-pool, repre-
306 sented here by the Chinese CHB population, and the Cabo Verdean gene-pool, as a community from China is
307 established in the archipelago since at least the 1950's. Note that for every value of K above 3, the light-pink
308 cluster mainly represented by Chinese CHB individuals is found in three ASW and one ACB individuals, as
309 previously identified (10), but is virtually absent in the Cabo Verdean individuals that were included in our
310 study without criteria of geographic origins nor community belonging (see also **Appendix 3**).

311 Altogether, these ADMIXTURE results, differentiating patterns of genetic resemblance across Cabo
312 Verde and with respect to varied continental African and European populations, have been possible to uncover
313 due to inclusion of varied reference populations from continental Atlantic Africa and Europe, treating all Cabo
314 Verdean islands of birth as differentiated in the analyses (3,23,34).

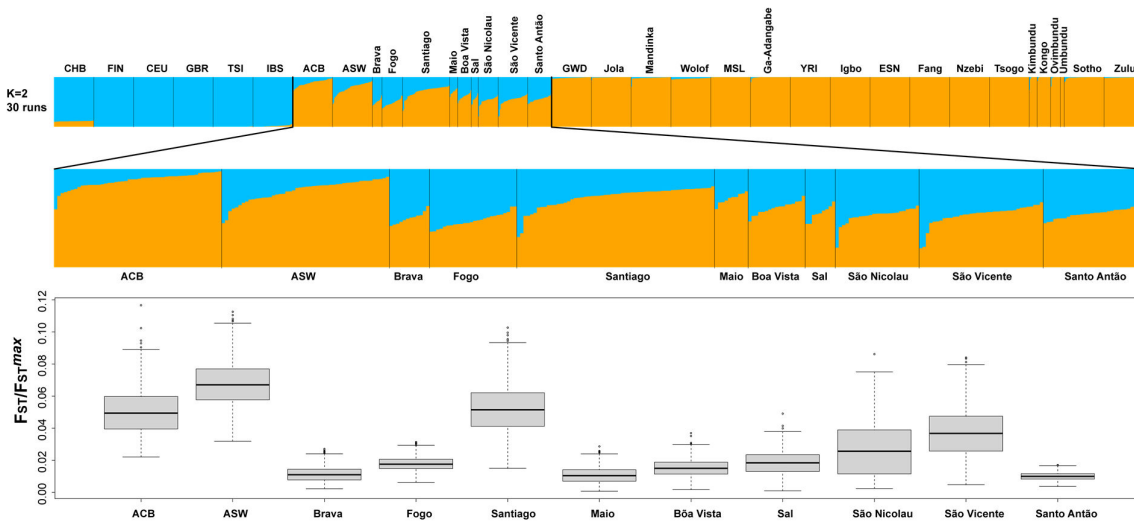
315
316

338 **Figure 3-figure supplement 2:**
339 *f₃*-admixture tests of admixture for each Cabo Verdean birth-island, the Barbadian-ACB, and the African-American ASW
340 populations related to the TAST.
341
342

343 **Figure 3-figure supplement 1:**
344 **Population F_{ST}/F_{ST}^{max} values for the ASW, ACB, and each Cabo Verdean birth-island separately considering the ADMIX-**
345 **TURE mode result at $K=2$ in Figure 3A.**

346 F_{ST}/F_{ST}^{max} values were computed using FSTruct (49) with 1000 bootstrap replicates per population. All population pairwise distributions of bootstrap F_{ST}/F_{ST}^{max} values were significantly different from one another after Bonferroni correction (Wilcoxon two-sided rank sum test $p < 3.96 \times 10^{-8}$), except the following pairwise comparisons: ACB-Santiago, Brava-Maio, Fogo-Sal, and Maio-Santo Antão.

349



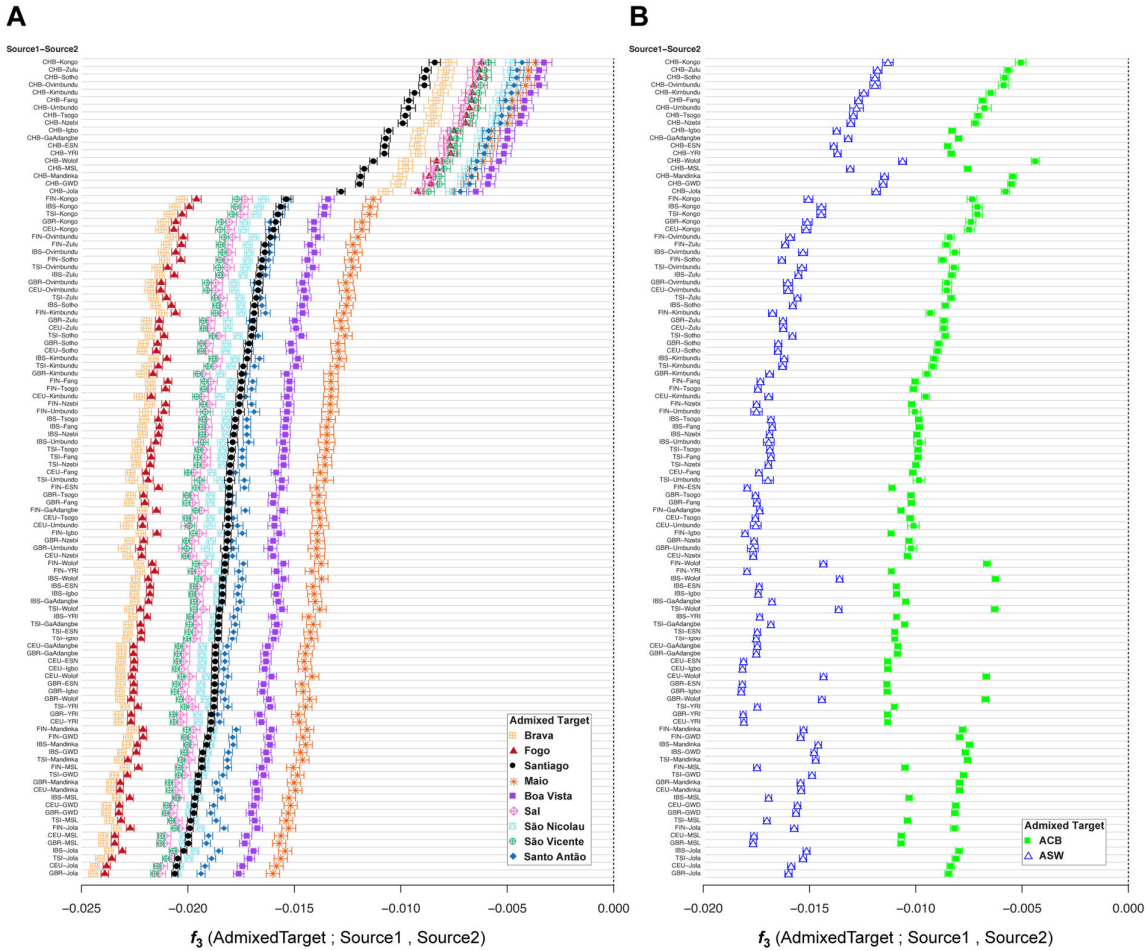
350
351

352
353
354
355
356
357
358
359
360
361
362

Figure 3-figure supplement 2:

f_3 -admixture tests of admixture for each Cabo Verdean birth-island, the Barbadian-ACB, and the African-American ASW populations related to the TAST.

As mentioned in the main text of the article, we calculated f_3 -admixture (50) considering as admixture targets each Cabo Verdean birth-island (panel A), the ASW (panel B), and the ACB (panel B) separately, with, as admixture sources, all 108 possible pairs of one continental European population (Source 1) and one continental African population (Source 2), or the East Asian CHB (Source 1) and one continental African population (Source2), using the same individuals, population groupings, and genotyping dataset as in the previous ADMIXTURE analyses (Figure 1-resource table 1). Results for each pair of possible sources are plotted in diminishing values of f_3 -admixture obtained specifically with Cabo Verde individuals born on Santiago as targets. Target population symbols are indicated in the legend at the bottom-right of each panel.



363
364
365

366 **3. Local-ancestry in Cabo Verde and other TAST-related admixed populations**

367 ASD-MDS and ADMIXTURE descriptive analyses do not formally test admixture and putative source popu-
368 lations of origins, they rather disentangle genetic resemblances among groups of individuals. The resulting
369 ADMIXTURE patterns could be due either to admixture from populations represented in our dataset, to ad-
370 mixture from populations un-represented in our dataset, or to common origins and drift (48,51–54). We further
371 analyzed the observed ADMIXTURE results by computing f_3 -admixture tests (50). We considered as admix-
372 ture targets each Cabo Verdean birth-island, the ASW, and the ACB separately, with, as admixture sources, in
373 turn all 108 possible pairs of one continental African population and one continental European population, or
374 one continental African population and the East Asian CHB, using the same individuals, population groupings,
375 and genotyping dataset as in the previous ADMIXTURE analyses.

376 For each Cabo Verdean birth island as a separate target population and for all pairs of possible sources
377 tested, we obtain negative values of f_3 -admixture (**Figure 3-figure supplement 2**), indicative of possible ad-
378 mixture signals (50). Altogether for the admixture of each Cabo Verdean birth-island, f_3 -admixture tests do not
379 allow us to clearly discriminate among possible African sources, nor among possible European sources, due
380 to largely overlapping f_3 -admixture values across tests (**Figure 3-figure supplement 2**). Note that f_3 and f_4
381 statistics have been recently shown to be strongly geometrically related to MDS/PCA and that its results need
382 not be due to admixture only (55), similarly to MDS/PCA or ADMIXTURE results (48,51–54). Therefore, we
383 conducted admixture-LD haplotypic local-ancestry inferences with the SHAPEIT2-CHROMOPAINTER-
384 SOURCEFIND pipeline (56–58), to more precisely identify the possible European and African populations at
385 the sources of genetic patterns observed in enslaved-African descendant populations and Cabo Verdeans in
386 particular.

387 **Figure 3B** shows striking differences concerning both the European and the African source populations
388 involved in the admixture history of ACB, ASW, and individuals born on different Cabo Verdean islands. We
389 find that individuals from all Cabo Verdean islands share almost all their European haplotypic ancestry with
390 the Iberian-IBS population rather than other European populations. Santiago-born individuals present the
391 smallest (27%) average haplotypic ancestry shared with IBS, and Fogo-born the highest (51%). Conversely,
392 the ASW and ACB both share haplotypic ancestries only with the USA-CEU of North-Western European
393 origin (20% and 12% respectively).

394 Furthermore, we find that all Cabo Verdeans almost exclusively share African haplotypic ancestries with
395 two Senegambian populations (Mandinka and Wolof) and very reduced to no shared ancestries with other
396 regions of Africa. More specifically, we find that the Mandinka from Senegal are virtually the sole African
397 population to share haplotypic ancestry with Cabo Verdeans born on Brava, Fogo, Santiago, Maio, and Boa
398 Vista, and the majority of the African shared ancestry for Sal, São Nicolau, São Vicente, and Santo Antão. In
399 individuals from these four latter islands, we find shared haplotypic ancestry with the Wolof population rang-
400 ing from 4%-5% for individuals born on Sal (considering four or six possible sources, respectively), up to
401 16%-22% for Santo Antão. Finally, we find limited (1%-6%) shared haplotypic ancestry with East Western
402 (Igbo, YRI, or Ga-Adangbe) or South-West Central (Kimbundu, Kongo, or Ovimbundu) African populations
403 in all Cabo Verdean islands, except Fogo and Brava, and the specific populations identified and their relative
404 proportions of shared haplotypic ancestries vary across analyses. Conversely, we find that the ASW and ACB
405 populations share African haplotypic ancestries in majority with East Western African populations (YRI, Ga-
406 Adangbe, and Igbo), and substantial shared ancestries with Senegambian populations (5-10%), the MSL from
407 Sierra Leone in Central Western Africa (5-12%), and South-West Central African populations (3-18%), albeit
408 variable depending on the number of putative sources considered.

409

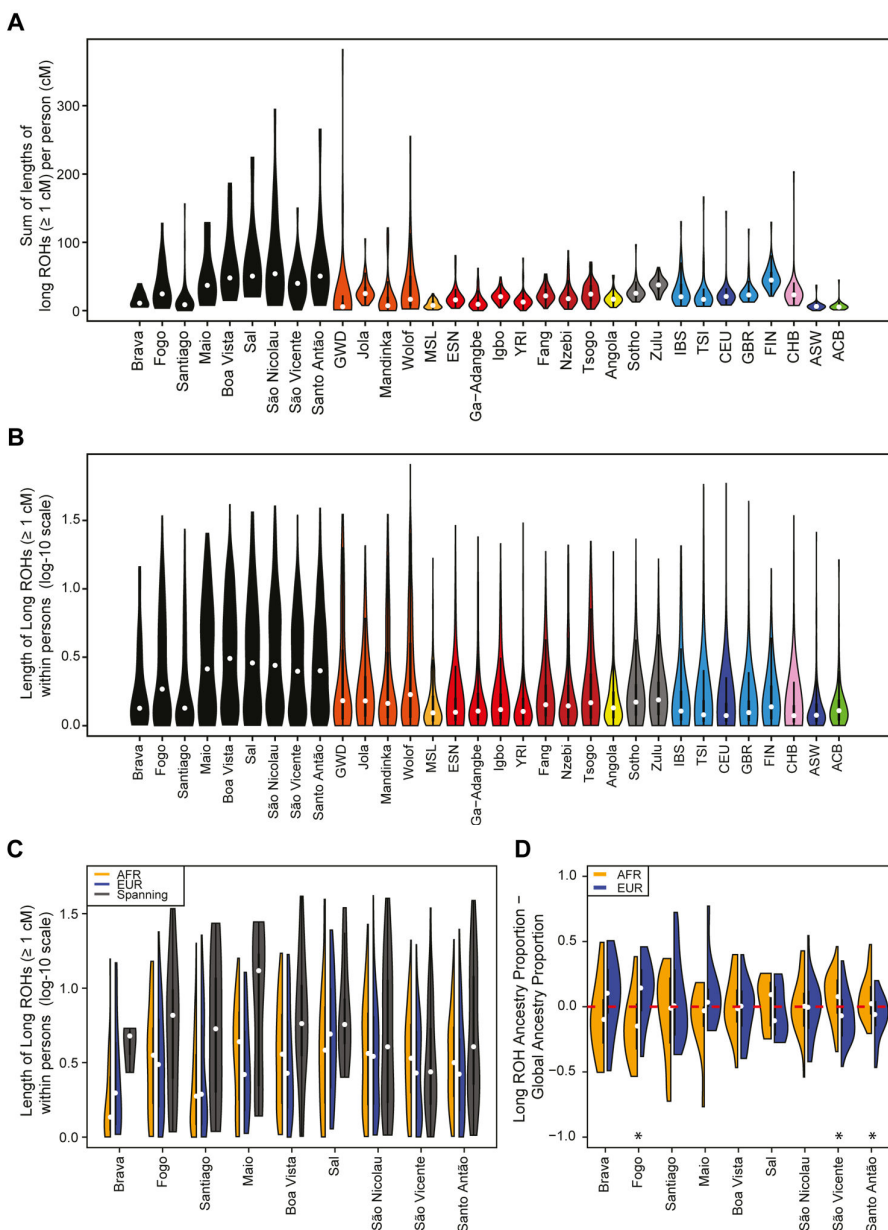
410 **4. Runs of homozygosity (ROH) and admixture patterns within Cabo Verde**

411 Runs of homozygosity (ROH) are Identical-By-Descent haplotypes resulting from recent parental
412 relatedness and present in individuals as long stretches of homozygous genotypes. Their length and abundance
413 can reflect demographic events, such as population bottlenecks and founder events, natural selection, and
414 cultural preferences for endogamy (59–61); and ROH have not been seen to depend strongly on recombination
415 or mutation rate variation across the genome (62).

416 We find higher levels of long ROH ($\geq 1\text{cM}$) in Cabo Verdeans compared to most other analyzed
417 populations, including ASW and ACB (**Figure 4A** and **Appendix 4-figure 1**). We find the highest levels of
418 long-ROH in individuals born on Maio, Boa Vista, Sal, São Nicolau, São Vicente, and Santo Antão, with a
419 mean individual length of long-ROHs around 3cM (**Figure 4B**), and the lowest levels of long-ROH in Santiago
420 and Brava-born individuals. Among long ROH (**Appendix 4-figure 2C**), we find little to no correlation with
421 total non-ROH levels for African local-ancestry segments (Pearson $\rho = -0.06689$, $p = 0.3179$), European
422 ($\rho = 0.1551$, $p = 0.01989$), or East Asian ($\rho = 0.06239$, $p = 0.3516$). Of all ROH identified, the mean proportion of
423 ROH that were long ranged from 0.065 to 0.280 (**Figure 4-resource table 1**).

424 In admixed populations, we expected that some of the long ROH spanned local ancestry breakpoint
425 switches (see **Materials and Methods 4**), indicating that the most recent common ancestor existed after the
426 initial admixture event having generated local-ancestry patterns. Furthermore, we expected that these
427 “spanning” ROH would be among the longest ROH observed if admixture occurred only in the past few
428 generations. We find that (**Figure 4C**), almost uniformly across Cabo Verde, the longest ROH identified
429 indeed spanned at least one ancestry breakpoint, excluding the very few East Asian ancestry regions identified.
430 Furthermore, correcting ancestry-specific long-ROH sizes (**Figure 4-figure supplement 1**) for individuals’
431 total ancestry fraction of that ancestry, we find that individuals born in Fogo have, on average, an
432 overrepresentation of European ancestry (and a corresponding underrepresentation of African ancestry) in
433 long-ROH (**Figure 4D**; permutation $p < 10^{-4}$; **Figure 4-figure supplement 2, Figure 4-resource table 2**), and
434 that individuals from Santo Antão and São Vicente have, conversely, an apparent overrepresentation of
435 African ancestry and underrepresentation of European ancestry in long ROH (permutation $p = 10^{-4}$ and $p < 10^{-4}$,
436 respectively; **Figure 4-figure supplement 2, Figure 4-resource table 2**). Finally, we find that individuals
437 from Brava, Santiago, Maio, Boa Vista, São Nicolau, and Sal have relatively similar long-ROH levels in
438 African and European segments (permutation $p > 0.01$; **Figure 4-figure supplement 2, Figure 4-resource**
439 **table 2**). This latter pattern may be consistent with these populations being founded by admixed individuals,
440 while the former patterns could indicate, in addition to such admixture founding effects, more recent or
441 recurring contributions from the sources (60).

442



443
444
445
446
447
448
449
450
451
452
453
454
455
456
457
458
459

Figure 4:

Distributions of long ROHs (≥ 1 cM) in Cabo Verde.

A) The distribution of the sum of long-ROH (≥ 1 cM) lengths per person for each Cabo Verdean birth-island and other populations. **B)** The length distribution (log-10 scale) of individual long-ROHs identified within samples for each Cabo Verdean birth-island and other populations (e.g., for a distribution with mass at 1.0, this suggests individual ROHs of length 10 cM were identified among samples from that group). **C)** The length distribution of ancestry-specific and ancestry-spanning individual long-ROHs for each Cabo Verdean birth-island. **D)** The distribution of differences between individuals' long-ROH ancestry proportion and their global ancestry proportion, for African and European ancestries separately and for each Cabo Verdean birth-island. * indicates significantly ($\alpha < 1\%$) different proportions of ancestry-specific long-ROH, based on non-parametric permutation tests, see **Material and Methods 4, Figure 4-resource table 2, and Figure 4-figure supplement 2.**

Figure 4-figure supplement 1:

The distribution of total ancestry in long ROH per individual for each Cabo Verdean birth-island.

Figure 4-figure supplement 2:

460 **Permutation distributions for over/under representation of ancestry in long ROH (≥ 1 cM) for each Cabo Verdean island of**
461 **birth.**

462

463 **Figure 4-resource table 1: *provided in .xls format***

464 **Mean proportion of total length of ROH that are classified as long ($cM \geq 1$) for each Cabo Verdean island of birth.**

465

466 **Figure 4-resource table 2: *provided in .xls format***

467 **Permutation tests' p-values for over/under representation of ancestry in long ROH ($cM \geq 1$) for each Cabo Verdean island of**
468 **birth.**

469

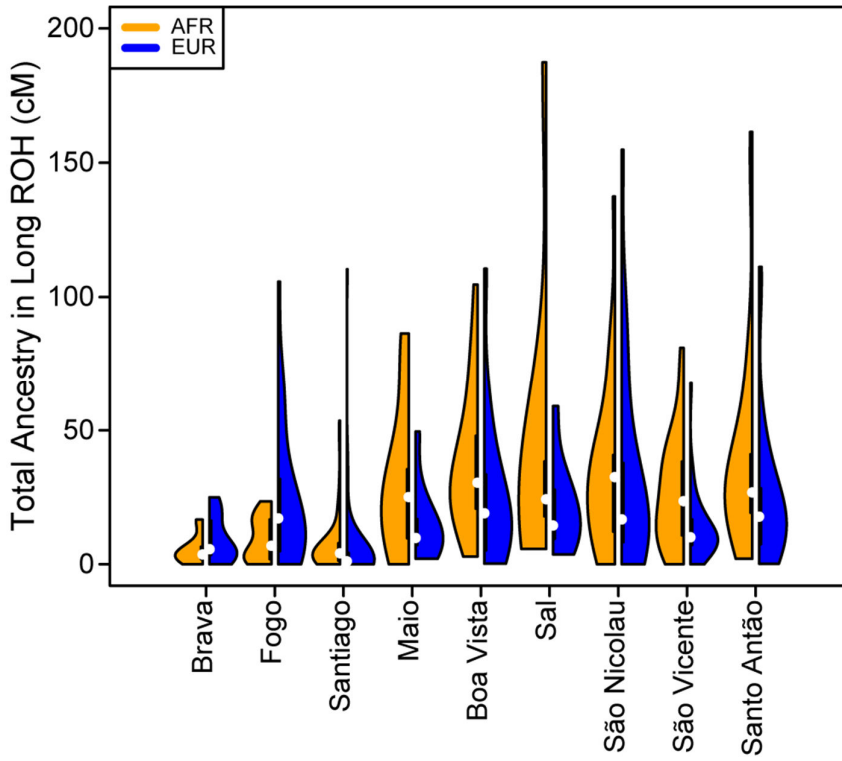
470 **Figure 4-resource table 3: *provided in .xls format***

471 **Mean proportion of total length of long ROH ($cM \geq 1$) that have heterozygous ancestry (AFR and EUR), for each Cabo Verdean**
472 **island of birth.**

473

474

475 **Figure 4-figure supplement 1:**
476 **The distribution of total ancestry in long ROH per individual for each Cabo Verdean birth-island.**
477



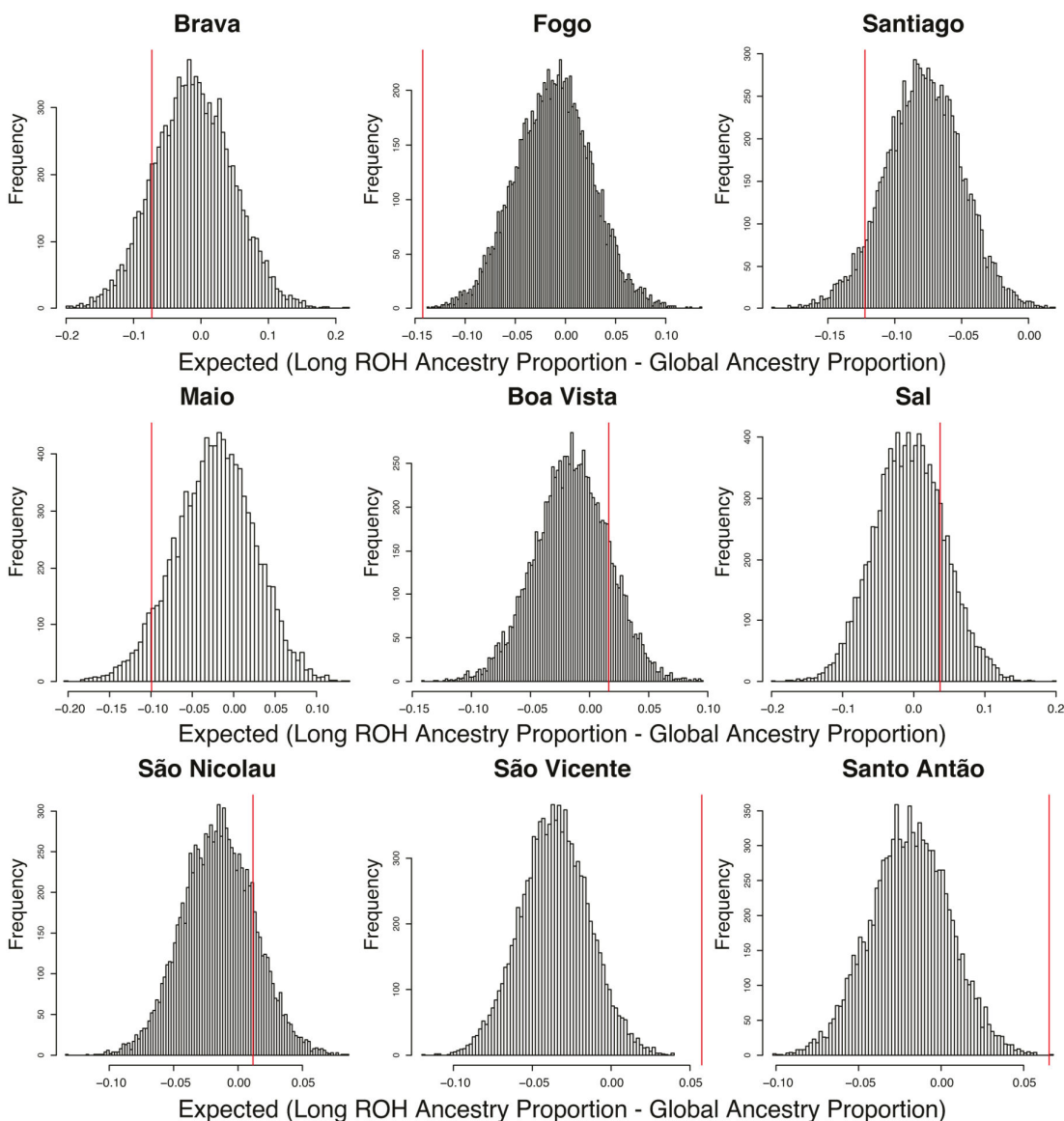
478
479
480

481
482
483
484
485
486
487
488
489
490
491

Figure 4-figure supplement 2:

Permutation distributions for over/under representation of ancestry in long ROH (≥ 1 cM) for each Cabo Verdean island of birth.

As mentioned in **Material and Methods 4**, for each individual in each island, we randomly permuted the location of all long ROH (ensuring that no permuted ROH overlap), re-computed the local AFR ancestry proportion falling within these permuted ROH, and then subtracted the global ancestry proportion. We then take the mean of this difference across all individuals for each island and repeat the process 10,000 times. As there is negligible ASN ancestry across these individuals, the AFR and EUR proportions essentially add to 1, and therefore we consider an over/under representation of AFR ancestry in long ROH to be equivalent to an under/over representation of EUR ancestry in long ROH. Observed values in the real data set are provided as a red vertical line for each island of birth separately. Permutation p-values are reported in **Figure 4-resource table 2**.



492
493

494 **5. Genetic and linguistic isolation-by-distance within Cabo Verde**

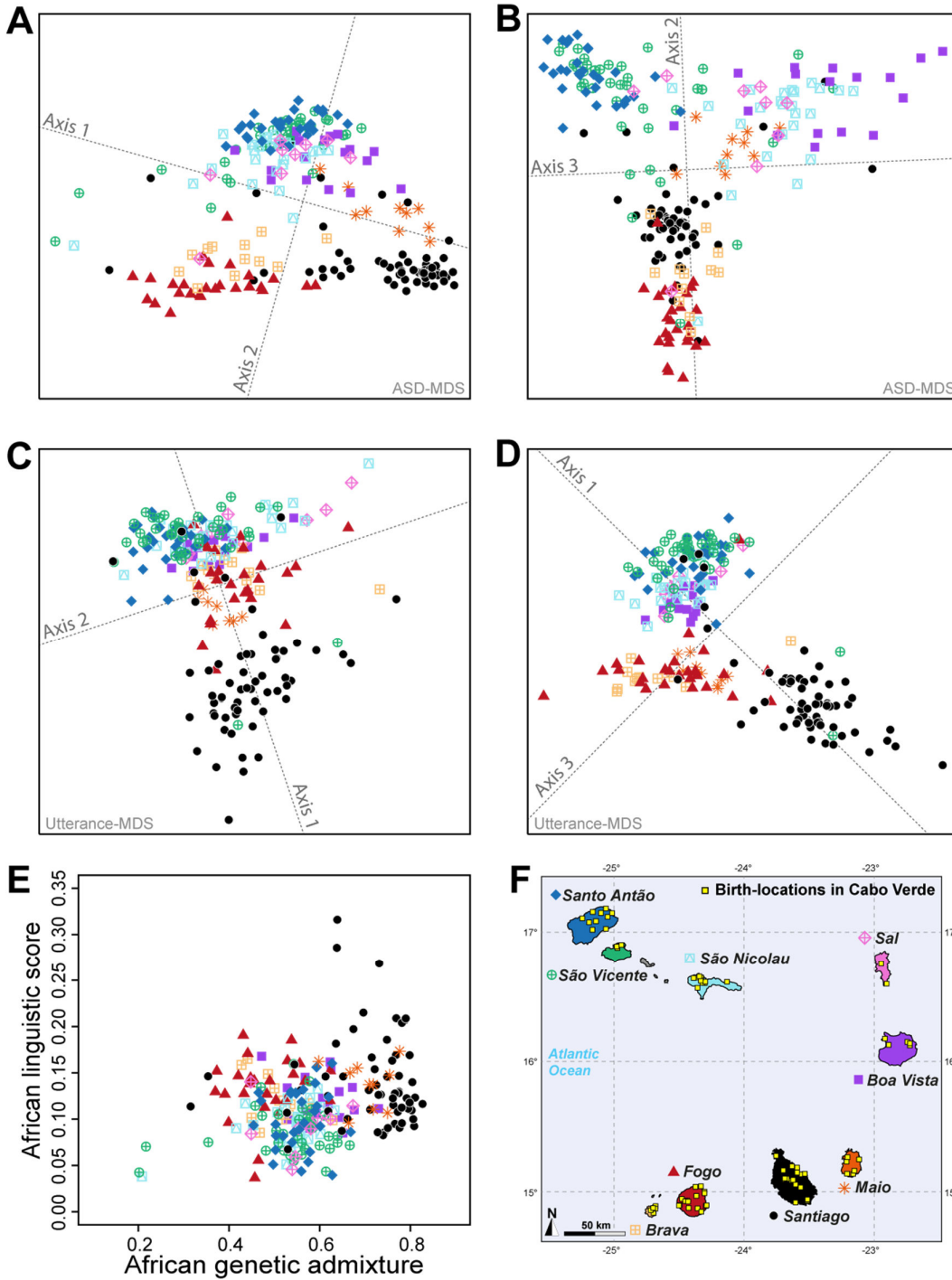
495 The above ASD-MDS, ADMIXTURE, local-ancestry inferences, and ROH results suggest substantial genetic
496 differentiation at a very reduced geographical scale within the archipelago across Cabo Verdean birth-islands
497 of individuals. Following previous linguistic investigations highlighting Kriolu qualitative linguistic variation
498 across islands within the archipelago (15,17,29,30), we aim at further characterizing possible patterns of joint
499 genetic and linguistic isolation (39) at very reduced geographical scale across islands as well as within islands.
500 Indeed, while the geographic distribution of genetic diversity has been previously extensively explored across
501 human populations to reveal population migration routes, in particular in island and archipelago contexts (e.g.
502 (63,64)), the underlying parent-offspring genetic and linguistic dispersal mechanisms have been seldom ex-
503 plored in humans at extremely local scales to our knowledge (39,42–44). Nevertheless, knowledge about such
504 dispersal mechanisms can be built by exploring the influence of isolation-by-distance mechanisms on genetic
505 and linguistic diversity distributions at very reduced geographical scales (~50km) within a population (39–41).
506 We thus explored both pairwise ASD and inter-individual variation in manners of speaking Kriolu (character-
507 ized as differences in the frequencies of use of Kriolu utterances among individual discourses; see **Material**
508 **and Methods 1.c-d**), in the same set of 225 Cabo Verde-born individuals. To do so, we used MDS and Mantel
509 testing of correlations between, respectively, genetic and linguistic pairwise differentiation, and socio-cultural
510 and geographical covariates including age, duration of academic education, residence locations, birth-places,
511 and parental birth-places (**Figure 5**, **Table 1**, and **Table 1-resource table 1**).

512 The first ASD-MDS axis differentiates mainly individuals born on Brava and Fogo compared to Santiago
513 (**Figure 5A-B**). The second axis mainly differentiates individuals from Santiago, Fogo, and Brava from all
514 other islands, while the third axis differentiates individuals from Boa Vista, São Nicolau, Sal, and Maio from
515 all other birth-islands. Furthermore, we find a significant positive correlation between ASD and actual indi-
516 vidual birth-locations across Cabo Verde (**Table 1**; Spearman $\rho=0.2916$, two-sided Mantel $p<2\times 10^{-4}$). This
517 correlation increases when considering only within-islands pairwise comparisons and excluding all inter-island
518 comparisons (Spearman $\rho=0.3460$, two-sided Mantel $p<2\times 10^{-4}$), thus illustrating the strong signal of genetic
519 isolation-by-distance (39) within Cabo Verde at very reduced geographical scales.

520 Furthermore, the first utterance-MDS axis of pairwise inter-individual Euclidean distances between utter-
521 ance frequencies mainly differentiates Santiago and Santo Antão/São Vicente-born individuals' speech-varie-
522 ties; all other Cabo Verdeans cluster intermediately (**Figure 5C-D**). The third axis further separates speech-
523 varieties recorded in individuals from Fogo, Maio, and Brava. Analogously to genetic differentiation patterns,
524 we find a positive correlation between differences in utterance frequencies and actual birth-places' distances
525 (Spearman $\rho=0.2794$, two-sided Mantel $p<2\times 10^{-4}$), as well as paternal and maternal birth-places respectively
526 (**Table 1**). However, unlike for to ASD, we find that utterance-frequencies differences stem from inter-birth-
527 islands' distances, rather than shorter distances within islands only. Extending previous results from Santiago
528 only (23), these results altogether show that speech-varieties are significantly transmitted from one generation
529 to the next throughout Cabo Verde, anchored in individuals' birth-places. Importantly, note, however, that this
530 vertical transmission of manners of speaking Kriolu does not account for the majority of observed linguistic
531 variation across individuals in our dataset. Indeed, we find that age-differences also substantially correlate with
532 utterance-frequency differences even when correcting for individual birth-places (Spearman $\rho=0.2294$, two-
533 sided partial-Mantel $p<2\times 10^{-4}$). Finally, while we might intuitively expect that academic education influences
534 idiolects, we find instead that differences in education-duration do not correlate with Kriolu utterance-frequen-
535 cies differences, whether correcting for residence or birth-places distances, or not (**Table 1**). This shows the
536 modest influence of academic education on Kriolu variation. Altogether, our results highlight strong genetic
537 and linguistic isolation-by-distance patterns at reduced geographic distances within Cabo Verde.

538 Altogether, we find here genetic and linguistic isolation-by-distance anchored in inter-individual birth-
539 places distances across, and sometimes within, Cabo Verdean islands. These results demonstrate the reduced

540 dispersal of Cabo Verdeans at very local scales within the archipelago, both genetically and linguistically, a
 541 fundamental mobility-behavior mechanism likely explaining genetic and linguistic isolation across islands and
 542 sometimes even within islands despite the large self-reported exploration mobility of Cabo Verdeans.
 543



544
 545
 546
 547
 548
 549
 550

Figure 5:
Utterance and genetic diversity and admixture within Cabo Verde.

A-B) 3D MDS projection of Allele Sharing Dissimilarities computed among 225 unrelated Cabo-Verde-born individuals using 1,899,878 autosomal SNPs. Three-dimensional Euclidean distances between pairs of individuals in this MDS significantly correlated with ASD (Spearman $\rho=0.6863$; $p<2.2\times 10^{-16}$). **C-D)** 3D MDS projection of individual pairwise Euclidean distances between uttered

551 linguistic items frequencies based on the 4831 unique uttered items obtained from semi-spontaneous discourses. Three-dimensional
552 Euclidean distances between pairs of individuals in this MDS significantly correlated with the utterance-frequencies distances (Spear-
553 man $\rho=0.8647$; $p<2.2\times 10^{-16}$). **E**) Spearman correlation between individual African utterance scores and individual genetic African
554 admixture rates obtained with ADMIXTURE at $K=2$. **F**) Birth-locations of 225 individuals in Cabo Verde. Symbols for individuals'
555 birth-island in panels **A-E** are shown in panel **F**. Panel **A-D** were Procrustes-transformed according to individual actual birth-places'
556 geographical locations in panel **F** (65).

Mantel variable	Partial-Mantel control	n	Geographic scale	Genetic ASD - 1,899,978 SNPs		Utterance-frequency Euclidean distances - 4831 uttered items	
				Spearman rho	10000 Mantel two-sided permutation p	Spearman rho	10000 Mantel two-sided permutation p
abs(Age difference)	--	225	within and between islands	0.1303	< 2.10 ⁻⁴	0.2215	< 2.10 ⁻⁴
abs(Age difference)	log(Birth-loc. dist.)	225	within and between islands	0.1348	< 2.10 ⁻⁴	0.2294	< 2.10 ⁻⁴
log(Birth-loc. dist.)	--	225	within and between islands	0.2916	< 2.10 ⁻⁴	0.2794	< 2.10 ⁻⁴
log(Birth-loc. dist.)	abs(Age difference)	225	within and between islands	0.2935	< 2.10 ⁻⁴	0.2855	< 2.10 ⁻⁴
abs(Education duration difference)	--	186	within and between islands	<i>0.0168</i>	<i>0.2730</i>	<i>0.0962</i>	<i>0.0024</i>
abs(Education duration difference)	log(Birth-loc. dist.)	186	within and between islands	<i>-0.0023</i>	<i>0.4900</i>	<i>0.0834</i>	<i>0.0071</i>
abs(Education duration difference)	--	185	within and between islands	<i>0.0159</i>	<i>0.2825</i>	<i>0.1001</i>	<i>0.0014</i>
abs(Education duration difference)	log(Residence dist.)	185	within and between islands	<i>-0.0041</i>	<i>0.4651</i>	<i>0.0824</i>	<i>0.0068</i>
log(Residence dist.)	--	224	within and between islands	0.1658	< 2.10 ⁻⁴	0.2145	< 2.10 ⁻⁴
log(Residence dist.)	log(Birth-loc. dist.)	224	within and between islands	-0.0488	0.0005	<i>0.0306</i>	<i>0.0682</i>
log(Birth-loc. dist.)	--	224	within and between islands	0.2889	< 2.10 ⁻⁴	0.2800	< 2.10 ⁻⁴
log(Birth-loc. dist.)	log(Residence dist.)	224	within and between islands	0.2445	< 2.10 ⁻⁴	0.1863	< 2.10 ⁻⁴
log(Father Birth-loc. dist.)	--	222	within and between islands	0.2424	< 2.10 ⁻⁴	0.1704	< 2.10 ⁻⁴
log(Father Birth-loc. dist.)	log(Birth-loc. dist.)	222	within and between islands	<i>0.0846</i>	<i>0.0014</i>	<i>0.0066</i>	<i>0.3915</i>
log(Mother Birth-loc. dist.)	--	224	within and between islands	0.2619	< 2.10 ⁻⁴	0.2634	< 2.10 ⁻⁴
log(Mother Birth-loc. dist.)	log(Birth-loc. dist.)	224	within and between islands	<i>0.0748</i>	<i>0.0057</i>	<i>0.0853</i>	<i>0.0071</i>
abs(Age difference)	--	225	within islands only	0.2124	0.0006	0.2727	< 2.10 ⁻⁴
abs(Age difference)	log(Birth-loc. dist.)	225	within islands only	<i>0.1648</i>	<i>0.0041</i>	0.2546	< 2.10 ⁻⁴
log(Birth-loc. dist.)	--	225	within islands only	0.3460	< 2.10 ⁻⁴	<i>0.1412</i>	<i>0.0401</i>
log(Birth-loc. dist.)	abs(Age difference)	225	within islands only	0.3212	< 2.10 ⁻⁴	<i>0.0990</i>	<i>0.1030</i>
abs(Education duration difference)	--	186	within islands only	<i>-0.0370</i>	<i>0.3077</i>	<i>0.1287</i>	<i>0.0440</i>
abs(Education duration difference)	log(Birth-loc. dist.)	186	within islands only	<i>-0.0537</i>	<i>0.2330</i>	<i>0.1239</i>	<i>0.0496</i>
abs(Education duration difference)	--	185	within islands only	<i>-0.0382</i>	<i>0.3037</i>	<i>0.1421</i>	<i>0.0292</i>
abs(Education duration difference)	log(Residence dist.)	185	within islands only	<i>-0.0491</i>	<i>0.2566</i>	<i>0.1202</i>	<i>0.0546</i>
log(Residence dist.)	--	224	within islands only	<i>-0.0667</i>	<i>0.1907</i>	<i>0.0982</i>	<i>0.0911</i>
log(Residence dist.)	log(Birth-loc. dist.)	224	within islands only	<i>-0.0549</i>	<i>0.2319</i>	<i>0.1063</i>	<i>0.0704</i>
log(Birth-loc. dist.)	--	224	within islands only	0.3465	< 2.10 ⁻⁴	<i>0.1537</i>	<i>0.0282</i>
log(Birth-loc. dist.)	log(Residence dist.)	224	within islands only	0.3446	< 2.10 ⁻⁴	<i>0.1589</i>	<i>0.0230</i>
log(Father Birth-loc. dist.)	--	222	within islands only	0.2660	0.0006	<i>0.0160</i>	<i>0.4123</i>
log(Father Birth-loc. dist.)	log(Birth-loc. dist.)	222	within islands only	<i>0.2187</i>	<i>0.0045</i>	<i>-0.0111</i>	<i>0.4546</i>
log(Mother Birth-loc. dist.)	--	224	within islands only	<i>0.2240</i>	<i>0.0034</i>	<i>0.1283</i>	<i>0.0423</i>
log(Mother Birth-loc. dist.)	log(Birth-loc. dist.)	224	within islands only	<i>0.1563</i>	<i>0.0303</i>	<i>0.1000</i>	<i>0.0925</i>

557

Table 1:

558

Mantel and partial-Mantel correlations between utterance frequency differences and covariables, and between genetic ASD and the same covariables, in 225 genetically unrelated Cabo Verde-born Kriolu-speaking individuals.

559

Spearman correlations ρ are indicated in bold when significant at $\alpha < 0.001$, and in italics otherwise. Spearman correlations and Mantel-tests among covariables are provided in **Table 1-resource table 1**.

560

561

562

563

Table 1-resource table 1: provided in .xls format

564

Mantel correlations among individual birth-places, residence-places, maternal and paternal birth places, age, and academic education duration.

565

566 **6. Geographic distribution of genetic and linguistic admixture within Cabo Verde**

567 Based on these results of genetic and linguistic diversity isolation-by-distance patterns anchored in individual's
568 birth-places, we aim at investigating whether individual genetic and/or linguistic admixture levels also exhibit
569 isolation-by-distance patterns across and within islands, beyond the qualitative observation that genetic and
570 linguistic admixture patterns vary across different islands of Cabo Verde obtained above and in previous results
571 (23,34). Interestingly, we find that absolute differences in inter-individual genetic admixture levels from Africa,
572 estimated with ADMIXTURE or ASD-MDS, significantly correlate with actual birth-places distance across
573 islands (Spearman $\rho=0.1865$, two-sided Mantel $p<2\times 10^{-4}$ and $\rho=0.1813$, $p<2\times 10^{-4}$, respectively), but not
574 within-islands only ($\rho=0.0342$ $p=0.3094$ and $\rho=0.0282$ $p=0.3385$, respectively). This shows that two individ-
575 uals born on far-away islands are likely to differ more in African genetic admixture levels, than two individuals
576 born on close-by islands, a form of isolation-by-distance pattern for genetic admixture across Cabo Verdean
577 islands.

578 We explored inter-individual variation in Kriolu utterance frequencies specifically for uttered items of
579 clearly African and dual European-African origins (utterance categories A and B; **Material and Methods 1.e**)
580 providing an estimate of individual African linguistic-admixture scores (23). We find that African linguistic-
581 admixture score differences significantly correlate with actual birth-places' distances throughout Cabo Verde
582 (Spearman $\rho=0.1297$, two-sided Mantel $p<2\times 10^{-4}$), and even marginally significantly correlate with birth-
583 places' distances at short distances within birth-islands (Spearman $\rho=0.1209$, two-sided Mantel $p=0.0419$).

584 Finally, we find a significant positive correlation (Spearman $\rho=0.2070$, $p=0.0018$) between genetic and
585 linguistic admixture in Cabo Verde (**Figure 5E**), indicating that individuals who frequently use African-related
586 utterances in their manner of speaking Kriolu are more likely to exhibit higher levels of African genetic-ad-
587 mixture. This correlation remains, respectively, marginally significant and significant when considering utter-
588 ances of strictly African-origin (Category A) or utterances with a dual European-African etymology (Category
589 B) separately (Spearman $\rho=0.1631$, $p=0.0143$, and $\rho=0.1829$, $p=0.0059$, respectively). These positive correla-
590 tions between genetic and linguistic admixture generalize to the whole archipelago our previous results ob-
591 tained in Santiago only (23), and further suggest that genetic and linguistic admixture histories may have oc-
592 curred in parallel all throughout Cabo Verde.

593 Therefore, not only we identify isolation-by-distance patterns within Cabo Verdean islands for genetic
594 and linguistic diversities, but also identify a form of isolation-by-distance for genetic and linguistic admixture
595 levels at very reduced geographical scales. This suggests that processes of reduced dispersal of individuals can
596 also be identified in the genetic and linguistic admixture patterns, which has never been previously observed
597 in human admixed populations to our knowledge, nor previously suspected whether genetically or linguisti-
598 cally in Cabo Verde (3,15,17,23,30,33).

599 Together with the above LAI and ROH results, the various isolation-by-distance patterns here identified
600 suggest that different founding events followed by local isolation due to reduced genetic and linguistic disper-
601 sal ranges, as well as different admixture histories, are at the root of patterns of genetic and linguistic diversity
602 and admixture throughout Cabo Verde, anchored in individual birth places across islands, and even sometimes
603 within islands.

604

605 7. Genetic admixture histories in Cabo Verde inferred with *MetHis-ABC*

606 Highly complex admixture histories, with more than two separate pulses and/or periods of recurring admixture
607 from each source population, are often impossible to infer from observed genetic data using maximum-likeli-
608 hood approaches; whether the likelihood itself cannot be explicitly formulated or whether its maximization is
609 computationally intractable for such high levels of complexity (8,9,66,67). Instead, Approximate Bayesian
610 Computation allows, in principle, formal comparison of competing scenarios underlying the observed data and
611 estimation of the posterior distribution of the parameters under the winning model (68,69). The user simulates
612 numerous genetic datasets under competing scenarios, drawing randomly the parameter values of each simu-
613 lation in prior distributions. ABC then allows to formally compare a set of summary statistics calculated on
614 the observed data with the same set of summary statistics calculated on each simulated genetic dataset sepa-
615 rately, in order to identify which of the competing scenarios produces simulations for which summary-statistics
616 are closest to the observed ones. Under the winning scenario, ABC then estimates the joint posterior distribu-
617 tion of parameter values which produced simulations whose summary statistics most resemble the observed
618 ones. Therefore, ABC allows, in principle, to infer arbitrarily complex demographic models underlying the
619 data, provided that data can be efficiently simulated under these scenarios drawing randomly parameter values
620 from prior distributions explicitly set by the user, and provided that calculated summary statistics are indeed
621 informative about the scenarios' parameters (70).

622 We reconstruct the admixture histories of each Cabo Verde island separately using the *MetHis-ABC*
623 framework (45,71,72). It was recently developed to investigate highly complex admixture histories using ma-
624 chine-learning ABC, by simulating independent autosomal SNPs forward-in-time in an admixed population
625 under any two source-population versions of a general admixture model (73), and calculating, for each simu-
626 lation, sets of summary statistics shown to be informative about the underlying admixture models' parameters
627 for ABC inferences (45). See **Material and Methods 7** and **Appendix 1** for the detailed description of simu-
628 lations and ABC machine-learning scenario-choice and posterior parameter estimation procedures.

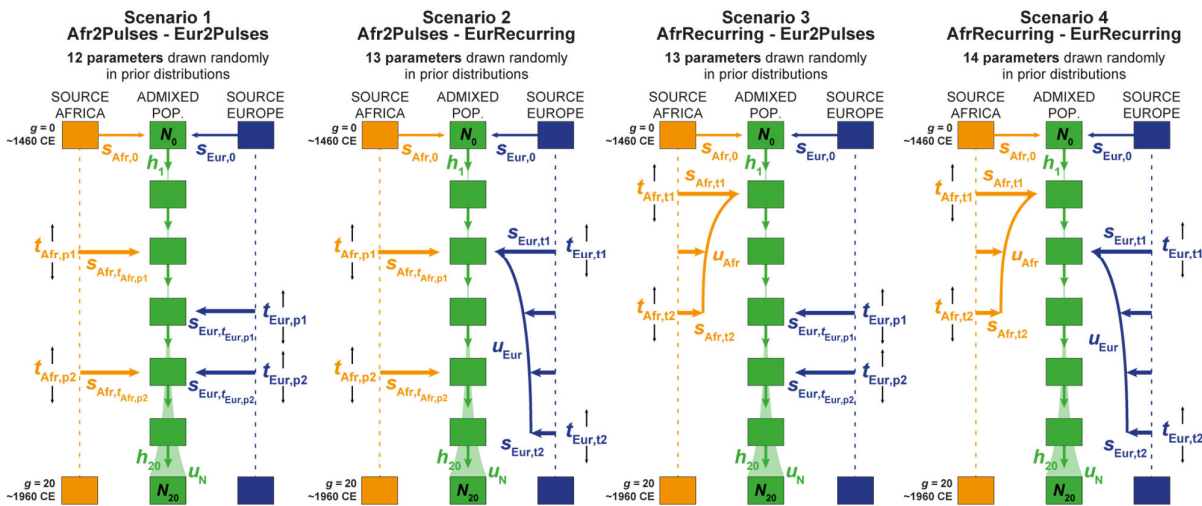
629 *MetHis-ABC* prior checking

631 We considered four competing genetic-admixture scenarios described in **Figure 6** and **Table 2**, tested
632 separately for individuals born on each Cabo Verdean island and for the 225 Cabo Verde-born unrelated indi-
633 viduals grouped altogether, with *MetHis-ABC* machine-learning scenario-choice and posterior parameter in-
634 ferences (45,71,72). ABC inferences are based on 42 summary statistics (**Table 3**), calculated for each simu-
635 lation under each competing scenario separately using 60,000 independent autosomal SNPs in Cabo Verdean
636 individuals, the African Mandinka and the European Iberian-IBS proxy source populations.

637 Note that we did not explicitly simulate genotype data in the European and African source-populations.
638 Instead, we built gamete reservoirs at each 21 generation of the forward-in-time admixture process, matching
639 in frequency the observed allele frequencies at the 60,000 independent SNPs for the Iberian IBS and Mandinka
640 populations, respectively. As in our previous *MetHis-ABC* investigation of the admixture history of the Afri-
641 can-American ASW and Barbadian ACB populations (45), we therefore consider that the African and Euro-
642 pean proxy populations at the source of the admixture history of Cabo Verde are large and unaffected by
643 mutation during the 21 generations of the admixture process; this assumption is reasonable provided that we
644 consider only independent genotyped SNPs and the very recent demographic history of the archipelago, dis-
645 covered un-inhabited and first settled in the 1460's. Therefore, although we cannot reconstruct the evolutionary
646 history of the African and European source populations with our design, we nevertheless implicitly take the
647 real demographic histories of these source populations into account in our simulations, as we use observed
648 genetic patterns themselves, the product of this demographic history, to create the virtual source populations
649 at the root of the admixture history of Cabo Verde.

650 We find that the summary-statistics calculated from the observed datasets fall well within the space of
651 summary-statistics obtained from 10,000 simulated-datasets under each of the four competing scenarios (**Ap-**
652 **pendix 1-figure 3, Appendix 1-figure 3-resource figure 1-10**), considering non-significant ($\alpha > 5\%$) good-
653 ness-of-fit, visual inspection of summary-statistics PCA-projections, and each summary-statistic's distribution,
654 for each Cabo Verdean birth-island and for all Cabo Verde-born individuals grouped in a single population,
655 separately. Prior-checks thus demonstrate that *MetHis* simulations are appropriate for further ABC scenario-
656 choice and posterior parameter inferences using observed data in the African Mandinka and the European
657 Iberian IBS source populations and each Cabo Verde islands separately or grouped altogether, as they allow
658 to mimic the observed summary-statistics, despite the assumption that the European and African proxy source
659 populations are at the drift-mutation equilibrium over the last 21 generations.
660
661

662



663

664

665

666

Figure 6:

667

Four competing scenarios for the genetic admixture histories of each Cabo Verde island.

668

For all scenarios, the duration of the admixture process is set to 20 generations after the initial founding admixture event occurring at generation 0, which corresponds roughly to the initial peopling of Cabo Verde in the 1460's, considering 25 years per generation and sampled individuals born on average between the 1960s and 1980's.

669

670

Scenario 1 Afr2Pulses-Eur2Pulses: after the initial founding pulse of admixture, the admixed population receives two separate introgression pulses from the African and European sources, respectively. **Scenario 2 Afr2Pulses-EurRecurring:** after the initial founding pulse of admixture, the admixed population receives two separate introgression pulses from the African source, and a period of monotonically constant or decreasing recurring introgression from the European source. **Scenario 3 AfrRecurring-Eur2Pulses:** after the initial founding pulse of admixture, the admixed population receives a period of monotonically constant or decreasing recurring introgression from the African source, and two separate introgression pulses from the European source. **Scenario 4 AfrRecurring-EurRecurring:** after the initial founding pulse of admixture, the admixed population receives a period of monotonically constant or decreasing recurring introgression from the African source, and, separately, a period of monotonically constant or decreasing recurring introgression from the European source.

671

672

673

674

675

676

677

678

679

For all scenarios, we consider demographic models corresponding to either a constant reproductive population size N_g between the founding event and the present, or, instead, a linear or hyperbolic increase between N_0 and N_{20} , depending on the values of N_0 , N_{20} , and u_N used for each simulation respectively.

680

681

682

Time for admixture pulses or time for the onset and offset of admixture periods are schematically represented as $t_{\text{Source},g}$. We define (73), $s_{\text{Afr},g}$, $s_{\text{Eur},g}$, and h_g as the proportion of parents of individuals in the admixed population at generation g coming from, respectively, the African source population, the European one, and the admixed population itself at the previous generation. Thus, for $g = 0$, $s_{\text{Afr},0} + s_{\text{Eur},0} = 1$, and for each value of g in $[1,20]$, $s_{\text{Afr},g} + s_{\text{Eur},g} + h_g = 1$. The number of “free” scenario-parameters drawn randomly in prior distributions set by the user for simulations and subsequent Approximate Bayesian Computation inferences is indicated below the name of each scenario respectively.

683

684

685

686

687

688

See **Table 2** for parameter prior distributions, and **Materials and Methods 7** for detailed descriptions of scenario-parameters.

689

690

691

692

Description	Scenario	Model parameter	Prior	Conditions
African admixture-pulse times	1, 2	$t_{Afr,p1}$ $t_{Afr,p2}$	Uniform [1, 20] in discrete generations, a range corresponding to between ~1485 and ~1960 in years CE	$t_{Afr,p1} > t_{Afr,p2}$
European admixture-pulse times	1, 3	$t_{Eur,p1}$ $t_{Eur,p2}$	Uniform [1, 20] in discrete generations, a range corresponding to between ~1485 and ~1960 in years CE	$t_{Eur,p1} > t_{Eur,p2}$
African admixture period start and end times	2, 4	$t_{Afr,t1}$ $t_{Afr,t2}$	Uniform [1, 20] in discrete generations, a range corresponding to between ~1485 and ~1960 in years CE	$t_{Afr,t1} > t_{Afr,t2}$
European admixture period start and end times	3, 4	$t_{Eur,t1}$ $t_{Eur,t2}$	Uniform [1, 20] in discrete generations, a range corresponding to between ~1485 and ~1960 in years CE	$t_{Eur,t1} > t_{Eur,t2}$
African admixture-pulse intensities	1, 2	$S_{Afr,tAfr,p1}$ $S_{Afr,tAfr,p2}$	Uniform [0, 1]	$S_{Afr,g} + S_{Eur,g} = 1 - h_g$, with h_g in [0,1]
European admixture-pulse intensities	1, 3	$S_{Eur,tEur,p1}$ $S_{Eur,tEur,p2}$	Uniform [0, 1]	
African admixture period intensity parameters	2, 4	$S_{Afr,tAfr,t1}$	Uniform [0, 1]	$S_{Afr,tAfr,t1} \geq S_{Afr,tAfr,t2}$
		$S_{Afr,tAfr,t2}$	Uniform [0, 1]	$S_{Afr,g} + S_{Eur,g} = 1 - h_g$, with h_g in [0,1]
		u_{Afr}	Uniform [0, 0.5]	
European admixture period intensity parameters	3, 4	$S_{Eur,tEur,t1}$	Uniform [0, 1]	$S_{Eur,tEur,t1} \geq S_{Eur,tEur,t2}$
		$S_{Eur,tEur,t2}$	Uniform [0, 1]	$S_{Afr,g} + S_{Eur,g} = 1 - h_g$, with h_g in [0,1]
		u_{Eur}	Uniform [0, 0.5]	
Admixture pulse at the foundation	1, 2, 3, 4	$S_{Afr,0}$	Uniform [0, 1]	$S_{Eur,0} = 1 - S_{Afr,0}$
Founding reproductive population size	1, 2, 3, 4	N_0	Uniform [10, 1000]	
Current reproductive population size	1, 2, 3, 4	N_{20}	Uniform [100, 100000]	$N_0 \leq N_{20}$
Steepness of the reproductive population size increase	1, 2, 3, 4	u_N	Uniform [0, 0.5]	

693
694
695
696
697

Table 2:
Prior distributions for the parameters of four competing scenarios for the admixture history of Cabo Verde islands.
Parameters are presented in **Figure 6** and described in **Materials and Methods 7**.

Summary Statistics for ABC inference		Number of statistics	Reference	
within population	Mean ASD within population H	1	(46)	
	Mean Heterozygosity (SNP by SNP) within population H	1	(74)	
	Variance Heterozygosity (SNP by SNP) within population H	1	(74)	
	Mean inbreeding F within population H	1	(75)	
	Variance inbreeding F within population H	1	(75)	
admixture pattern	Mode ASD-MDS African admixture proportions in population H	1	(45,73)	
	Mean ASD-MDS African admixture proportions in population H	1	(45,73)	
	Variance ASD-MDS African admixture proportions in population H	1	(45,73)	
	Skewness ASD-MDS African admixture proportions in population H	1	(45,73)	
	Kurtosis ASD-MDS African admixture proportions in population H	1	(45,73)	
	Min ASD-MDS African admixture proportions in population H	1	(45,73)	
	Max ASD-MDS African admixture proportions in population H	1	(45,73)	
	Deciles of ASD-MDS African admixture proportions in population H	9	(45,73)	
	Mode ASD-MDS "African-European angles" in population H	1	This study; Appendix 1-figure 2	
	Mean ASD-MDS "African-European angles" in population H	1	This study; Appendix 1-figure 2	
	Variance ASD-MDS "African-European angles" in population H	1	This study; Appendix 1-figure 2	
	Skewness ASD-MDS "African-European angles" in population H	1	This study; Appendix 1-figure 2	
	Kurtosis ASD-MDS "African-European angles" in population H	1	This study; Appendix 1-figure 2	
	Min ASD-MDS "African-European angles" in population H	1	This study; Appendix 1-figure 2	
	Max ASD-MDS "African-European angles" in population H	1	This study; Appendix 1-figure 2	
	Deciles of ASD-MDS "African-European angles" in population H	9	This study; Appendix 1-figure 2	
	between populations	FST(African Source - Population H)	1	(76)
		FST(European Source - Population H)	1	(76)
Mean ASD (African Source - Population H)		1	(46)	
Mean ASD (European Source - Population H)		1	(46)	
f3 (Population H ; European Source, African Source)		1	(50)	

698

699

700

701

702

703

Table 3:

Summary-statistics used for *MetHis*-machine-learning ABC inferences.

All 42 statistics were computed using the summary-statistics computation tool embedded in *MetHis* (45).

704 MetHis–Random Forest (RF)-ABC scenario-choices

705 Overall (**Figure 7B**), *MetHis*-RF-ABC scenario-choices indicate that multiple pulses of admixture from the
706 European and African source populations (after the founding admixture pulse, two independent admixture
707 pulses from both Africa and Europe: “Afr2Pulses-Eur2Pulses” scenarios, **Figure 6 – Scenario 1**), best explain
708 the genetic history of individuals born on six of nine Cabo Verdean islands. Furthermore, we find that even
709 more complex scenarios involving a period of recurring admixture from either source best explain the history
710 of the remaining three islands. Scenarios with periods of recurring admixture from both Africa and Europe
711 (“AfrRecurring-EurRecurring”, **Figure 6 – Scenario 4**) are the least favored across Cabo Verde.

712 RF-ABC cross-validation prior-errors for each of the 40,000 simulations used, in-turn, as pseudo-ob-
713 served data indicate a reasonably good, albeit not perfect, discriminatory power of the RF (**Appendix 1-figure**
714 **4A**). RF-ABC scenario-choices identify the correct scenario in the majority of cross-validations for most sce-
715 narios and most islands. Furthermore, asymmetrical scenarios are the least confused with one-another (AfrRe-
716 curring-Eur2Pulses vs Afr2Pulses-EurRecurring, or Afr2Pulses-Eur2Pulses vs AfrRecurring-EurRecurring).
717 As expected and previously shown empirically with *MetHis*-RF-ABC scenario-choice (45,77), these results
718 are consistent with increased assignation-errors in the parts of the parameter-space where the different scenar-
719 ios are highly nested and thus biologically equivalent. Finally (**Appendix 1-figure 4B**), the mean, variance,
720 skewness, kurtosis, minimum, and maximum of individual admixture proportions’ distributions are systemat-
721 ically among the most informative summary-statistics for RF-ABC scenario-choice in every island or in Cabo
722 Verde as a whole, consistently with theoretical expectations (45,73).

723 Finally, when considering all Cabo Verde-born individuals as a single random-mating population without
724 distinguishing birth-islands, our *MetHis*-RF-ABC scenario-choice identifies the Afr2Pulses-Eur2Pulses sce-
725 nario as the winning scenario (**Appendix 1-figure 4B**), thus consistent with the scenario most often found as
726 the winner among Cabo Verde islands considered as the target admixed population in nine separate *MetHis*-
727 RF-ABC analyses.

728 MetHis–Neural Network (NN)-ABC posterior parameter estimations

730 For individuals on each Cabo Verdean birth island separately, we performed NN-ABC joint posterior param-
731 eter estimation based on 100,000 *MetHis* simulations under the winning scenario (45): Afr2Pulses-Eur2Pulses
732 in Santiago, Fogo, Santo Antão São Nicolau, Brava, and Maio; Afr2Pulses-EurRecurring in Boa Vista and Sal;
733 and AfrRecurring-Eur2Pulses in São Vicente (**Figure 7B**). For each island separately, detailed posterior pa-
734 rameters’ distributions, Credibility Intervals (CI), and cross-validation errors are provided in **Figure 7-figure**
735 **supplement 1-3** and **Appendix 5-table 1-10**. We synthesized our results considering median point-estimates
736 and 50%-CI for each scenario parameter in the admixture history of each island in **Figure 7C-D**. We detailed
737 our results and discussion for admixture history inferences for each island separately in **Appendix 5**, in the
738 light of historical data about the peopling of Cabo Verde (**Figure 7-resource table 1**).

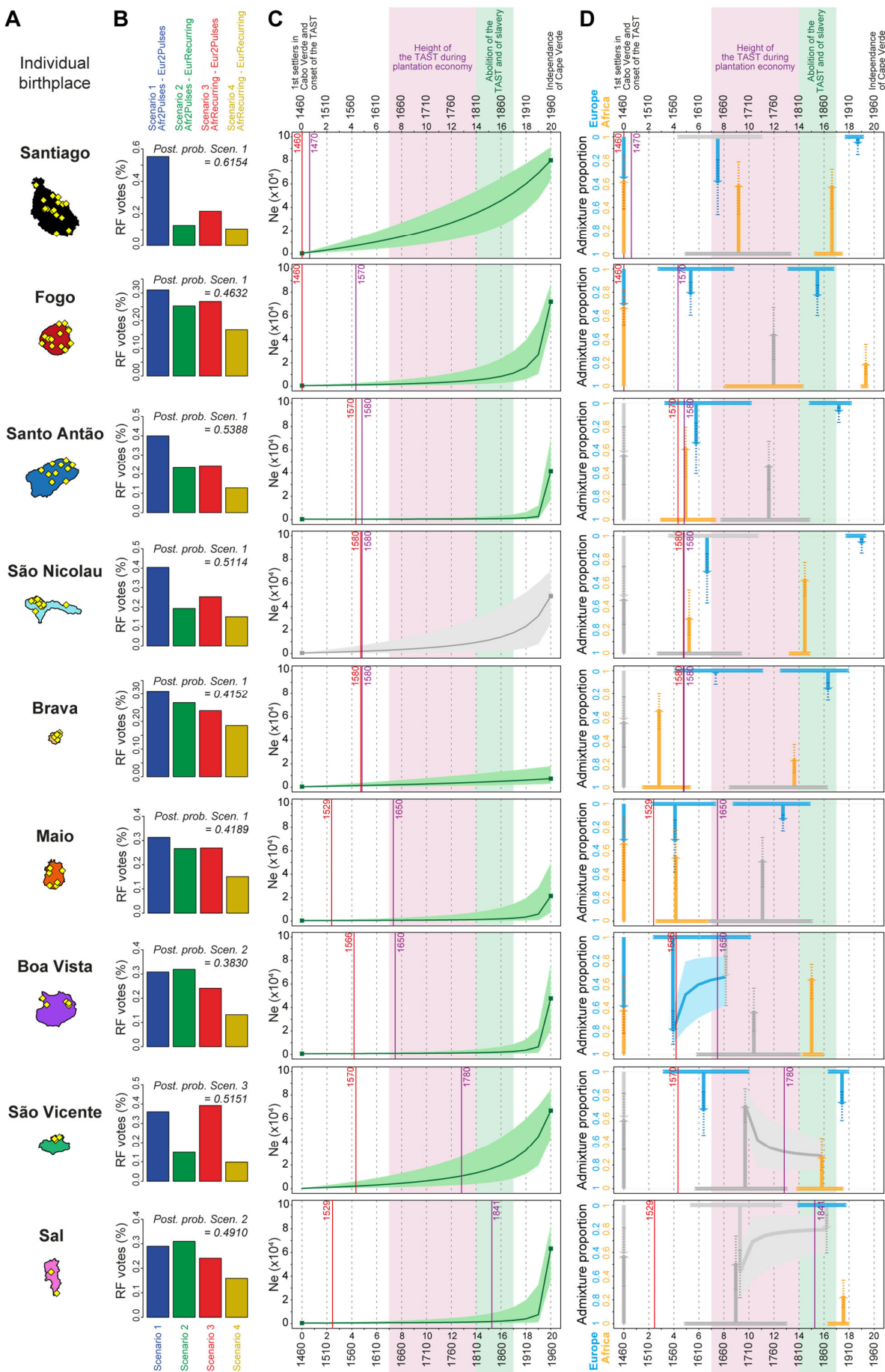
739 **Figure 7C** shows that the reproductive population size of Cabo Verde islands remained very low until a
740 strong increase in the last three generations for all islands but Santiago and Brava. In Santiago the population
741 expansion was more linear since the founding of Cabo Verde in the 1460’s, while the reproductive size of
742 Brava remained almost constant and low until today.

743 In summary, **Figure 7D** shows that European and African admixture events throughout the archipelago
744 occurred first during the early peopling history of each island, before the mid-17th century massive expansion
745 of the TAST due to the expansion of the plantation economy (1). We find that other admixture events from
746 Europe or Africa, or both, likely occurred much later during, or immediately after, the 19th century abolition
747 of the TAST and of slavery in European colonial empires. Altogether our *MetHis*-ABC results support limited
748 historical admixture having occurred in Cabo Verde during the most intense periods of the TAST between the

749 mid-17th and early 19th centuries. Furthermore, note that we find admixture events often earlier than, or con-
750 comitant with, the first perennial peopling of an island. For the islands of Santiago, Fogo, Santo Antão and, to
751 a lesser extent, São Nicolau, initial historical admixture events occurred synchronously to the first perennial
752 settlement of the island. For the islands of Brava, Maio, Boa Vista, and São Vicente, early admixture events
753 occurred long before their first perennial peopling, thus showing that their founding was already largely com-
754 posed of already admixed individuals. Importantly, note that our *MetHis*-NN-ABC posterior parameter infer-
755 ences cannot infer all scenario-parameters accurately, as some parameters hardly depart from their respective
756 priors (**Figure 7-figure supplement 1-3**), and the admixture history of the island of Sal remains overall poorly
757 inferred.

758 Interestingly, *MetHis*-NN-ABC posterior parameter inference results obtained for the 225 Cabo Verde-
759 born individuals grouped in a single random-mating population instead of separately for each island of birth,
760 are largely undifferentiated from their prior distributions, and have very wide CI and large cross-validation
761 errors, for all admixture-history parameters except for the two parameters associated with the most recent pulse
762 of admixture from the African source (**Figure 7-figure supplement 1-3; Appendix 5-table 10**). This contrasts
763 with the substantial number of informative posterior-parameter estimations obtained for all islands of birth
764 separately except Sal (**Figure 7, Figure 7-figure supplement 1-3; Appendix 5-table 1-9**), despite the much
765 smaller sample sizes used in each one of these separate analyses compared to the analysis considering Cabo
766 Verde as a single population. These results further show that the history of admixture substantially differs
767 across Cabo Verde islands and that considering the Cabo Verde archipelago as a single random mating popu-
768 lation is inadequate to successfully infer the parameters of its admixture history, consistently with our results
769 from ADMIXTURE, LAI, ROH and Isolation-By-Distance analyses.

770



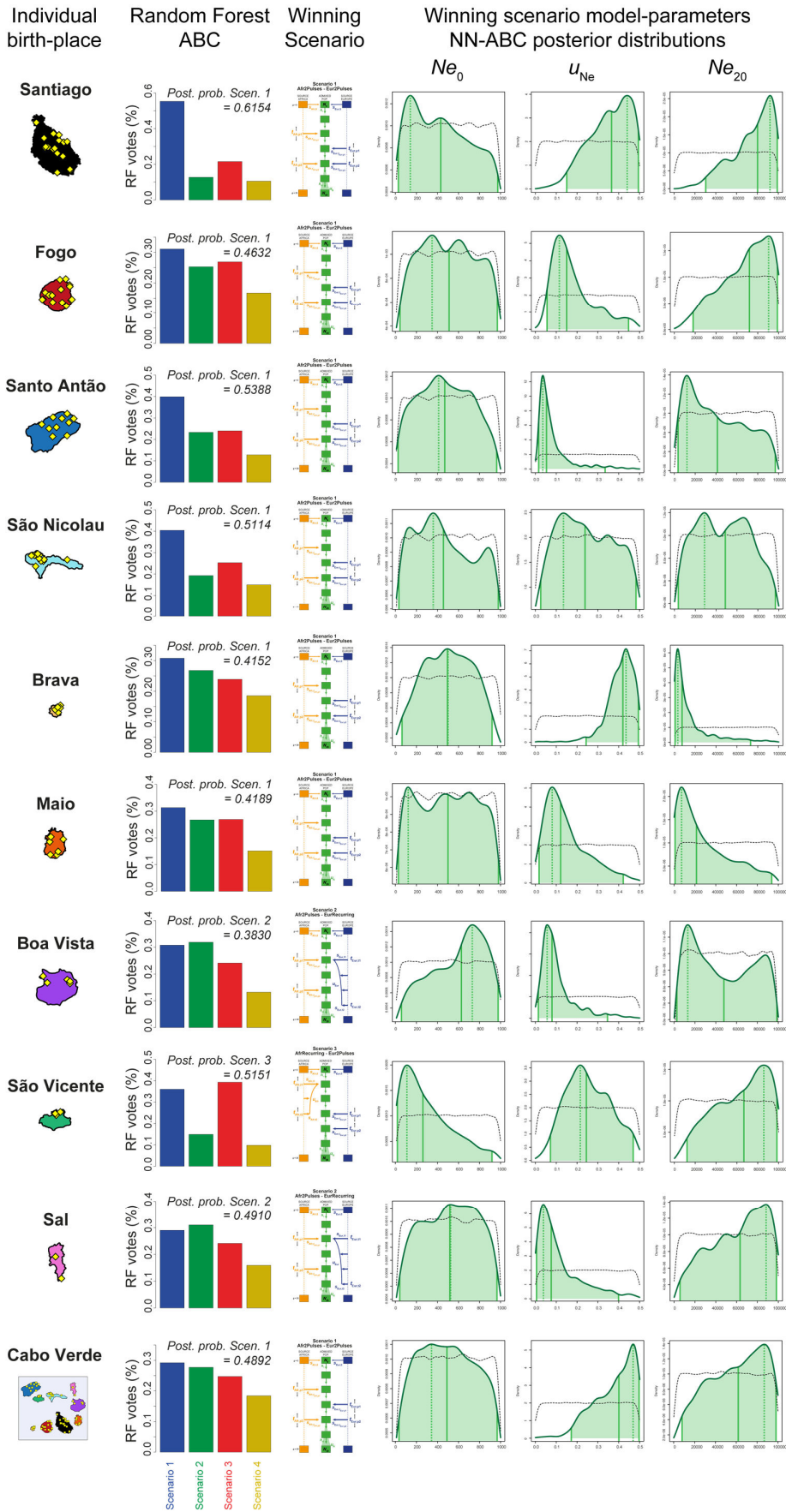
772 **Figure 7:**
773 **Genetic admixture histories of Cabo Verde islands inferred with *MetHis*-Approximate Bayesian Computation.**
774 Elements of the peopling-history of Cabo Verde islands are synthesized in **Figure 7-resource table 1**, stemming from historical work
775 cited therein. Islands are ordered from top to bottom in the chronological order of the first historical census perennially above 100
776 individuals within an island, indicated with the purple vertical lines. First historical records of the administrative, political, and religious,
777 settlement of an island are indicated with the red vertical lines.
778 **A)** Within-island birth-places of 225 Cabo-Verde-born individuals. **B)** *MetHis*-Random Forest-ABC scenario-choice vote results for
779 each island separately in histogram format. Posterior probabilities of correctly identifying a scenario if correct are indicated for the
780 winning scenario as “Post. prob. Scen.”, above each histogram. **C)** *MetHis*-Neural Network-ABC posterior parameter distributions
781 with 50% Credibility Intervals for the reproductive population size history of each birth-island separately. **D)** Synthesis of *MetHis*-NN-
782 ABC posterior parameter median point-estimates and associated 50%CI, for the admixture history of each island under the winning
783 scenario identified with RF-ABC in panel **B**. European admixture history appears in blue, African admixture history in orange. Hori-
784 zontal bars indicate 50%CI for the admixture time parameters, vertical arrows correspond to median admixture intensity estimates with
785 50%CI in dotted lines.
786 For **C)** and **D)**, posterior parameter distributions showing limited departure from their respective priors and large CI are greyed, as they
787 were largely unidentifiable in our ABC procedures. Detailed parameter posterior distributions, 95%CI, and cross-validation errors are
788 provided in **Figure 7-figure supplement 1-3** and **Appendix 5-table1-9**. Detailed results description for each island are provided in
789 **Appendix 5**.
790 **C-D)** The period between the 1630’s and the abolition of the TAST in the 1810’s, when most enslaved-Africans were deported from
791 Africa by European empires concomitantly to the expansion of the plantation economy (1,2), is indicated in light-pink. The period
792 between the abolition of the TAST in the 1810’s and the abolition of slavery enacted between 1856 and 1878 throughout the Portuguese
793 empire is indicated in light-green (25). The independence of Cabo Verde occurred in 1975.
794
795 **Figure 7-figure supplement 1:**
796 **Reproductive-size posterior parameter distributions and associated priors obtained with Neural Network ABC inference for**
797 **each island, and for the 225 Cabo Verde-born individuals grouped in a single random mating population “Cabo Verde”, sepa-**
798 **rately.**
799
800 **Figure 7-figure supplement 2:**
801 **African admixture histories posterior parameter distributions and associated priors obtained with Neural Network ABC in-**
802 **ference for each island, and for the 225 Cabo Verde-born individuals grouped in a single random mating population “Cabo**
803 **Verde”, separately.**
804
805
806 **Figure 7-figure supplement 3:**
807 **European admixture histories posterior parameter distributions and associated priors obtained with Neural Network ABC**
808 **inference for each island, and for the 225 Cabo Verde-born individuals grouped in a single random mating population “Cabo**
809 **Verde”, separately.**
810
811
812 **Figure 7-resource table 1: provided in .xls format**
813 **Historical landmark chronology for the peopling history of Cabo Verde as provided by previous historical work, respectively**
814 **for each island.**
815
816

817 **Figure 7-figure supplement 1:**

818 **Reproductive-size posterior parameter distributions and associated priors obtained with Neural Network ABC inference for**
819 **each island separately.**

820 We considered, for each island separately, and for all 225 Cabo Verde-born individuals grouped in a single random mating population
821 separately, Neural Network tolerance levels and number of neurons in the hidden layer, for each island and for Cabo Verde as a whole,
822 separately, are chosen based on posterior parameter cross-validation error minimization procedures conducted on 1,000 random simu-
823 lations used in-turn, as pseudo observed data (see **Appendix 1**, and **Appendix 1-table 1**). For each island and for Cabo Verde as a
824 whole, separately, posterior parameter distributions correspond to the solid lines and corresponding priors correspond to the dotted
825 black lines. Density distributions are based on the logit transformation of parameter values (see **Appendix 1**) using an Epanechnikov
826 kernel between the corresponding prior bounds. See **Results 7**, main **Discussion**, and **Appendix 5** for descriptions and discussions of
827 the results. Synthesis in **Figure 7**.

828

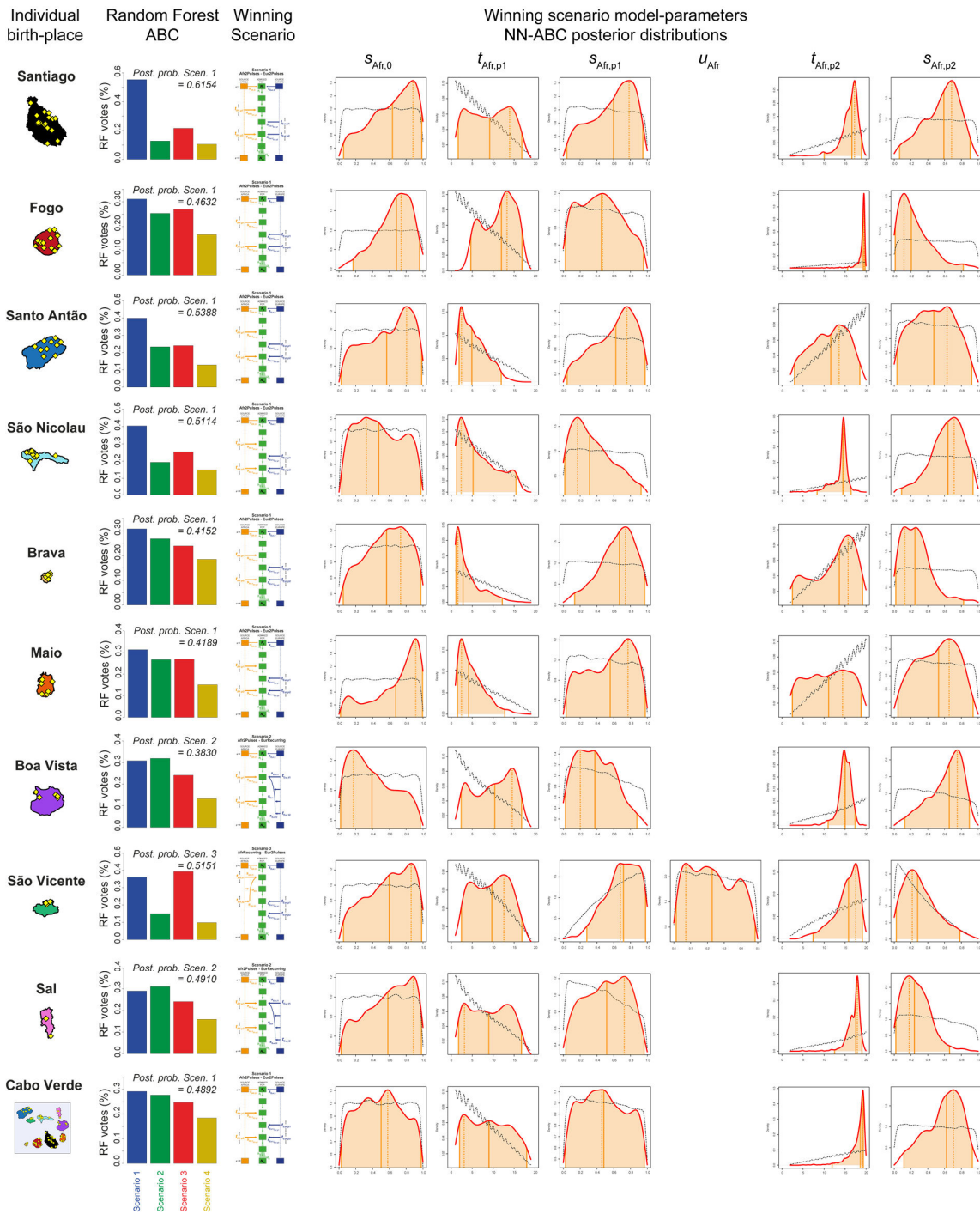


830 **Figure 7-figure supplement 2:**

831 **African admixture histories posterior parameter distributions and associated priors obtained with Neural Network ABC in-**
832 **ference for each island separately.**

833 We considered, for each island separately, and for all 225 Cabo Verde-born individuals grouped in a single random mating population
834 separately, Neural Network tolerance levels and number of neurons in the hidden layer, for each island and for Cabo Verde as a whole,
835 separately, are chosen based on posterior parameter cross-validation error minimization procedures conducted on 1,000 random simu-
836 lations used in-turn, as pseudo observed data (see **Appendix 1**, and **Appendix 1-table 1**). For each island and for Cabo Verde as a
837 whole, separately, posterior parameter distributions correspond to the solid lines and corresponding priors correspond to the dotted
838 black lines. Density distributions are based on the logit transformation of parameter values (see **Appendix 1**) using an Epanechnikov
839 kernel between the corresponding prior bounds. See **Results 7**, main **Discussion**, and **Appendix 5** for descriptions and discussions of
840 the results. Synthesis in **Figure 7**.

841

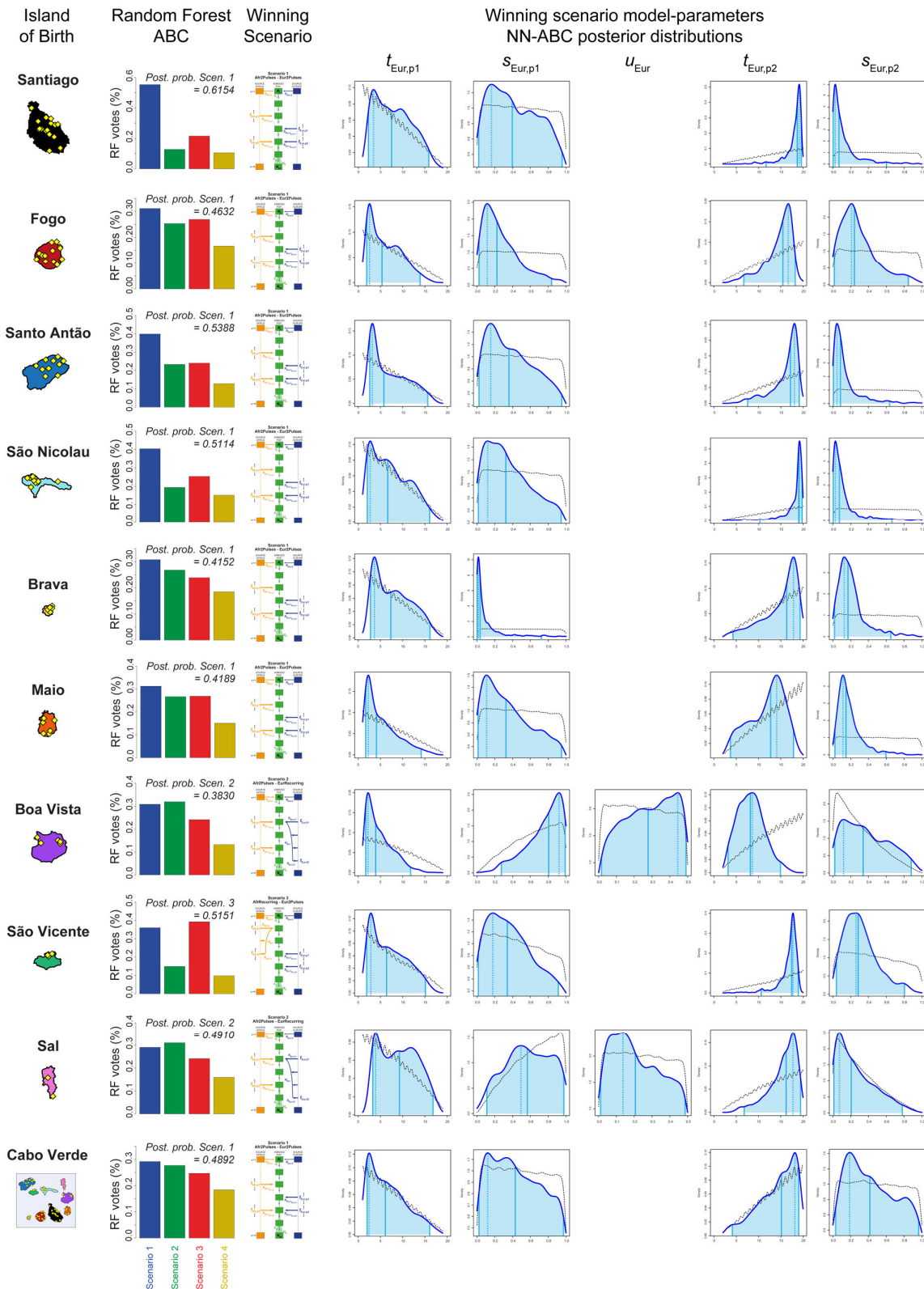


843 **Figure 7-figure supplement 3:**

844 **European admixture histories posterior parameter distributions and associated priors obtained with Neural Network ABC**
845 **inference for each island separately.**

846 We considered, for each island separately, and for all 225 Cabo Verde-born individuals grouped in a single random mating population
847 separately, 100,000 simulations computed under the winning scenario obtained with RF-ABC scenario-choice procedures and provided
848 on the left of the figure. Neural Network tolerance levels and number of neurons in the hidden layer, for each island and for Cabo
849 Verde as a whole, separately, are chosen based on posterior parameter cross-validation error minimization procedures conducted on
850 1,000 random simulations used in-turn, as pseudo observed data (see **Appendix 1**, and **Appendix 1-table 1**). For each island and for
851 Cabo Verde as a whole, posterior parameter distributions correspond to the solid lines and corresponding priors correspond to the dotted
852 black lines. Density distributions are based on the logit transformation of parameter values (see **Appendix 1**) using an Epanechnikov
853 kernel between the corresponding prior bounds. See **Results 7**, main **Discussion**, and **Appendix 5** for descriptions and discussions of
854 the results. Synthesis in **Figure 7**.

855



857 **DISCUSSION**

858

859 **Which African and European populations contributed genetically to Cabo Verde?**

860

861 *The genetic heritage of continental Africa in Cabo Verde*

862 Numerous enslaved-African populations from Western, Central, and South-Western Central Africa were forcibly deported during the TAST to both Cabo Verde and the Americas, as shown by historical demographic records (1,25). There is still extensive debate about whether enslaved-Africans remained or more briefly transited in Cabo Verde during the most intense period of the TAST, in the 18th and 19th centuries, when the archipelago served as a slave-trade platform between continents (25,78,79); the question of the duration of stay of enslaved individuals at a given location being also of major interest throughout the Americas during the TAST (18,37). In this context, previous genetic studies considering a relatively limited number of populations from mainland Europe and Africa, and/or limited numbers of Cabo Verdean islands of birth, suggested that mainly continental West Africans and South Europeans were at the root of Cabo Verde genetic landscape (3,23,34).

871 In this context, our genetic results favor scenarios where mostly certain West Western African Senegambian populations only (Mandinka and Wolof in our study) contribute to the genetic makeup of Cabo Verde (Figure 2-3). Other Western, Central, and South-Western African populations historically also forcibly deported during the TAST seem to have had very limited contributions to the genomic diversity of most Cabo Verde islands, and virtually no contribution to that of Brava, Fogo, and Santiago.

876 This could be due to Cabo Verde being only a temporarily waypoint for these latter enslaved-African populations between Africa, the Americas, and Europe, but would also be consistent with additional socio-historical processes (see below). Interestingly, and further echoing these genetic results, the Cabo Verdean Kriolu language carries specific signatures mainly from the Mande language-family, and Wolof and Temne languages from Western Africa, and largely more limited signatures of Kikongo and Kimbundu Bantu languages from Central and South-Western Africa (15,30).

882 These results contrast with the admixture patterns identified in other enslaved-African descendant populations in the Americas in our dataset (African-American and Barbadian, Figure 2-3), and in previous studies (3,4,10,38,80). Indeed, the origins of African ancestries in numerous populations throughout the Caribbean and the Americas traced to varied continental African regions, from Western to South-Western Africa, thus qualitatively consistent with the known diversity of slave-trade routes used between continents and within the Americas after the Middle Passage.

888

889 *The genetic heritage of continental Europe in Cabo Verde*

890 After the initial settlement of Cabo Verde by Portuguese migrants, temporary changes of European dominion in certain islands, newly developing commercial opportunities, and intense piracy during the 16th and 17th centuries have triggered different European populations to migrate to the archipelago (26,27,36).

893 Nevertheless, these latter historical events do not seem to have left a major signature in the genetic landscape of Cabo Verde (Figure 2-3). Instead, we find that Cabo Verdean-born individuals in our dataset share virtually all their European genetic ancestry with Iberian populations, with extremely limited evidence of contributions from other European regions, consistent with previous studies (3,23). Interestingly, the reduced diversity of European populations' contributions to the genomic landscape of Cabo Verde is also identified in other enslaved-African descendant populations in our study, as well as in previous studies in Caribbean and American populations (11,12,38). Our results thus show that European admixture in enslaved-African descendant populations on both sides of the Atlantic, as represented here by Cabo Verde, the Barbadians ACB and the African American ASW, mainly stem from the gene-pool of the European empires historically and socio-economically dominant locally, rather than subsequent European migrations (2).

902

903 Altogether, note that, in our local-ancestry inferences, we considered as reference source populations varied existing populations from continental mainland Africa and Europe, categorized as such from sampling information and geographic location only, prior to any genetic investigation. Therefore, in these analyses, we cannot disentangle the fraction of European admixture in Cabo Verdean genomes stemming directly from European migrations after the 1460's, from the fraction stemming from the European genetic legacy in continental African source populations acquired whether during more ancient migrations which occurred before the peopling of Cabo Verde (e.g. (81)), or since then during the European colonial expansion in Sub-Saharan Africa. Symmetrically, we cannot disentangle the fraction of African admixture in Cabo Verde stemming directly from continental Africa after the 1460's, from the fraction inherited from Africa-Europe admixture events that may have occurred in Europe prior to the peopling of Cabo Verde or during the colonial era until today. Disentangling both genetic heritages will require, in future studies, the explicit modelling of such possible admixture histories within African and European ancestral populations at the source of the Cabo Verde genetic landscape, and would also benefit from including data from North-African populations in our reference panels.

916

917 **Genetic and linguistic isolation-by-distance and recent demographic expansion in Cabo Verde**

918 A scenario of island peopling via a series of founding events followed by slow-growing population sizes and local isolation due to reduced genetic and linguistic parent-offspring dispersal would consistently explain the increasing differentiation of island-specific patterns with increasing values of K found with ADMIXTURE, ASD-MDS, and isolation-by-distance results (**Figure 2-5, Table 1**), as well as *MetHis*-ABC demographic inferences (**Figure 7C**).

924 Indeed, *MetHis*-ABC results (**Figure 7C**) show the long period of small relatively constant reproductive sizes until the very recent strong, hyperbolic, increases in most Cabo Verdean islands; with the notable exceptions of, *i*) the linear increase in Santiago, the political and commercial center of Cabo Verde throughout the colonial history of the archipelago, and *ii*) the relatively constant reduced reproductive sizes in Brava until today. Altogether, this result was expected as the dry Sahelian climate of Cabo Verde with scarcely accessible water resources, recurring famines and epidemic outbreaks, and the Portuguese crown maintaining a strong control over population movements within Cabo Verde, rendered difficult the perennial peopling of most islands (see **Figure 7-resource table 1** and references therein, **Appendix 5**). Furthermore, such demographic scenarios are also consistent with long-ROH patterns reflecting isolation on each Cabo Verdean islands, whereas elevated shorter ancestry-specific ROH patterns likely stemmed from admixture (**Figure 4**), similarly to our results in the ASW and ACB populations and as previously identified (61). Note, however, that while we explored and found, *a posteriori*, a different demographic regime for each Cabo Verde island separately, with constant, hyperbolic, or linear increases of reproductive sizes, we did not consider possible demographic bottlenecks which may also have occurred as a result of the difficult settlement history of Cabo Verde described above. Such possible bottleneck events will need to be explored in the future, a particularly challenging task given the extensive number of competing models to be considered and given that bottleneck intensities and duration parameters have to be co-estimated with admixture parameters over a very short history of 21 generations.

942 Investigating isolation-by-distance anchored in individual birth-places at a very reduced geographical scale (39–41) within a population and a language allowed us to reveal that effective dispersal from one generation to the next across Cabo Verde islands, and sometimes even within-islands, was surprisingly reduced compared to the large mobility self-reported by participants (**Figure 5, Table 1**). Patterns of parent-offspring dispersal at a very local scale ~50 km within populations has seldom been tested using genetics, to our knowledge, in human populations (39,42–44); although isolation-by-distance genetic patterns have been extensively explored to investigate serial founding events and migrations across human populations at varied

948

949 geographical scales, including in archipelagos contexts (20,63,64,82). Furthermore, while the geographic dis-
950 tribution of genetic admixture patterns have been explored at much larger geographical scales (e.g 55,78,79),
951 and in particular in enslaved-African descendant populations (11,12), isolation-by-distance patterns for inter-
952 individual differences of genetic admixture fractions at very reduced geographical scales have never been
953 reported to our knowledge.

954 We also found substantial signals of isolation-by-distance among Kriolu idiolects (i.e. individual manners
955 of uttering Cabo Verdean Kriolu), also anchored in individual birth-places (**Figure 5, Table 1**), thus showing
956 striking parallels between the history of biological and cultural dispersal and isolation in Cabo Verde at a
957 micro-geographical scale. Our results show that linguistic admixture patterns were isolated-by-distance within
958 the archipelago, similarly to genetic admixture patterns, which was previously unsuspected in both genetics
959 and linguistic studies of Cabo Verde (15,23,29,34).

960 Altogether, these joint genetic-linguistic patterns highlight the limited effective genetic and linguistic dis-
961 persal from one generation to the next within Cabo Verde, including for genetic and linguistic admixture levels,
962 despite extended mobility of individuals within the archipelago. Both mechanisms may thus underline indi-
963 vidual linguistic identity construction processes and the genetic relative isolation across and within Cabo Verd-
964 ean islands.

965 Importantly, we considered only random mating processes in our inferences and interpretations. However,
966 the almost complete lack of identifiability of the admixture-history parameters obtained when considering
967 Cabo Verde as a single random-mating population in our ABC inferences (**Figure 7-figure supplement 1-3,**
968 **Appendix 5-table 1-9**), and our ROH results together with recent work (85), altogether suggest that non-
969 random mating processes significantly influenced Cabo Verdean genetic patterns. Therefore, future studies
970 will need to evaluate how possible deviations from random-mating in Cabo Verde, such as assortative mating
971 (85,86), may have influenced our results and interpretations. Note that this is a conceptually particularly chal-
972 lenging task in a small census-size population with strong marital stratification where mate-choices have been,
973 by definition, limited during most of the TAST (87). Nevertheless, such complex processes may also underlie
974 the joint genetic-linguistic isolation-by-distance patterns anchored in birth-place distances here observed for
975 both diversity and admixture patterns; and would also explain that genetic and linguistic histories of admixture
976 apparently occurred in parallel in Cabo Verde.

977

978 **Histories of genetic admixture in Cabo Verde**

979 *Early admixture in Cabo Verde, limited admixture during the plantation economy era*

980 While we expected recurring African admixture processes due to the known history of regular forced migra-
981 tions from Africa during most of Cabo Verde history (25), our *MetHis*-ABC scenario-choices indicate that,
982 qualitatively, these demographic migrations did not necessarily translate into clearly recurring gene-flow pro-
983 cesses to shape genetic patterns in most of Cabo Verde islands (**Figure 7B**). Indeed, African admixture pro-
984 cesses in all islands, except São Vicente, seem to have occurred during much more punctual periods of Cabo
985 Verdean history. Our *MetHis*-ABC posterior parameter estimations further highlighted often largely differing
986 admixture histories across Cabo Verde islands (**Figure 7C-D** and **Appendix 5**).

987 We find that admixture from continental Europe and Africa occurred first early during the TAST history,
988 concomitantly with the successive settlement of each Cabo Verdean island between the 15th and the early 17th
989 centuries (**Figure 7D**). Furthermore, we find that the most intense period of enslaved-African deportations
990 during the TAST via Cabo Verde, between the mid-17th and early-19th centuries during the expansion of the
991 plantation economic system in the Americas and Africa (1,25–27), seem to have left a limited signature in the
992 admixture patterns of most Cabo Verdean islands today. Interestingly, previous studies also highlighted that
993 admixture in enslaved-African descendants in the Caribbean may have occurred first early in the European
994 colonial expansion in the region in the 16th century, and then much later towards the end of the TAST at the

995 end of the 18th century, and had thus been relatively limited during most of the plantation economy era (11,88).
996 Together with our results, this illustrates the apparent discrepancy between intense demographic forced migra-
997 tions during the TAST and genetic admixture signatures at least in certain populations on both sides of the
998 Atlantic. Indeed, in contrast with these results, numerous other enslaved-African populations in the Americas
999 have, instead, shown substantial historical admixture inferred to have occurred during the plantation economy
1000 era, hence exemplifying the diversity of admixture histories experienced locally by enslaved-Africans descend-
1001 ant populations during the TAST (4,12).

1002 The inferred lack of admixture events in Cabo Verde during the height of the TAST could be due to newly
1003 deported enslaved-Africans being only transiting via Cabo Verde before being massively re-deported to other
1004 European colonies during this era (25,78,79). Furthermore, and not mutually exclusive with this latter hypoth-
1005 esis, historians reported, in Cabo Verde and other European colonies in the Americas, that relationships be-
1006 tween enslaved and non-enslaved communities largely changed with the expansion of plantation economy at
1007 the end of the 17th century. These changes are often referred to as the shift from Societies-with-Slaves to Slave-
1008 Societies (1,19,89). Slave-Societies legally enforced the socio-marital and economic segregation between com-
1009 munities, and coercively controlled relationships between new enslaved-African migrants and pre-existing en-
1010 slaved-African descendant communities more systematically and violently than Societies-with-Slaves (19)^{p.15-}
1011 ^{46,95-108,(25)^{p.281-319}}. The high prevalence of segregation during the height of the plantation economy could have
1012 limited genetic admixture between enslaved-African descendants and non-enslaved communities of European
1013 origin, as well as admixture between new migrants, forced or voluntary, and pre-existing Cabo Verdeans;
1014 notwithstanding the known history of dramatic sexual abuses during and before this era. This could consist-
1015 ently explain our observations of a relative lack of diverse African or European origins in Cabo Verdean ge-
1016 nomes despite the known geographical diversity of populations deported and emigrated to the archipelago
1017 throughout the TAST. Furthermore, with legally enforced segregation, we might expect more marital pairings
1018 than before to occur among individuals with common origins; i.e. between two individuals with the same
1019 continental African or European origin. Such ancestry-specific marriages triggered by socio-cultural segrega-
1020 tion would be consistent with our ROH patterns (**Figure 4**), also depending on how long such mate-choice
1021 behaviors persisted after the end of legal segregation. We note, however, that we have not formally tested this
1022 influence on ROH and ancestry patterns and that a careful consideration of alternate explanations, such as
1023 temporally varying admixture contributions over time or a severe bottleneck in one of the ancestral populations,
1024 would be important to consider in such future analyses.

1025 In this context, the diversified African ancestries here found in the Americas (**Figure 2-3**), consistently
1026 with previous studies showing admixture events occurring before or during the height of plantation economy
1027 in the Americas (3,4,12), would suggest that the gene-pool of enslaved-Africans communities admixing with
1028 Europeans in the Americas since the 16th century often involved, at a local scale, multiple African source
1029 populations, thus reflecting the multiple slave-trade routes between continents and within the Americas. Con-
1030 versely in Cabo Verde, the early onset of the TAST during the 15th century likely privileged commercial routes
1031 with nearby Senegambia (25)^{p.31-54,281-319}, thus favoring almost exclusively admixture events with individuals
1032 from this region and from certain populations only. Altogether, our results in Cabo Verde contrasting with
1033 certain other enslaved-African descendant populations in the Americas, highlight the importance of early ad-
1034 mixture processes and socio-cultural constraints changes on intermarriages throughout the TAST, which likely
1035 durably influenced genomic diversities in descendant populations locally, on both sides of the Atlantic.

1036 1037 Admixture in Cabo Verde after the abolition of the TAST and of Slavery

1038 Finally, we find that recent European and African admixture in Cabo Verde occurred mainly during the
1039 complex historical transition after the abolition of the TAST in European colonial empires in the 1800's and
1040 the subsequent abolition of slavery between the 1830's and the 1870's (**Figure 7D**). Historians have showed

1041 that these major historical shifts strongly disrupted pre-existing segregation systems between enslaved and
1042 non-enslaved communities (1)^{p.271-290}, (25)^{p.335-362}, (90). In addition, an illegal slave-trade flourished during this
1043 era, bringing numerous enslaved-Africans to Cabo Verde outside of the official routes (25)^{p.363-384}. Altogether,
1044 our results indicate increased signals of European and African admixture events in almost every island of Cabo
1045 Verde during this period, and were thus consistent with a change of the social constraints regarding admixture
1046 and forced displacements of enslaved-descendants that had prevailed over the preceding 200 years of the TAST.
1047 These results were largely consistent with previous studies elsewhere in the Caribbean (11,88), and Central
1048 and South America (4,38); showing, at a local scale, the major influence of this recent and global socio-histor-
1049 ical change in inter-community relationships in European colonial empires on either sides of the ocean.

1050

1051 **Perspectives**

1052 Altogether, our results highlight both the unity and diversity of the genetic peopling and admixture histories
1053 of Cabo Verde islands, the first colony peopled by Europeans in Sub-Saharan Africa, resulting from the soci-
1054 ocultural and historical complexity of the Trans-Atlantic Slave Trade and European colonial expansions since
1055 the 15th century. Our results obtained at a micro-geographical scale reveal the fundamental importance of the
1056 early TAST history, before the expansion of the plantation economy, in durably shaping the genomic and
1057 cultural diversities of enslaved-African descendant populations in both Africa and the Americas.

1058 Importantly, we considered only the genome-wide autosomal admixture history of Cabo Verde in this
1059 study, and therefore did not explore possible sex-biased admixture processes. However, previous studies
1060 demonstrated the strong sex-biased admixture processes involved in Cabo Verde using sex-specific genetic
1061 markers (32,33), similarly as in other enslaved-African descendant populations in the Americas (2). Further-
1062 more, previous theoretical work considering sex-specific mechanistic admixture models showed that sex-bi-
1063 ased admixture processes may possibly bias historical inferences based only on autosomal data (91). It will
1064 thus be important, in future studies, to explore how this sex-biased admixture history may have influenced the
1065 ABC inferences here conducted; for instance, via sex-specific developments of *MetHis*-ABC.

1066 Future work will need to formally test the serial-founder hypothesis here proposed to be at the root of the
1067 observed genetic and linguistic patterns within Cabo Verde, and thus compare the numerous possible routes
1068 for such a peopling history across islands within the archipelago. In particular, it will be of interest to investi-
1069 gate, then, the series of bottlenecks concomitant to each genetic and linguistic founding event; a much needed
1070 but challenging task considering the very recent history of the archipelago founded only 21 generations ago,
1071 and the historically-known small census sizes echoed in the relatively small reproductive sizes here identified
1072 in almost every island until the 20th century.

1073 Our novel results together with their methodological limitations massively beg for future work further
1074 complexifying the admixture models here considered, as well as incorporating other summary-statistics such
1075 as admixture-LD and sex-specific statistics. This will allow to further dissect the admixture processes that gave
1076 birth to enslaved-African descendant populations, on both sides of the Atlantic.

1077

1078

1079 MATERIALS AND METHODS

1080

1081 **1. Cabo Verde genetic and linguistic datasets**

1082 We conducted joint sampling of anthropological, genetic, and linguistic data in Cabo Verde with the only
1083 inclusion criteria that volunteer-participants be healthy adults with Cabo Verdean citizenship and self-report-
1084 ing speaking Kriolu (23). Between 2010 and 2018, six interdisciplinary sampling-trips were conducted to in-
1085 terview 261 participants from more than thirty interview-locations throughout the archipelago (**Figure 1**).

1086

1087 **1.a. Familial anthropology and geography data**

1088 The 261 Cabo Verdean individuals were each interviewed to record a classical familial anthropology question-
1089 naire on self-reported life-history mobility. In particular, we recorded primary residence location, birth location,
1090 parental and grand-parental birth and residence locations, and history of islands visited in Cabo Verde and
1091 foreign experiences (23). Furthermore, we also recorded age, sex, marital status, and cumulative years of
1092 schooling and higher education (for 211 individuals only), and languages known and their contexts of use.

1093 GPS coordinates for each reported location were acquired on site during field-work, supplemented by
1094 paper maps and Google Earth™ for non-Caboverdean locations and islands that we did not visit (Sal and Maio).
1095 While participants' birth-locations were often precise, increasing levels of uncertainty arose for the reported
1096 parental and grand-parental locations. We arbitrarily assigned the GPS coordinates of the main population
1097 center of an island when only the island of birth or residence could be assessed with some certainty by partic-
1098 ipants. All other uncertain locations were recorded as missing data. Figure maps were designed with the
1099 software *QuantumGIS* v3.10 "București" and using Natural Earth free vector and raster map data
1100 (<https://www.naturalearthdata.com>).

1101

1102 **1.b. Genome-wide genotyping data**

1103 The 261 participants each provided 2mL saliva samples collected with DNAGenotek™ OG-250 kits, and com-
1104 plete DNA was extracted following manufacturer's recommendations. DNA samples were genotyped using
1105 an Illumina HumanOmni2.5Million-BeadChip genotyping array following manufacturer's instructions. We
1106 followed the quality-control procedures for genotypic data curation using Illumina's GenomeStudio® Geno-
1107 typing Module v2.0 described in (23). Genotype-calling, population-level quality-controls, and merging pro-
1108 cedures are detailed in **Appendix 1-figure 1**.

1109 In summary, we extracted a preliminary dataset of 259 Cabo Verdean Kriolu-speaking individuals, in-
1110 cluding relatives, genotyped at 2,118,835 polymorphic di-allelic autosomal SNPs genome-wide. We then
1111 merged this dataset with 2,504 worldwide samples from the 1000 Genomes Project Phase 3 (92); with 1,307
1112 continental African samples from the African Genome Variation Project (93) (EGA accession number
1113 EGAD00001000959); and with 1,235 African samples (7) (EGA accession number EGAS00001002078). We
1114 retained only autosomal SNPs common to all data sets, and excluded one individual for each pair of individuals
1115 related at the 2nd degree (at least one grand-parent in common) as inferred with KING (94), following previous
1116 procedures (23).

1117 After merging all datasets (**Appendix 1-figure 1**), we considered a final working-dataset of 5,157 world-
1118 wide unrelated samples, including 233 unrelated Cabo Verdean Kriolu-speaking individuals, of which 225
1119 were Cabo-Verde-born, genotyped at 455,705 autosomal bi-allelic SNPs (**Figure 1; Figure 1-resource table**
1120 **1**). Note that, for this working-dataset, the fraction of missing genotypes was very low and equaled 7.0×10^{-4}
1121 on average within Cabo Verdean islands of birth ($SD = 3.0 \times 10^{-4}$ across islands).

1122

1123 **1.c. Individual utterances of Kriolu**

1124 We collected linguistic data for each of the 261 Cabo Verdean individuals using anthropological linguistics
1125 questionnaires, and semi-directed interviews. Each participant was shown a brief (~6 min) speech-less movie,
1126 “*The Pear Story*” (95), after which they were asked to narrate the story as they wanted in “the Kriolu they
1127 speak every day at home”. Discourses were fully recorded without interruption, whether individuals’ dis-
1128 courses were related to the movie or not. Then each discourse was separately fully transcribed using the ortho-
1129 graphic convention of the Cabo Verdean Kriolu official alphabet “Alfabeto Unificado para a Escrita da Língua
1130 Cabo-verdiana (ALUPEC)” (Decreto-Lei nº 67/98, 31 de Dezembro 1998, I Série nº 48, Sup. B. O. da
1131 República de Cabo Verde).

1132 Building on the approach of (23), we were interested in inter-individual variation of “ways of speaking
1133 Kriolu” rather than in a prescriptivist approach to the Kriolu language. Thus, we considered each utterance as
1134 defined in (96)^{p.107}: “a particular instance of actually-occurring language as it is pronounced, grammatically
1135 structured, and semantically interpreted in its context”. Transcripts were parsed together and revealed 4831
1136 ($L=4831$) unique uttered items among the 92,432 uttered items transcribed in total from the 225 discourses
1137 from the genetically-unrelated Cabo Verde-born individuals. To obtain these counts, we considered phonetic,
1138 morphological, and syntactic variation of the same lexical root items that were uttered/pronounced differently,
1139 and we excluded from the utterance-counts onomatopoeia, interjections, and names. Note that we were here
1140 interested in the diversity of realizations in the Kriolu lexicon, including within the same individuals. In other
1141 words, we are interested in both between-speaker and within-speaker variation. Also note that a very limited
1142 number of English words were pronounced by particular individuals (10 utterances each occurring only once),
1143 and were kept in utterance-counts.

1144

1145 **1.d. Individual Kriolu utterance frequencies**

1146 The list of unique uttered items was then used to compute individual’s specific vectors of uttered items’ relative
1147 frequencies as, for each genetically unrelated Cabo Verde-born individual i (in $[1, 225]$) and each unique ut-
1148 tered item l (in $[1, L=4831]$), $f_{i,l} = n_{i,l} / \sum_{j=1}^L n_{i,j}$, where $n_{i,l}$ is the absolute number of times individual i uttered
1149 the unique item l over her/his entire discourse, f_i being the vector $(f_{i,1}, f_{i,2}, \dots, f_{i,L})$. We compared vectors of
1150 individuals’ utterance-frequencies by computing the inter-individual pairwise Euclidean distance matrix as,

1151 for all pairs of individuals i and j , $d(f_i, f_j) = \sqrt{\sum_{l=1}^L (f_{i,l} - f_{j,l})^2}$ (23).

1152

1153 **1.e. African origin of Kriolu utterances**

1154 We categorized each of the 4831 unique uttered items separately into five linguistic categories (23). Category
1155 A included only unique utterances directly tracing to a known African language and comprised 88 unique
1156 items occurring 3803 times out of the 92,432 utterances. Category B included only items with a dual African
1157 and European etymology, i.e. items of a European linguistic origin strongly influenced in either meaning,
1158 syntax, grammar, or form by African languages or vice versa, attesting to the intense linguistic contacts at the
1159 origins of Cabo Verdean Kriolu, and comprised 254 unique items occurring 6960 times. Category C included
1160 4432 items (occurring 73,799 times) with strictly Portuguese origin and not carrying identifiable traces of
1161 significant African linguistic origin or influence. Category D included 26 items occurring 6762 times with
1162 potential, not attested by linguists, traces of African languages’ phonetic or morphologic influences. Finally,
1163 Category U included the 10 English utterances occurring 10 times and the 21 unique Kriolu utterances occur-
1164 ring 1089 times of unknown origin as they could not be traced to African or European languages.

1165 Following (23), we defined an “African-utterances score” based, conservatively, on the utterance frequen-
1166 cies obtained separately for items in Category A, Category B, and merging Categories A and B, as, for indi-
1167 vidual i and the set of utterances in each category denoted Cat (in [A; B; A&B]), $Z_{i,Cat} = \sum_{l=1}^{L_{Cat}} f_{i,l}$, with L_{Cat}
1168 the number of uttered items in the corresponding category, and $f_{i,l}$ defined as previously.

1169

1170 **2. Population genetics descriptions**

1171

1172 **2.a. Allele Sharing Dissimilarities, Multidimensional Scaling, and ASD-MDS admixture estimates**

1173 We calculated pairwise Allele Sharing Dissimilarities (46) using the *asd* software (v1.1.0a;
1174 <https://github.com/szpiech/asd>), among the 5,157 individuals in our worldwide dataset (**Figure 1; Figure 1-**
1175 **resource table 1**), using 455,705 autosomal SNPs, considering, for a given pair of individuals, only the SNPs
1176 with no missing data. We then projected this dissimilarity matrix in three dimensions with metric Multidimen-
1177 sional Scaling using the *cmdscale* function in R (97). We conducted successive MDS analyses on different
1178 individual subsets of the original ASD matrix, by excluding, in turn, groups of individuals and recomputing
1179 each MDS separately (**Appendix 2-figure 1-4; Figure 2-figure supplement 1**). Lists of populations included
1180 in each analysis can be found in **Figure 1-resource table 1**. 3D MDS animated plots in *gif* format for **Figure**
1181 **2, Figure 2-figure supplement 1, and Appendix 2-figure 1-4** were obtained with the *plot3d* and *movie3d*
1182 functions from the R packages *rgl* and *magick*.

1183 Recently admixed individuals are intuitively expected to be at intermediate distances between the clusters
1184 formed by their putative proxy source populations on ASD-MDS two-dimensional plots. A putative estimate
1185 of individual admixture rates can then be obtained by projecting admixed individuals orthogonally on the line
1186 joining the respective centroids of each proxy-source populations and, then, calculating the distance between
1187 the projected points and either centroid, scaled by the distance between the two centroids (**Appendix 1-figure**
1188 **2; (45,98)**). We estimated such putative individual admixture rates in Cabo Verdean, ASW, and ACB individ-
1189 uals, considering sets of individuals for the putative proxy-source populations identified visually and resulting
1190 from our ASD-MDS decomposition (**Appendix 2**).

1191

1192 **2.b. ADMIXTURE-CLUMPP-DISTRUCT and f_3 -admixture analyses**

1193 Based on ASD-MDS explorations, we focused on the genetic structure of individuals born in Cabo Verde
1194 compared to that of other admixed populations related to TAST migrations. Therefore, we conducted ADMIX-
1195 TURE analyses (48) using 1,100 individuals from 22 populations: four from Europe, 14 from Africa, the USA-
1196 CEU, the African-American ASW, the Barbadian-ACB populations, and the North Chinese-CHB population
1197 as an outgroup (**Figure 1-resource table 1**). To limit clustering biases due to uneven sampling, we randomly
1198 resampled without replacement 50 individuals, once, for each one of these 22 populations. Furthermore, we
1199 also included all 44 Angolan individuals from four populations in the analyses, as no other samples from the
1200 region were available in our dataset. In addition to the 1,100 individuals hence obtained, we included the 225
1201 Cabo Verde-born individuals.

1202 Following constructor recommendations, we pruned the initial 455,705 SNPs set for low LD using *plink*
1203 (99) function *--indep-pairwise* for a 50 SNP-window moving in increments of 10 SNPs and a r^2 threshold of
1204 0.1. We thus conducted all subsequent ADMIXTURE analyses considering 1,369 individuals genotyped at
1205 102,543 independent autosomal SNPs.

1206 We performed 30 independent runs of ADMIXTURE for values of K ranging from 2 to 15. For each value
1207 of K separately, we identified groups of runs providing highly similar results (ADMIXTURE “modes”), with
1208 Symmetric Similarity Coefficient strictly above 99.9% for all pairs of runs within a mode, using CLUMPP
1209 (100). We plotted each modal result comprising two ADMIXTURE runs or more, for each value of K sepa-

1210 rately, using DISTRUCT (101). We evaluated within-population variance of individual membership propor-
1211 tions as F_{st}/F_{st}^{max} values using FSTruct (102) with 1000 Bootstrap replicates per population, for the ADMIX-
1212 TURE mode result at $K=2$ (**Figure 3-figure supplement 1**).

1213 Finally, we computed, using ADMIXTOOLS (50,103), f_3 -admixture tests considering as admixture tar-
1214 gets each Cabo Verdean birth-island, the ASW, and the ACB separately, with, as admixture sources, in turn
1215 all 108 possible pairs of one continental European population (Source 1) and one continental African popula-
1216 tion (Source2), or the East Asian CHB (Source1) and one continental African population (Source2). For all
1217 tests we used the same individuals, population groupings, and genotyping dataset as in the previous ADMIX-
1218 TURE analyses (**Figure 3-figure supplement 2**), and considered the no-inbreeding option in ADMIXTOOLS.

1219

1220 **3. Local-ancestry inferences**

1221 To identify all populations sharing a likely common ancestry with the Cabo Verdean, ASW or ACB individuals
1222 in our dataset using local-ancestry haplotypic inferences, we considered the same sample-set as for the AD-
1223 MIXTURE analysis (**Figure 1-resource table 1**), including all 455,705 SNPs from the merged dataset.

1224

1225 *Phasing with ShapeIT2*

1226 We first phased individual genotypes using SHAPEIT2 (57) for the 22 autosomal chromosomes separately
1227 using the joint Hap Map Phase 3 Build GRCh38 genetic recombination map (104). We considered default
1228 parameters using phasing windows of 2Mb and 100 states per SNP. We considered by default 7 burn-in itera-
1229 tions, 8 pruning iterations, 20 main iterations, and missing SNPs were imputed as monomorphic. Finally, we
1230 considered a “Ne” parameter of 30,000, and all individuals were considered unrelated.

1231

1232 *Chromosome painting with ChromoPainter2*

1233 We determined the possible origins of each Cabo Verdean, ASW, and ACB individual pair of phased haplo-
1234 types among European, African, USA-CEU, and Chinese-CHB populations using CHROMOPAINTER v2
1235 (56) with the same recombination map used for phasing. Following authors’ recommendations, we conducted
1236 a first set of 10 replicated analyses on a random subset of 10% of the individuals for chromosomes 2, 5, 12,
1237 and 19, which provided a posteriori $Ne=233.933$ and $\theta=0.0004755376$, on average by chromosome weighted
1238 by chromosome sizes, to be used in the subsequent analysis. We then conducted a full CHROMOPAINTER
1239 analysis using these parameters to paint all individuals in our dataset, in turn set as Donor and Recipient, except
1240 for Cabo Verde, ACB, and ASW individuals set only as Recipient. Finally, we combined painted chromosomes
1241 for each individual in the Cabo Verdean, ASW, and ACB population, separately.

1242

1243 *Estimating possible source populations for the Cabo Verde gene-pool using SOURCEFIND*

1244 We used CHROMOPAINTER results aggregated for each Cabo Verdean, ACB, and ASW individual sepa-
1245 rately and conducted two SOURCEFIND (58) analyses using all other populations in the dataset as a possible
1246 source, separately for four or six possible source populations (“surrogates”), to allow *a priori* for symmetric
1247 or asymmetric numbers of African and European source populations for each target admixed population. We
1248 considered 400,000 MCMC iteration steps (including 100,000 burn-in) and kept only one MCMC step every
1249 10,000 steps for final likelihood estimation. Each individual genome was divided in 100 slots with possibly
1250 different ancestry, with an expected number of surrogates equal to 0.5 times the number of surrogates, for each
1251 SOURCEFIND analysis. We aggregated results obtained for all individuals in the ACB, ASW, and each Cabo
1252 Verdean birth-island, separately. We present the highest likelihood results across 20 separate iterations of the
1253 SOURCEFIND analysis in **Figure 3B**. The second-best results were highly consistent and thus not shown.

1254

1255 **4. Runs of homozygosity (ROH)**

1256

1257 **4.a. Calling ROHs**

1258 Considering the same sample and SNP set as in the above local-ancestry analyses (**Figure 1-resource table**
1259 **1**), we called ROH with GARLIC (105). For each population separately, we ran GARLIC using the weighted
1260 logarithm of the odds (wLOD) score-computation scheme, with a genotyping-error rate of 10^{-3} (a likely
1261 overestimate), and using the same recombination map as for phasing, window sizes ranging from 30 to 90
1262 SNPs in increments of 10 SNPs, 100 resampling to estimate allele frequencies, and all other GARLIC
1263 parameters set to default values. We only considered results obtained with a window size of 40 SNPs, which
1264 was the largest window size associated with a bimodal wLOD score distribution and a wLOD score cutoff
1265 between the two modes, for all populations.

1266 For each population and Cabo Verdean island separately, we considered three classes of ROH that
1267 correspond to the approximate time to the most recent common ancestor of the IBD haplotypes, which can be
1268 estimated from the equation $g=100/2l$, where l is the ROH length in cM and g is the number of generations to
1269 the most recent common ancestor of the haplotypes (59). Short ROH are less than 0.25cM, reflecting
1270 homozygosity of haplotypes from more than 200 generations ago; medium ROH are between 0.25cM and 1cM
1271 reflecting demographic events having occurred between approximately 200 and 50 generations ago; and long
1272 ROH are longer than 1cM, reflecting haplotypes with a recent common ancestor less than 50 generations ago.
1273 In **Figure 4A-B** and **Appendix 4-figure 1**, we plot the distribution of the summed length of ROH per individual
1274 per size-classes.

1275

1276 **4.b. Intersecting ROH and local ancestry painting**

1277 Using the same phasing results as described above, we conducted 10 EM iterations of the RFMIX2 (106)
1278 algorithm to assign, for each Cabo Verdean individual and each SNP on each chromosome, separately, its
1279 putative source population of origin among the 24 African, European, Chinese-CHB, and USA-CEU popula-
1280 tions. We collapsed the local ancestry assignments for each SNP in each Cabo Verdean individual hence ob-
1281 tained into three continental regions, representing broadly African, broadly European, and broadly East Asian
1282 ancestries respectively. Any ancestry call that was assigned a population from the African continent was as-
1283 signed a category of AFR, any ancestry call that was assigned a population from the European continent was
1284 assigned a category of EUR, and any ancestry call that was assigned a population from the East Asian continent
1285 was assigned a category of ASN. We considered an approach similar to previous work (61), and intersected
1286 local ancestry calls with ROH calls (**Figure 4C-D**).

1287 RFMIX2 only makes local ancestry calls at loci that are present in the dataset. Therefore, a gap of unclas-
1288 sified ancestry exists where inferred ancestry switches between two successive genotyped loci as called by
1289 RFMIX2. These gaps necessarily each contain an odd number of ancestry switch points (≥ 1) absent from our
1290 marker set. Therefore, when computing the total ancestry content of an ROH that overlaps one of these ancestry
1291 breakpoints, we assign half of the length of this gap to each ancestry classification, effectively extending each
1292 local ancestry segment to meet at the midpoint.

1293 We then plotted the length distribution of long ROH for each island and we break out the distributions by
1294 ancestral haplotype background: those with only African ancestry, those with only European ancestry, and
1295 those that span at least one ancestry breakpoint (**Figure 4C**). We excluded long ROH in East Asian ancestry
1296 segments from this and the following analyses, as we found such ancestry overall very limited in the samples
1297 (**Appendix 4-figure 2**). We also excluded ROH called with heterozygous ancestry calls (e.g., called with one
1298 haplotype called as AFR and the other as EUR). These regions were also rare (**Figure 4-resource table 3**).

1299 Finally, we explored how total African/European ancestry in long ROH varies between islands. For each
1300 individual we summed the total amount of each ancestry in long-ROH and plot the distributions across islands
1301 (**Figure 4-figure supplement 1**). High levels of a given ancestry in long ROH could stem from an overall high

1302 level of that ancestry in that individual. Therefore, for each individual, we computed their global ancestry
1303 proportions by summing up the total length of the genome inferred as a given ancestry and dividing by the
1304 length of the genome. We then plotted (**Figure 4D**), the difference of an individual's long-ROH ancestry pro-
1305 portion and their global ancestry proportion, for African and European ancestries separately. Values above
1306 zero indicated that a given ancestry is overrepresented in long-ROH relative to genome-wide proportions of
1307 that ancestry.

1308 To assess the significance of these deviations, we performed a non-parametric permutation test. For each
1309 individual in each island, we randomly permuted the location of all long ROH (ensuring that no permuted
1310 ROH overlap), re-computed the local AFR ancestry proportion falling within these permuted ROH, and then
1311 subtracted the global ancestry proportion. We then took the mean of this difference across all individuals for
1312 each island and repeated the process 10,000 times. As there is negligible ASN ancestry across these individuals,
1313 the AFR and EUR proportions essentially add to 1, and therefore we consider an over/under representation of
1314 AFR ancestry in long ROH to be equivalent to an under/over representation of EUR ancestry in long ROH.
1315 Permutation distributions with observed values are plotted in **Figure 4-figure supplement 2** and permutation
1316 p-values are given in **Figure 4-resource table 2**.

1317

1318 **5. Isolation-by-distance: genetic and linguistic diversity within Cabo Verde**

1319 We explored genetic pairwise levels of differentiation calculated with ASD as previously, considering the
1320 1,899,878 non-monomorphic SNPs within Cabo Verde obtained after QC Stage 3 (**Appendix 1-figure 1**). We
1321 projected the matrix for the 225 unrelated Cabo Verde-born individuals using metric MDS as above. Note that
1322 pruning this data set for very low LD using *plink* function *--indep-pairwise* for a 50 SNPs window moving in
1323 increments of 10 SNPs and a r^2 threshold of 0.025 resulted in 85,425 SNPs for which the ASD matrix was
1324 highly correlated with the one using all SNPs (Spearman $\rho=0.8745$, $p<2.2\times 10^{-16}$). In parallel, we described the
1325 diversity of Kriolu idiolects (i.e. individuals' manners of speaking Kriolu) among the 225 genetically unrelated
1326 Cabo Verde-born individuals by projecting, with metric MDS, the matrix of pairwise Euclidean distances be-
1327 tween vectors of individuals' utterance-frequencies (**Material and Methods 1.d**), considering the 4831 unique
1328 uttered items.

1329 We then conducted a series of Mantel and partial Mantel correlation tests (Legendre and Legendre 1998),
1330 using the *partial.mantel.test* function in the R package *ncf*, with Spearman correlation and 10,000 Mantel per-
1331 mutations, to explore possible isolation-by-distance (39) patterns as well as correlations with other variables
1332 of interest. We conducted correlation tests between either the pairwise Euclidean distances between vectors of
1333 individuals' utterance-frequencies or genetic ASD separately, and individual pairwise matrices of *i*) absolute
1334 age differences, *ii*) absolute differences in academic education duration, *iii*) geographic distances between
1335 residence-locations (logarithmic scale), *iv*) between birth-locations, *v*) between mothers' birth-locations, *vi*)
1336 between fathers' birth-locations (**Table 1, Table 1-resource table 1**). All pairwise geographic distances were
1337 calculated with the Haversine great-circle distance formulation (107), taking 6,371 km for the radius of the
1338 Earth, using the *rdist.earth* function in the R package *fields*. Before computing logarithmic distances, we added
1339 1km to all pairwise distances.

1340

1341 **6. Isolation-by-distance: genetic and linguistic admixture within Cabo Verde**

1342 We further explored isolation-by-distance patterns within Cabo Verde specifically for African genetic and
1343 linguistic individual admixture levels. We considered African genetic admixture levels estimated from AD-
1344 MIXTURE at $K=2$ or ASD-MDS approaches (**Material and Methods 2-3, Figure 3, Appendix 1-figure 2**),
1345 and individual African linguistic admixture as "African-utterances scores" $Z_{i,Cat}$ as defined in **Material and**
1346 **Methods 1.e** for utterance lists contained in Category A, Category B, or Category A&B respectively (23). For

1347 genetic or linguistic admixture levels separately, we computed the pairwise matrix of individual absolute ad-
1348 mixture levels differences, and conducted Mantel testing with the different geographical distance matrices as
1349 above. Finally, we compared African genetic and linguistic admixture scores using Spearman correlations,
1350 throughout Cabo Verde and within all birth-islands, separately.

1351

1352 **7. Inferring genetic admixture histories in Cabo Verde with *MetHis*-ABC**

1353 We aimed at reconstructing the detailed genetic admixture history of each Cabo Verde island separately. To
1354 do so, we first design *MetHis* v1.0 (45) forward-in-time simulations of four competing complex admixture
1355 scenarios. We then couple *MetHis* simulation and summary-statistics calculation tools with ABC Random-
1356 Forest scenario-choice implemented in the R package *abcrf* (71), followed by Neural-Network posterior pa-
1357 rameter estimation with the R package *abc* (72), under the winning scenario for each island separately.

1358

1359 **7.a. Simulating four competing scenarios of complex historical admixture for each Cabo Verde island**

1360 ABC inference relies on simulations conducted with scenario-parameter values drawn randomly within prior
1361 distributions set explicitly by the user. We used *MetHis* v1.0 (45) to simulate 60,000 independent autosomal
1362 SNP markers in the admixed population H, forward-in-time and individual centered, under the four competing
1363 scenarios presented in **Figure 6** and **Table 2** and explicated below. In all four scenarios (**Figure 6; Table 2**),
1364 we considered, forward-in-time, that the admixed population (Population H) is founded at generation 0, 21
1365 generations before present. Generation 0 thus roughly corresponds to the 15th century when considering an
1366 average generation-time of 25 years and sampled individuals born on average between the 1960's and the
1367 1980's and no later than 1990 in our dataset. This is reasonable as historical records showed that Cabo Verde
1368 was likely un-inhabited before its initial colonial settlement established in the 1460s on Santiago (26). Due to
1369 the recent admixture history of Cabo Verde and as we considered only independent genotyped SNPs, we ne-
1370 glected mutation in our simulations for simplicity.

1371 Following our descriptive analyses results, we considered scenarios with only one “European” and one
1372 “African” source population, and each Cabo Verde island, separately, as the “Admixed” recipient population
1373 H. This corresponds to the “two-source” version of the general admixture model from Verdu and Rosenberg
1374 (73), also explored with *MetHis* previously (45). We therefore considered a single African and European pop-
1375 ulation at the source of all admixture in Cabo Verde, and further considered that both source populations were
1376 very large and at the drift-mutation equilibrium during the 21 generations of the admixture process until present.
1377 Furthermore, we considered that these source populations were accurately represented, respectively, by the
1378 Mandinka from Senegambia and the Iberian-IBS populations in a random genotyping dataset of 60,000 inde-
1379 pendent autosomal SNPs (see **Results 1-3**).

1380 In brief (see below), at each generation, *MetHis* performs simple Wright-Fisher (108,109) forward-in-
1381 time discrete simulations, individual-centered, in a randomly-mating (without selfing) admixed population of
1382 N_g diploid individuals. Separately for each N_g individual in the admixed population at generation g , *MetHis*
1383 draws parents randomly from the source populations and the admixed population itself at the previous gener-
1384 ation according to given parameter-values drawn from prior distributions separately for each simulation.

1385

1386 *Hyperbolic increase, linear increase, or constant reproductive population size in the admixed population*

1387 We considered, for the admixed population H, a reproductive population size of N_0 diploid individuals at gen-
1388 eration 0, with N_0 in $[10,1000]$, and N_{20} in $[100,100,000]$ at generation 20, such that $N_0 < N_{20}$. In between these
1389 two values, we considered for the N_g values at each generation the discrete numerical solutions of an increasing
1390 rectangular hyperbola function of parameter u_N in $[0,1/2]$ (45). Therefore, values of the demographic param-
1391 eters $N_0 \sim N_{20}$ correspond to simulations with a constant admixed-population H reproductive population size of
1392 N_0 diploid individuals during the entire 21 generations of the admixture process, whichever the value of u_N .

1393 Instead, parameter values $N_0 \neq N_{20}$ necessarily correspond to simulations with an increase in reproductive size
1394 between N_0 and N_{20} , steeper with values of u_N closer to 0. Note, thus, that parameter values $N_0 \neq N_{20}$ and u_N
1395 close to 0 correspond to simulations where the reproductive size of the admixed population H is roughly con-
1396 stant and equal to N_0 at each generation until a very sharp increase to reach N_{20} at the last generation before
1397 present. Instead, parameter values $N_0 \neq N_{20}$ and u_N close to $1/2$ correspond to simulations with a linear increase
1398 in reproductive size between N_0 and N_{20} .

1399 Therefore, while we do not formally compare competing scenarios with different demographic regimes
1400 in this work, each scenario comprises simulations whose parameter values correspond to a variety of constant,
1401 hyperbolic increase, or linear increase in reproductive size over the course of the admixture history of each
1402 Cabo Verdean island separately. Therefore, ABC parameter estimation of the demographic parameters N_0 , N_{20} ,
1403 and u_N should determine, *a posteriori*, which of the three demographic regimes best explain our data, which-
1404 ever is the winning admixture scenario among the four in competition.

1405

1406 Founding the admixed population

1407 At generation 0 (**Figure 6**), the admixed population of size N_0 diploid individuals drawn in $[10,1000]$ is
1408 founded with a proportion $s_{Eur,0}$ of admixed individuals' parents originating from the European source drawn
1409 in $[0,1]$, and a proportion of $s_{Afr,0}$ parents from the African source drawn in $[0,1]$, with $s_{Eur,0} + s_{Afr,0} = 1$. Note
1410 that parameter-values of $s_{Afr,0}$, or $s_{Eur,0}$, close to 0 correspond to simulations where the "admixed" population
1411 is initially founded by only one of the sources, and that genetic admixture *per se* may only occur at the follow-
1412 ing admixture event.

1413 After the founding of the admixed population H, we considered two different admixture scenarios for
1414 either source population's contribution to the gene-pool of population H. In all cases, for all generations g in
1415 $[1,20]$ after the initial founding of the admixed population at $g = 0$, *MetHis* randomly draws parents from the
1416 African source, the European source and the admixed population H respectively in proportions $s_{Afr,g}$, $s_{Eur,g}$, and
1417 h_g , each in $[0,1]$ and satisfying $s_{Afr,g} + s_{Eur,g} + h_g = 1$. Then, the software randomly builds gametes for each
1418 parent and randomly pairs them, without selfing, to produce N_g diploid individuals in the admixed population.

1419

1420 Two admixture pulses after foundation

1421 For a given source population hereafter designated "Source" ("European" or "African" in our case), after
1422 founding at generation 0, we considered scenarios with two additional pulses of admixture ("Source"-2Pulses
1423 scenarios). The two pulses occur, respectively, at generation $t_{Source,p1}$ and $t_{Source,p2}$ in $[1,20]$, with $t_{Source,p1} \neq$
1424 $t_{Source,p2}$; and with intensity $s_{Source,tSource,p1}$ and $s_{Source,tSource,p2}$ in $[0,1]$, respectively.

1425 Note that simulations considering values of parameters $t_{Source,p1} = t_{Source,p2} + 1$, and simulations with either
1426 $s_{Source,tSource,p1}$ or $s_{Source,tSource,p2}$ close to 0, may strongly resemble those expected under scenarios with only one
1427 pulse of admixture after the founding of the admixed population H.

1428

1429 A period of recurring admixture after foundation

1430 For a given Source population, after founding at generation 0, we considered scenarios with a possible period
1431 of recurring admixture, where, during this period, admixture intensity followed a monotonically decreasing
1432 trend ("Source"-Recurring scenarios). The period of admixture occurs between times $t_{Source,t1}$ and $t_{Source,t2}$ in
1433 $[1,20]$ with $t_{Source,t2} \geq t_{Source,t1} + 1$. The beginning of the admixture period at $t_{Source,t1}$ is associated with admixture
1434 intensity $s_{Source,tSource,t1}$ in $[0,1]$. The end of the admixture period at $t_{Source,t2}$ is associated with intensity
1435 $s_{Source,tSource,t2}$ in $[0,1]$ such that $s_{Source,tSource,t1} \geq s_{Source,tSource,t2}$. In between, the admixture intensity values at each
1436 generation of the admixture period are the discrete numerical solutions of a decreasing rectangular hyperbola
1437 function of parameter u_{Source} in $[0,1/2]$ (45).

1438 Intuitively, a u parameter value close to 0 corresponds to a sharp pulse of admixture occurring at the
1439 beginning of the admixture period of intensity $s_{\text{Source},t_{\text{Source},t1}}$, followed at the next generation by constant recur-
1440 ring admixture of intensity $s_{\text{Source},t_{\text{Source},t2}}$ until the end of the admixture period. Alternatively, a u parameter
1441 value close to 1/2 corresponds to a linearly decreasing admixture at each generation of the admixture period,
1442 from $s_{\text{Source},t_{\text{Source},t1}}$ to $s_{\text{Source},t_{\text{Source},t2}}$.

1443 Note that in the limit when $s_{\text{Source},t_{\text{Source},t1}} \sim s_{\text{Source},t_{\text{Source},t2}}$, Recurring scenarios correspond to constant recur-
1444 ring admixture of that intensity. Furthermore, simulations with u and $s_{\text{Source},t_{\text{Source},t2}}$ parameter values both close
1445 to 0 correspond to scenarios with a single pulse of admixture from a given source after the founding pulse,
1446 occurring at time $t_{\text{Source},t1}$ and with intensity $s_{\text{Source},t_{\text{Source},t1}}$.

1447

1448 Four competing scenarios of admixture from two-source populations in each Cabo Verde island

1449 Finally, we combined the 2Pulses and Recurring scenarios from either the African and European Source pop-
1450 ulations in order to produce four competing scenarios of admixture for the genetic history of Cabo Verde
1451 (**Figure 6**), with the only constraint that at each generation g between 1 and 20, $s_{\text{Afr},g} + s_{\text{Eur},g} = 1 - h_g$, where h_g
1452 is the contribution of the admixed population H to itself at the following generation in $[0,1]$.

1453

1454 Simulating the admixed population from source-populations for 60,000 independent SNPs with MetHis

1455 As introduced previously, our results showed that the Mandinka from West Western Africa and the Iberian
1456 IBS from South West Europe were reasonable proxies of the main source populations for the gene-pool of
1457 Cabo Verde, at least when considering a relatively small number of independent autosomal SNPs. We decided
1458 to consider both populations as very large and at the drift-mutation equilibrium since the 1460's and the initial
1459 founding of Cabo Verde. We thus chose not to explicitly simulate the evolutionary history of the two European
1460 and African populations at the source of the genetic history of the Cabo Verde islands.

1461 Instead, we first randomly drew 60,000 independent SNPs, avoiding singletons, from the LD-pruned
1462 102,543 independent SNPs employed for the ADMIXTURE analyses. We then built a single reservoir of “Af-
1463 rican” gametes comprising 20,000 haploid genomes of 60,000 independent SNP-sites each, where each allele
1464 at each site of a gamete was randomly drawn in the site frequency spectrum observed for the corresponding
1465 SNP in the Mandinka proxy source population. Separately, we proceeded similarly to build a reservoir of
1466 20,000 European gametes matching instead the site-frequency spectrum observed in the Iberian IBS at the
1467 60,000 SNPs.

1468 For a given simulation with, at generation 0, given parameter values $s_{\text{Afr},0}$ and $s_{\text{Eur},0}$, each in $[0,1]$ such that
1469 $s_{\text{Afr},0} + s_{\text{Eur},0} = 1$, and a given value (in $[10,1000]$) of N_0 diploid individuals in the admixed population H, *MetHis*
1470 randomly draws two different gametes in the African gamete-reservoir and randomly pairs them to produce
1471 one parent from the African source and repeats the process $s_{\text{Afr},0} \times 2N_0$ times to obtain that number of African
1472 parents. In parallel and using the same procedure, *MetHis* randomly builds $s_{\text{Eur},0} \times 2N_0$ parents from the Euro-
1473 pean gamete-reservoirs. For each of N_0 individuals in the admixed population separately, *MetHis* then draws
1474 randomly a pair of parents among the European and African parents hence obtained, and for each parent sep-
1475 arately, builds one haploid gamete by randomly drawing one allele for each 60,000 genotypes. Finally, *MetHis*
1476 pairs both hence obtained gametes to create the novel individual in the admixed population at the following
1477 generation, and repeats the procedure (replacing the pair of parents after each random draw in the parental
1478 pool) for each of N_0 individuals separately.

1479 Then, for the same given simulation, admixture from a source population is set to occur at a given gener-
1480 ation g (in $[1,20]$) associated with a given intensity $s_{\text{source},g}$, keeping in mind that at all g in $[1,20]$, $s_{\text{Afr},g} + s_{\text{Eur},g}$
1481 $+ h_g = 1$. *MetHis* then builds anew $s_{\text{source},g} \times 2N_g$ reproductive parents from this source population's gamete-
1482 reservoir as previously, and in parallel randomly draws $h_g \times 2N_g$ parents from the admixed population H itself
1483 at the previous generation. Then, for each of N_g individuals in the admixed population separately, *MetHis*

1484 randomly draws a pair of different parents (replacing the pair of parents after each random draw in the parental
1485 pool), randomly builds haploid gametes from each parent, and pairs them similarly as previously to obtain a
1486 new individual at the following generation.

1487 Thus, note that while our source-populations' gamete reservoirs were fixed during the admixture process,
1488 the African or the European diploid parents possibly contributing to the gene-pool of the admixed population
1489 are randomly built anew, and each produce novel gametes, at each generation and in each simulation separately.
1490 Importantly, note that recombination is thus not a parameter in *MetHis* simulations as all SNPs are considered
1491 statistically independent.

1492

1493 Sampling simulated source and admixed populations

1494 At the end of each simulation, we randomly drew individual samples from each source and the admixed pop-
1495 ulation H matching observed sample sizes. We randomly sampled 60 individuals in the African source gamete
1496 reservoirs, 60 individuals in the European source, and the number of admixed individuals corresponding to the
1497 sample size of each Cabo Verde island of birth of individuals or to all 225 Cabo Verde-born individuals
1498 grouped in a single random mating population, in turn (**Figure 1-resource table 1**). We sampled individuals
1499 without grand-parents in common, as allowed in *MetHis* by explicit genealogical flagging of individuals during
1500 the last two generations of the admixture process, hence mimicking our observed family unrelated dataset
1501 within Cabo Verde.

1502

1503 Number of simulations and scenario-parameter priors for ABC inference

1504 We performed 10,000 such *MetHis* simulations under each of four admixture scenarios for each of the nine
1505 birth-islands of Cabo Verde and for all Cabo Verde-born individuals grouped in a single population, separately.
1506 Each simulation was performed under a vector of scenario parameters drawn from prior distributions described
1507 above and in **Table 2**, using *MetHis parameter generator* tools. Separately for each island and for Cabo Verde
1508 as a single population, we used this set of simulations to determine which scenario best explained the observed
1509 data using Random-Forest ABC (see below). Under the winning scenario for each birth-island and separately
1510 for Cabo Verde as a whole, we then performed an additional 90,000 simulations each corresponding to a dif-
1511 ferent vector of parameter values drawn randomly from the priors set by the user for this scenario, to produce
1512 a total of 100,000 simulations to be used for Neural-Network ABC posterior parameter estimation, for each
1513 ten – 9 islands and Cabo Verde as a whole, separately – analysis separately.

1514

1515 **7.b. *MetHis*-ABC Random Forest scenario-choice and Neural Network posterior parameter estimations**

1516 To reconstruct highly complex admixture histories in Cabo Verde using genetic data, we conducted machine-
1517 learning Approximate Bayesian Computation inferences based on the simulations produced with *MetHis* as
1518 described above under the four competing admixture history scenarios. We performed Random-Forest ABC
1519 scenario-choice (71), and Neural Network ABC posterior parameter inferences (72), for each Cabo Verde
1520 island and for all Cabo Verde-born individuals grouped in a single population, separately. We followed the
1521 *MetHis*-ABC approach proposed in (45) for summary-statistics calculation, prior-checking, out-of-bag cross-
1522 validation, machine-learning ABC predictions and inferences parameterization, and posterior parameter cross-
1523 validation error calculations.

1524 All the details and results of these ABC procedures can be found in corresponding **Appendix 1, Appendix**
1525 **1-table 1, Appendix 5-table 1-10, Appendix 1-figure 3-4, Appendix 1-figure 3-resource figure 1-10,** and
1526 **Figure 7-figure supplement 1-3**. Briefly, we performed 10,000 simulations of 60,000 independent SNPs un-
1527 der each of the four competing scenarios described above, drawing parameter values in prior distributions
1528 detailed in **Table 2**. As listed in **Table 3** and described in details in **Appendix 1**, we then computed 42 sum-

1529 summary-statistics separately for each simulated dataset comprising 60,000 independent SNPs, by drawing ran-
1530 domly 60 parents in the African and European source populations, and randomly drawing sample-sets match-
1531 ing the observed sample-sizes of each Cabo Verde birth-island or all Cabo Verde-born individuals as a single
1532 population, separately. Note that we considered summary-statistics specifically aiming at describing the dis-
1533 tribution of individual admixture fractions in the sample set, known theoretically and empirically to be highly
1534 informative about complex admixture history parameters (45,73). We thus performed RF-ABC scenario-
1535 choices using 40,000 vectors of 42 summary-statistics (10,000 under each four competing scenarios), each
1536 corresponding to a vector of parameter values randomly drawn in prior distributions and used for *MetHis*
1537 simulations, for each nine birth-island and for Cabo Verde as a whole, separately. We then performed NN-
1538 ABC joint posterior parameter inferences of all scenario-parameters under the winning scenarios obtained with
1539 RF-ABC, using 100,000 vectors of 42 summary statistics obtained from additional *MetHis* simulations under
1540 the winning scenarios respectively for each nine birth-island and for Cabo Verde as a whole, separately.
1541
1542

1543 **ACKNOWLEDGEMENTS**

1544 The authors would like to warmly thank all Cabo Verdean participants to this study as well as the UniCV for
1545 facilitating the project. This project was funded in part by the French “Agence Nationale pour la Recherche”
1546 grant ANR METHIS 15-CE32-0009-1, and by a grant from the France-Stanford Center for Interdisciplinary
1547 Studies. MB was supported in part by the Linguistics Department at the University of Michigan (MI, USA).
1548 ZAS was supported in part by startup funds from the Department of Biology at the Pennsylvania State Uni-
1549 versity (PA, USA), and by the NIH grant R35 GM146926. CAFL was supported in part by the Marcus
1550 Borgströms Foundation for Genetic Research and the Bertil Lundman Foundation for Anthropological Studies
1551 (Sweden). We thank the platform “Paléogénomique et génétique moléculaire” (P2GM) of the French Muséum
1552 National d’Histoire Naturelle at the Musée de l’Homme for support handling biological samples and generating
1553 genetic data. We thank the BIOMICS platform from the Pasteur institute for performing genotyping analyses.
1554 Finally, the authors warmly thank two independent reviewers and the editors of *eLife*, as well as Frank Alvarez-
1555 Pereyre, Erkan O. Buzbas, Marta Ciccarella, Pierre Darlu, Evelyne Heyer, Ethan M. Jewett, Marie-France
1556 Mifune, Etienne Patin, Jorge M. Rocha, Lara Rubio Arauna, and Bruno Toupance, for useful comments and
1557 discussions about this work.

1558

1559

1560 **CONFLICT OF INTEREST STATEMENT**

1561 The authors declare no conflict of interests for this work.

1562

1563

1564 **REFERENCES**

1565

- 1566 1. Eltis D, Richardson D. Atlas of the transatlantic slave trade. 2015. 336 p.
- 1567 2. Fortes-Lima C, Verdu P. Anthropological genetics perspectives on the transatlantic slave
1568 trade. *Human Molecular Genetics* [Internet]. 2021 Apr 26 [cited 2021 Jun 4];30(R1):R79–87.
1569 Available from: <https://academic.oup.com/hmg/article/30/R1/R79/6040749>
- 1570 3. Micheletti SJ, Bryc K, Ancona Esselmann SG, Freyman WA, Moreno ME, Poznik GD, et al.
1571 Genetic Consequences of the Transatlantic Slave Trade in the Americas. *The American*
1572 *Journal of Human Genetics* [Internet]. 2020 Aug [cited 2021 Jun 4];107(2):265–77. Available
1573 from: <https://linkinghub.elsevier.com/retrieve/pii/S0002929720302007>
- 1574 4. Ongaro L, Scliar MO, Flores R, Raveane A, Marnetto D, Sarno S, et al. The Genomic Impact
1575 of European Colonization of the Americas. *Current Biology* [Internet]. 2019 Dec [cited 2022
1576 Apr 8];29(23):3974–3986.e4. Available from:
1577 <https://linkinghub.elsevier.com/retrieve/pii/S0960982219313065>
- 1578 5. Winkler CA, Nelson GW, Smith MW. Admixture Mapping Comes of Age. *Annu Rev Genom*
1579 *Hum Genet* [Internet]. 2010 Sep [cited 2021 Jun 4];11(1):65–89. Available from:
1580 <http://www.annualreviews.org/doi/10.1146/annurev-genom-082509-141523>
- 1581 6. Wojcik GL, Graff M, Nishimura KK, Tao R, Haessler J, Gignoux CR, et al. Genetic analyses
1582 of diverse populations improves discovery for complex traits. *Nature* [Internet]. 2019 Jun
1583 [cited 2021 Jun 4];570(7762):514–8. Available from: [http://www.nature.com/articles/s41586-](http://www.nature.com/articles/s41586-019-1310-4)
1584 [019-1310-4](http://www.nature.com/articles/s41586-019-1310-4)
- 1585 7. Patin E, Lopez M, Grollemund R, Verdu P, Harmant C, Quach H, et al. Dispersals and genetic
1586 adaptation of Bantu-speaking populations in Africa and North America. *Science* [Internet].
1587 2017 May 5 [cited 2021 Jun 4];356(6337):543–6. Available from:
1588 <https://www.sciencemag.org/lookup/doi/10.1126/science.aal1988>
- 1589 8. Gravel S. Population Genetics Models of Local Ancestry. *Genetics* [Internet]. 2012 Jun 1
1590 [cited 2021 Jun 4];191(2):607–19. Available from:
1591 <https://academic.oup.com/genetics/article/191/2/607/5935164>
- 1592 9. Hellenthal G, Busby GBJ, Band G, Wilson JF, Capelli C, Falush D, et al. A Genetic Atlas of
1593 Human Admixture History. *Science* [Internet]. 2014 Feb 14 [cited 2021 Jun
1594 4];343(6172):747–51. Available from:
1595 <https://www.sciencemag.org/lookup/doi/10.1126/science.1243518>
- 1596 10. Mathias RA, Taub MA, Gignoux CR, Fu W, Musharoff S, O'Connor TD, et al. A continuum
1597 of admixture in the Western Hemisphere revealed by the African Diaspora genome. *Nat*
1598 *Commun* [Internet]. 2016 Nov [cited 2021 Jun 4];7(1):12522. Available from:
1599 <http://www.nature.com/articles/ncomms12522>
- 1600 11. Moreno-Estrada A, Gravel S, Zakharia F, McCauley JL, Byrnes JK, Gignoux CR, et al.
1601 Reconstructing the Population Genetic History of the Caribbean. Tarazona-Santos E, editor.
1602 *PLoS Genet* [Internet]. 2013 Nov 14 [cited 2021 Jun 4];9(11):e1003925. Available from:
1603 <https://dx.plos.org/10.1371/journal.pgen.1003925>
- 1604 12. Baharian S, Barakatt M, Gignoux CR, Shringarpure S, Errington J, Blot WJ, et al. The Great

- 1605 Migration and African-American Genomic Diversity. Gibson G, editor. PLoS Genet [Internet].
1606 2016 May 27 [cited 2021 Jun 4];12(5):e1006059. Available from:
1607 <https://dx.plos.org/10.1371/journal.pgen.1006059>
- 1608 13. Holm JA. An introduction to pidgin and creoles. Cambridge [England] ; New York:
1609 Cambridge University Press; 2000. 282 p. (Cambridge textbooks in linguistics).
- 1610 14. Escure G, Schwegler A. Creoles, contact, and language change: linguistics and social
1611 implications. Amsterdam ; Philadelphia: John Benjamins Pub; 2004. 354 p. (Creole language
1612 library).
- 1613 15. Quint N. Le cap-verdien: origines et devenir d'une langue métisse. Paris, France:
1614 L'Harmattan; 2000. 353 p.
- 1615 16. Essegbey J, Migge B, Winford D. Cross-linguistic influence in language creation: Assessing
1616 the role of the Gbe languages in the formation of the Creoles of Suriname. *Lingua* [Internet].
1617 2013 May [cited 2021 Jun 4];129:1–8. Available from:
1618 <https://linkinghub.elsevier.com/retrieve/pii/S002438411300048X>
- 1619 17. Baptista M. Continuum and variation in Creoles: Out of many voices, one language. *JPCL*
1620 [Internet]. 2015 Oct 20 [cited 2021 Jun 4];30(2):225–64. Available from: [http://www.jbe-](http://www.jbe-platform.com/content/journals/10.1075/jpcl.30.2.02bap)
1621 [platform.com/content/journals/10.1075/jpcl.30.2.02bap](http://www.jbe-platform.com/content/journals/10.1075/jpcl.30.2.02bap)
- 1622 18. Eltis D, editor. Coerced and free migration: global perspectives. Stanford, Calif: Stanford
1623 University Press; 2002. 447 p. (The making of modern freedom).
- 1624 19. Berlin I. Many Thousands Gone: the First Two Centuries of Slavery in North America.
1625 [Internet]. Cambridge: Harvard University Press; 2009 [cited 2021 Jun 7]. 512 p. Available
1626 from: <https://public.ebookcentral.proquest.com/choice/publicfullrecord.aspx?p=3300728>
- 1627 20. Creanza N, Ruhlén M, Pemberton TJ, Rosenberg NA, Feldman MW, Ramachandran S. A
1628 comparison of worldwide phonemic and genetic variation in human populations. *Proc Natl*
1629 *Acad Sci USA* [Internet]. 2015 Feb 3 [cited 2022 Nov 30];112(5):1265–72. Available from:
1630 <https://pnas.org/doi/full/10.1073/pnas.1424033112>
- 1631 21. Cavalli-Sforza LL, Piazza A, Menozzi P, Mountain J. Reconstruction of human evolution:
1632 bringing together genetic, archaeological, and linguistic data. *Proc Natl Acad Sci USA*
1633 [Internet]. 1988 Aug [cited 2023 Jan 20];85(16):6002–6. Available from:
1634 <https://pnas.org/doi/full/10.1073/pnas.85.16.6002>
- 1635 22. Ansari-Pour N, Moñino Y, Duque C, Gallego N, Bedoya G, Thomas MG, et al. Palenque de
1636 San Basilio in Colombia: genetic data support an oral history of a paternal ancestry in Congo.
1637 *Proc R Soc B* [Internet]. 2016 Mar 30 [cited 2021 Jun 4];283(1827):20152980. Available
1638 from: <https://royalsocietypublishing.org/doi/10.1098/rspb.2015.2980>
- 1639 23. Verdu P, Jewett EM, Pemberton TJ, Rosenberg NA, Baptista M. Parallel Trajectories of
1640 Genetic and Linguistic Admixture in a Genetically Admixed Creole Population. *Current*
1641 *Biology* [Internet]. 2017 Aug [cited 2022 Feb 2];27(16):2529–2535.e3. Available from:
1642 <https://linkinghub.elsevier.com/retrieve/pii/S096098221730859X>
- 1643 24. Hagemeyer T, Rocha J. Creole languages and genes: the case of São Tomé and Príncipe. *Faits*
1644 *Lang* [Internet]. 2019 Aug 23 [cited 2021 Jun 4];49(1):167–82. Available from:

- 1645 https://brill.com/view/journals/fdl/49/1/article-p167_11.xml
- 1646 25. Carreira A. Cabo Verde: formação e extinção de uma sociedade escravocrata (1460-1878). 3rd
1647 ed. Praia, Cabo Verde: IPC; 2000. 522 p. (Estudos e ensaios).
- 1648 26. Albuquerque L de, Santos MEM, editors. História geral de Cabo Verde T1. Vol. 1. Lisboa :
1649 Praia [Cape Verde]: Centro de Estudos de História e Cartografia Antiga, Instituto de
1650 Investigação Científica Tropical ; Instituto Nacional da Cultura de Cabo Verde; 1991. 523 p.
- 1651 27. Albuquerque L de, Santos MEM, editors. História geral de Cabo Verde T2. 2. ed. Vol. 2.
1652 Lisboa: Centro de Estudos de História e Cartogr. Antiga; 1995. 596 p.
- 1653 28. Albuquerque L de, Santos MEM, editors. História concisa de Cabo Verde (Resumo da História
1654 geral de Cabo Verde T1-3). Lisboa: Inst. de Investigação Científica Tropical; 2007. 427 p.
- 1655 29. Baptista M. The syntax of Cape Verdean Creole: the Sotavento varieties. Amsterdam ;
1656 Philadelphia: John Benjamins Pub; 2002. 289 p. (Linguistik aktuell = Linguistics today).
- 1657 30. Lang J. Les langues des autres dans la créolisation: théorie et exemplification par le créole
1658 d’empreinte wolof à l’île Santiago du Cap Vert. Tübingen: Narr; 2009. 275 p.
- 1659 31. Brehm A, Pereira L, Bandelt HJ, Prata MJ, Amorim A. Mitochondrial portrait of the Cabo
1660 Verde archipelago: the Senegambian outpost of Atlantic slave trade. *Ann Hum Genet*
1661 [Internet]. 2002 Jan [cited 2021 Jun 4];66(1):49–60. Available from:
1662 <http://doi.wiley.com/10.1017/S0003480001001002>
- 1663 32. Gonçalves R, Rosa A, Freitas A, Fernandes A, Kivisild T, Villems R, et al. Y-chromosome
1664 lineages in Cabo Verde Islands witness the diverse geographic origin of its first male settlers.
1665 *Human Genetics* [Internet]. 2003 Nov 1 [cited 2021 Jun 4];113(6):467–72. Available from:
1666 <http://link.springer.com/10.1007/s00439-003-1007-4>
- 1667 33. Beleza S, Campos J, Lopes J, Araújo II, Hoppfer Almada A, e Silva AC, et al. The Admixture
1668 Structure and Genetic Variation of the Archipelago of Cape Verde and Its Implications for
1669 Admixture Mapping Studies. Relethford JH, editor. *PLoS ONE* [Internet]. 2012 Nov 30 [cited
1670 2021 Jun 4];7(11):e51103. Available from: <https://dx.plos.org/10.1371/journal.pone.0051103>
- 1671 34. Beleza S, Johnson NA, Candille SI, Absher DM, Coram MA, Lopes J, et al. Genetic
1672 Architecture of Skin and Eye Color in an African-European Admixed Population. Spritz RA,
1673 editor. *PLoS Genet* [Internet]. 2013 Mar 21 [cited 2021 Jun 4];9(3):e1003372. Available from:
1674 <https://dx.plos.org/10.1371/journal.pgen.1003372>
- 1675 35. Hamid I, Korunes KL, Beleza S, Goldberg A. Rapid adaptation to malaria facilitated by
1676 admixture in the human population of Cabo Verde. *eLife* [Internet]. 2021 Jan 4 [cited 2021
1677 Jun 4];10:e63177. Available from: <https://elifesciences.org/articles/63177>
- 1678 36. Soares MJ. The British Presence on the Cape Verdean Archipelago (Sixteenth to Eighteenth
1679 centuries). *African Economic History*. 2011;39:129–46.
- 1680 37. Berlin I. *The making of African America: the four great migrations*. New York: Penguin
1681 Books; 2010. 304 p.
- 1682 38. Gouveia MH, Borda V, Leal TP, Moreira RG, Bergen AW, Kehdy FSG, et al. Origins,

- 1683 Admixture Dynamics, and Homogenization of the African Gene Pool in the Americas. Nielsen
1684 R, editor. *Molecular Biology and Evolution*. 2020 Jun 1;37(6):1647–56.
- 1685 39. Rousset F. Genetic Differentiation and Estimation of Gene Flow from F -Statistics Under
1686 Isolation by Distance. *Genetics* [Internet]. 1997 Apr 1 [cited 2022 Feb 2];145(4):1219–28.
1687 Available from: <https://academic.oup.com/genetics/article/145/4/1219/6018124>
- 1688 40. Barbujani G. Autocorrelation of Gene Frequencies Under Isolation by Distance. *Genetics*
1689 [Internet]. 1987 Dec 1 [cited 2022 Nov 30];117(4):777–82. Available from:
1690 <https://academic.oup.com/genetics/article/117/4/777/5997427>
- 1691 41. Malécot G. Heterozygosity and relationship in regularly subdivided populations. *Theoretical*
1692 *Population Biology* [Internet]. 1975 Oct [cited 2022 Nov 30];8(2):212–41. Available from:
1693 <https://linkinghub.elsevier.com/retrieve/pii/0040580975900337>
- 1694 42. Barbujani G, Sokal RR. Genetic population structure of Italy. II. Physical and cultural barriers
1695 to gene flow. *Am J Hum Genet*. 1991 Feb;48(2):398–411.
- 1696 43. Cavalli-Sforza LL, Moroni A, Zei G. *Consanguinity, Inbreeding, and Genetic Drift in Italy*.
1697 Princeton: Princeton University Press; 2004.
- 1698 44. Verdu P, Leblois R, Froment A, Théry S, Bahuchet S, Rousset F, et al. Limited dispersal in
1699 mobile hunter–gatherer Baka Pygmies. *Biol Lett* [Internet]. 2010 Dec 23 [cited 2022 Nov
1700 30];6(6):858–61. Available from:
1701 <https://royalsocietypublishing.org/doi/10.1098/rsbl.2010.0192>
- 1702 45. Fortes-Lima CA, Laurent R, Thouzeau V, Toupance B, Verdu P. Complex genetic admixture
1703 histories reconstructed with Approximate Bayesian Computation. *Mol Ecol Resour* [Internet].
1704 2021 May [cited 2021 Jun 4];21(4):1098–117. Available from:
1705 <https://onlinelibrary.wiley.com/doi/10.1111/1755-0998.13325>
- 1706 46. Bowcock AM, Ruiz-Linares A, Tomfohrde J, Minch E, Kidd JR, Cavalli-Sforza LL. High
1707 resolution of human evolutionary trees with polymorphic microsatellites. *Nature* [Internet].
1708 1994 Mar [cited 2022 Feb 2];368(6470):455–7. Available from:
1709 <http://www.nature.com/articles/368455a0>
- 1710 47. Hastie T, Tibshirani R, Friedman JH, Friedman JH. *The elements of statistical learning: data*
1711 *mining, inference, and prediction*. Vol. 2. Springer; 2009.
- 1712 48. Alexander DH, Novembre J, Lange K. Fast model-based estimation of ancestry in unrelated
1713 individuals. *Genome Research* [Internet]. 2009 Sep 1 [cited 2021 Jun 4];19(9):1655–64.
1714 Available from: <http://genome.cshlp.org/cgi/doi/10.1101/gr.094052.109>
- 1715 49. Morrison ML, Alcalá N, Rosenberg NA. FSTruct: An F_{ST} -based tool for measuring ancestry
1716 variation in inference of population structure. *Molecular Ecology Resources* [Internet]. 2022
1717 Oct [cited 2023 Jan 20];22(7):2614–26. Available from:
1718 <https://onlinelibrary.wiley.com/doi/10.1111/1755-0998.13647>
- 1719 50. Patterson N, Moorjani P, Luo Y, Mallick S, Rohland N, Zhan Y, et al. Ancient Admixture in
1720 Human History. *Genetics* [Internet]. 2012 Nov 1 [cited 2022 Feb 2];192(3):1065–93.
1721 Available from: <https://academic.oup.com/genetics/article/192/3/1065/5935193>

- 1722 51. Pritchard JK, Stephens M, Donnelly P. Inference of population structure using multilocus
1723 genotype data. *Genetics*. 2000 Jun;155(2):945–59.
- 1724 52. Rosenberg NA. Genetic Structure of Human Populations. *Science* [Internet]. 2002 Dec 20
1725 [cited 2021 Jun 4];298(5602):2381–5. Available from:
1726 <https://www.sciencemag.org/lookup/doi/10.1126/science.1078311>
- 1727 53. Falush D, Stephens M, Pritchard JK. Inference of population structure using multilocus
1728 genotype data: linked loci and correlated allele frequencies. *Genetics*. 2003 Aug;164(4):1567–
1729 87.
- 1730 54. Lawson DJ, van Dorp L, Falush D. A tutorial on how not to over-interpret STRUCTURE and
1731 ADMIXTURE bar plots. *Nat Commun* [Internet]. 2018 Dec [cited 2021 Jun 4];9(1):3258.
1732 Available from: <http://www.nature.com/articles/s41467-018-05257-7>
- 1733 55. Peter BM. A geometric relationship of F_2 , F_3 and F_4 -statistics with principal component
1734 analysis. *Phil Trans R Soc B* [Internet]. 2022 Jun 6 [cited 2023 Jan 20];377(1852):20200413.
1735 Available from: <https://royalsocietypublishing.org/doi/10.1098/rstb.2020.0413>
- 1736 56. Lawson DJ, Hellenthal G, Myers S, Falush D. Inference of Population Structure using Dense
1737 Haplotype Data. Copenhaver GP, editor. *PLoS Genet* [Internet]. 2012 Jan 26 [cited 2021 Jun
1738 4];8(1):e1002453. Available from: <https://dx.plos.org/10.1371/journal.pgen.1002453>
- 1739 57. Delaneau O, Marchini J, Zagury JF. A linear complexity phasing method for thousands of
1740 genomes. *Nat Methods* [Internet]. 2012 Feb [cited 2021 Jun 4];9(2):179–81. Available from:
1741 <http://www.nature.com/articles/nmeth.1785>
- 1742 58. Chacón-Duque JC, Adhikari K, Fuentes-Guajardo M, Mendoza-Revilla J, Acuña-Alonzo V,
1743 Barquera R, et al. Latin Americans show wide-spread Converso ancestry and imprint of local
1744 Native ancestry on physical appearance. *Nat Commun* [Internet]. 2018 Dec [cited 2021 Jun
1745 4];9(1):5388. Available from: <http://www.nature.com/articles/s41467-018-07748-z>
- 1746 59. Thompson EA. Identity by Descent: Variation in Meiosis, Across Genomes, and in
1747 Populations. *Genetics* [Internet]. 2013 Jun 1 [cited 2021 Jun 4];194(2):301–26. Available
1748 from: <https://academic.oup.com/genetics/article/194/2/301/6065409>
- 1749 60. Mooney JA, Huber CD, Service S, Sul JH, Marsden CD, Zhang Z, et al. Understanding the
1750 Hidden Complexity of Latin American Population Isolates. *The American Journal of Human
1751 Genetics* [Internet]. 2018 Nov [cited 2022 Feb 2];103(5):707–26. Available from:
1752 <https://linkinghub.elsevier.com/retrieve/pii/S0002929718303513>
- 1753 61. Szpiech ZA, Mak ACY, White MJ, Hu D, Eng C, Burchard EG, et al. Ancestry-Dependent
1754 Enrichment of Deleterious Homozygotes in Runs of Homozygosity. *The American Journal of
1755 Human Genetics* [Internet]. 2019 Oct [cited 2021 Jun 4];105(4):747–62. Available from:
1756 <https://linkinghub.elsevier.com/retrieve/pii/S0002929719303374>
- 1757 62. Pemberton TJ, Absher D, Feldman MW, Myers RM, Rosenberg NA, Li JZ. Genomic Patterns
1758 of Homozygosity in Worldwide Human Populations. *The American Journal of Human
1759 Genetics* [Internet]. 2012 Aug [cited 2022 Nov 30];91(2):275–92. Available from:
1760 <https://linkinghub.elsevier.com/retrieve/pii/S0002929712003230>
- 1761 63. Arauna LR, Bergstedt J, Choin J, Mendoza-Revilla J, Harmant C, Roux M, et al. The genomic

- 1762 landscape of contemporary western Remote Oceanians. *Current Biology* [Internet]. 2022 Nov
1763 [cited 2022 Nov 30];32(21):4565-4575.e6. Available from:
1764 <https://linkinghub.elsevier.com/retrieve/pii/S096098222201377X>
- 1765 64. Hunley K, Dunn M, Lindström E, Reesink G, Terrill A, Healy ME, et al. Genetic and
1766 Linguistic Coevolution in Northern Island Melanesia. Pritchard JK, editor. *PLoS Genet*
1767 [Internet]. 2008 Oct 31 [cited 2022 Nov 30];4(10):e1000239. Available from:
1768 <https://dx.plos.org/10.1371/journal.pgen.1000239>
- 1769 65. Wang C, Szpiech ZA, Degnan JH, Jakobsson M, Pemberton TJ, Hardy JA, et al. Comparing
1770 Spatial Maps of Human Population-Genetic Variation Using Procrustes Analysis. *Statistical*
1771 *Applications in Genetics and Molecular Biology* [Internet]. 2010 Jan 27 [cited 2022 Apr
1772 27];9(1). Available from: [https://www.degruyter.com/document/doi/10.2202/1544-](https://www.degruyter.com/document/doi/10.2202/1544-6115.1493/html)
1773 [6115.1493/html](https://www.degruyter.com/document/doi/10.2202/1544-6115.1493/html)
- 1774 66. Foll M, Shim H, Jensen JD. WFABC: a Wright-Fisher ABC-based approach for inferring
1775 effective population sizes and selection coefficients from time-sampled data. *Mol Ecol Resour*
1776 [Internet]. 2015 Jan [cited 2022 Nov 30];15(1):87–98. Available from:
1777 <https://onlinelibrary.wiley.com/doi/10.1111/1755-0998.12280>
- 1778 67. Ni X, Yuan K, Liu C, Feng Q, Tian L, Ma Z, et al. MultiWaver 2.0: modeling discrete and
1779 continuous gene flow to reconstruct complex population admixtures. *Eur J Hum Genet*
1780 [Internet]. 2019 Jan [cited 2022 Nov 30];27(1):133–9. Available from:
1781 <http://www.nature.com/articles/s41431-018-0259-3>
- 1782 68. Tavaré S, Balding DJ, Griffiths RC, Donnelly P. Inferring coalescence times from DNA
1783 sequence data. *Genetics*. 1997 Feb;145(2):505–18.
- 1784 69. Beaumont MA, Zhang W, Balding DJ. Approximate Bayesian computation in population
1785 genetics. *Genetics*. 2002 Dec;162(4):2025–35.
- 1786 70. Sisson SA, Fan Y, Beaumont MA, editors. *Handbook of Approximate Bayesian Computation*
1787 [Internet]. 1st ed. Boca Raton, Florida : CRC Press, [2019]: Chapman and Hall/CRC; 2018
1788 [cited 2022 Nov 30]. Available from: <https://www.taylorfrancis.com/books/9781439881514>
- 1789 71. Pudlo P, Marin JM, Estoup A, Cornuet JM, Gautier M, Robert CP. Reliable ABC model
1790 choice via random forests. *Bioinformatics* [Internet]. 2016 Mar 15 [cited 2021 Jun
1791 4];32(6):859–66. Available from:
1792 <https://academic.oup.com/bioinformatics/article/32/6/859/1744513>
- 1793 72. Csilléry K, François O, Blum MGB. abc: an R package for approximate Bayesian computation
1794 (ABC): *R package: abc*. *Methods in Ecology and Evolution* [Internet]. 2012 Jun [cited 2021
1795 Jun 4];3(3):475–9. Available from: <http://doi.wiley.com/10.1111/j.2041-210X.2011.00179.x>
- 1796 73. Verdu P, Rosenberg NA. A General Mechanistic Model for Admixture Histories of Hybrid
1797 Populations. *Genetics* [Internet]. 2011 Dec 1 [cited 2021 Jun 4];189(4):1413–26. Available
1798 from: <https://academic.oup.com/genetics/article/189/4/1413/6089061>
- 1799 74. Nei M. Estimation of average heterozygosity and genetic distance from a small number of
1800 individuals. *Genetics* [Internet]. 1978 Jul 20 [cited 2022 Feb 2];89(3):583–90. Available from:
1801 <https://academic.oup.com/genetics/article/89/3/583/5992737>

- 1802 75. Danecek P, Auton A, Abecasis G, Albers CA, Banks E, DePristo MA, et al. The variant call
1803 format and VCFtools. *Bioinformatics* [Internet]. 2011 Aug 1 [cited 2022 Feb 2];27(15):2156–
1804 8. Available from: [https://academic.oup.com/bioinformatics/article-
1805 lookup/doi/10.1093/bioinformatics/btr330](https://academic.oup.com/bioinformatics/article-lookup/doi/10.1093/bioinformatics/btr330)
- 1806 76. Weir BS, Cockerham CC. Estimating F-statistics for the analysis of population-structure.
1807 *Evolution* [Internet]. 1984 Nov [cited 2022 Feb 2];38(6):1358–70. Available from:
1808 <https://onlinelibrary.wiley.com/doi/10.1111/j.1558-5646.1984.tb05657.x>
- 1809 77. Robert CP, Mengersen K, Chen C. Model choice versus model criticism. *Proceedings of the*
1810 *National Academy of Sciences* [Internet]. 2010 Jan 19 [cited 2021 Jun 4];107(3):E5–E5.
1811 Available from: <http://www.pnas.org/cgi/doi/10.1073/pnas.0911260107>
- 1812 78. Patterson KD. Epidemics, Famines, and Population in the Cape Verde Islands, 1580-1900. *The*
1813 *International Journal of African Historical Studies* [Internet]. 1988 [cited 2021 Jun
1814 4];21(2):291. Available from: <https://www.jstor.org/stable/219938?origin=crossref>
- 1815 79. Brooks GE. Cabo Verde: Gulag of the South Atlantic: Racism, Fishing Prohibitions, and
1816 Famines. *Hist Afr*. 2006;33:101–35.
- 1817 80. Martin AR, Gignoux CR, Walters RK, Wojcik GL, Neale BM, Gravel S, et al. Human
1818 Demographic History Impacts Genetic Risk Prediction across Diverse Populations. *The*
1819 *American Journal of Human Genetics* [Internet]. 2017 Apr [cited 2022 Apr 8];100(4):635–49.
1820 Available from: <https://linkinghub.elsevier.com/retrieve/pii/S0002929717301076>
- 1821 81. Busby GB, Band G, Si Le Q, Jallow M, Bougama E, Mangano VD, et al. Admixture into and
1822 within sub-Saharan Africa. *eLife* [Internet]. 2016 Jun 21 [cited 2022 Feb 2];5:e15266.
1823 Available from: <https://elifesciences.org/articles/15266>
- 1824 82. Ramachandran S, Deshpande O, Roseman CC, Rosenberg NA, Feldman MW, Cavalli-Sforza
1825 LL. Support from the relationship of genetic and geographic distance in human populations for
1826 a serial founder effect originating in Africa. *Proc Natl Acad Sci USA* [Internet]. 2005 Nov
1827 [cited 2022 Nov 30];102(44):15942–7. Available from:
1828 <https://pnas.org/doi/full/10.1073/pnas.0507611102>
- 1829 83. Bradburd GS, Ralph PL, Coop GM. A Spatial Framework for Understanding Population
1830 Structure and Admixture. Slatkin M, editor. *PLoS Genet* [Internet]. 2016 Jan 15 [cited 2022
1831 Nov 30];12(1):e1005703. Available from: <https://dx.plos.org/10.1371/journal.pgen.1005703>
- 1832 84. Gneccchi-Ruscione GA, Jeong C, De Fanti S, Sarno S, Trancucci M, Gentilini D, et al. The
1833 genomic landscape of Nepalese Tibeto-Burmans reveals new insights into the recent peopling
1834 of Southern Himalayas. *Sci Rep* [Internet]. 2017 Dec [cited 2022 Nov 30];7(1):15512.
1835 Available from: <http://www.nature.com/articles/s41598-017-15862-z>
- 1836 85. Korunes KL, Soares-Souza GB, Bobrek K, Tang H, Araújo II, Goldberg A, et al. Sex-biased
1837 admixture and assortative mating shape genetic variation and influence demographic inference
1838 in admixed Cabo Verdeans. Hernandez R, editor. *G3 Genes|Genomes|Genetics* [Internet].
1839 2022 Sep 30 [cited 2023 Jan 20];12(10):jkac183. Available from:
1840 <https://academic.oup.com/g3journal/article/doi/10.1093/g3journal/jkac183/6647844>
- 1841 86. Zaitlen N, Huntsman S, Hu D, Spear M, Eng C, Oh SS, et al. The Effects of Migration and
1842 Assortative Mating on Admixture Linkage Disequilibrium. *Genetics* [Internet]. 2017 Jan 1

- 1843 [cited 2021 Jun 4];205(1):375–83. Available from:
1844 <https://academic.oup.com/genetics/article/205/1/375/6095598>
- 1845 87. Versluys TMM, Mas-Sandoval A, Flintham EO, Savolainen V. Why do we pick similar mates,
1846 or do we? *Biol Lett* [Internet]. 2021 Nov [cited 2022 Feb 2];17(11):20210463. Available from:
1847 <https://royalsocietypublishing.org/doi/10.1098/rsbl.2021.0463>
- 1848 88. Fortes-Lima C, Bybjerg-Grauholm J, Marin-Padrón LC, Gomez-Cabezas EJ, Bækvad-Hansen
1849 M, Hansen CS, et al. Exploring Cuba’s population structure and demographic history using
1850 genome-wide data. *Sci Rep* [Internet]. 2018 Dec [cited 2021 Jun 4];8(1):11422. Available
1851 from: <http://www.nature.com/articles/s41598-018-29851-3>
- 1852 89. Chaudenson R, Mufwene SS. *Creolization of language and culture*. London ; New York:
1853 Routledge; 2001. 340 p.
- 1854 90. Cooper F, Holt TC, Scott RJ. *Beyond slavery: explorations of race, labor, and citizenship in
1855 postemancipation societies*. Chapel Hill: University of North Carolina Press; 2000. 198 p.
- 1856 91. Goldberg A, Verdu P, Rosenberg NA. Autosomal Admixture Levels Are Informative About
1857 Sex Bias in Admixed Populations. *Genetics* [Internet]. 2014 Nov 1 [cited 2021 Jun
1858 4];198(3):1209–29. Available from:
1859 <https://academic.oup.com/genetics/article/198/3/1209/6065659>
- 1860 92. The 1000 Genomes Project Consortium. A global reference for human genetic variation.
1861 *Nature*. 2015 Oct 1;526(7571):68–74.
- 1862 93. Gurdasani D, Carstensen T, Tekola-Ayele F, Pagani L, Tachmazidou I, Hatzikotoulas K, et al.
1863 The African Genome Variation Project shapes medical genetics in Africa. *Nature* [Internet].
1864 2015 Jan 15 [cited 2021 Jun 4];517(7534):327–32. Available from:
1865 <http://www.nature.com/articles/nature13997>
- 1866 94. Manichaikul A, Mychaleckyj JC, Rich SS, Daly K, Sale M, Chen WM. Robust relationship
1867 inference in genome-wide association studies. *Bioinformatics* [Internet]. 2010 Nov 15 [cited
1868 2021 Jun 4];26(22):2867–73. Available from: [https://academic.oup.com/bioinformatics/article-
1869 lookup/doi/10.1093/bioinformatics/btq559](https://academic.oup.com/bioinformatics/article-lookup/doi/10.1093/bioinformatics/btq559)
- 1870 95. Chafe WL, editor. *The Pear stories: cognitive, cultural, and linguistic aspects of narrative
1871 production*. Norwood, N.J: Ablex Pub. Corp; 1980. 327 p. (Advances in discourse processes).
- 1872 96. Croft W. Linguistic Selection: An Utterance-based Evolutionary Theory of Language Change.
1873 *Nordic Journal of Linguistic* [Internet]. 1996 Dec [cited 2021 Jun 4];19(2):99–139. Available
1874 from:
1875 https://www.cambridge.org/core/product/identifier/S0332586500003358/type/journal_article
- 1876 97. R Development Core Team. *R: A language and environment for statistical computing*.
1877 [Internet]. R Foundation for Statistical Computing; 2020. Available from: [http://www.R-proje
1878 ct.org](http://www.R-project.org)
- 1879 98. Paschou P, Ziv E, Burchard EG, Choudhry S, Rodriguez-Cintron W, Mahoney MW, et al.
1880 PCA-Correlated SNPs for Structure Identification in Worldwide Human Populations. Allison
1881 DB, editor. *PLoS Genet* [Internet]. 2007 Sep 21 [cited 2023 Jan 20];3(9):e160. Available
1882 from: <https://dx.plos.org/10.1371/journal.pgen.0030160>

- 1883 99. Purcell S, Neale B, Todd-Brown K, Thomas L, Ferreira MAR, Bender D, et al. PLINK: A
1884 Tool Set for Whole-Genome Association and Population-Based Linkage Analyses. *The*
1885 *American Journal of Human Genetics* [Internet]. 2007 Sep [cited 2021 Jun 4];81(3):559–75.
1886 Available from: <https://linkinghub.elsevier.com/retrieve/pii/S0002929707613524>
- 1887 100. Jakobsson M, Rosenberg NA. CLUMPP: a cluster matching and permutation program for
1888 dealing with label switching and multimodality in analysis of population structure.
1889 *Bioinformatics* [Internet]. 2007 Jul 15 [cited 2021 Jun 4];23(14):1801–6. Available from:
1890 <https://academic.oup.com/bioinformatics/article-lookup/doi/10.1093/bioinformatics/btm233>
- 1891 101. Rosenberg NA. DISTRUCT: a program for the graphical display of population structure.
1892 *Molecular Ecology Notes* [Internet]. 2003 Dec 10 [cited 2021 Jun 4];4(1):137–8. Available
1893 from: <http://doi.wiley.com/10.1046/j.1471-8286.2003.00566.x>
- 1894 102. Morrison ML, Alcalá N, Rosenberg NA. FSTruct: an FST-based tool for measuring ancestry
1895 variation in inference of population structure [Internet]. *Evolutionary Biology*; 2021 Sep [cited
1896 2022 Feb 2]. Available from: <http://biorxiv.org/lookup/doi/10.1101/2021.09.24.461741>
- 1897 103. Maier R, Flegontov P, Flegontova O, Changmai P, Reich D. On the limits of fitting complex
1898 models of population history to genetic data [Internet]. *Evolutionary Biology*; 2022 May [cited
1899 2022 Nov 30]. Available from: <http://biorxiv.org/lookup/doi/10.1101/2022.05.08.491072>
- 1900 104. The International HapMap 3 Consortium. Integrating common and rare genetic variation in
1901 diverse human populations. *Nature*. 2010 Sep;467(7311):52–8.
- 1902 105. Szpiech ZA, Blant A, Pemberton TJ. GARLIC: Genomic Autozygosity Regions Likelihood-
1903 based Inference and Classification. Berger B, editor. *Bioinformatics* [Internet]. 2017 Jul 1
1904 [cited 2021 Jun 4];33(13):2059–62. Available from:
1905 <https://academic.oup.com/bioinformatics/article/33/13/2059/3000374>
- 1906 106. Maples BK, Gravel S, Kenny EE, Bustamante CD. RFMix: A Discriminative Modeling
1907 Approach for Rapid and Robust Local-Ancestry Inference. *The American Journal of Human*
1908 *Genetics* [Internet]. 2013 Aug [cited 2022 Feb 2];93(2):278–88. Available from:
1909 <https://linkinghub.elsevier.com/retrieve/pii/S0002929713002899>
- 1910 107. Snyder JP. Map projections--a working manual [Internet]. 1987 [cited 2022 Feb 2]. Available
1911 from: <https://purl.fdlp.gov/GPO/gpo93084>
- 1912 108. Fisher RA. Darwinian evolution of mutations. *Eugen Rev*. 1922 Apr;14(1):31–4.
- 1913 109. Wright S. Evolution in Mendelian Populations. *Genetics*. 1931 Mar;16(2):97–159.
- 1914 110. Buzbas EO, Verdu P. Inference on admixture fractions in a mechanistic model of recurrent
1915 admixture. *Theoretical Population Biology* [Internet]. 2018 Jul [cited 2022 Feb 2];122:149–57.
1916 Available from: <https://linkinghub.elsevier.com/retrieve/pii/S0040580918300662>
- 1917 111. Pritchard JK, Seielstad MT, Perez-Lezaun A, Feldman MW. Population growth of human Y
1918 chromosomes: a study of Y chromosome microsatellites. *Molecular Biology and Evolution*
1919 [Internet]. 1999 Dec 1 [cited 2023 Jan 20];16(12):1791–8. Available from:
1920 <https://academic.oup.com/mbe/article-lookup/doi/10.1093/oxfordjournals.molbev.a026091>
- 1921 112. Raynal L, Marin JM, Pudlo P, Ribatet M, Robert CP, Estoup A. ABC random forests for

- 1922 Bayesian parameter inference. Stegle O, editor. *Bioinformatics* [Internet]. 2019 May 15 [cited
1923 2022 Feb 2];35(10):1720–8. Available from:
1924 <https://academic.oup.com/bioinformatics/article/35/10/1720/5132692>
- 1925 113. Jay F, Boitard S, Austerlitz F. An ABC Method for Whole-Genome Sequence Data: Inferring
1926 Paleolithic and Neolithic Human Expansions. Hernandez R, editor. *Molecular Biology and*
1927 *Evolution* [Internet]. 2019 Jul 1 [cited 2022 Feb 2];36(7):1565–79. Available from:
1928 <https://academic.oup.com/mbe/article/36/7/1565/5345566>
- 1929 114. Pereira L, Černý V, Cerezo M, Silva NM, Hájek M, Vašíková A, et al. Linking the sub-
1930 Saharan and West Eurasian gene pools: maternal and paternal heritage of the Tuareg nomads
1931 from the African Sahel. *Eur J Hum Genet*. 2010 Aug;18(8):915–23.
- 1932 115. Henn BM, Botigué LR, Gravel S, Wang W, Brisbin A, Byrnes JK, et al. Genomic Ancestry of
1933 North Africans Supports Back-to-Africa Migrations. Schierup MH, editor. *PLoS Genet*
1934 [Internet]. 2012 Jan 12 [cited 2022 Feb 2];8(1):e1002397. Available from:
1935 <https://dx.plos.org/10.1371/journal.pgen.1002397>
- 1936
1937

1938
1939
1940
1941
1942
1943
1944
1945
1946
1947
1948
1949
1950
1951
1952

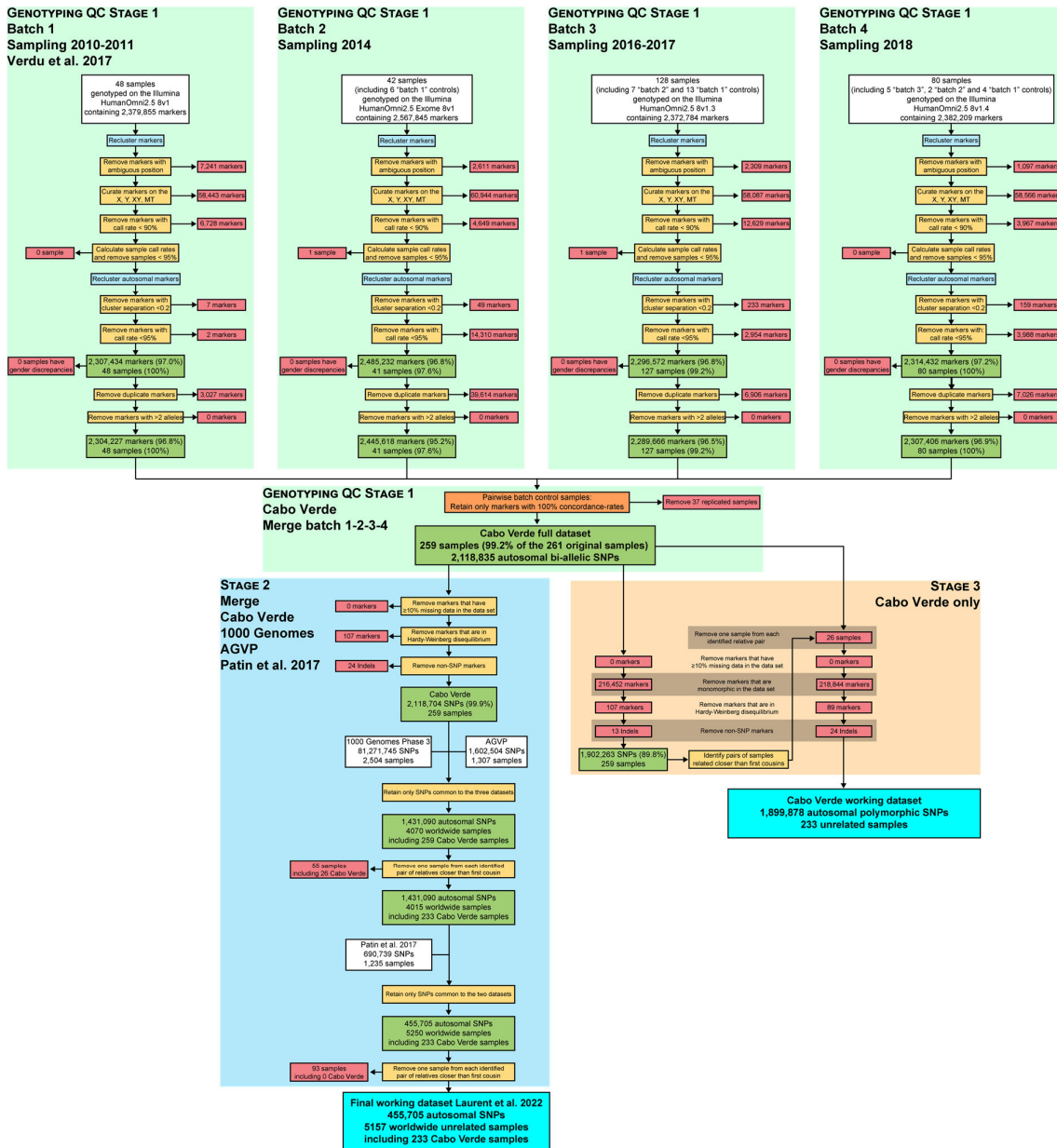
APPENDIX 1

1.a. Quality Control and genomic datasets merging procedures

Appendix 1-figure 1:

Quality-control and datasets merging procedures.

Quality controls at the genotyping call level (Stage 1) were conducted with Illumina's GenomeStudio® software Genotyping Module. Cabo Verde original DNA samples have been collected during six separate field-trips between 2010 and 2018, genotyped in four batches using four different versions of the Illumina Omni2.5Million Beadchip genotyping array. The resulting dataset was merged with 2,504 worldwide samples from the 1000 Genomes Project Phase 3 (1000 Genomes Project Consortium, 2015); with 1,307 continental African samples from the African Genome Variation Project (EGA accession number EGAD00001000959, (93)); and with 1,235 African samples from (7) (EGA accession number EGAS00001002078). We retained only autosomal SNPs common to all datasets, and excluded one individual for each pair of individuals related at the 2nd degree (at least one grand-parent in common) as inferred with KING (94), following previous procedures (23).



1953

1954 **1.b. Summary statistics for ABC inference**

1955

1956 We used *MetHis* (45) summary statistics calculation tools to calculate, for each simulated dataset, a
1957 vector of 42 summary statistics listed with references in main-text **Table 3**. We computed the same 42
1958 summary-statistics using the real data set for each Cabo Verdean island of birth and for all Cabo Verde-
1959 born individuals grouped in a single population, respectively. Henceforth, Population H refers to the
1960 admixed population simulated with *MetHis* corresponding, in turn, to each Cabo Verdean island of birth
1961 and the 225 Cabo Verde-born individuals grouped in a single population.

1962

1963 *Within-population summary statistics*

1964 We computed the mean and variance of interindividual ASD (46) within Population H. Furthermore,
1965 we computed the mean and variance of average heterozygosities (where the average is taken over inde-
1966 pendent SNPs for each individual and then over individuals within an island) as in (74). We also calcu-
1967 lated the mean and variance of inbreeding coefficient F (75). Intuitively, we *a priori* expected these
1968 statistics to be particularly sensitive to genetic-drift and possibly informative specifically about repro-
1969 ductive population size N_e parameters in our scenarios.

1970

1971 *Admixture patterns summary statistics*

1972 We analytically showed previously that the distribution of admixture fractions across individuals within
1973 admixed populations carried identifiable information about the history of admixture (73,110). Further-
1974 more, we showed with *MetHis* (45) that summary statistics describing this distribution could be suc-
1975 cessfully used in ABC inferences.

1976 Therefore, we considered the 16 admixture-related summary statistics describing the mode, the first
1977 four moments (as mean, variance, skewness, and kurtosis), and the minimum, maximum, and all deciles
1978 of the ASD-MDS admixture estimates of individual admixture fractions from the African source popu-
1979 lation (or one minus that from the European source in a two-source admixture scenario). ASD-MDS
1980 admixture estimates were obtained as described in **Material and Methods 2.**, represented schematically
1981 in **Appendix 1-figure 2**, considering the 2D-MDS centroids, respectively, of the African and European
1982 sources, and the projection on the line joining these two points of each Population H individual. Fur-
1983 thermore, to further capture the ASD-MDS admixture patterns, we calculated the distribution of the
1984 angles between population H's individuals and the source populations' centroids on the 2D ASD-MDS.
1985 We then considered as summary-statistics for ABC inference the mode, the first four moments (as mean,
1986 variance, skewness, and kurtosis), the minimum and maximum, and the deciles of this distribution of
1987 angles in radian (**Appendix 1-figure 2**).

1988

1989 *Among-populations summary statistics*

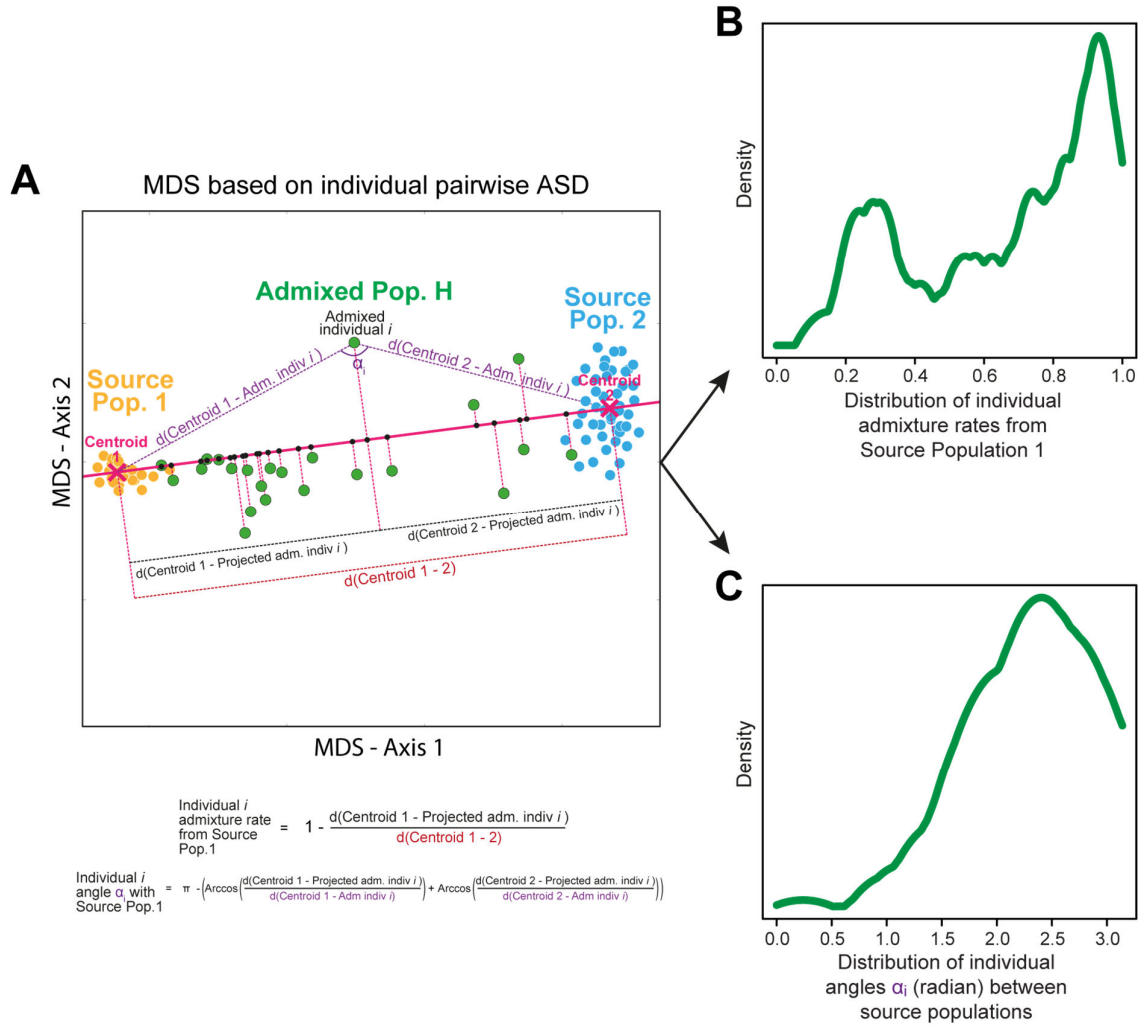
1990 Using *MetHis* summary-statistic calculation tools, we computed F_{ST} values between either Source pop-
1991 ulation (African or European) and Population H following (76). We also computed the mean ASD be-
1992 tween the Source Population and Population H. Finally, we computed the f_3 statistic (50) with African
1993 and European populations as the two sources and Population H as the targeted admixed population.

1994

1995

1996 **Appendix 1-figure 2:**
 1997 **Schematic representation of the ASD-MDS estimates of individual admixture proportions and angles, also used as sum-**
 1998 **mary statistics for ABC inference and implemented in *MetHis* summary-statistic calculation tools.**
 1999 All the panels of the figure are schematic.

2000
 2001



2002
 2003

2004 **1.c. Prior-ABC checking**

2005

2006 Before conducting any ABC inference, we needed to statistically evaluate whether the 42 summary-
2007 statistics calculated on the observed datasets were within the range of the sets of summary statistics
2008 computed on the simulated datasets with *MetHis*. To do so, we considered each Cabo Verdean birth-
2009 island and Cabo Verde as a whole, in turn as population H, and conducted the following three-step
2010 procedure whose results are provided in **Appendix 1-figure 3, Appendix 1-figure3-resource figure 1-**
2011 **10**.

2012 (i) first, we conducted a goodness-of-fit test between the 40,000 vectors of summary statistics com-
2013 puted for each simulation under the four competing scenarios, and the vector of observed summary
2014 statistics with the *gfit* function of the R package *abc* (72), with 1000 random repetitions and a 1% toler-
2015 ance level (**Appendix 1-figure 3A**).

2016 (ii) second, we computed a Principal Component Analysis considering each simulation as an indi-
2017 vidual and all the summary statistics as observed variables. By projecting the observed summary statis-
2018 tics onto this PCA along the first three PCA axes of variation (with the *princomp* function in R), we
2019 visually evaluated whether the observed data fell into the range of simulated statistics along the major
2020 PCA axes (**Appendix 1-figure 3B-C**).

2021 (iii) finally, we present the distribution of each summary statistic obtained for the 40,000 simula-
2022 tions and the observed value, for each summary statistic and each Cabo Verdean birth-island and for
2023 Cabo Verde as a whole, separately (**Appendix 1-figure 3-resource figure 1-10**).

2024

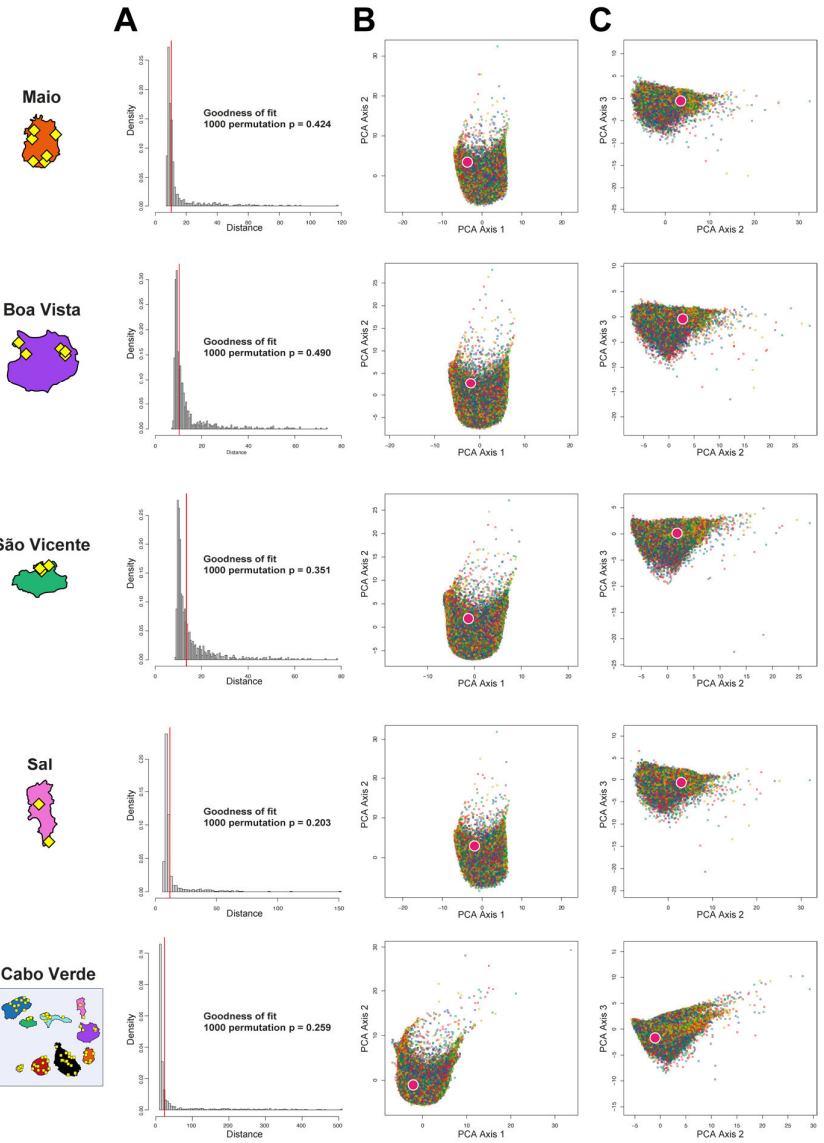
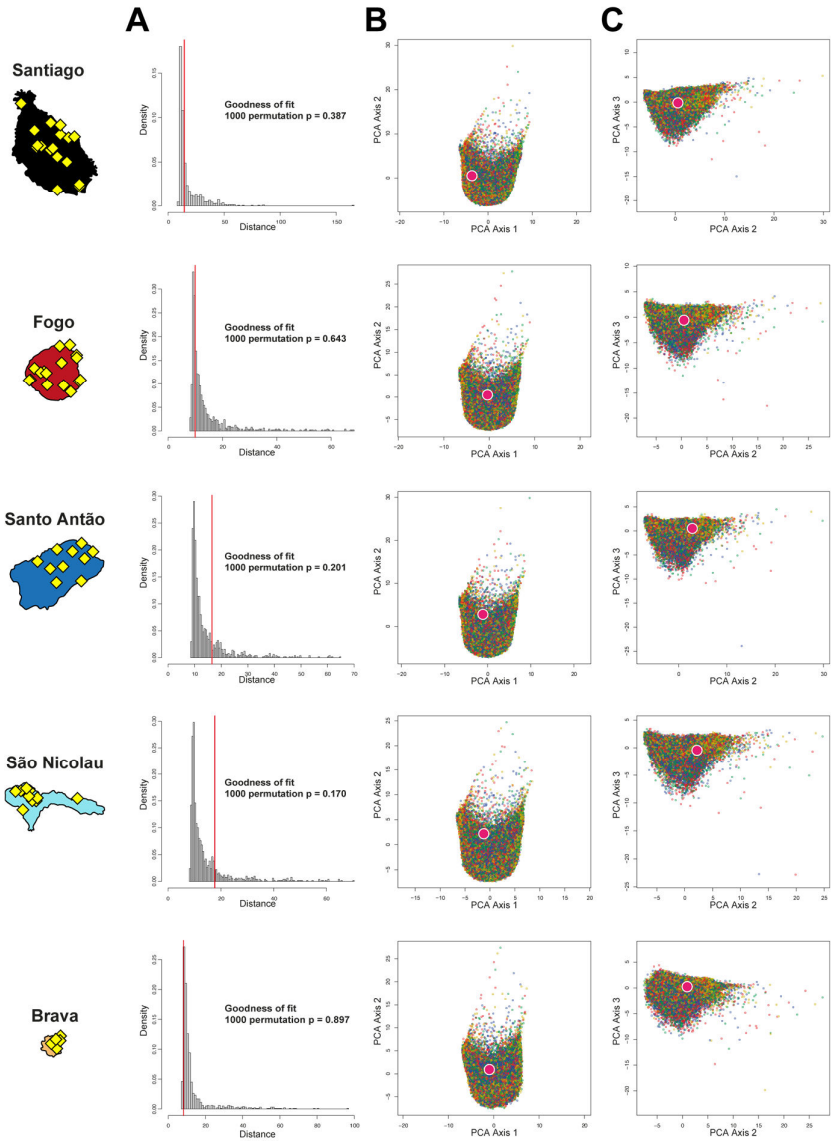
2025 **Appendix 1-figure 3:**

2026 **ABC Prior-checking for *MetHis* simulations for each island separately.**

2027 10,000 simulations are conducted under each four competing scenarios of historical admixture considered in Random-Forest
2028 ABC scenario-choice (see **Figure 6**). **A) Goodness-of-Fit tests:** we use as goodness-of-fit statistic the median of the distance
2029 between one target vector of 42 summary-statistics and the vectors of 42 statistics obtained for the 1% simulations in the 40,000
2030 simulations reference table that are closest to the target (as identified by simple rejection (111)). Results obtained with the
2031 observed data as target are indicated in the vertical red line. Null-distribution of the goodness-of-fit statistics as histograms are
2032 obtained by considering as target in-turn 1000 random simulations as pseudo-observed data, for each island and for the 225
2033 Cabo Verde-born individuals grouped in a single random-mating population, separately. **B)** First two axes of a principal com-
2034 ponent analysis performed on the 42 summary-statistics obtained for 40,000 simulations per island (10,000 simulations for
2035 each of four competing-scenarios). Each point corresponds to a single simulation colored per scenario: simulations under Sce-
2036 nario 1 are in blue; Scenario 2 in green; Scenario 3 in red; and Scenario 4 in yellow (**Figure 6-7**). The pink white-circled dot
2037 corresponds to the vector of summary-statistics from the observed dataset. **C)** Axes 1 and 3 of the same PCA projection as in
2038 panel **B**.

2039

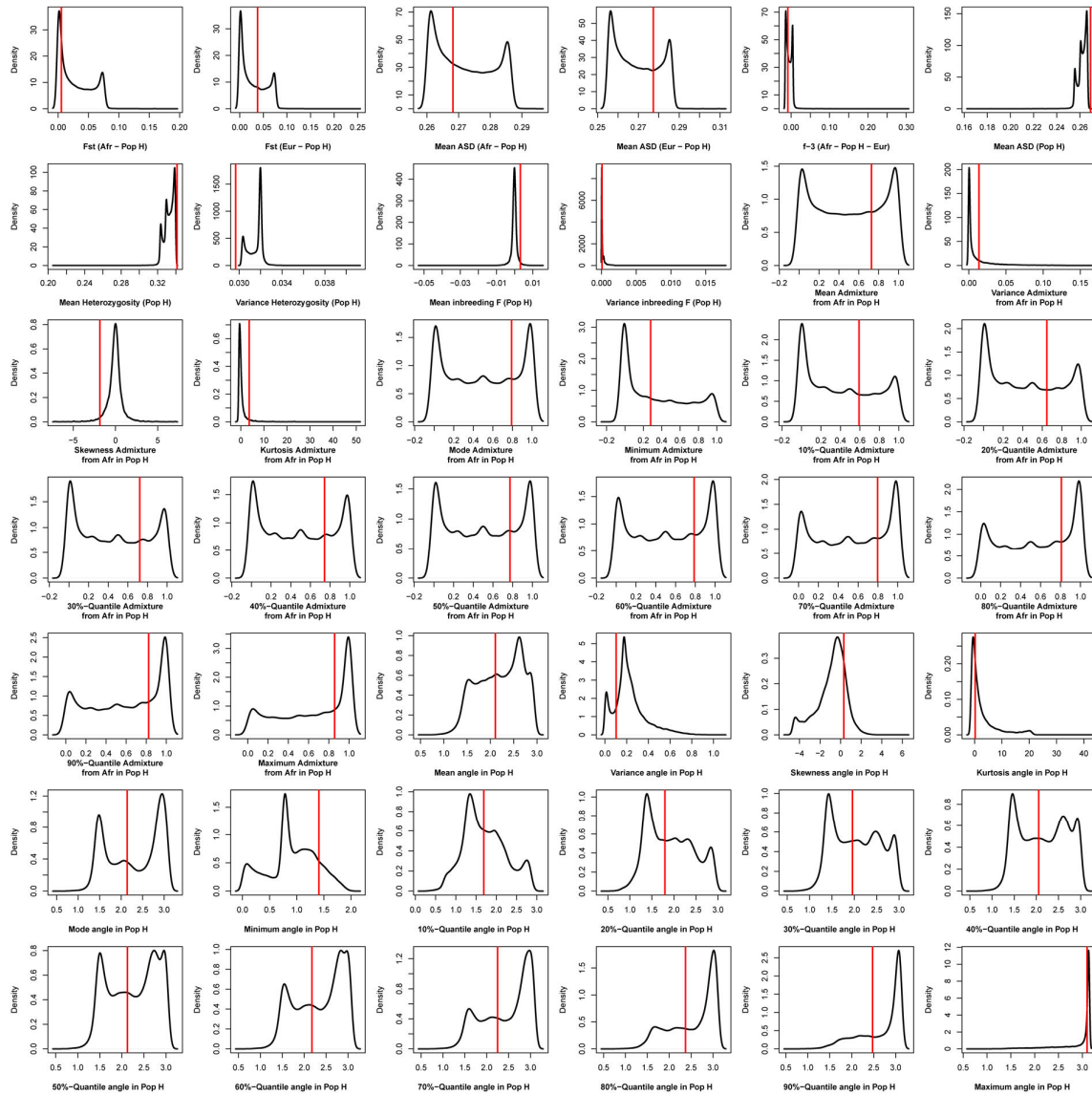
2040



2042
2043
2044
2045
2046

Appendix 1-figure 3-resource figure 1:

Density distributions (black line) of each of 42 summary-statistics obtained from 40,000 simulations, 10,000 under each of four competing scenarios for Santiago, compared to the observed statistic obtained in this island (red vertical line). The four scenarios are synthetically described in Figure 6 and the 42 summary-statistics in Table 3.



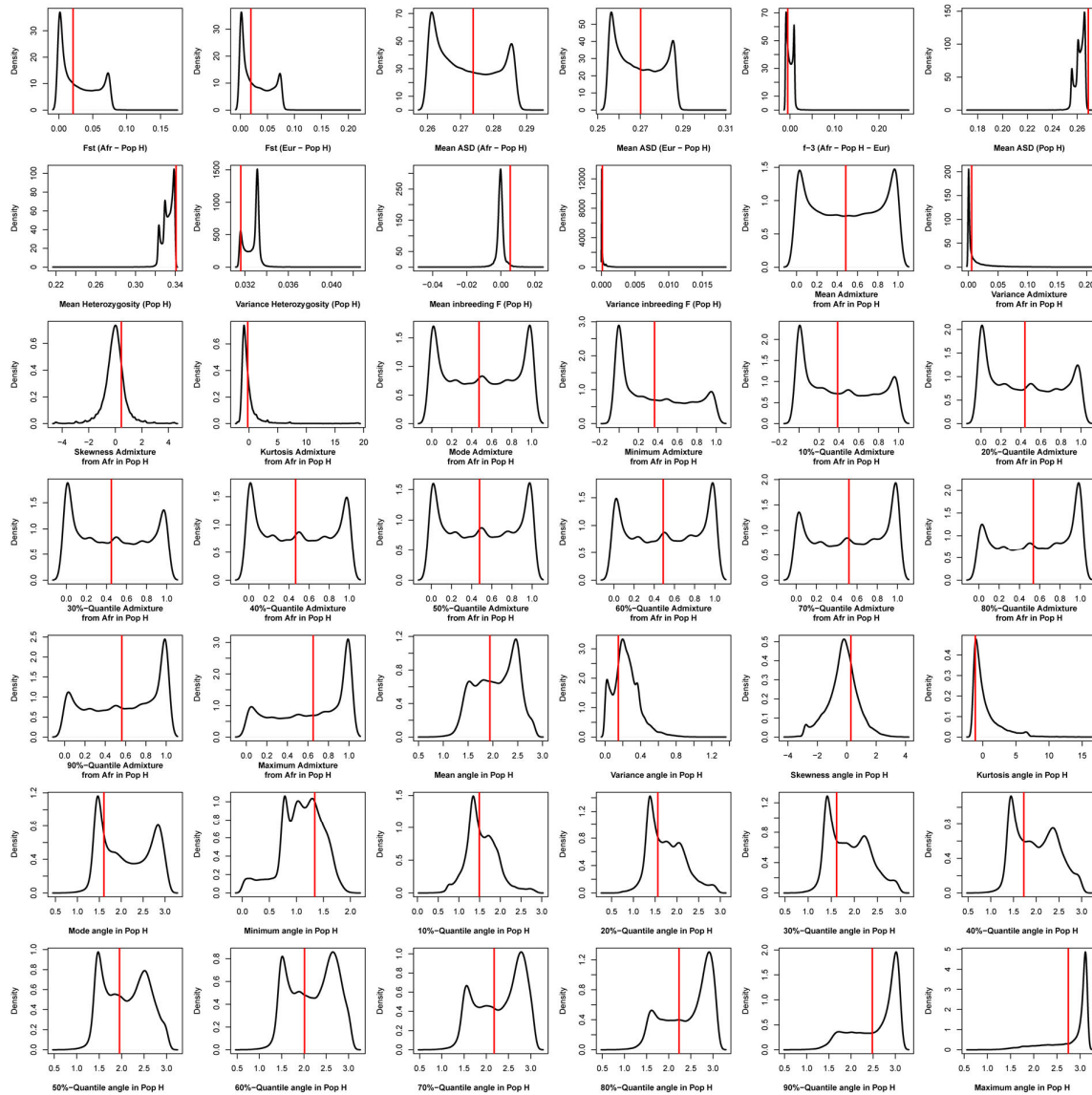
2047
2048
2049

2050
2051
2052
2053
2054

Appendix 1-figure 3-resource figure 2:

Density distributions (black line) of each of 42 summary-statistics obtained from 40,000 simulations, 10,000 under each of four competing scenarios for Fogo, compared to the observed statistic obtained in this island (red vertical line).

The four scenarios are synthetically described in **Figure 6** and the 42 summary-statistics in **Table 3**.



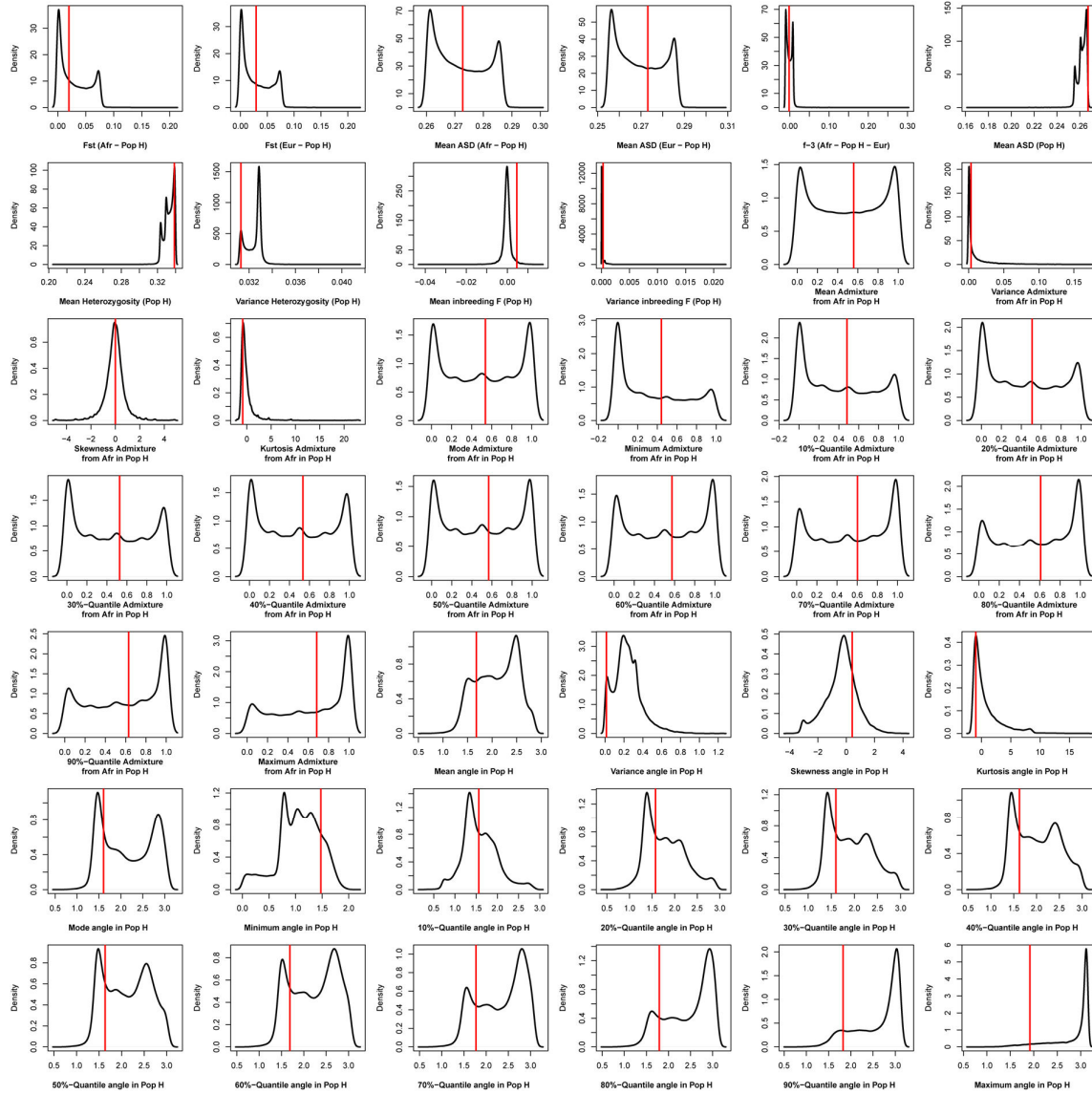
2055
2056
2057

2058
2059
2060
2061
2062
2063

Appendix 1-figure 3-resource figure 3:

Density distributions (black line) of each of 42 summary-statistics obtained from 40,000 simulations, 10,000 under each of four competing scenarios for Santo Antão, compared to the observed statistic obtained in this island (red vertical line).

The four scenarios are synthetically described in **Figure 6** and the 42 summary-statistics in **Table 3**.

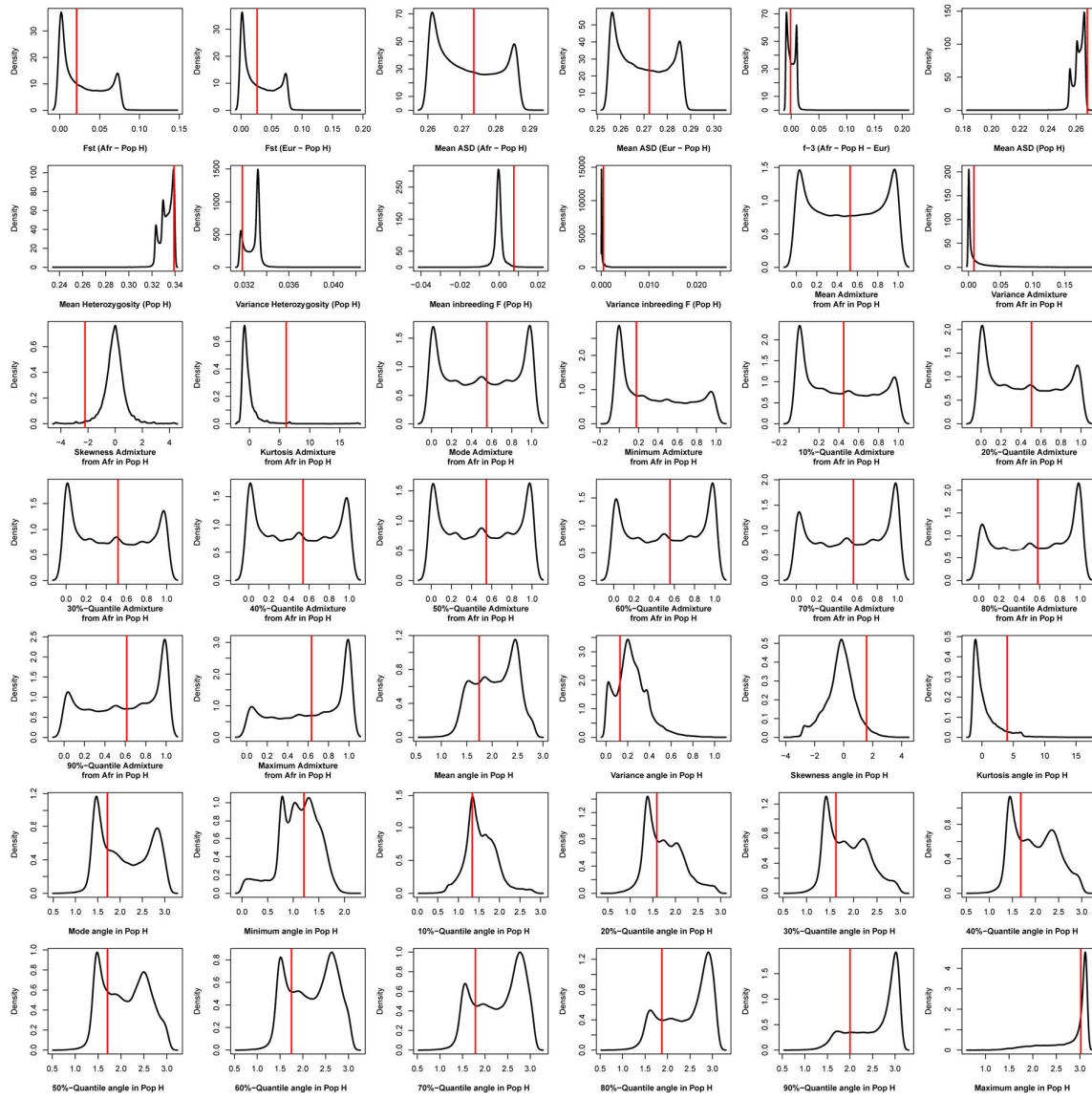


2064
2065
2066

2067
2068
2069
2070
2071

Appendix 1-figure 3-resource figure 4:

Density distributions (black line) of each of 42 summary-statistics obtained from 40,000 simulations, 10,000 under each of four competing scenarios for São Nicolau, compared to the observed statistic obtained in this island (red vertical line). The four scenarios are synthetically described in Figure 6 and the 42 summary-statistics in Table 3.



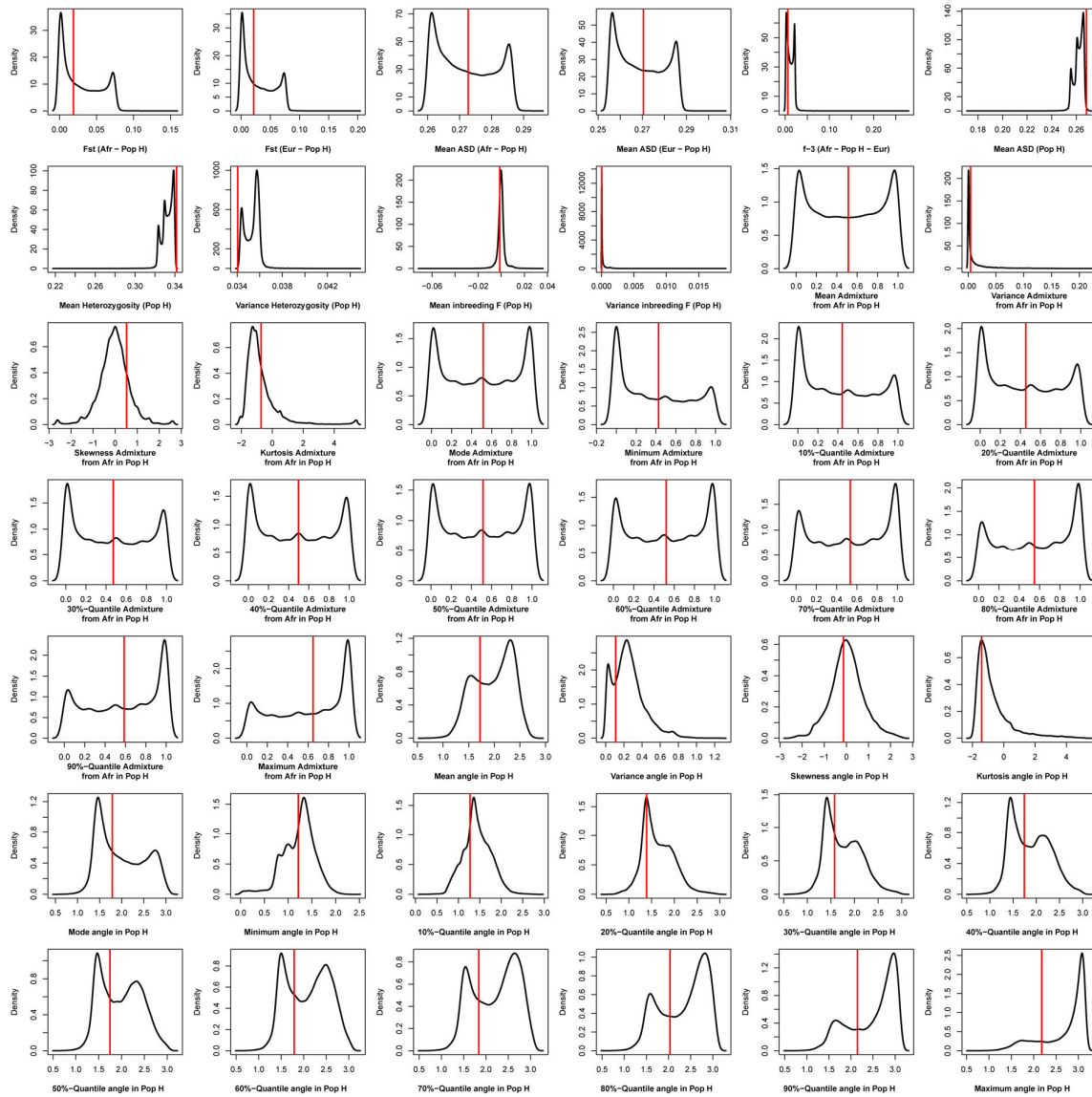
2072
2073

2074
2075
2076
2077
2078

Appendix 1-figure 3-resource figure 5:

Density distributions (black line) of each of 42 summary-statistics obtained from 40,000 simulations, 10,000 under each of four competing scenarios for Brava, compared to the observed statistic obtained in this island (red vertical line).

The four scenarios are synthetically described in **Figure 6** and the 42 summary-statistics in **Table 3**.



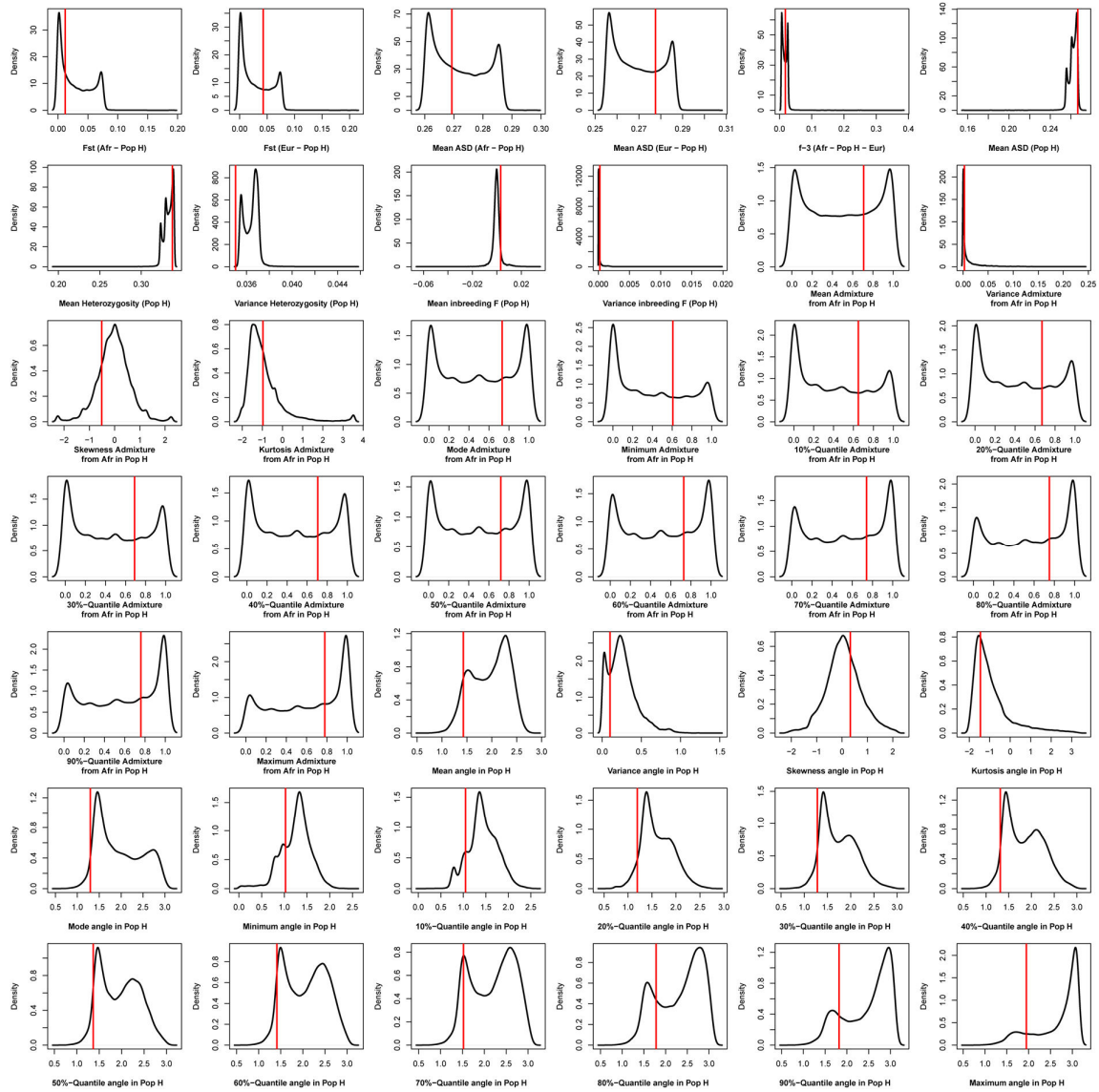
2079
2080
2081

2082
2083
2084
2085
2086

Appendix 1-figure 3-resource figure 6:

Density distributions (black line) of each of 42 summary-statistics obtained from 40,000 simulations, 10,000 under each of four competing scenarios for Maio, compared to the observed statistic obtained in this island (red vertical line).

The four scenarios are synthetically described in **Figure 6** and the 42 summary-statistics in **Table 3**.

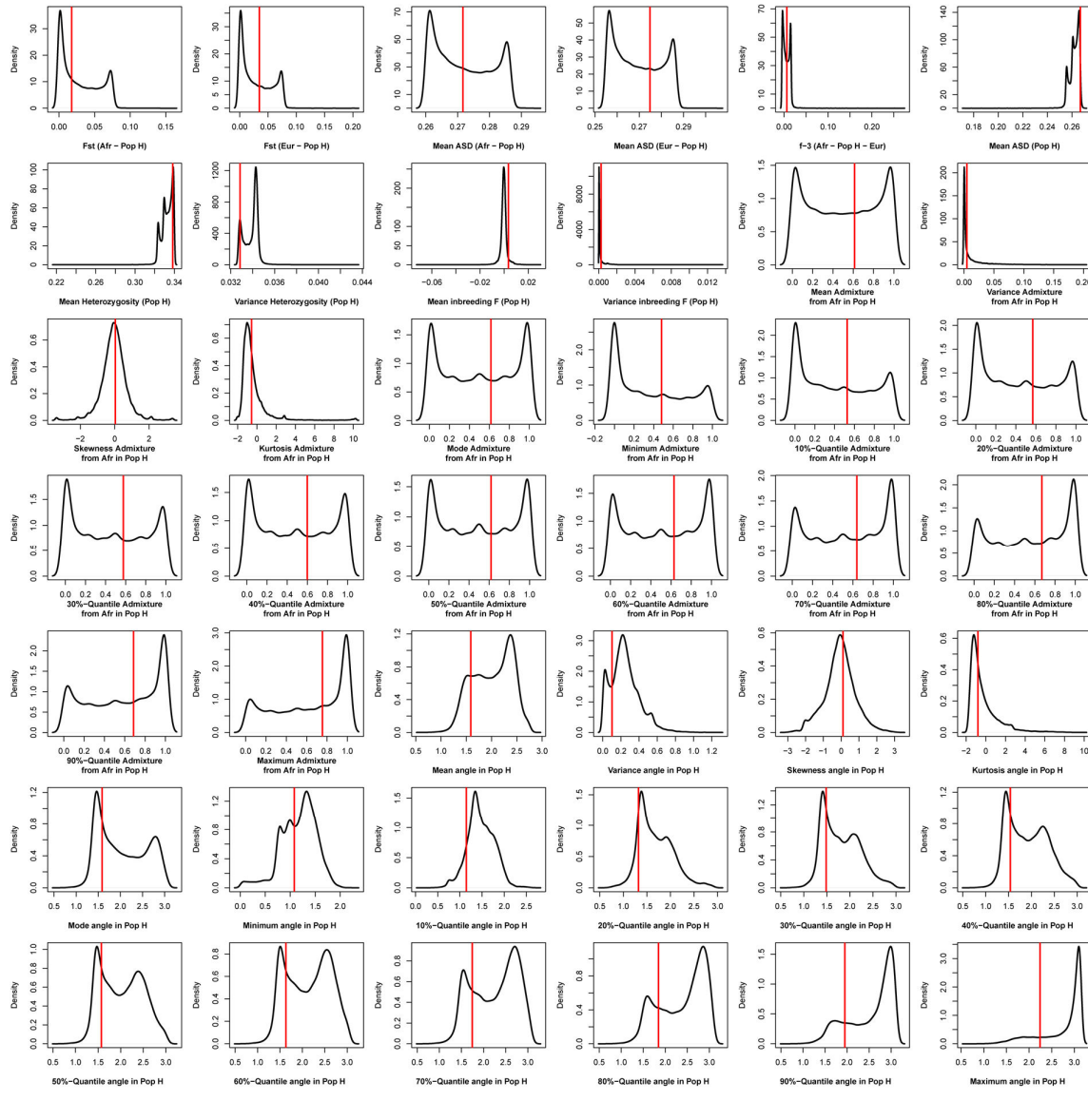


2087
2088

2089
2090
2091
2092
2093

Appendix 1-figure 3-resource figure 7:

Density distributions (black line) of each of 42 summary-statistics obtained from 40,000 simulations, 10,000 under each of four competing scenarios for Boa Vista, compared to the observed statistic obtained in this island (red vertical line). The four scenarios are synthetically described in Figure 6 and the 42 summary-statistics in Table 3.

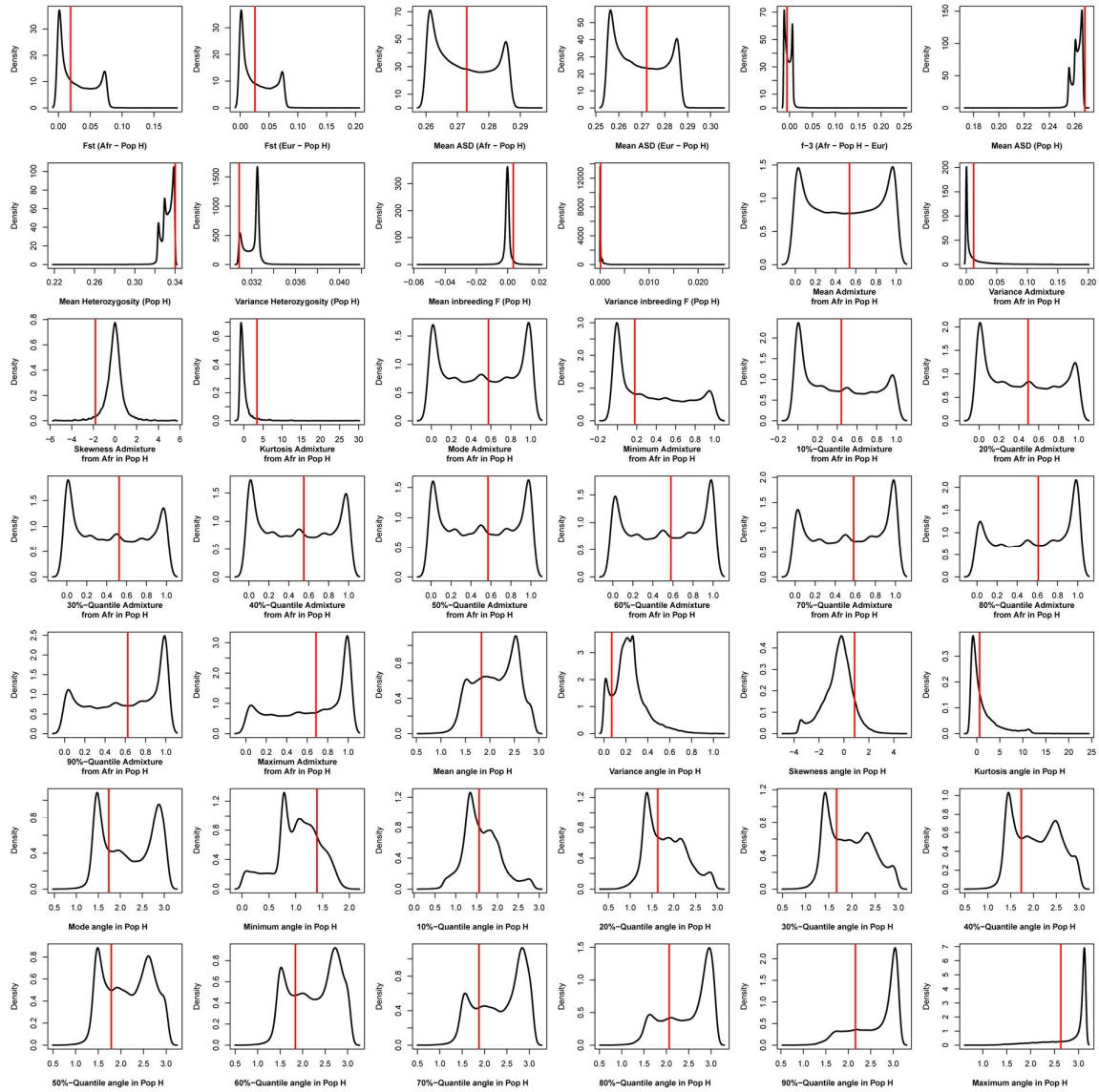


2094
2095

2096
2097
2098
2099
2100

Appendix 1-figure 3-resource figure 8:

Density distributions (black line) of each of 42 summary-statistics obtained from 40,000 simulations, 10,000 under each of four competing scenarios for São Vicente, compared to the observed statistic obtained in this island (red vertical line). The four scenarios are synthetically described in Figure 6 and the 42 summary-statistics in Table 3.



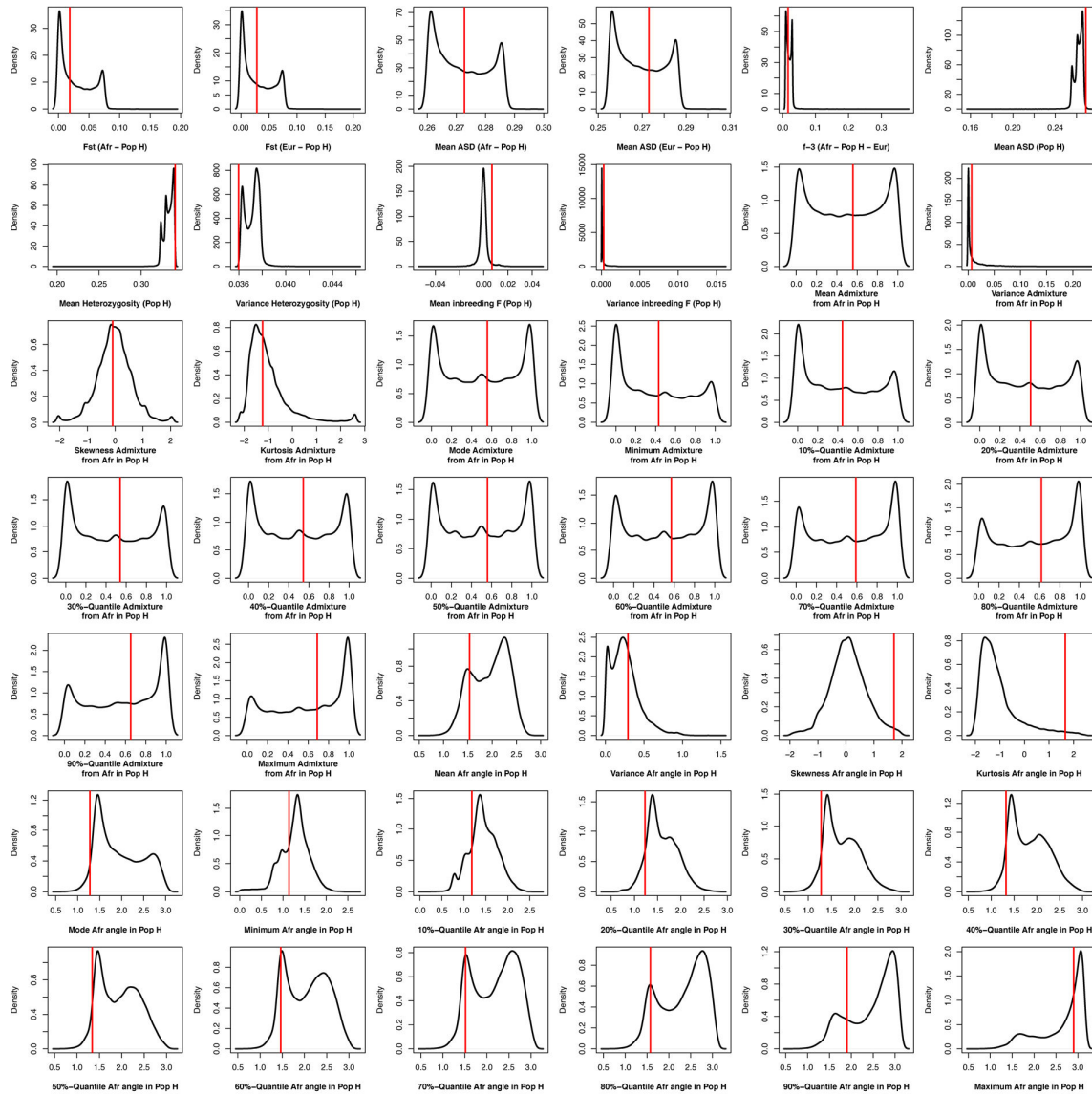
2101
2102

2103
2104
2105
2106
2107

Appendix 1-figure 3-resource figure 9:

Density distributions (black line) of each of 42 summary-statistics obtained from 40,000 simulations, 10,000 under each of four competing scenarios for Sal, compared to the observed statistic obtained in this island (red vertical line).

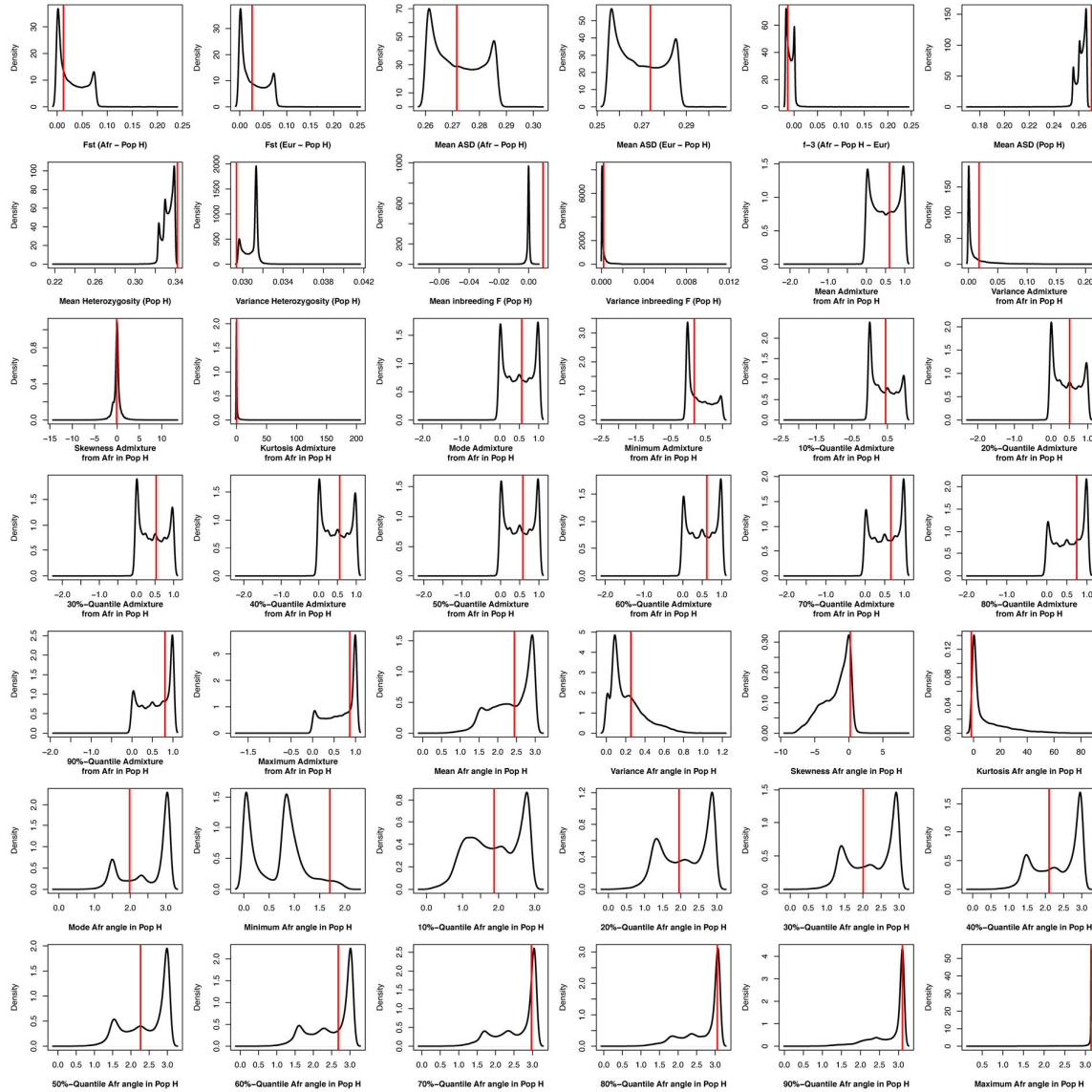
The four scenarios are synthetically described in **Figure 6** and the 42 summary-statistics in **Table 3**.



2108
2109

2110 **Appendix 1-figure 3-resource figure 10:**
 2111 **Density distributions (black line) of each of 42 summary-statistics obtained from 40,000 simulations, 10,000 under each**
 2112 **of four competing scenarios for the 225 Cabo Verde-born individuals grouped in a single random-mating population,**
 2113 **compared to the observed statistic obtained in this dataset (red vertical line).**

2114 The four scenarios are synthetically described in **Figure 6** and the 42 summary-statistics in **Table 3**.
 2115



2116
 2117

2118 **1.d. Random-Forest (RF) ABC scenario-choice cross-validation**

2119

2120 We used the Random-Forest ABC algorithm implemented in the *abcrf* package in R (71,112) for sce-
2121 nario-choice, as in the *MetHis*-ABC pipeline previously described (45). Random-Forest classification
2122 has been shown to allow for robust ABC scenario-choice with relatively small numbers of simulations
2123 and, most importantly, to be unaffected by correlations among summary statistics; thus outperforming
2124 local linear regression classically used in ABC scenario-choice (69). Here, we considered the same prior
2125 probability (25%) for the four competing scenarios.

2126 First, for each island separately, we used the *abcrf* function in this R package to conduct ABC
2127 scenario-choice cross-validation. Each of 40,000 simulations served in-turn as pseudo-observed data
2128 and the remaining 39,999 simulations as training (**Appendix 1-figure 4A**), using 1000 decision trees in
2129 the Random-Forest. We visually checked that prior error rates (the rates of erroneously assigned sce-
2130 nario in the cross-validation) were minimized for this number of decision trees, using the *err.abcrf* func-
2131 tion in the same R package. Each summary-statistic's importance to the cross-validation accurate deci-
2132 sion was calculated and plotted using the *abcrf* function (**Appendix 1-figure 4B**).

2133 Second, for each birth-island and for Cabo Verde as a whole, separately, we used the *predict.abcrf*
2134 function on the trained Random Forest with all simulations in the reference table, to determine which
2135 competing scenario produced simulations whose summary statistics most resembled those from the ob-
2136 served data. We then estimate the posterior probability of accurately finding such winning scenario in
2137 our framework (indicated as “Post. prob. Scen.” in **Figure 7B**).

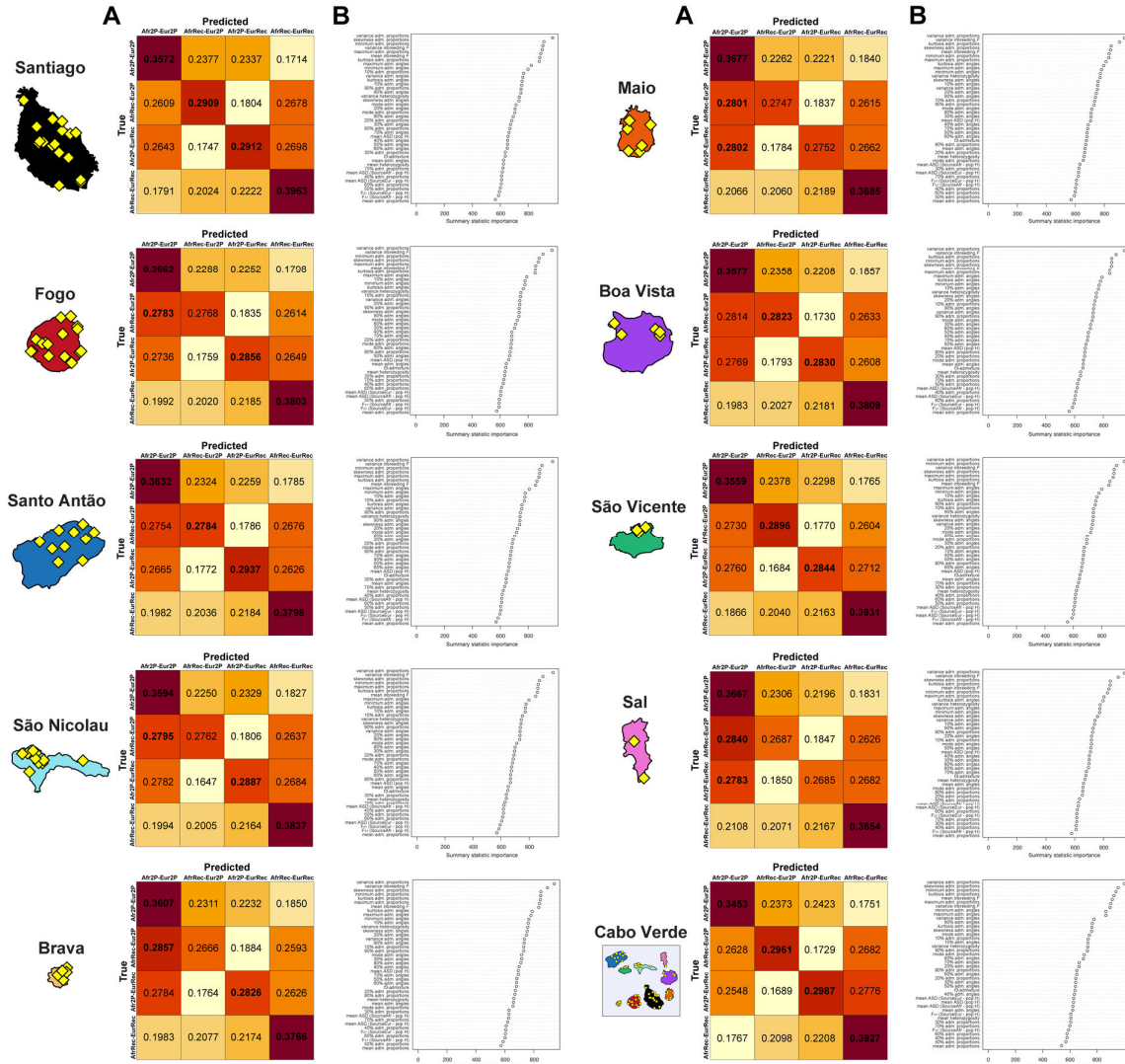
2138

2139
2140
2141
2142
2143
2144
2145
2146
2147
2148

Appendix 1-figure 4:

Random-Forest ABC scenario-choice cross validation results and summary-statistics' importance.

We considered four competing scenarios as described in **Material and Methods 7** and in **Figure 6**, with associated prior parameter distributions in **Table 2** and 42 summary-statistics described in **Table 3**, for each Cabo Verdean birth-island and the 225 Cabo Verde-born individuals grouped in a single random mating population, separately. Cross-validation results are obtained by conducting RF scenario-choices using, in-turn, each 40,000 simulations (10,000 per competing scenario) as pseudo-observed data and the remaining 39,999 simulations as the reference table. We considered 1,000 trees in the random-forest for each analysis. Cross-validation results and associated summary-statistics' importance for the RF decisions are obtained from the function *abcrf* in the R package *abcrf*.



2149
2150

2151 1.e. Neural Network ABC posterior parameter inference procedures

2152

2153 While RF-ABC scenario-choice procedures are specifically designed to accurately work with a rela-
2154 tively small number of simulations compared to classical regression ABC (69,71), posterior joint-esti-
2155 mations of all scenario-parameters under the winning scenario remain difficult in Random-Forest
2156 (45,112). In this context, our previous benchmarking of various ABC posterior-parameter estimation
2157 under the *MetHis* framework showed that Neural Network ABC joint parameter estimations outper-
2158 formed other approaches (45). However, Neural Network ABC posterior parameter inferences have
2159 been shown in multiple previous investigations, including ours with *MetHis*, to require substantial
2160 amounts of information in the reference table to perform satisfactorily (45,72,113). Therefore, we con-
2161 ducted anew 90,000 simulations with *MetHis*, for each birth-island and for Cabo Verde as a whole,
2162 separately, under the winning scenario determined with RF-ABC, thus obtaining a total 100,000 simu-
2163 lations under the winning scenario, for each birth-island or for Cabo Verde as a whole, separately, for
2164 further Neural Network ABC posterior parameter estimation using the *abc* package in R (72).

2165

2166 NN-ABC parameter inference settings

2167 We followed the same empirical approach as in *MetHis*-ABC (45) to determine the most suitable num-
2168 ber of neurons in the hidden layer and associated number of simulations closest to the target data and
2169 retained for training the Neural Network (called “tolerance level”) for further NN-ABC posterior pa-
2170 rameter estimation for this target. Indeed, there is no rule-of-thumb to determine these parameters *a*
2171 *priori* in order to obtain the most informative posterior parameter inference while minimizing overfitting
2172 using a Neural-Network approach under a given scenario (72,113).

2173 Therefore, we empirically tested three different tolerance-level values to be used in NN-ABC pos-
2174 terior parameter estimation: 1%, 5%, or 10% of the total 100,000 simulations generated under the win-
2175 ning scenario determined by our RF-ABC procedure for each Cabo Verdean island and for Cabo Verde
2176 as a whole, respectively. Furthermore, for each one of the three tolerance-level values, we tested asso-
2177 ciated numbers of neurons in the hidden layer between 5 and 11, or 12, the number of free parameters
2178 minus one in the winning scenario for each Cabo Verdean island and for Cabo Verde as a whole, re-
2179 spectively (**Figure 6-7**).

2180 Then, for each pair of tolerance-level value and number of neurons for each targeted data separately,
2181 we performed 1,000 cross-validation NN-ABC posterior parameter inferences using the *cv4abc* function
2182 in the *abc* package (72). This procedure draws 1,000 simulations at random and considers them, in turn,
2183 as pseudo-observed data for posterior-parameter inference using the remaining 99,999 simulations as
2184 the reference table. For the 1,000 pseudo-observed cross-validations and each pair of tolerance level and
2185 number of hidden neurons, we calculated the error between the median posterior point-estimate of each
2186 parameter ($\hat{\theta}_i$) and its’ known true-value used for simulation (θ_i), as the mean-square error (MSE)
2187 scaled by the parameter’s variance across the 1,000 cross-validations (72):

2188

$$\text{Scaled MSE}(\hat{\theta}_i) = \sum_1^{1000} (\hat{\theta}_i - \theta_i)^2 / (1000 \times \text{Variance}(\theta_i)).$$

2189

2190 Therefore, we conducted, in total, 219,000 NN-ABC cross-validation parameter inference proce-
2191 dures to identify the NN-ABC settings most suitable for further posterior parameter estimations using
2192 the observed data for each Cabo Verdean birth-island and for Cabo Verde as a whole. For each Cabo
2193 Verdean island and for Cabo Verde as a whole, separately under the corresponding winning scenario,
2194 we chose the pair of tolerance-level values and number of hidden neurons that minimized the average
2195 error across all estimated parameters, as the Neural-Network setting used in further ABC posterior pa-
parameter inferences based on the observed data (**Appendix 1-table 1**).

2196
2197
2198
2199
2200
2201
2202
2203
2204
2205
2206
2207
2208
2209
2210
2211
2212
2213

Appendix 1-table 1:

Average parameter posterior random cross-validation error across all model parameters as a function of the number of neurons in the hidden layer and the rejection tolerance level (number of simulations retained for training the Neural-Network) under the winning scenario for each island respectively.

For each island separately, and for the 225 Cabo Verde-born individuals grouped as a single “Cabo Verde” population, we considered, 1,000 random simulations in-turn as pseudo-observed data to estimate posterior parameter distributions and 100,000 total simulations in the reference table. For each cross-validation procedure, we considered between 5 and 11 neurons in the hidden layer (“NN-HL”) for the winning scenarios with 12 original parameters, and between 5 and 12 NN-HL for the winning scenarios with 13 original parameters. We considered three different tolerance levels of 0.01, 0.03, and 0.1 (“Tol.”) corresponding, respectively, to 1,000, 3,000, and 10,000 simulations, in turn closest to each one of the 1,000 cross-validation pseudo-observed simulation retained for training the NN. The median values of posterior parameter distributions were used as point estimates for the calculation of the error of each parameter (72).

For each birth-island and Cabo Verde as a whole, and corresponding winning scenario, separately, we considered, for further posterior parameter estimation using the observed “real” data, only the pair of tolerance level and number of hidden neurons that minimized the average error on posterior parameter estimations across all parameters (indicated in bold in the table).

Individual birth-island	SANTIAGO	FOGO	SANTO ANTAO	SAO NICO-LAU	BRAVA	MAIO	BOA VISTA	SAO VICENTE	SAL	CABO VERDE
Winning scenario	Scenario 1: Afr2pulses-Eur2pulses	Scenario 1: Afr2pulses-Eur2pulses	Scenario 1: Afr2pulses-Eur2pulses	Scenario 1: Afr2pulses-Eur2pulses	Scenario 1: Afr2pulses-Eur2pulses	Scenario 1: Afr2pulses-Eur2pulses	Scenario 2: Afr2pulses-EurRecurring	Scenario 3: Afr-Recurring-Eur2pulses	Scenario 2: Afr2pulses-EurRecurring	Scenario 1: Afr2pulses-Eur2pulses
Number of scenario parameters	12	12	12	12	12	12	13	13	13	12
NN-HL = 5 Tol. = 0.01	0.79264	0.79943	0.80170	0.79380	0.81251	0.83232	0.79972	0.77795	0.82888	0.79532
NN-HL = 5 Tol. = 0.03	0.80899	0.81292	0.81257	0.80771	0.81703	0.83470	0.79739	0.82028	0.81753	0.83438
NN-HL = 5 Tol. = 0.1	0.84025	0.84031	0.84662	0.84870	0.84526	0.85366	0.83374	0.83312	0.83264	0.83271
NN-HL = 6 Tol. = 0.01	0.77139	0.80186	0.79800	0.80765	0.81085	0.82516	0.79239	0.77743	0.81601	0.82118
NN-HL = 6 Tol. = 0.03	0.79501	0.81397	0.80533	0.80463	0.83318	0.83673	0.80492	0.80127	0.81325	0.82882
NN-HL = 6 Tol. = 0.1	0.84684	0.84072	0.84028	0.84484	0.85753	0.85428	0.82136	0.81617	0.83773	0.84745
NN-HL = 7 Tol. = 0.01	0.78525	0.79836	0.79075	0.81595	0.82657	0.82662	0.79304	0.77898	0.80415	0.80413
NN-HL = 7 Tol. = 0.03	0.80899	0.81151	0.81000	0.81035	0.83069	0.83474	0.80060	0.79491	0.81855	0.83622
NN-HL = 7 Tol. = 0.1	0.85600	0.84544	0.83704	0.84737	0.86071	0.85582	0.81033	0.81619	0.83739	0.85601
NN-HL = 8 Tol. = 0.01	0.78512	0.79805	0.79127	0.80886	0.82241	0.83387	0.83387	0.78077	0.80992	0.80783
NN-HL = 8 Tol. = 0.03	0.80995	0.81077	0.81583	0.82452	0.82334	0.83715	0.79490	0.78639	0.80565	0.83356
NN-HL = 8 Tol. = 0.1	0.83938	0.83593	0.83681	0.85231	0.84982	0.84614	0.83469	0.81671	0.82696	0.84774
NN-HL = 9 Tol. = 0.01	0.77910	0.79889	0.81027	0.80103	0.81898	0.82483	0.79744	0.78619	0.81770	0.80542
NN-HL = 9 Tol. = 0.03	0.81192	0.81046	0.81474	0.81642	0.82593	0.82631	0.80630	0.78640	0.82512	0.84165
NN-HL = 9 Tol. = 0.1	0.84379	0.84721	0.83676	0.84813	0.86218	0.85223	0.83254	0.81698	0.81723	0.85381
NN-HL = 10 Tol. = 0.01	0.78993	0.79615	0.80275	0.79444	0.80692	0.82095	0.80121	0.77644	0.81801	0.80485
NN-HL = 10 Tol. = 0.03	0.80159	0.80518	0.81143	0.80949	0.83496	0.82787	0.79804	0.78801	0.81555	0.82157
NN-HL = 10 Tol. = 0.1	0.85245	0.84242	0.84222	0.85444	0.85410	0.85424	0.83049	0.81742	0.84660	0.84183
NN-HL = 11 Tol. = 0.01	0.79994	0.81073	0.78479	0.78709	0.82927	0.84091	0.79414	0.77365	0.79984	0.80238
NN-HL = 11 Tol. = 0.03	0.82611	0.80882	0.80825	0.81653	0.82511	0.82334	0.80234	0.80333	0.81730	0.82939
NN-HL = 11 Tol. = 0.1	0.84914	0.83830	0.84011	0.84941	0.85471	0.85756	0.82120	0.81919	0.83044	0.85282
NN-HL = 12 Tol. = 0.01	na	na	na	na	na	na	0.79915	0.78138	0.81418	na
NN-HL = 12 Tol. = 0.03	na	na	na	na	na	na	0.79959	0.79306	0.81551	na
NN-HL = 12 Tol. = 0.1	na	na	na	na	na	na	0.81731	0.82090	0.82284	na

2214
2215

2216 *NN-ABC posterior parameter estimation*

2217 For each Cabo Verdean island and for all Cabo Verde-born individuals grouped in a single population,
2218 separately, under the winning scenario identified with RF-ABC, we jointly estimated the posterior dis-
2219 tributions of all parameters using NN-ABC “*neuralnet*” method option in the function *abc* of the R
2220 package *abc* (72), with logit-transformed parameters (“*logit*” transformation option) using the tolerance
2221 level and number of neurons in the hidden layer identified previously in **Appendix 1-table 1**. For each
2222 birth-island and for Cabo Verde as a whole, separately, a synthetic schematic figure of the complex
2223 admixture processes identified using median point estimates of the posterior scenario-parameter distri-
2224 bution is provided in **Figure 7**, and full posterior parameter distributions with 95% Credibility-Intervals
2225 (CI) are provided in **Figure 7-figure supplement 1-3** and **Appendix 5-table 1-10**.

2227 *NN-ABC posterior parameter errors*

2228 We evaluated posterior parameter error rates and 95%-CI accuracies in the vicinity of the observed data,
2229 for each island and for Cabo Verde as a whole, separately, and for each corresponding NN-ABC poste-
2230 rior parameter joint estimation.

2231 First, we identified the 1,000 simulations closest to the observed “real” data for each target data
2232 separately using a 1% tolerance level in the “*neuralnet*” option from the *abc* function. We then used
2233 each one of these 1,000 specific simulations, in turn, as pseudo-observed target data for cross-validation
2234 NN-ABC posterior parameter estimation using the same NN settings as previously, logit-transformed
2235 parameters, and the 99,999 remaining simulations in the reference table. We then compared the median
2236 posterior estimate of each scenario parameter ($\hat{\theta}_i$), with the original parameter value used for the sim-
2237 ulation (θ_i), respectively for each 1,000 cross-validation posterior parameter estimation; and calculated
2238 the cross-validation mean absolute error (MAE), for each scenario parameter (**Appendix 5-table 1-10**):

2239
$$MAE(\hat{\theta}_i) = \sum_1^{1000} |\hat{\theta}_i - \theta_i| / 1000.$$

2240

2241 Second, for each island and for Cabo Verde as a whole, and for each scenario-parameter separately,
2242 we calculated how many times the true parameter values (θ_i), used for simulating the 1,000 simulations
2243 closest to the observed data, fell within the 95%-CI [2.5% quantile($\hat{\theta}_i$); 97.5% quantile($\hat{\theta}_i$)] estimated
2244 using the observed data. Thus, if the 1,000 cross-validation true parameter values fell more than 95% of
2245 the time within the estimated 95%-CI, the length of the estimated 95%-CI was considered over-esti-
2246 mated and thus excessively conservative; and, alternatively, if it was the case less than 95% of the time,
2247 the length of the 95%-CI was considered under-estimated thus indicating a less conservative behavior
2248 of our CI estimation procedure (**Appendix 5-table 1-10**).

2249

2250

2251

2252 **APPENDIX 2**

2253

2254 **Genetic diversity patterns with ASD-MDS at different geographical scales,**
2255 **complementary to Results 1.**

2256

2257 At the worldwide scale (**Appendix 2-figure 1**), the first MDS axis is mainly driven by genetic differen-
2258 tiation between African individuals and non-African individuals, the second MDS axis by differentiation
2259 between European and East Asian individuals, and the third axis by differentiation between South Asian
2260 and American individuals.

2261 We explored successive subsamples of this worldwide dataset in order to decompose apparent pre-
2262 ferred relationships between each admixed population related to the TAST with respect to African and
2263 European populations only. We find (**Appendix 2-figure 2**) that the first MDS axis differentiates Afri-
2264 can and European individuals; the second axis differentiates mainly Senegambian West Western African
2265 individuals from Congo Basin hunter-gatherer individuals (namely the Baka, Ba.Bongo, Ba.Koya,
2266 Ba.Mbuti, Ba.Twa and Bezan); and the third axis differentiates further these latter populations from
2267 Eastern African individuals. In this context, we find Cabo Verdean individuals clustering along an axis
2268 going from the European cluster to a cluster formed mainly by West Western African individuals, with
2269 the sole exception of two individuals with fathers born on Angola as per our familial anthropology
2270 questionnaires and consistently clustering closer to our Angolan samples. Instead, ASW, ACB and PUR
2271 individuals are found on a slightly different trajectory going from European individuals towards East
2272 Western Africa mainly (**Appendix 2-figure 2**).

2273 Further resampling our ASD matrix (**Appendix 2-figure 3**), we find no signs of particular genetic
2274 affinity, along the first three MDS axes, between enslaved-African descendants and Eastern and South-
2275 ern African individuals.

2276 Notably, we find Cabo Verdean individuals clustering similarly to Senegambian Fulani individuals
2277 in between European and other Senegambian populations, the Fulani being known to have historically
2278 received gene-flow from Northern African populations (81,93,114,115). In the absence of Northern Af-
2279 rican populations in our dataset, the South-Western European Iberian-IBS population represented the
2280 best such proxy-populations with known historical relationship with Northern Africa, hence resulting,
2281 at this geographical scale, in the similar clustering of Cabo Verdean and Fulani individuals. Note that
2282 Fulani and Cabo Verdean individuals substantially departed from each other along higher MDS axes,
2283 the Cabo Verdeans remaining on a European-African axis while the Fulani departed from this trajectory
2284 on the European side (**Appendix 2-figure 3**).

2285 Finally, considering only populations related to the TAST with respect to European and East, Cen-
2286 tral, and West Western African populations (excluding the Fulani), we find (**Appendix 2-figure 4**) that
2287 Cabo Verdeans cluster separately from other TAST populations not only with respect to African popu-
2288 lations, but also with respect to their relationships to European populations (**Figure 2**).

2289

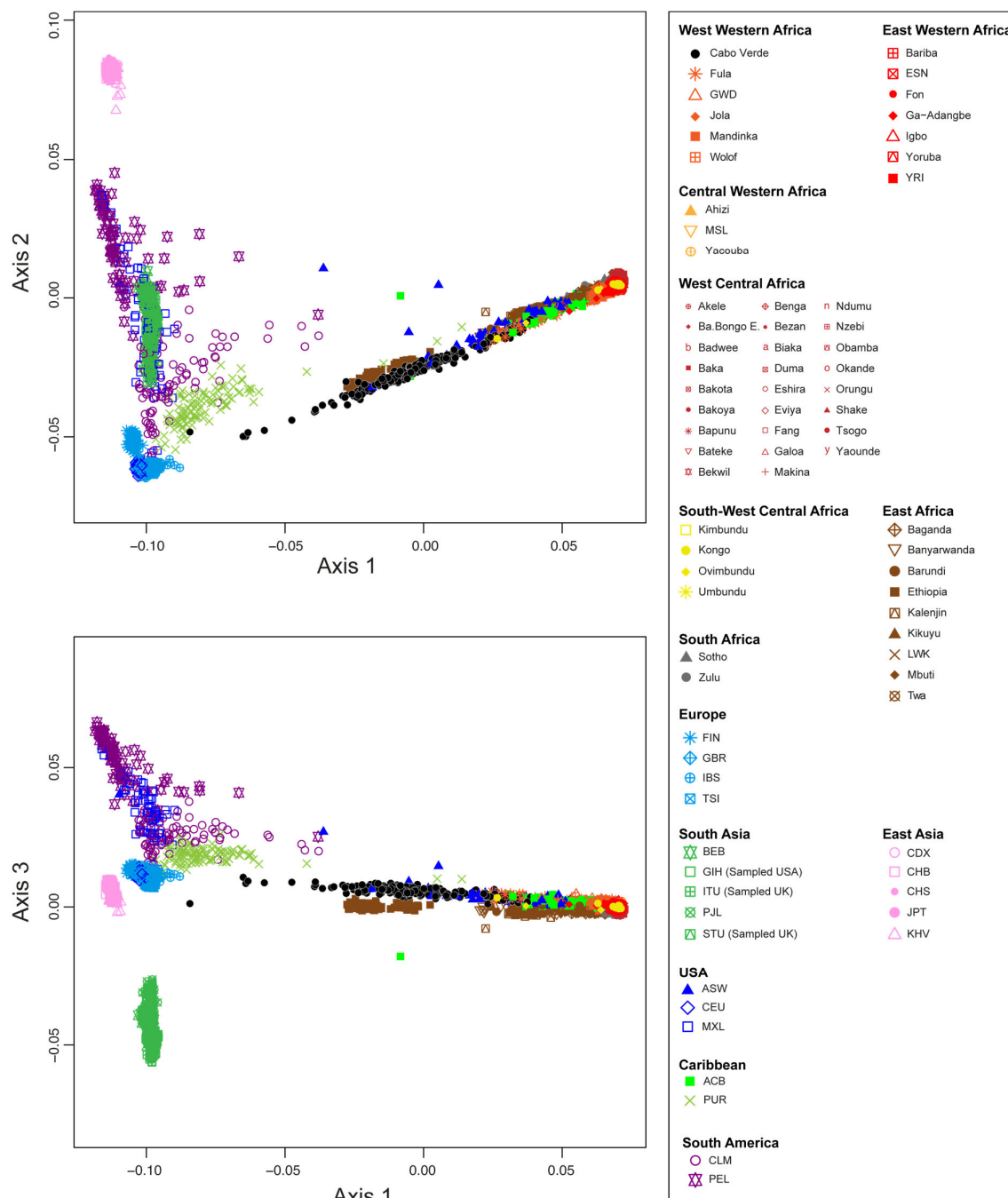
2290

2291 **Appendix 2-figure 1:**
 2292 **Multidimensional scaling three-dimensional projection of allele sharing pairwise dissimilarities, for all worldwide pop-**
 2293 **ulations in our dataset.**

2294 Each individual in the plot is represented by a single point. See **Figure 1-resource table 1** for the population list used and
 2295 **Figure 1** for sample locations and symbols.

2296 **A) Axis 1 and 2; B) Axis 1 and 3.** 3D animated plot is provided in .gif format.

2297 We evaluate the Spearman correlation between 3D MDS projections and the original ASD pairwise matrix to evaluate the
 2298 precision of the dimensionality reduction along the first three axes of the MDS. We find significant Spearman ρ of 0.9796
 2299 ($p < 2.2 \times 10^{-16}$).
 2300



2301
 2302

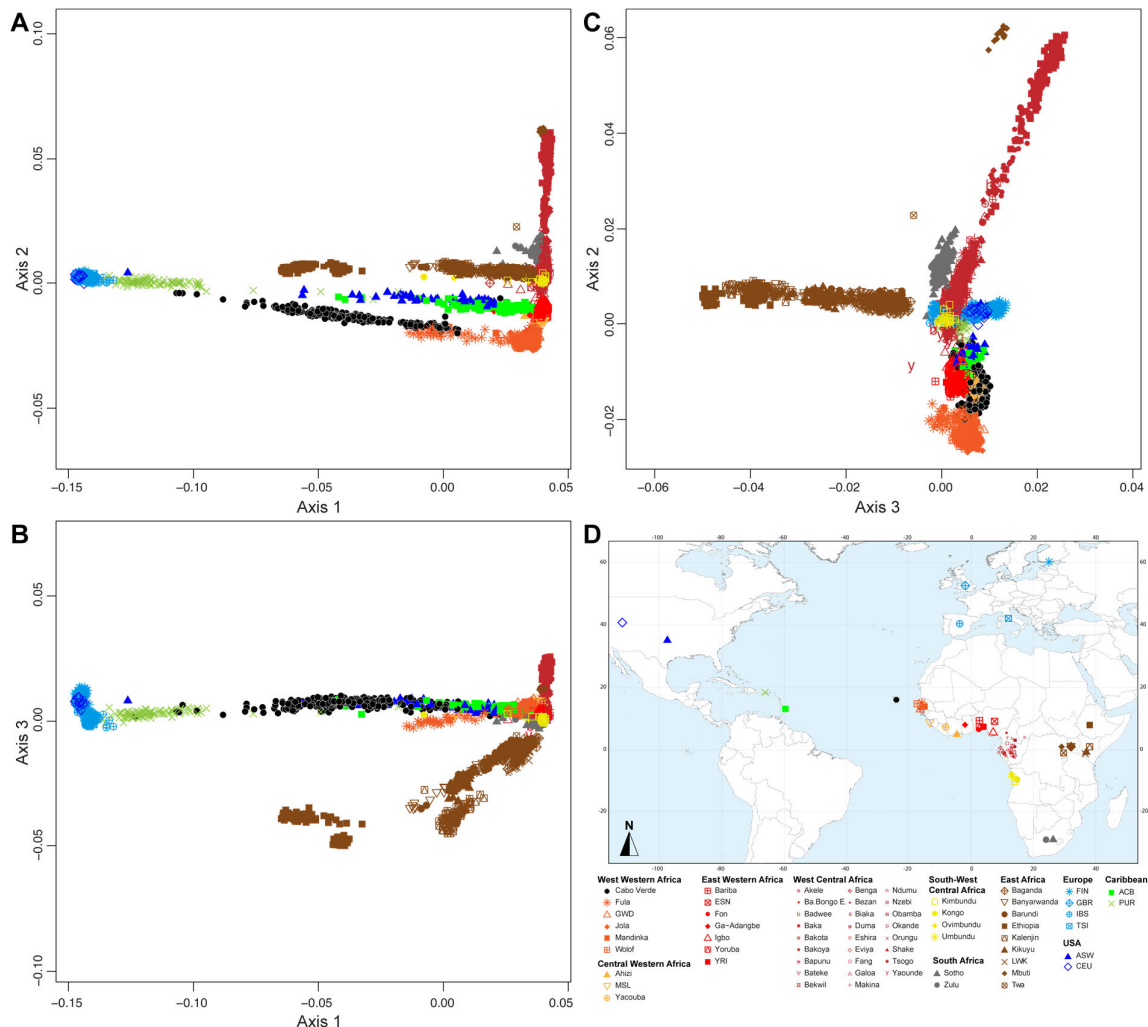
2303 **Appendix 2-figure 2:**

2304 **Multidimensional scaling three-dimensional projection of allele sharing pairwise dissimilarities, for all of the African,**
 2305 **European and other admixed populations related to the TAST.**

2306 Each individual is represented by a single point. We removed all Asian and South American samples compared to the sample set employed in **Appendix 2-figure 1**, and recomputed the MDS based on this reduced sample set. See **Figure 1-resource**
 2307 **table 1** for the population list used in these analyses. The sample map used in these analyses is extracted from **Figure 1** and
 2308 provided in panel **D**.

2309 A) **Axis 1 and 2; B) Axis 2 and 3; C) Axis 1 and 3.** 3D animated plot is provided in .gif format.

2310 We evaluate the Spearman correlation between 3D MDS projections and the original ASD pairwise matrix to evaluate the
 2311 precision of the dimensionality reduction along the first three axes of the MDS. We find Spearman ρ of 0.9392 ($p < 2.2 \times 10^{-16}$).
 2312
 2313
 2314



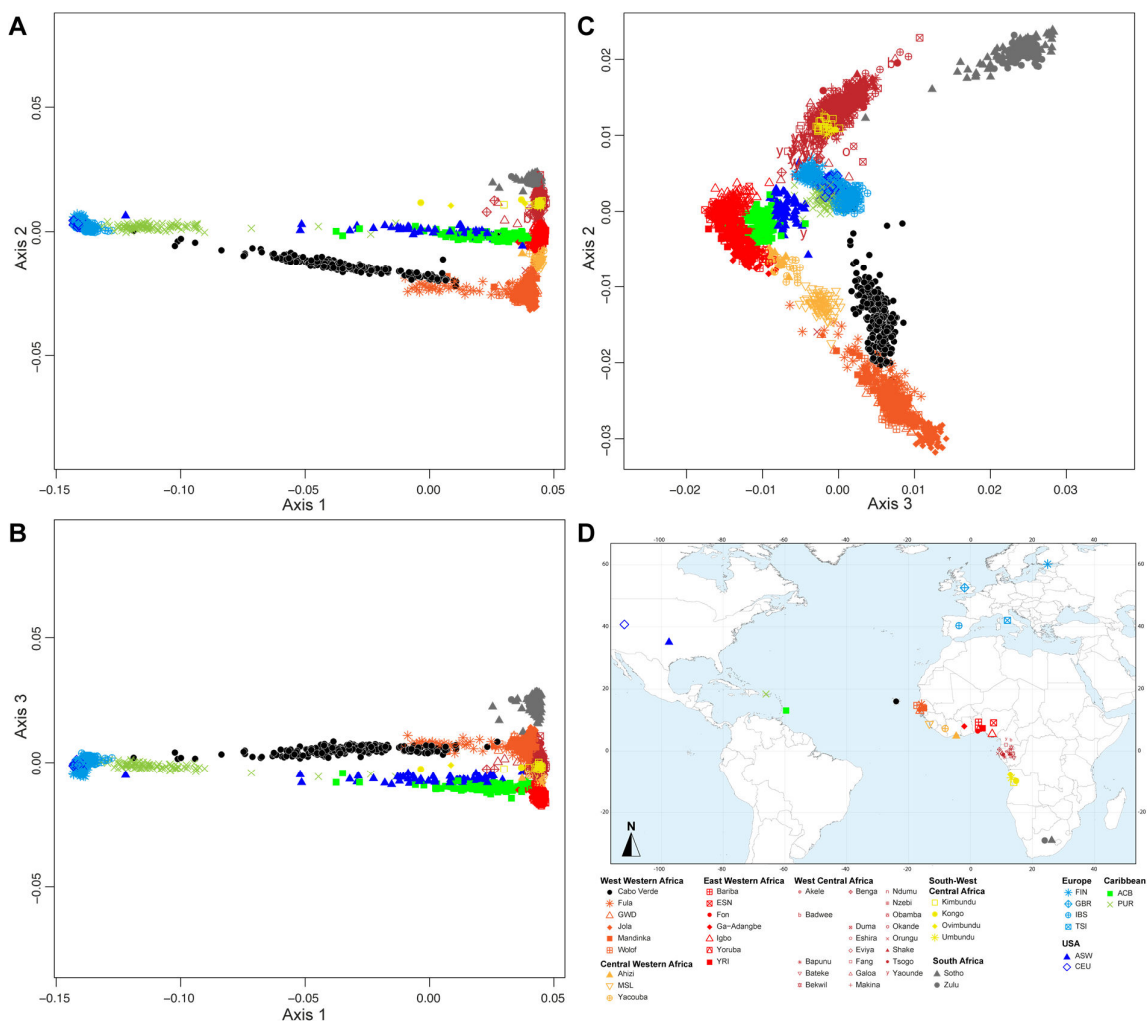
2315
 2316
 2317

2318 **Appendix 2-figure 3:**
 2319 **Multidimensional scaling three-dimensional projection of allele sharing pairwise dissimilarities, for a subset of African,**
 2320 **European and other admixed populations related to the TAST.**

2321 Each individual is represented by a single point. We removed all East African and Central African hunter-gatherer samples
 2322 (Baka, Bezan, Ba.Bongo, Ba.Koya, Ba.Twa, Bi.Aka, Mbuti) compared to the sample set employed in **Appendix 2-figure 2**,
 2323 and recomputed the MDS based on this reduced sample set. See **Figure 1-resource table 1** for the population list used in these
 2324 analyses. Sample map used in these analyses is extracted from **Figure 1** and provided in panel **D**.

2325 **A) Axis 1 and 2; B) Axis 2 and 3; C) Axis 1 and 3.** 3D animated plot is provided in .gif format.

2326 We evaluate the Spearman correlation between 3D MDS projections and the original ASD pairwise matrix to evaluate the
 2327 precision of the dimensionality reduction along the first three axes of the MDS. We find Spearman ρ of 0.9450 ($p < 2.2 \times 10^{-16}$).
 2328



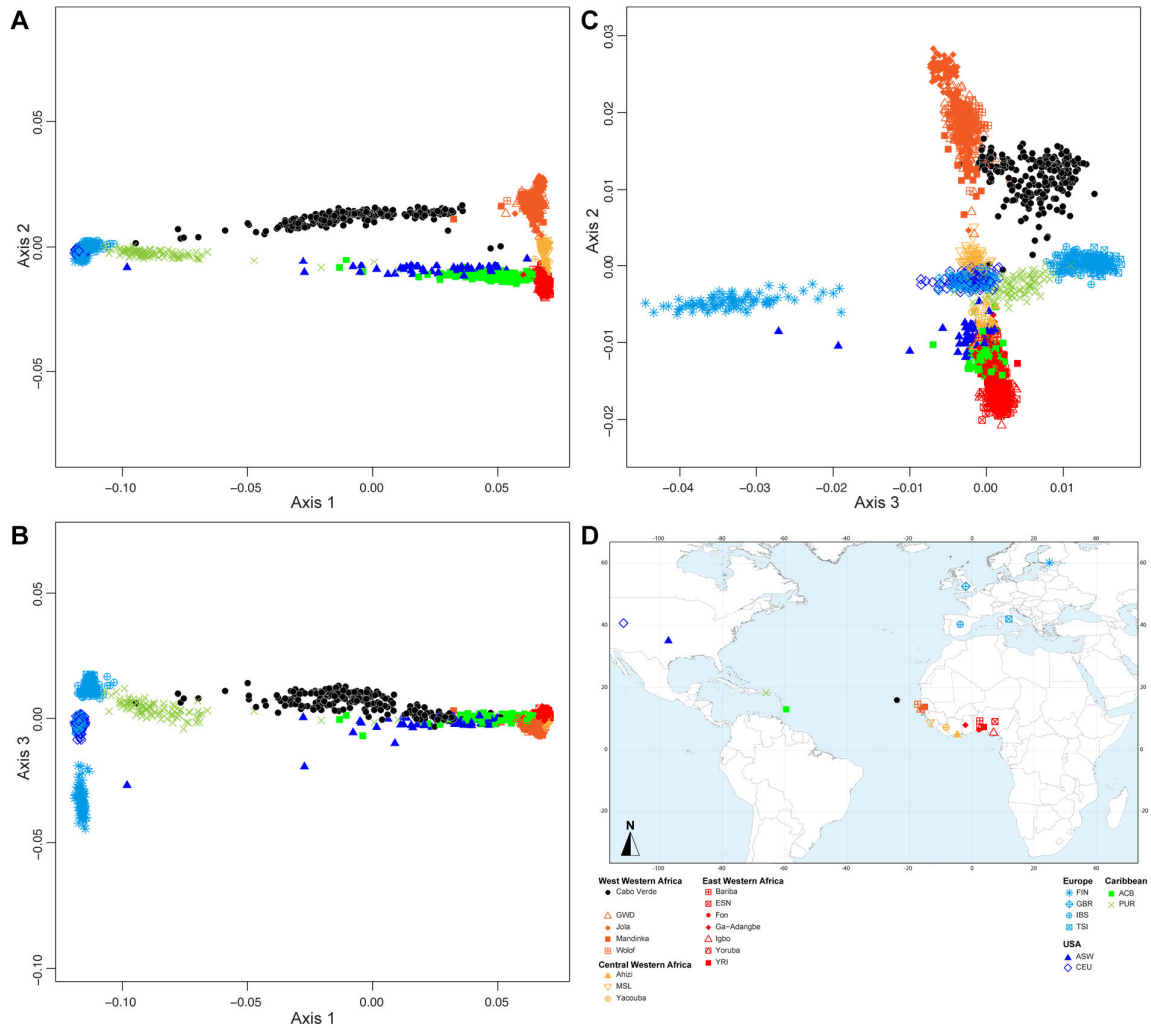
2329
 2330

2331 **Appendix 2-figure 4:**
 2332 **Multidimensional scaling three-dimensional projection of allele sharing pairwise dissimilarities, for the closest subsets**
 2333 **of West African, European and other admixed populations related to the TAST.**

2334 Each individual is represented by a single point. We removed all West and South-West Central African samples, as well as
 2335 South African samples, compared to the sample set employed in **Appendix 2-figure 3**, and recomputed the MDS based on this
 2336 reduced sample set. See **Figure 1-resource table 1** for the population list used in these analyses. Sample map used in these
 2337 analyses is extracted from **Figure 1** and provided in panel **D**.

2338 **A) Axis 1 and 2; B) Axis 2 and 3; C) Axis 1 and 3.** 3D animated plot is provided in .gif format.

2339 We evaluate the Spearman correlation between 3D MDS projections and the original ASD pairwise matrix to evaluate the
 2340 precision of the dimensionality reduction along the first three axes of the MDS. We find Spearman ρ of 0.9636 ($p < 2.2 \times 10^{-16}$).
 2341



2342
 2343
 2344
 2345

2346 **APPENDIX 3**

2347

2348

Alternative ADMIXTURE modes, complementary to Results 2.

2349

2350

2351

2352

2353

2354

2355

2356

2357

2358

In **Figure 3A**, ADMIXTURE results at $K=3$ show that the new pink cluster is maximized in East Asian Chinese-CHB individuals, with a few African-American ASW and Barbadian-ACB individuals exhibiting relatively high membership to this cluster as visually identified in the ASD-MDS analysis (**Appendix 2-figure 1**), and previously reported (10). While Finnish-FIN individuals all exhibit low membership to this cluster, such signal probably emerges from unresolved clustering for this population geographically between Western Europe and East Asia. This is further evidenced by the almost complete disappearing of this resemblance of FIN individuals with the pink cluster at higher values of K . No other individuals or populations in our analysis show signals of strong resemblance with the East Asian Chinese-CHB for higher values of K .

2359

2360

2361

2362

2363

2364

2365

2366

2367

2368

2369

2370

2371

2372

2373

2374

2375

2376

2377

The fourth gray cluster at $K=4$ in **Figure 3A** is maximized in Southern African individuals from the Soto and Zulu populations. At this value of K , the original orange cluster is maximized in the West Western African Jola from Senegambia and all other African populations exhibit intermediate membership between the gray and the orange cluster. Interestingly, the average membership to the gray “Southern African” cluster decreases with increasing geographic distance from Southern Africa, along the Atlantic Ocean coast of the continent. This echoes the relatively continuous clustering observed in the ASD-MDS analysis for the Atlantic African populations in our dataset (**Appendix 2-figure supplement 2-4**). Notably, the Cabo Verdean individuals born on Brava, Fogo, Santiago, and Maio, exhibit membership to both the orange and the gray clusters, albeit with a majority of membership to the orange cluster rather than the gray cluster. All other Cabo Verdean individuals show virtually no membership to the gray cluster. While indicating the stronger resemblance between all Cabo Verdean individuals with genetic patterns observed mostly in West Western Africa and Senegambian populations, this provides a first indication of differentiated genetic structure across islands within Cabo Verde. Conversely, the orange cluster previously identified in the ASW and ACB is, at $K=4$ in **Figure 3A**, divided into gray and orange with a slight excess of gray. A similar pattern is found among Central and East Western African populations, such as the Yoruba-YRI, the Nigerian-ESN, the Igbo, and the Ga-Adangbe populations, hence providing a first indication of a closer resemblance of the individuals of these two enslaved-African descendant populations with East Western Africa rather than with West Western Africa.

2378

2379

2380

2381

2382

2383

2384

2385

2386

2387

2388

2389

2390

2391

2392

2393

At $K=5$ in **Figure 3A**, note that West Central and South-West African populations exhibit a distinctive unique pattern with high membership to both the red and gray clusters. However, note that ADMIXTURE clustering is largely unresolved at this value of K as no individuals exhibit close (<1% to 100% membership to the red cluster, and as only 27 out of the 30 ADMIXTURE iterations provide similar results. Indeed, an alternative minor mode is identified at this value of K (**Appendix 3-figure 1**).

At $K=7$ in **Figure 3A**, the novel light-blue cluster is maximized only in Finnish-FIN individuals, while the blue cluster is now maximized only in Tuscan-TSI individuals. British-GBR and USA-CEU individuals exhibit intermediate membership between the two clusters while Iberian-IBS individuals strongly resemble TSI individuals. This clustering patterns further echoes the observed ASD-MDS clustering of European populations identified in **Figure 2**. Importantly, the “European” membership of all Cabo Verdean islands resembles, relatively, the patterns exhibited in TSI and IBS individuals (with high proportions of blue and minimal proportion of light-blue), while African-American ASW and Barbadian-ACB individuals show relatively much higher proportions of light-blue, hereby resembling, for this genotype membership, GBR and CEU individuals rather than other Europeans. Nevertheless, variable results across runs at this value of K indicate unresolved clustering and these interpretations should be considered cautiously at this point (see alternative ADMIXTURE modes at $K=7$, **Appendix 3-figure 1**).

2394 At $K=8$ in **Figure 3A**, the novel dark-red cluster is maximized in West Central African Tsogho
2395 individuals and at very high proportions in all other individuals from West-Central and South-West
2396 Africa, hence resolving the unresolved clustering identified for these populations at $K=5$. Interestingly,
2397 substantial traces of this cluster are found in YRI, Igbo and ESN East Western African populations as
2398 well as ASW and ACB individuals, but virtually absent from Cabo Verdeans or any other African pop-
2399 ulation. This further indicates the closer resemblances of ASW and ACB African genetic component to
2400 East Western and West Central Africa than to other African populations in our dataset, as echoed in our
2401 ASD-MDS analyses (**Figure 2, Figure 2-figure supplement 1**).

2402 At $K=9$ in **Figure 3A**, the novel light-yellow cluster is maximized in Sierra Leone-MSL population
2403 from Central West Africa, albeit imperfectly. This further illustrates the intermediate clustering of Cen-
2404 tral Western African populations in between Senegambian and East Western African populations,
2405 largely overlapping on both sides, and observed in ASD-MDS analyses (**Appendix 2-figure supple-**
2406 **ment 1-4**). Nevertheless, patterns should be interpreted with caution at this value of K , as clustering is
2407 largely unresolved, also indicated by the alternative ADMIXTURE solutions (**Appendix 3-figure 1**).

2408 At $K=11$ in **Appendix 3-figure 1**, we find five alternative ADMIXTURE solutions to **Figure 3**. In
2409 one alternative solution, the novel dark blue cluster is maximized either in the Fang from West Central
2410 Africa hereby distinguished from the Tsogho from the same geographic region. Other modal results
2411 show this novel dark-blue cluster maximized instead in the Wolof from West Western Africa, hence
2412 distinguished from the Jola from the same geographic region; or instead in the British GBR, thus distin-
2413 guishing three different ADMIXTURE patterns among Western European populations and hence res-
2414 solving minoritarian modes observed previously at $K=10$; or, finally, among individuals from Fogo is-
2415 land, and Brava to a lesser extent, thus indicating further sub-structure among Cabo Verdean islands.
2416 Interestingly, note that for all ADMIXTURE solutions at this value of K , the light-yellow cluster is
2417 majoritarian in Sierra Leone MSL individuals, hence more clearly differentiated from either West West-
2418 ern and East Western African individuals compared to results obtained at previous values of K .

2419 At $K=12$ in **Appendix 3-figure 1**, we find three alternative modes to the results presented in **Figure**
2420 **3**. These results resolve alternative modes obtained at the previous values of K , thus further differenti-
2421 ating populations within Africans and Europeans sub-regions, respectively.

2422 At $K=13$ in **Appendix 3-figure 1**, we find five alternative mode results compared to the one pre-
2423 sented in **Figure 3**. These further resolve the various modal results obtained at previous values of $K=10$,
2424 11, and 12. Furthermore, note that three minoritarian such modes maximize the novel light-brown clus-
2425 ter in Boa Vista individuals, while memberships to this specific cluster are virtually absent from all other
2426 individuals in our data set, except for a substantial proportion in individuals born on Maio.

2427 At $K=14$ in **Appendix 3-figure 1**, we find three alternative solutions compared to **Figure 3**. Note
2428 that some such solutions resolve separate modal solutions obtained at previous values of K . Furthermore,
2429 interestingly, in one modal solution, the novel bright yellow cluster is maximized in Ga-Adangabe in-
2430 dividuals, hence differentiating this population from others in the East Western African sub-region.

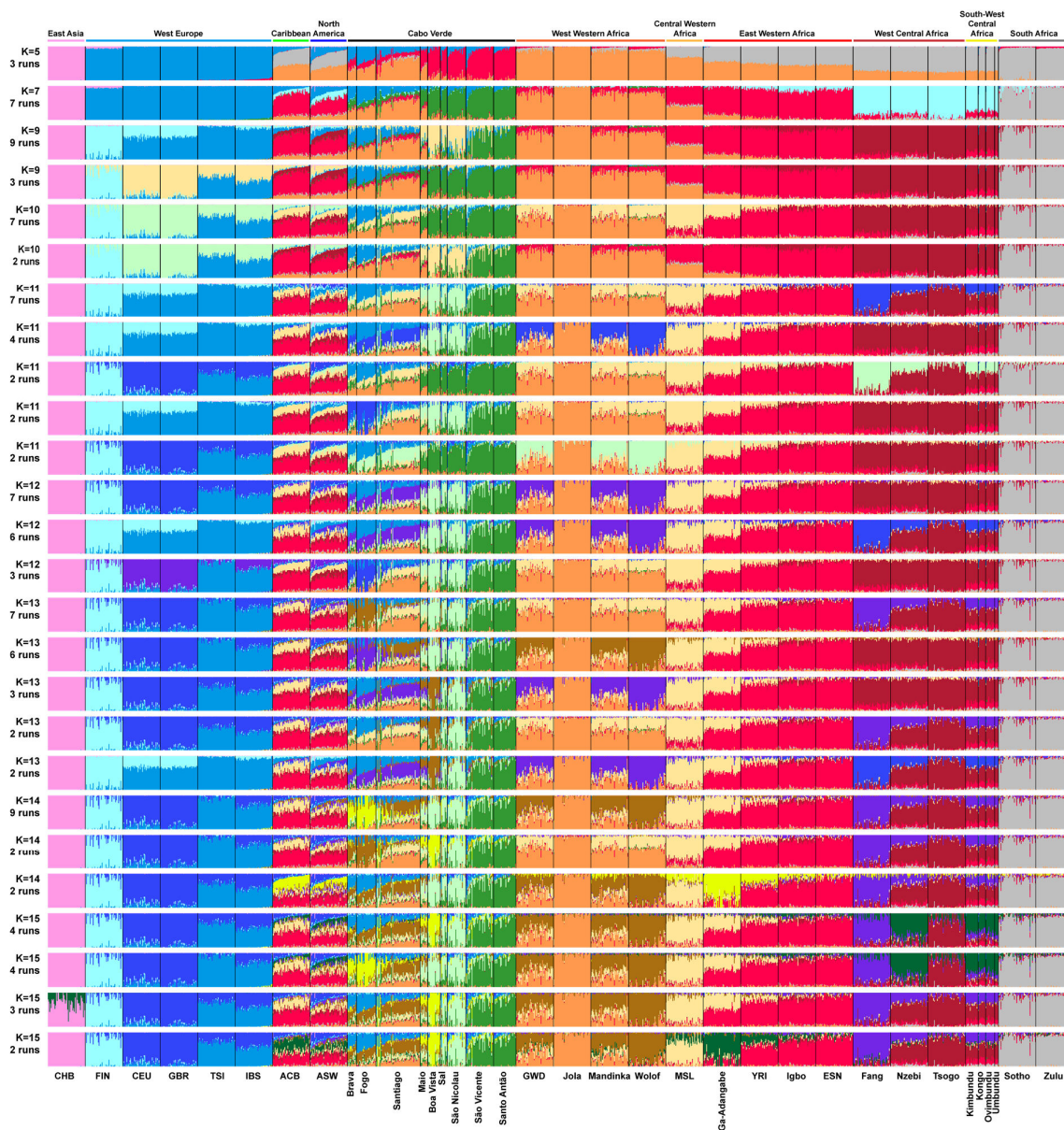
2431 Finally, at $K=15$ in **Appendix 3-figure 1**, we obtain four alternative solutions compared to **Figure**
2432 **3** results. Interestingly, in two such solutions, the novel dark-green cluster is maximized in Nzebi West
2433 Central Africans thus further differentiating the three populations from Gabon (the Fang, the Tsogho
2434 and the Nzebi) in three different cluster. Note that in these cases, geographically close South-West Central
2435 African individuals from Angola exhibit membership proportion patterns resembling more the Nzebi
2436 than the two other Gabonese populations. An alternative mode interestingly differentiates some individ-
2437 uals within the CHB East Asian population, and is virtually absent from all other individuals in our data
2438 set. Finally, the last alternative mode encompasses the smallest number of runs and resolves some of the
2439 alternative solutions previously obtained at $K=14$ (**Figure 3A, Appendix 3-figure 1**).

2440
2441
2442
2443
2444
2445
2446
2447
2448
2449

Appendix 3-figure 1:

Alternative ADMIXTURE mode results for the individual genetic structure among Cabo Verdean, Barbadian-ACB and African-American ASW populations related to the TAST.

ADMIXTURE (48) analyses using resampled individual sets for the population sets originally containing more than 50 individuals (**Figure 1-resource table 1**). 225 unrelated Cabo Verdean-born individuals are grouped by island of birth (**Figure 1-resource table 1**). All analyses considered 102,543 independent autosomal SNPs, for values of K between 2 and 15. 30 independent ADMIXTURE runs were performed for each value of K , and groups of runs (>2) providing similar results (all pairwise SSC > 99.9%) were averaged in a single “mode” result using CLUMPP (100), and plotted with DISTRUCT (101). Number of runs in the presented modes are indicated below the value of K . All other modes are presented in **Figure 3**.



2450
2451
2452

2453 **APPENDIX 4**

2454

2455 **Runs of homozygosity patterns in Cabo Verde and other admixed populations related to**
2456 **the TAST, complementary to Results 4.**

2457

2458 Examining patterns of ROH less than 1cM long, we find generally low levels of short and medium ROH
2459 in continental Africa (**Appendix 4-figure 1**), with the lowest levels in Southern Africa. Conversely, we
2460 found high levels of such short and medium-size ROH among European and East Asian populations,
2461 likely reflecting ancient migration bottlenecks during the Out-of-Africa expansion (61). We note that
2462 the Cabo Verdean individuals have slightly elevated levels of short and medium ROH compared to
2463 continental Africa, similarly to the ACB and ASW populations. This may stem from the known
2464 admixture with European populations that occurred recently during the TAST. Admixture can be
2465 intuitively expected to decrease ROH levels compared to the source populations in general. However,
2466 recent admixture between African and European populations, the latter who exhibit much higher levels
2467 of short and medium ROH than the former (**Appendix 4-figure 1**), may inflate levels of such ROHs in
2468 the admixed population compared to continental African sources. Consistently with our findings for the
2469 African American ASW and Barbadian ACB (**Appendix 4-figure 1**), such phenomenon had been
2470 previously reported (60). Finally, overall total ROH levels reflected the generally higher levels of ROH
2471 in Cabo Verde compared to continental African and other admixed populations from the Americas
2472 (**Appendix 4-figure 1C**), patterns likely related to the relative isolation of populations within the
2473 archipelago (**Figure 5, Table 1**).

2474

2475 Exploring how local ancestry intersects with ROH less than 1cM long, since short and medium
2476 ROH are comprised of old haplotypes that likely predate over 50 generations ago (59), the colonization
2477 of the Cabo Verde islands and the subsequent admixture histories of their populations, we expected that
2478 the local ancestry content of these ROH classes should be correlated with total non-ROH local ancestry
2479 levels. **Appendix 4-figure 2** illustrates the relationship between total ancestry in a given ROH size class
2480 versus the total ancestry not in that ROH size class for all Cabo Verdean individuals. We find strong
2481 correlations among the short ROH and local ancestry (**Appendix 4-figure 2A**; African local ancestry:
2482 Pearson $\rho=0.9372$, $p < 2.2 \times 10^{-16}$; European local ancestry: Pearson $\rho=0.9496$, $p < 2.2 \times 10^{-16}$; Asian local
2483 ancestry: Pearson $\rho=0.7516$, $p < 2.2 \times 10^{-16}$), and medium ROH and local ancestry (**Appendix 4-figure**
2484 **2B**; African local ancestry: Pearson $\rho=0.9071$, $p < 2.2 \times 10^{-16}$; European local ancestry: Pearson $\rho=0.9379$,
2485 $p < 2.2 \times 10^{-16}$; Asian local ancestry: Pearson $\rho=0.3905$, $p < 1.298 \times 10^{-9}$).

2485

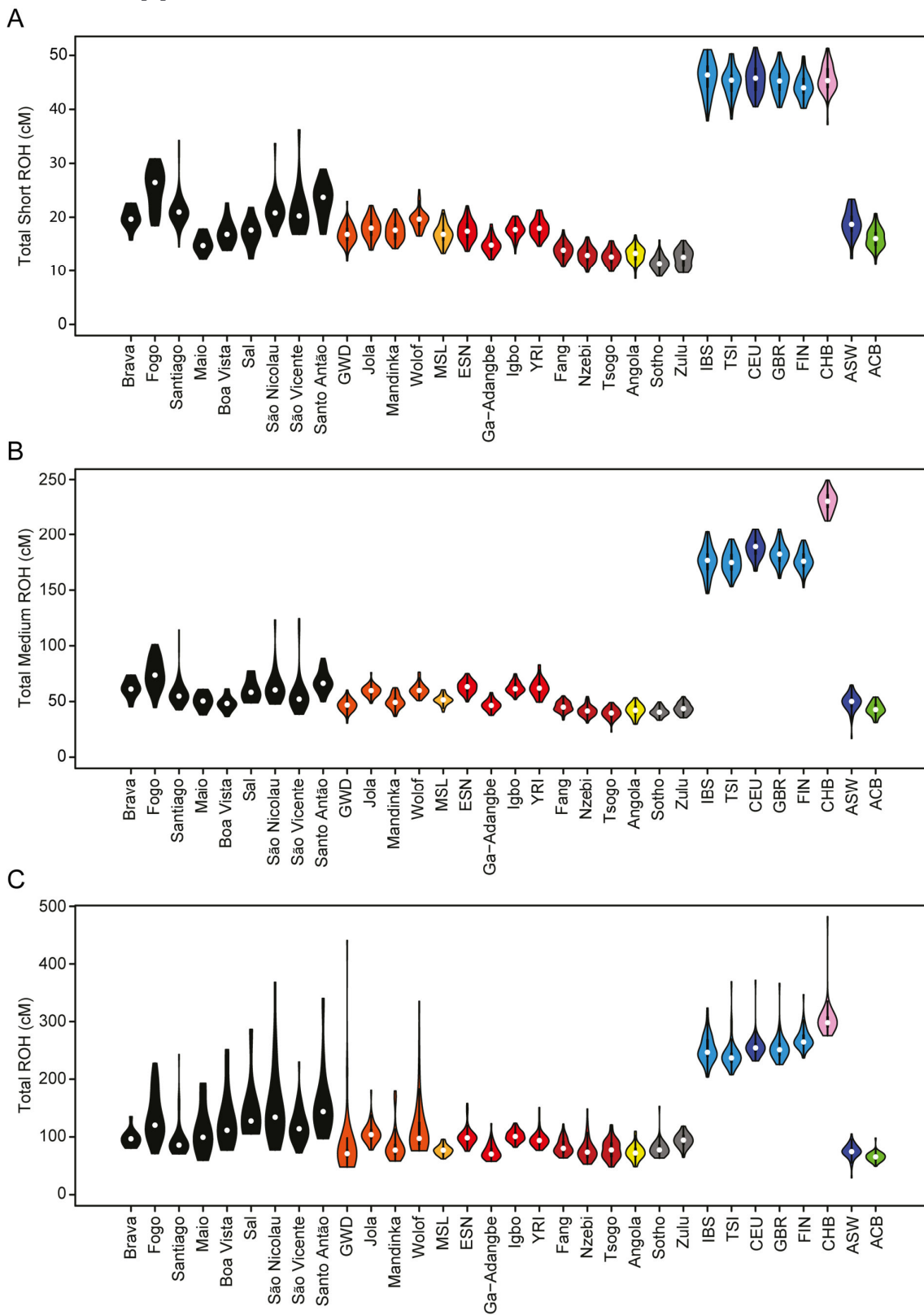
2486

2487

2488
2489
2490

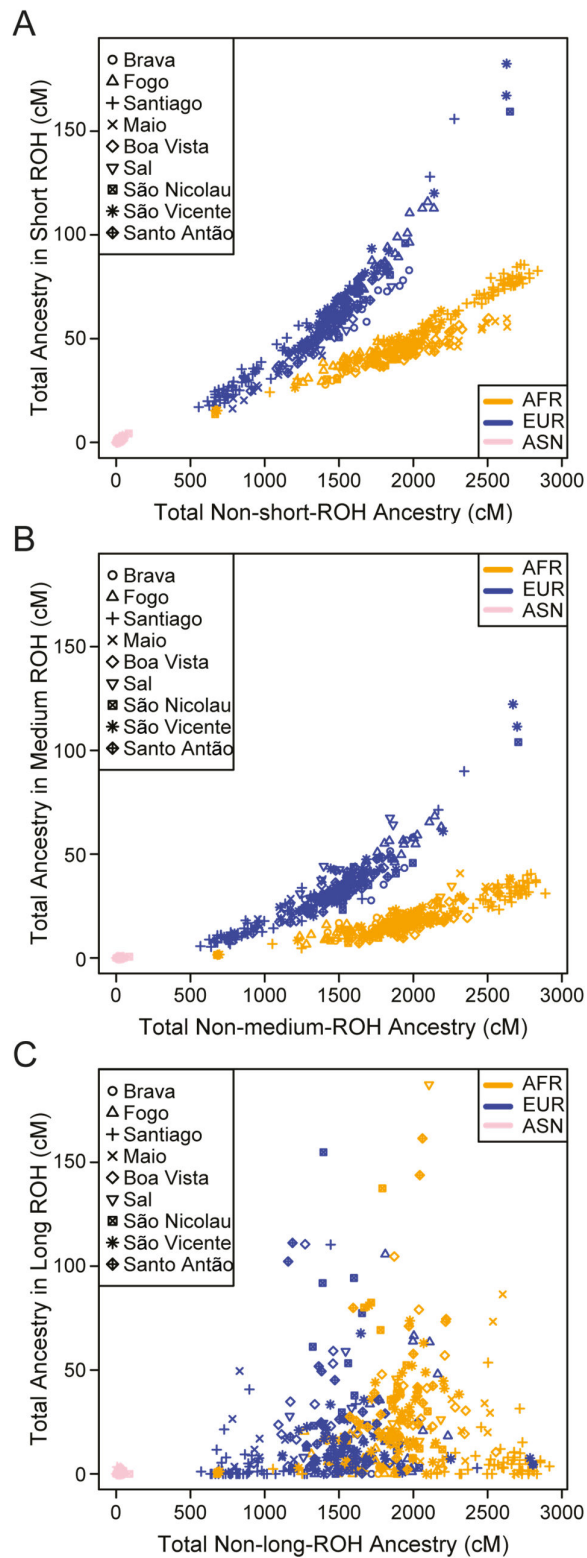
Appendix 4-figure 1:

The distribution of (A) short, (B) medium, and (C) all ROH per individual, for each Cabo Verdean birth-island and other worldwide populations.



2491
2492

2493 **Appendix 4-figure 2:**
2494 **Individual total ancestry contained in (A) short, (B) medium, and (C) long ROH versus total ancestry not in that class**
2495 **ROH, for each Cabo Verdean birth-island and other worldwide populations.**
2496



2497
2498

2499 **APPENDIX 5**

2500

2501 **Genetic admixture histories of each Cabo Verdean island of birth inferred with *MetHis-***
2502 **ABC, complementary to Results 7. and Discussion sections.**

2503

2504 Results for the detailed admixture history of each island separately are henceforth presented in the chron-
2505 ological order of the first time in an islands' history when more than 100 individuals are reported in
2506 historical census information, and after which further census reports always exceeded this number until
2507 today; hereafter called "first perennial peopling" of an island (**Figure 7D, Figure 7-resource table 1**).
2508 As in the main text of the article, note that this historical date can vastly differ from the date for the first
2509 official settlement of an island inferred via political, administrative and tax records, and witnessed by
2510 parishes foundations, illustrating the complex and versatile peopling history of each Cabo Verdean is-
2511 land after the initial establishment of the Portuguese dominion over the archipelago.

2512

2513 **Admixture history of Santiago (First official settlement 1460; Perennial peopling: 1470)**

2514 ***MetHis-ABC inferences detailed results for Santiago***

2515 For individuals born on Santiago island, we find that the most recent pulses of admixture from Africa
2516 and Europe, respectively, occurred after the official abolition of the TAST in the Portuguese Empire in
2517 the 1830's, and after the effective abolition of slavery in the Portuguese empire in the 1860's (**Figure**
2518 **7**). Both admixture pulses are characterized by posterior distributions with narrow 95%CI's clearly de-
2519 parting from their respective priors, both for the timing of each pulse and their respective intensities, in
2520 particular for the European admixture pulse (**Figure 7-figure supplement 1-3, Appendix 5-table 1**).
2521 For these recent events, observed genetic patterns are consistent with a relatively intense African ad-
2522 mixture event (median=0.5913, mode=0.6837, 95%CI=[0.0642–0.9038]), occurring between genera-
2523 tion sixteen and seventeen after the founding of Cabo Verde at generation 0 (generation median=16.6,
2524 mode=17.2, 95%CI=[10.0–18.9]). Furthermore, we find strong evidence for the most recent European
2525 admixture pulse being weak (median=0.0684, mode=0.0258, 95%CI=[0.0028–0.6021]), and having oc-
2526 curred between one and two generations before the sampled generation (generation median=18.7, mode
2527 =19.1, 95%CI=[11.7–19.6]).

2528 NN-ABC posterior parameter estimations perform less accurately to infer the dates of the earlier
2529 admixture pulses and their associated intensities, both from Africa and Europe respectively, as shown
2530 by posterior distribution departing less clearly from their respective priors and overall large 95%CI.
2531 Nevertheless, results indicate that both the African and European pulses may have occurred in a more
2532 remote past; the African pulse was inferred at generation 9.2 (median) after founding at generation 0
2533 (mode=13.9, 95%CI=[1.7–16.8]); the European pulse at generation 7.5 (median, mode=3.4,
2534 95%CI=[2.3–15.9]), towards the beginning of the plantation economy era in the Americas and during
2535 the intensification of the TAST in the second half of the 17th century (1,2) (**Figure 7D**). Conversely, the
2536 initial founding admixture pulse, set to occur at generation 0 at the beginning of Cabo Verde settlement
2537 history in the 1460's, is more accurately estimated *a posteriori*, as indicated by substantial departure
2538 from the prior distribution and relatively narrow CI. Results here indicate a stronger contribution from
2539 Africa than Europe (median=0.6365, mode=0.8816, 95%CI=[0.0538–0.9858]), at the root of the genetic
2540 make-up of Santiago-born individuals in our sample set.

2541 Finally, effective population sizes in Santiago indicate a strong, relatively linear (u_{Ne} median=0.365,
2542 mode=0.440, 95%CI=[0.150–0.494]), increase since the 1460's up to 80,077 effective individuals (me-
2543 dian, mode=92,109, 95%CI=[30,408–98,975]), in the sampled generation born on average between the
2544 1960's and the 1980's.

2545 **Appendix 5-table 1-Santiago:**

2546 **NN-ABC posterior parameter estimations for Santiago island, cross-validation posterior parameter errors, and cross-**
 2547 **validation 95% Credibility Interval accuracies.**

2548 Cross-validation errors and 95% CI accuracies are based on 1,000 NN-ABC posterior parameter inferences using, in turn, each
 2549 one of the 1,000 simulations closest to the observed data used as pseudo-observed data, and the remaining 99,999 simulations
 2550 as the reference table.

2551 Error calculations are based on the mode and, separately, the median point estimate for each 1,000 pseudo-observed simulations
 2552 posterior parameter estimation, compared to the known parameter used for simulation. We considered 6 neurons in the hidden
 2553 layer and a tolerance level of 0.01 (1000 simulations) for all posterior parameter estimation in this analysis as identified in
 2554 **Appendix 1-table 1**. Plotted distributions for posterior parameter estimations can be found in **Figure 7-figure supplement 1-**
 2555 **3**.

2556
 2557

SANTIAGO Afr2P-Eur2P scenario parameters	Parameter posterior estimation				1,000 cross-validation errors		
	Mode	Median	50% Credibility Interval	95% Credibility Interval	Mode mean absolute error	Median mean absolute error	95% CI length accuracy
Ne.0	142	431	[194 - 692]	[28 - 974]	305	255	0.059
Ne.20	92109	80077	[63220 - 91349]	[30408 - 98975]	25426	21558	0.045
u.Ne	0.440	0.365	[0.284 - 0.438]	[0.150 - 0.494]	0.113	0.096	0.042
sAfr,0	0.8816	0.6365	[0.3884 - 0.8415]	[0.0538 - 0.9858]	0.3147	0.2507	0.056
tAfr,p1	13.9	9.2	[4.9 - 13.4]	[1.7 - 16.8]	5.3	4.2	0.101
sAfr,tAfr,p1	0.7844	0.5986	[0.3421 - 0.7861]	[0.0420 - 0.9479]	0.2618	0.2204	0.054
tAfr,p2	17.2	16.6	[15.2 - 17.5]	[10.0 - 18.9]	1.8	1.6	0.199
sAfr,tAfr,p2	0.6837	0.5913	[0.3894 - 0.7241]	[0.0642 - 0.9038]	0.1597	0.1458	0.052
tEur,p1	3.4	7.5	[4.3 - 11.1]	[2.3 - 15.9]	4.0	3.1	0.161
sEur,tEur,p1	0.1617	0.3969	[0.1957 - 0.6606]	[0.0185 - 0.9564]	0.3042	0.2439	0.056
tEur,p2	19.1	18.7	[17.7 - 19.2]	[11.7 - 19.6]	3.0	2.9	0.115
sEur,tEur,p2	0.0258	0.0684	[0.0250 - 0.1501]	[0.0028 - 0.6021]	0.2749	0.2254	0.057

2558
 2559

2560 *Discussion for the admixture history of Santiago*

2561 Altogether, our results indicate that admixture in Santiago occurred mainly between Senegambian and
 2562 South Western European populations (**Figure 2-3**), at the very beginning of the Portuguese colonization
 2563 of the archipelago in the 15th century. This early admixture history is likely due to an initial peopling of
 2564 Cabo Verde strongly biased towards solitary males (familial permanent migrations from Portugal being
 2565 a minority), who reproduced with African enslaved women, and whose admixed offspring constituted
 2566 the first Cabo Verdean generations, as shown by some recorded instances of legitimizations of the ad-
 2567 mixed offspring to allow them to legally inherit dating back to the early 16th century (25).

2568 Our results further indicate that two substantial admixture events from Africa and Europe, respec-
 2569 tively, occur concomitantly to the early expansion of the TAST during the 17th-century, although we are
 2570 unable to precisely date both events. Nevertheless, our results support a more tenuous genetic admixture
 2571 history from Africa experienced by Cabo Verdeans from Santiago during the most intense period of the
 2572 TAST (18th-century) and the height of plantation economy in European colonial empires (1,2). This
 2573 apparent reduced influence of the most intense period of the TAST on admixture pattern in Santiago is
 2574 also echoed in our ASD-MDS, ADMIXTURE, and SOURCEFIND results, where Santiago Cabo Ver-
 2575 deans today share ancestry with Senegambian Mandinka almost exclusively (**Figure 2-3**). However, his-
 2576 torical records unquestionably demonstrated that numerous other populations from West Central and
 2577 South Western Africa were enslaved and forcibly deported to Cabo Verde during this era (25). Thus,
 2578 our results highlight that the strong and recurrent demographic migrations of enslaved Africans brought
 2579 to Santiago during the second half of the TAST do not seem to have left a similar genetic admixture

2580 signature. This is consistent with several, mutually non-exclusive, historical scenarios, where enslaved
2581 African populations brought to Santiago may have been mostly re-deported to the Americas and Europe
2582 after the 17th century, without substantially contributing to the genetic landscape of this island, whether
2583 due to rapid re-deportation, and/or to slave-owners and colonial society strongly preventing marriages
2584 and reproduction between newly arrived enslaved individuals and pre-existing enslaved or non-enslaved
2585 communities in Santiago (see **Discussion** in main text).

2586 Conversely, our results indicate an intense introgression event from Africa in Santiago, occurring
2587 shortly after the TAST and the abolition of slavery in the Portuguese empire in the 1860's. This may
2588 have been caused by a relaxation of the socio-economic constraints that predominated during most of
2589 the TAST against marriages between enslaved and non-enslaved communities as well as the control of
2590 marriages among enslaved individuals imposed by slave-owners; concomitant with the strong intensifi-
2591 cation of the illegal slave-trade which deported numerous enslaved Africans in a short amount of time
2592 shortly after the end of the TAST (25–28).

2593 Our results also clearly identify a European introgression event in Santiago having occurred at the
2594 beginning of the 20th century, which may be explained by the European migrations towards African
2595 colonies triggered by European empires' policies during the first half of this century. Interestingly, we
2596 find that this recent admixture event was of very limited intensity, thus indicating that European emi-
2597 gration to Santiago during the 20th century only had a quantitatively limited, albeit precisely detectable,
2598 influence on genetic admixture patterns.

2599 Finally, Santiago-born individuals also show the lowest ROH levels and generally some of the
2600 shortest ROH in Cabo Verde (**Figure 4** and **Appendix 4-figure 1-2**). When examining ancestry patterns
2601 within ROH in Santiago-born individuals, although proportions within ROH are on average consistent
2602 with an individuals' overall genetic ancestry, there are some outlier individuals with much higher Euro-
2603 pean ancestry within ROH compared to the remainder of the genome. This could possibly reflect his-
2604 torical marriage prohibitions and other social constraints against intercommunity reproductions (see
2605 **Discussion** in main text). These ROH results combined with the evidence for the relatively constantly
2606 increasing reproductive population in Santiago over the course of the peopling of Cabo Verde (**Figure**
2607 **7C**), was consistent with this island being the administrative historical capital, and principal entry to the
2608 archipelago throughout its' history (26,27).

2609
2610
2611
2612

2613 **Admixture history of Fogo (First official settlement 1460; Perennial settlement: 1570)**

2614 *MetHis-ABC inferences detailed results for Fogo*

2615 For individuals born on Fogo island, we find that both European admixture pulses were precisely in-
2616 ferred with NN-ABC, for the time of their occurrence and for their respective intensities, as posterior
2617 parameter distributions and 95%CI substantially depart from their respective priors (**Figure 7, Figure**
2618 **7-figure supplement 1-3, Appendix 5-table 2**). The most recent European admixture pulse in Fogo
2619 occurred concomitantly to the abolition of the TAST and of slavery in the Portuguese empire in the
2620 1860's (generation median=15.5 after the founding of Cabo Verde at generation 0, mode=16.7,
2621 95%CI=[6.7–18.2]), and was of substantial intensity (median=0.2428, mode=0.2101, 95%CI=[0.0157–
2622 0.8485]). The older European pulse occurred much more remotely in the past (generation median=5.3,
2623 mode=2.5, 95%CI=[1.9 –13.9]), shortly after the first perennial census above 100 individuals in 1570
2624 for this island, and long before the increase in TAST intensity due to the expansion of Plantation Econ-
2625 omy in the Americas in the second half of the 17th century. Furthermore, note that our results indicate
2626 that this European pulse is of relatively similar intensity compared to the most recent one (me-
2627 dian=0.2234, mode=0.1149, 95%CI=[0.0223–0.8383]).

2628 Interestingly, we find that the African admixture history of individuals from Fogo occurred at very
2629 different periods of time than the European ones, the timing for both African admixture pulses being
2630 also well estimated with substantial departure from the prior and relatively narrow 95%CI. Indeed, we
2631 find strong indications of a very recent pulse of African admixture of overall limited intensity (me-
2632 dian=0.2034, mode=0.1174, 95%CI=[0.0120–0.8225]), having occurred around the first part of the 20th
2633 century (generation median=19.3 after the founding of Cabo Verde at generation 0, mode=19.5,
2634 95%CI=[15.6–19.8]). Furthermore, we find that the previous African admixture pulse likely occurred
2635 between six and eight generations before the sampled one (generation median=12.0 after Cabo Verde
2636 founding, mode=13.3, 95%CI=[4.7–16.9]), in the midst of the most intense period of the TAST and
2637 plantation economy in the Americas, around the 1760's. However, we cannot recover a precise estima-
2638 tion for the intensity of this older pulse, as its' posterior parameter distribution seldom depart from its'
2639 prior. We also find that the founding admixture event set to occur at the beginning of the colonization
2640 history of the archipelago in the 1460's is substantially departing from its' prior distribution and very
2641 similar to the founding admixture event found for individuals born on Santiago (median=0.6831,
2642 mode=0.7407, 95%CI=[0.1679–0.9600]).

2643 Finally, our posterior estimation of the demographic history of Fogo-born individuals substantially
2644 differs from that of Santiago. Indeed, while we find similar effective sizes towards the present between
2645 the two islands (median=72,023, mode=90,370, 95%CI=[18,011–98,846]), we find that the demo-
2646 graphic increase was much more recent and rapid in Fogo (u_{Ne} median=0.150, mode=0.115,
2647 95%CI=[0.055–0.447]) than in Santiago.

2648
2649

2650 **Appendix 5-table 2-Fogo:**

2651 **NN-ABC posterior parameter estimations for Fogo island, cross-validation posterior parameter errors, and cross-validation 95% Credibility Interval accuracies.**

2652 Cross-validation errors and 95% CI accuracies are based on 1,000 NN-ABC posterior parameter inferences using, in turn, each one of the 1,000 simulations closest to the observed data used as pseudo-observed data, and the remaining 99,999 simulations as the reference table.

2653 Error calculations are based on the mode and, separately, the median point estimate for each 1,000 pseudo-observed simulations posterior parameter estimation, compared to the known parameter used for simulation. We considered 10 neurons in the hidden layer and a tolerance level of 0.01 (1000 simulations) for all posterior parameter estimation in this analysis as identified in **Appendix 1-table 1**. Plotted distributions for posterior parameter estimations can be found in **Figure 7-figure supplement 1-3**.

2654
2655
2656
2657
2658
2659
2660
2661
2662

FOGO Afr2P-Eur2P scenario parameters	Parameter posterior estimation				1,000 cross-validation errors		
	Mode	Median	50% Credibility Interval	95% Credibility Interval	Mode mean absolute error	Median mean absolute error	95% CI length accuracy
Ne.0	349	511	[274 - 737]	[44 - 969]	295	253	0.063
Ne.20	90370	72023	[50948 - 87248]	[18011 - 98846]	27142	22749	0.057
u.Ne	0.115	0.150	[0.104 - 0.230]	[0.055 - 0.447]	0.085	0.081	0.074
sAfr,0	0.7407	0.6831	[0.5218 - 0.8152]	[0.1679 - 0.9600]	0.2936	0.2432	0.069
tAfr,p1	13.3	12.0	[8.1 - 14.4]	[4.7 - 16.9]	4.2	3.3	0.157
sAfr,tAfr,p1	0.4667	0.4549	[0.2286 - 0.6721]	[0.0251 - 0.9555]	0.2498	0.2315	0.056
tAfr,p2	19.5	19.3	[18.9 - 19.5]	[15.6 - 19.8]	2.6	2.5	0.100
sAfr,tAfr,p2	0.1174	0.2034	[0.1051 - 0.3560]	[0.0120 - 0.8225]	0.2032	0.1891	0.060
tEur,p1	2.5	5.3	[2.7 - 8.8]	[1.9 - 13.9]	3.6	3.0	0.216
sEur,tEur,p1	0.1149	0.2234	[0.1146 - 0.3943]	[0.0223 - 0.8383]	0.2804	0.2371	0.062
tEur,p2	16.7	15.5	[13.1 - 16.8]	[6.7 - 18.2]	3.2	3.0	0.070
sEur,tEur,p2	0.2101	0.2428	[0.1393 - 0.3966]	[0.0157 - 0.8485]	0.1751	0.1686	0.060

2663
2664

2665 Discussion for the admixture history of Fogo

2666 Our results indicate a very similar founding admixture event for Fogo island compared to that of Santiago, strongly suggesting that the admixture event at the root of Fogo peopling occurred early in Cabo Verde history, likely in Santiago island. This scenario is consistent with historical data suggesting an initial peopling of Fogo from Santiago at the end of the 15th century and the beginning of the 16th century, rather than independent founding events between islands (26,27).

2671 Interestingly, we find a European pulse of admixture concomitant with the perennial peopling of the island at the end of the 16th century and the establishment of Fogo as an important center of agricultural and free-range cattle herding in the economic triangle between Europe, Cabo Verde, and continental Africa. Later on, we identify traces of an African admixture pulse having occurred during the most intense period of the TAST in the mid-18th century, thus consistent with increased African enslaved individuals' forced deportations to Fogo as showed by historical records, but we could not infer its intensity, suggesting the difficult identifiability of such admixture event in the genetic landscape of Fogo island today with the methods here deployed.

2679 This history of admixture is likely related to the intense control on the island's economic expansion and regulated immigration imposed after 1532 by the central political, administrative, and commercial power of Santiago, with the notable exception of direct commercial relationships allowed between Fogo and Europe under the rule of the Portuguese crown (26–28). This could thus explain the limited African admixture during Fogo history and more intense European admixture on this island, identified with our ASD-MDS/ADMIXTURE, and SOURCEFIND results (**Figure 2-3**). Furthermore, these socio-political

2684

2685 factors likely also explain the maintaining of a relatively low reproductive population size on Fogo until
2686 very recently, as opposed to the more continuous population increase on Santiago (**Figure 7C**). In ad-
2687 dition, this demographic history may be further explained by the recurrent eruptions of the Fogo volcano,
2688 which unquestionably chronically disrupted the island's development, although historical records
2689 showed limited direct mortality due to these events and that communities fleeing the island often mi-
2690 grated back after each cataclysm (26).

2691 We identify a much more recent pulse of European admixture, having occurred in the first half of
2692 the 19th century, shortly after the abolition of the TAST in the Portuguese empire, possibly due to the
2693 profound socio-cultural changes in marital relationships between enslaved and non-enslaved communi-
2694 ties during the abolition of slavery in colonial empires (see **Discussion** in main text). Finally, we identify
2695 precisely a weak African admixture pulse having occurred in Fogo during the 20th century possibly
2696 consistent with more recent work-related migrations from Africa to Cabo Verde (28).

2697 Finally, ROH patterns in Fogo are similar to Santiago, in that ROH levels are relatively low and
2698 individual ROH are relatively short (**Figure 4, Appendix 4-figure 1-2**). This is consistent with Fogo's
2699 history of economic control and influx of European individuals. Interestingly, when exploring ancestry
2700 proportions within ROH relative to the remainder of the genome, we see on average more European
2701 ancestry within ROH. This could possibly reflect the historical influx of Europeans onto the island
2702 and/or a legacy of preferential marriages between individuals of shared family origin.

2703

2704 **Admixture history of Santo Antão (First official settlement 1570; Perennial settlement:**
2705 **1580)**

2706 *MetHis-ABC inferences detailed results for Santo Antão*

2707 For individuals born on Santo Antão island, we find that both European admixture pulses after the
2708 founding admixture event are substantially departing from their respective priors and have relatively
2709 narrow 95%CI, both for the timing of their occurrence and their respective intensities (**Figure 7, Figure**
2710 **7-figure supplement 1-3, Appendix 5-table 3**). We find that Santo Antão-born individuals have experi-
2711 enced a recent European admixture pulse of weak intensity (median=0.0847, mode=0.0467,
2712 95%CI=[0.0056–0.6382]), that occurred roughly three generations before the sampled generation, at the
2713 turn of the 20th century (generation median=17.2 after Cabo Verde founding at generation 0, mode=18.1,
2714 95%CI=[7.6–19.1]). Furthermore, we find a much more ancient European admixture pulse of strong
2715 intensity (median=0.3592, mode=0.1542, 95%CI=[0.0216–0.9522]), occurring concomitantly (genera-
2716 tion median=5.8, mode=3.2, 95%CI=[2.6–15.6]) with the first perennial census in this island dated in
2717 1580, and before the massive increase of TAST during the 17th century.

2718 Interestingly, we find that the first African admixture pulse after founding at generation 0 occurred
2719 at generation 4.9 (median, mode=2.4, 95%CI=[1.9–11.9]), almost synchronically to the oldest European
2720 admixture pulse and the first perennial settlement of the island recorded in 1580. Furthermore, this Af-
2721 rican admixture pulse was intense (median=0.6255, mode=0.7574; 95%CI=[0.0451–0.9749]), which
2722 summed close to 100% with the European admixture pulse having occurred at very similar times. This
2723 obliterated any older admixture events, consistently with the wide 95%CI obtained for the intensity of
2724 the founding admixture event for this island (median $s_{\text{Afr},0}$ =0.5681, mode=0.8047, 95%CI=[0.0260–
2725 0.9839]). Importantly, our NN-ABC posterior parameter estimation fail to infer the second African ad-
2726 mixture pulse identified by our RF-ABC scenario-choice. Indeed, the posterior distributions of both the
2727 timing of this most recent pulse and its' intensity depart little from their respective priors.

2728 Finally, despite the relatively poor performances of our inferences of demographic changes in Santo
2729 Antão, our results are indicative of a very reduced population in this island over the course of Cabo
2730 Verdean peopling history until a very recent increase up to 41,256 individuals (median, mode=12,056,
2731 95%CI=[3570–96,855]).

2732
2733

2734 **Appendix 5-table 3-Santo Antão:**

2735 **NN-ABC posterior parameter estimations for Santo Antão island, cross-validation posterior parameter errors, and**
 2736 **cross-validation 95% Credibility Interval accuracies.**

2737 Cross-validation errors and 95% CI accuracies are based on 1,000 NN-ABC posterior parameter inferences using, in turn, each
 2738 one of the 1,000 simulations closest to the observed data used as pseudo-observed data, and the remaining 99,999 simulations
 2739 as the reference table.

2740 Error calculations are based on the mode and, separately, the median point estimate for each 1,000 pseudo-observed simulations
 2741 posterior parameter estimation, compared to the known parameter used for simulation. We considered 11 neurons in the hidden
 2742 layer and a tolerance level of 0.01 (1000 simulations) for all posterior parameter estimation in this analysis as identified in
 2743 **Appendix 1-table 1**. Plotted distributions for posterior parameter estimations can be found in **Figure 7-figure supplement 1-**
 2744 **3**.

2745
 2746

SANTO ANTAO Afr2P-Eur2P scenario parameters	Parameter posterior estimation				1,000 cross-validation errors		
	Mode	Median	50% Credibility Interval	95% Credibility Interval	Mode mean absolute error	Median mean absolute error	95% CI length accuracy
Ne.0	411	469	[254 - 706]	[26 - 964]	254	228	0.071
Ne.20	12056	41256	[17145 - 69559]	[3570 - 96855]	32106	25308	0.051
u.Ne	0.035	0.053	[0.033 - 0.093]	[0.015 - 0.334]	0.072	0.067	0.056
sAfr,0	0.8047	0.5681	[0.2995 - 0.7964]	[0.0260 - 0.9839]	0.3029	0.2586	0.068
tAfr,p1	2.4	4.9	[2.9 - 7.4]	[1.9 - 11.9]	3.3	2.6	0.164
sAfr,tAfr,p1	0.7574	0.6255	[0.3644 - 0.7916]	[0.0451 - 0.9749]	0.2512	0.2283	0.055
tAfr,p2	13.6	11.6	[7.7 - 14.9]	[3.0 - 18.5]	2.8	2.7	0.072
sAfr,tAfr,p2	0.6294	0.4716	[0.2596 - 0.6733]	[0.0338 - 0.9233]	0.2435	0.2150	0.049
tEur,p1	3.2	5.8	[3.2 - 10.2]	[2.6 - 15.6]	2.6	2.4	0.265
sEur,tEur,p1	0.1542	0.3592	[0.1709 - 0.6051]	[0.0216 - 0.9522]	0.2767	0.2347	0.059
tEur,p2	18.1	17.2	[14.8 - 18.2]	[7.6 - 19.1]	3.2	3.0	0.074
sEur,tEur,p2	0.0467	0.0847	[0.0416 - 0.1656]	[0.0056 - 0.6382]	0.1868	0.1763	0.059

2747
 2748

2749 *Discussion for the admixture history of Santo Antão*

2750 Our results for the admixture history of Santo Antão indicate that individuals born today on this island
 2751 experienced an African-European admixture event concomitant with the first perennial settlement of the
 2752 island in the 1580's, at the root of the genetic makeup of this island.

2753 Most interestingly, we find no identifiable genetic admixture events, from Europe or Africa,
 2754 throughout the height of the TAST on Santo Antão, albeit this island experienced a strong agricultural
 2755 expansion during the plantation economy era which triggered recurrent African enslaved individuals'
 2756 deportations to this island, as shown by historical records (26–28). Thus, even more strikingly than
 2757 observed in Santiago, our results indicate that the enslaved-African forced deportations to Santo Antão
 2758 during most of the TAST did not leave a statistically significant genetic contribution to the genetic
 2759 landscape of the island, for likely the same complex socio-cultural reasons suggested for the rest of Cabo
 2760 Verde (see **Discussion** in main text).

2761 In this context, our ADMIXTURE and SOURCEFIND results identify two different Senegambian
 2762 populations, the Mandinka and the Wolof, sharing significant African haplotypic ancestry with Santo
 2763 Antão-born individuals, as well as a much more limited shared ancestry with the West Central Africa
 2764 Igbo population (**Figure 3B**). Our ABC results would thus be consistent with a scenario where different
 2765 enslaved-African populations from Senegambia and West Central Africa were brought together to set-
 2766 tle Santo Antão in the early stages of the TAST in the late 16th century, a pattern distinct to our findings
 2767 for Santiago and Fogo. Alternatively, it is possible that the Igbo shared ancestry identified in our anal-
 2768 yses stem from another admixture event that we failed to identify. This is likely due to an overall limited
 2769 shared ancestry between this population and Santo Antão identified only with haplotypic local ancestry

2770 inferences, as our *MetHis*-ABC procedure considered a single Senegambian population at the root of
2771 the admixture history of the island and a much more limited number of independent SNPs compared to
2772 the haplotypic local ancestry analysis.

2773 Finally, we find that a weak but significant European admixture pulse occurred at the turn between
2774 the 19th and the 20th centuries, substantially later than the end of the TAST and the abolition of slavery
2775 and before the 20th European colonial migrations, whose putative historical causes remain to be eluci-
2776 dated. Furthermore, we find that the reproductive population of Santo Antão remained overall small
2777 during its' entire history until a very recent expansion, although much more limited than the expansions
2778 observed in Santiago and Fogo. This is somewhat surprising with the census records showing that Santo
2779 Antão was the second most peopled island after Santiago during most of Cabo Verde history (**Figure 7-**
2780 **resource table 1**). Nevertheless, our results could be explained by the demographic collapse experi-
2781 enced by Santo Antão since the beginning of the 20th century, due to several intense famine episodes
2782 and rural-urban emigration from the island; a demographic history scenario thus much more complex
2783 than the relatively simple scenario here explored. Reflecting the historically small population size on
2784 the island, Santo Antão show high total ROH and generally quite long individual ROH among the is-
2785 lands (**Figure 4** and **Appendix 4-figure 1-2**).

2786

2787 **Admixture history of São Nicolau (First official settlement 1580; Perennial settlement:**
2788 **1580)**

2789 *MetHis-ABC inferences detailed results for São Nicolau*

2790 For individuals born on São Nicolau island, we find that the two most recent admixture pulses from
2791 Europe and Africa, respectively, are precisely estimated with posterior distributions substantially de-
2792 parting from their priors and reduced 95%CI, for the pulses' timing and intensities (**Figure 7, Figure 7-**
2793 **figure supplement 1-3, Appendix 5-table 4**). We find that the most recent pulse of European admixture
2794 is weak in intensity (median=0.0731, mode=0.0297, 95%CI=[0.0038–0.6642]), and occurred very re-
2795 cently at the generation before that of the sampled individuals (generation median=19.0 after the found-
2796 ing at generation 0, mode=19.2, 95%CI=[10.3–19.8]). Furthermore, we find that the most recent African
2797 admixture pulse is very intense (median=0.6398, mode=0.7132, 95%CI=[0.0877–0.9380]), and oc-
2798 curred at generation 14.5 after founding (median, mode=14.6, 95%CI=[8.3–16.4]), during the abolition
2799 of the TAST in the first half of the 19th century.

2800 Interestingly, for both the more ancient admixture pulses from either Africa or Europe, our NN-
2801 ABC posterior parameter estimation provide reasonably informative posterior distributions pointing to-
2802 wards relatively weak African and European admixture intensities (median=0.3133, mode=0.1695,
2803 95%CI=[0.0171–0.9262]; and median=0.3240, mode=0.1193, 95%CI=[0.0145–0.9460], respectively).
2804 However, our results only provide indications that both pulses were ancient and occurred synchronically
2805 (generation median=5.2 after founding, mode=2.4, 95%CI=[1.3–15.5]; generation median=6.7,
2806 mode=2.7, 95%CI=[2.0–16.1], for the African and European older pulses respectively), as posterior
2807 distributions for the timing of these events are largely confounded with their respective priors.

2808 Finally, we obtain a posterior distribution of the founding admixture intensity largely confounded
2809 with its prior, similarly as for the demographic parameters, thus showing a limit of our ABC inferences
2810 procedures.

2811

2812

2813 **Appendix 5-table 4-São Nicolau:**

2814 **NN-ABC posterior parameter estimations for São Nicolau island, cross-validation posterior parameter errors, and**
2815 **cross-validation 95% Credibility Interval accuracies.**

2816 Cross-validation errors and 95% CI accuracies are based on 1,000 NN-ABC posterior parameter inferences using, in turn, each
2817 one of the 1,000 simulations closest to the observed data used as pseudo-observed data, and the remaining 99,999 simulations
2818 as the reference table.

2819 Error calculations are based on the mode and, separately, the median point estimate for each 1,000 pseudo-observed simulations
2820 posterior parameter estimation, compared to the known parameter used for simulation. We considered 11 neurons in the hidden
2821 layer and a tolerance level of 0.01 (1000 simulations) for all posterior parameter estimation in this analysis as identified in
2822 **Appendix 1-table 1**. Plotted distributions for posterior parameter estimations can be found in **Figure 7-figure supplement 1-**
2823 **3**.

2824

2825

2826

SAO NICOLAU Afr2P-Eur2P scenario parameters	Parameter posterior estimation				1,000 cross-validation errors		
	Mode	Median	50% Credibility Interval	95% Credibility Interval	Mode mean absolute error	Median mean absolute error	95% CI length accuracy
Ne.0	360	457	[238 - 734]	[34 - 979]	309	255	0.059
Ne.20	28767	48793	[25155 - 70475]	[3686 - 96753]	27502	23452	0.055
u.Ne	0.135	0.238	[0.133 - 0.358]	[0.025 - 0.483]	0.132	0.113	0.057
sAfr,0	0.3249	0.4730	[0.2491 - 0.7393]	[0.0327 - 0.9752]	0.3017	0.2461	0.051
tAfr,p1	2.4	5.2	[2.7 - 9.5]	[1.3 - 15.5]	5.9	4.5	0.145
sAfr,tAfr,p1	0.1695	0.3133	[0.1584 - 0.5404]	[0.0171 - 0.9262]	0.2897	0.2363	0.069
tAfr,p2	14.6	14.5	[13.2 - 14.9]	[8.3 - 16.4]	1.5	1.4	0.522
sAfr,tAfr,p2	0.7132	0.6398	[0.4900 - 0.7736]	[0.0877 - 0.9380]	0.1044	0.0981	0.055
tEur,p1	2.7	6.7	[3.5 - 10.8]	[2.0 - 16.1]	4.6	3.5	0.139
sEur,tEur,p1	0.1193	0.3240	[0.1547 - 0.5711]	[0.0145 - 0.9460]	0.2806	0.2394	0.048
tEur,p2	19.2	19.0	[17.7 - 19.4]	[10.3 - 19.8]	3.3	2.9	0.199
sEur,tEur,p2	0.0297	0.0731	[0.0295 - 0.1465]	[0.0038 - 0.6642]	0.2419	0.2067	0.065

2827

2828

2829 *Discussion for the admixture history of São Nicolau*

2830 Our results for the admixture history of São Nicolau indicate that two moderate admixture pulses from
 2831 Africa and Europe occurred synchronically between the date for the first perennial settlement of this
 2832 island in the 1580s and the onset of the intensification of the TAST at the beginning of the 17th century.
 2833 Much later in the course of Cabo Verde peopling history at the beginning of the 19th century, we find an
 2834 intense introgression event from Africa, probably occurring for the same reasons as in Santiago (see
 2835 above) and other Cabo Verde islands (see below and **Discussion** in main text).

2836 Interestingly, our haplotypic local ancestry inferences identify three African populations with
 2837 shared ancestries with São Nicolau-born individuals (**Figure 3**); Senegambian Wolof and Mandinka
 2838 shared-ancestry representing the majority similarly to the rest of Cabo Verde and as expected historically
 2839 (see **Discussion** in the main text, (25–28)), and South West Central African Angolan Ovimbundu a small
 2840 minority. Analogous to the Santo Antão inferences' limitations, our analyses cannot disentangle whether
 2841 either or both African pulses in São Nicolau involved the limited South West Central African popula-
 2842 tions shared ancestry here identified.

2843 Finally, we identify, much later during the 20th century, a weak event of European introgression for
 2844 the genetic admixture history of São Nicolau (**Figure 7D**), similarly likely due to labor-induced migra-
 2845 tions in the former Lusophone empire as for other islands, and in particular possibly due to the expansion
 2846 of fishing and cannery industry in São Nicolau at this time (28).

2847 Altogether, our genetic data contain little identifiable information for the demographic history of
 2848 this island (**Figure 7C, Figure 7-figure supplement 1**). This may be due to the recurrent demographic
 2849 collapses of the permanent settlement in this island due to intense starvation events, epidemic outbreaks,
 2850 and destructive pirate raids that affected the peopling of this island throughout history (**Figure 7-re-**
 2851 **source table 1**). Nevertheless, one genetic pattern that was consistent with these recurrent demographic
 2852 collapses is the high total levels of ROH observed in the data (**Figure 4** and **Appendix 4-figure 1-2**).

2853

2854

2855 **Admixture history of Brava (First official settlement 1580; Perennial settlement: 1580)**

2856 **MetHis-ABC inferences detailed results for Brava**

2857 For individuals born on Brava island, we find that the most recent pulse of European admixture is rela-
 2858 tively weak (median=0.1697, mode=0.1281, 95%CI=[0.0188–0.6504]), and occurred towards the abo-
 2859 lition of slavery in the Portuguese empire in the second half of the 19th century (generation median=16.3
 2860 after the founding of Cabo Verde at generation 0, mode=17.9, 95%CI=[4.2–19.3]), as indicated by pos-
 2861 terior distributions of parameters for this event largely differing from their priors (**Figure 7, Figure 7-**
 2862 **figure supplement 1-3, Appendix 5-table 5**). We identify a similarly intense pulse of admixture from
 2863 Africa (median=0.2473, mode=0.1261, 95%CI=[0.0191–0.8266]), for which our inferences only bore
 2864 indications that it occurred during the second half of the 18th century during the TAST, as the 95%CI
 2865 for the timing of this event is wide (generation median=13.6 after founding at generation 0, mode=15.7,
 2866 95%CI=[2.4–19.2]).

2867 More remotely in the past, we identify strong indications that a very weak European admixture
 2868 pulse (median=0.0352, mode=0.0157, 95%CI=[0.0007–0.7239]) may have occurred at the beginning of
 2869 the 17th century (generation median=7.3 after founding, mode=3.6, 95%CI=[2.8–16.1]). Furthermore,
 2870 we identify a strong signal for an intense African admixture pulse (median=0.6688, mode=0.7403,
 2871 95%CI=[0.1358–0.9685]), occurring at the beginning of Cabo Verdean peopling history, during the
 2872 early 16th century, at generation 2.8 after the founding of the archipelago at generation 0 (median,
 2873 mode=1.6, 95%CI=[1.1–12.2]), and thus largely before the first perennial settlement of this island.

2874 Finally, our results strongly support a very limited effective size linear increase (u_{Ne} median=0.420,
 2875 mode=0.435, 95%CI=[0.243–0.494]) throughout the entire history of the island reaching 7337 effective
 2876 individuals (median, mode=3278, 95%CI=[647–73,114]) in the present.

2877

2878 **Appendix 5-table 5-Brava:**

2879 **NN-ABC posterior parameter estimations for Brava island, cross-validation posterior parameter errors, and cross-**
 2880 **validation 95% Credibility Interval accuracies.**

2881 Cross-validation errors and 95% CI accuracies are based on 1,000 NN-ABC posterior parameter inferences using, in turn, each
 2882 one of the 1,000 simulations closest to the observed data used as pseudo-observed data, and the remaining 99,999 simulations
 2883 as the reference table.

2884 Error calculations are based on the mode and, separately, the median point estimate for each 1,000 pseudo-observed simulations
 2885 posterior parameter estimation, compared to the known parameter used for simulation. We considered 10 neurons in the hidden
 2886 layer and a tolerance level of 0.01 (1000 simulations) for all posterior parameter estimation in this analysis as identified in
 2887 **Appendix 1-table 1**. Plotted distributions for posterior parameter estimations can be found in **Figure 7-figure supplement 1-**
 2888 **3**.
 2889

BRAVA Afr2P-Eur2P scenario parameters	Parameter posterior estimation				1,000 cross-validation errors		
	Mode	Median	50% Credibility Interval	95% Credibility Interval	Mode mean absolute error	Median mean absolute error	95% CI length accuracy
Ne.0	495	501	[309 - 696]	[63 - 919]	308	254	0.068
Ne.20	3278	7337	[2908 - 17935]	[647 - 73114]	31523	24989	0.056
u.Ne	0.435	0.420	[0.374 - 0.455]	[0.243 - 0.494]	0.077	0.073	0.050
sAfr,0	0.7337	0.5666	[0.3452 - 0.7698]	[0.0497 - 0.9737]	0.2836	0.2405	0.059
tAfr,p1	1.6	2.8	[1.5 - 5.3]	[1.1 - 12.2]	3.9	3.1	0.159
sAfr,tAfr,p1	0.7403	0.6688	[0.4987 - 0.7995]	[0.1353 - 0.9685]	0.2418	0.2232	0.060
tAfr,p2	15.7	13.6	[8.4 - 16.3]	[2.4 - 19.2]	2.8	2.7	0.069
sAfr,tAfr,p2	0.1261	0.2473	[0.1272 - 0.3647]	[0.0191 - 0.8266]	0.2118	0.1905	0.058
tEur,p1	3.6	7.3	[4.1 - 11.1]	[2.8 - 16.1]	3.4	2.9	0.204
sEur,tEur,p1	0.0157	0.0352	[0.0116 - 0.1161]	[0.0007 - 0.7239]	0.2658	0.2338	0.064
tEur,p2	17.9	16.3	[12.5 - 18.0]	[4.2 - 19.3]	3.3	3.1	0.054
sEur,tEur,p2	0.1281	0.1697	[0.1054 - 0.2554]	[0.0188 - 0.6504]	0.1844	0.1716	0.057

2890

2891
2892
2893
2894
2895
2896
2897
2898
2899
2900
2901
2902
2903
2904
2905
2906
2907
2908
2909
2910
2911
2912
2913
2914
2915
2916
2917
2918
2919
2920
2921
2922

Discussion for the admixture history of Brava

We find an intense first African admixture pulse roughly three generations prior the first official and perennial peopling of the island in the 1580's (**Figure 7-resource table 1, Figure 7**), thus strongly suggesting that Brava was initially peopled by individuals already admixed and originating from another Cabo Verdean island, similarly to what was suggested for Fogo (see above). We hypothesize that Fogo admixed individuals were originally at the root of this peopling, as the patterns of shared haplotypic ancestry in Brava-born individuals strongly resemble that of Fogo, rather than Santiago, with shared ancestry exclusively with Senegambian Mandinka and in similar proportion, as well as a significant (albeit very reduced) signal for a shared ancestry with Tuscan TSI otherwise only found in Fogo (**Figure 3**). We find a limited introgression event from Europe during the late 17th century, possibly consistent with a known immigration event from Madeira and the Açores, and from Fogo after a volcano eruption, around this time (27). We also find a relatively weak African admixture pulse at some point during the height of the TAST for which the timing remains poorly inferred, and which will require further investigations.

Finally, we identify a more intense pulse of European admixture shortly after the abolition of slavery in the Portuguese empire in the second half of the 19th century. This later event may be due to the expansion of the whaling industry at this time, particularly in Brava due to favorable maritime currents and routes for this industry, which brought European and European-North American sailors to the island and increased locally contacts with Europe, and North America. Most interestingly, this historical scenario is also consistent with the signal, virtually unique across Cabo Verde, of a significant albeit reduced shared haplotypic ancestry between Brava-born individuals and the British GBR.

Notably, our results indicate that the effective population of Brava remained low during the entire peopling history of Cabo Verde and until today (**Figure 7C**), consistent with this island being the smallest inhabited and the most south-west ward in the archipelago (**Figure 7-resource table 1**). Surprisingly, in spite of the historically low effective population size, Brava shows low total ROH levels and relatively short ROH lengths (**Figure 4** and **Appendix 4-figure 1-2**), which remains to be elucidated in the future by considering larger sample sizes from the island.

2923 **Admixture history of Maio (First official settlement 1529; Perennial settlement: 1650)**

2924 *MetHis-ABC inferences detailed results for Maio*

2925 For individuals born on Maio island, we find evidence that the most recent pulse of European admixture
2926 was of relatively modest intensity (median=0.1472, mode=0.1134, 95%CI=[0.0233–0.5957]), and likely
2927 occurred during the 18th century, in the midst of the TAST (generation median=12.7 after founding at
2928 generation 0, mode=14.1, 95%CI=[3.7–17.9]), as both posterior distributions substantially departe from
2929 their respective priors (**Figure 7, Figure 7-figure supplement 1-3, Appendix 5-table 6**). Although our
2930 RF-ABC scenario-choice favors several pulses of admixture from both sources, our NN-ABC posterior
2931 parameter estimation fails to capture sufficient information to infer satisfactorily the most recent pulse
2932 of admixture from Africa, as both the posterior distribution of the timing of this event and its intensity
2933 seldom depart from their respective priors and have wide 95%CI.

2934 However, we capture substantial information strongly suggesting two, much older, admixture
2935 pulses from Europe and Africa, respectively, occurring virtually synchronically in the middle 16th
2936 century (generation median=4.1 after founding for the European pulse, mode=2.3, 95%CI=[1.7–14.2]; gen-
2937 eration median=4.2 after founding for the African pulse, mode=2.4, 95%CI=[1.5–12.8]), thus much ear-
2938 lier than the first perennial settlement of this island dated in 1650 by historians (**Figure 7-resource table**
2939 **1**). Furthermore, we find that the respective intensities of the two pulses (median=0.3260 for the Euro-
2940 pean pulse, mode=0.1075, 95%CI=[0.0117–0.9497]; median=0.5589 for the African pulse,
2941 mode=0.7703, 95%CI=[0.0346–0.9769]), sum close to 100%. This suggests a large replacement of the
2942 Maio population at that time, with indications that these synchronic admixture events occur on the basis
2943 of a founding admixed population largely of African origin (median $s_{Afr,0}$ =0.6757, mode=0.9135,
2944 95%CI=[0.017–0.421]).

2945 Finally, the demographic inference of reproductive size changes in Maio indicates, similarly as for
2946 Brava, that the reproductive size of the island remained relatively small during its entire history, and
2947 only very recently increased up to a median 21,454 effective individuals (mode=7159), albeit with a
2948 large 95%CI ([914–93,656]).

2949

2950 **Appendix 5-table 6-Maio:**

2951 **NN-ABC posterior parameter estimations for Maio island, cross-validation posterior parameter errors, and cross-val-
2952 idation 95% Credibility Interval accuracies.**

2953 Cross-validation errors and 95% CI accuracies are based on 1,000 NN-ABC posterior parameter inferences using, in turn, each
2954 one of the 1,000 simulations closest to the observed data used as pseudo-observed data, and the remaining 99,999 simulations
2955 as the reference table.

2956 Error calculations are based on the mode and, separately, the median point estimate for each 1,000 pseudo-observed simulations
2957 posterior parameter estimation, compared to the known parameter used for simulation. We considered 10 neurons in the hidden
2958 layer and a tolerance level of 0.01 (1000 simulations) for all posterior parameter estimation in this analysis as identified in
2959 **Appendix 1-table 1**. Plotted distributions for posterior parameter estimations can be found in **Figure 7-figure supplement 1-
2960 3**.

2961

2962

2963

MAIO Afr2P-Eur2P scenario parameters	Parameter posterior estimation				1,000 cross-validation errors		
	Mode	Median	50% Credibility Interval	95% Credibility Interval	Mode mean absolute error	Median mean absolute error	95% CI length accuracy
Ne.0	122	500	[241 - 746]	[29 - 980]	276	240	0.059
Ne.20	7159	21454	[7388 - 49176]	[914 - 93656]	30301	25378	0.072
u.Ne	0.080	0.121	[0.071 - 0.210]	[0.017 - 0.421]	0.082	0.078	0.064
sAfr,0	0.9135	0.6757	[0.3486 - 0.8841]	[0.0177 - 0.9941]	0.3150	0.2509	0.061
tAfr,p1	2.4	4.2	[2.5 - 6.8]	[1.5 - 12.8]	4.1	3.2	0.126
sAfr,tAfr,p1	0.7703	0.5589	[0.2768 - 0.7758]	[0.0346 - 0.9769]	0.2630	0.2350	0.051
tAfr,p2	14.4	11.1	[6.6 - 15.1]	[2.4 - 18.8]	2.5	2.4	0.112
sAfr,tAfr,p2	0.6543	0.5276	[0.2918 - 0.7126]	[0.0452 - 0.9393]	0.2168	0.1937	0.052
tEur,p1	2.3	4.1	[2.2 - 7.4]	[1.7 - 14.2]	3.2	2.8	0.219
sEur,tEur,p1	0.1075	0.3260	[0.1376 - 0.5818]	[0.0117 - 0.9497]	0.3014	0.2415	0.068
tEur,p2	14.1	12.7	[8.7 - 14.9]	[3.7 - 17.9]	3.3	3.1	0.048
sEur,tEur,p2	0.1134	0.1472	[0.0957 - 0.2301]	[0.0233 - 0.5957]	0.2145	0.1899	0.057

2964

2965

2966

Discussion for the admixture history of Maio

2967

2968

2969

2970

2971

2972

2973

Our results for the admixture history of Maio indicate a relatively simple scenario with a single pulse of European and African synchronic admixture having occurred in the mid-16th century in another Cabo Verdean island, long before the first perennial settlement of the island in 1650, similarly to Fogo or Brava. We hypothesize that this event occurred on Santiago, as shared local haplotypic ancestry patterns are highly resembling between islands (**Figure 3**), and also consistently with Maio being located very close to Santiago and historical records showing unequivocally the strong relationships between islands throughout history (25–28).

2974

2975

2976

2977

2978

2979

2980

After the descendants of this initial admixture event settled Maio, they experienced only a single identifiable admixture pulse of weak intensity from Europe, which likely occurred at the turn between the 18th and the 19th century during the TAST, and no clearly identifiable further signal of African admixture in the island. As for some other Cabo Verde islands, we cannot conclude about the timing of the African admixture event that brought the reduced signal of West Central and South West Central Africa shared haplotypic ancestry with Maio, observed in our ADMIXTURE and SOURCEFIND analyses (**Figure 3**).

2981

2982

2983

2984

Finally, the reduced population size throughout the history of Maio is consistent with the island being located close to Santiago and with much less water resources, having made it difficult to maintain and expand the settlement on this island, despite its first peopling having occurred early in the history of Cabo Verde almost exclusively dedicated to free-range cattle herding (25–27).

2985

2986

2987

2988

2989

2990

2991

ROH patterns are also consistent with this history, with high total ROH indicating long term isolation and population bottlenecks. Similar to Santiago there were some outlier individuals with much higher European ancestry within ROH compared to the remainder of the genome (**Figure 4** and **Appendix 4-figure 1-2**). This could possibly reflect historical marriage prohibitions and other social constraints against intercommunity reproductions (see **Discussion** in main text).

2992 **Admixture history of Boa Vista (First official settlement 1566; Perennial settlement:**
2993 **1650)**

2994 *MetHis-ABC inferences detailed results for Boa Vista*

2995 For the admixture history of individuals born on Boa Vista, we find an intense admixture pulse from
2996 Africa (median=0.6553, mode=0.7516, 95%CI=[0.1262–0.8949]), that occurred in the mid-19th century
2997 (generation median=15.0 after Cabo Verde founding at generation 0, mode=14.8, 95%CI=[11.0–17.4]),
2998 during the abolition of the TAST, with posterior distributions for both these parameters substantially
2999 departing from their respective priors and relatively reduced 95%CI (**Figure 7, Figure 7-figure sup-**
3000 **plement 1-3, Appendix 5-table 7**). Prior to that event, we fail to estimate the timing and intensity of
3001 the older African admixture pulse into Boa Vista, as posterior parameter distributions seldom depart
3002 from their respective priors for this event.

3003 However, our results strongly support a scenario with an intense period of recurring monotonically
3004 decreasing admixture from Europe (median admixture intensity at the period's start=0.8057,
3005 mode=0.9219, 95%CI=[0.2736–0.9907]; median admixture intensity at the period's end=0.340,
3006 mode=0.120, 95%CI=[0.021–0.880]), between the first official settlement of the island in 1566 (genera-
3007 tion median at the start of the European period of admixture=3.9 after founding, mode=2.2,
3008 95%CI=[1.7–11.8]), until shortly after its first perennial peopling dated in 1650 (generation median at
3009 the end of the European period of admixture=8.2, mode=8.6, 95%CI=[3.1–14.9]). Interestingly, the in-
3010 itial founding admixture event at the root of the genetic patterns of Boa Vista-born individuals supports
3011 a substantially lower amount of African admixture (median=0.3917, mode=0.1706, 95%CI=[0.1814–
3012 0.6678]), compared to the rest of Cabo Verde where this parameter could be reliably identified.

3013 Finally, our results show that the demography of Boa Vista remained relatively constant throughout
3014 the history of Cabo Verde, and indicate a possible very recent increase in effective size, albeit posterior
3015 parameter estimation of the most recent effective size was ambiguous due to large 95%CI (median
3016 $N_{e20}=47,744$, mode=13,128, 95%CI=[2657–98,587]).

3017
3018

3019 **Appendix 5-table 7-Boa Vista:**
 3020 **NN-ABC posterior parameter estimations for Boa Vista island, cross-validation posterior parameter errors, and cross-**
 3021 **validation 95% Credibility Interval accuracies.**

3022 Cross-validation errors and 95% CI accuracies are based on 1,000 NN-ABC posterior parameter inferences using, in turn, each
 3023 one of the 1,000 simulations closest to the observed data used as pseudo-observed data, and the remaining 99,999 simulations
 3024 as the reference table.

3025 Error calculations are based on the mode and, separately, the median point estimate for each 1,000 pseudo-observed simulations
 3026 posterior parameter estimation, compared to the known parameter used for simulation. We considered 8 neurons in the hidden
 3027 layer and a tolerance level of 0.01 (1000 simulations) for all posterior parameter estimation in this analysis as identified in
 3028 **Appendix 1-table 1**. Plotted distributions for posterior parameter estimations can be found in **Figure 7-figure supplement 1-**
 3029 **3**.

3030

BOA VISTA Afr2P-Eur Rec. scenario parameters	Parameter posterior estimation				1,000 cross-validation errors		
	Mode	Median	50% Credibility Interval	95% Credibility Interval	Mode mean absolute error	Median mean absolute error	95% CI length accuracy
Ne.0	731	627	[357 - 793]	[57 - 977]	263	230	0.049
Ne.20	13128	47744	[20486 - 76777]	[2657 - 98587]	30386	25219	0.074
u.Ne	0.056	0.079	[0.051 - 0.125]	[0.014 - 0.346]	0.067	0.066	0.059
sAfr,0	0.1706	0.3917	[0.1814 - 0.6678]	[0.0188 - 0.9677]	0.3186	0.2517	0.061
tAfr,p1	14.6	10.4	[5.8 - 14.2]	[2.4 - 16.8]	4.6	3.7	0.137
sAfr,tAfr,p1	0.2027	0.3760	[0.1998 - 0.5640]	[0.0261 - 0.8771]	0.2494	0.2213	0.056
tAfr,p2	14.8	15.0	[14.2 - 16.0]	[11.0 - 17.4]	1.7	1.7	0.113
sAfr,tAfr,p2	0.7516	0.6553	[0.4758 - 0.7671]	[0.1262 - 0.8949]	0.1962	0.1801	0.048
tEur,p1	2.2	3.9	[2.3 - 6.6]	[1.7 - 11.8]	3.7	3.1	0.192
tEur,p2	8.6	8.2	[6.0 - 10.2]	[3.1 - 14.9]	3.3	3.2	0.090
sEur,tEur,p1	0.9219	0.8057	[0.6300 - 0.9141]	[0.2736 - 0.9907]	0.2723	0.2319	0.076
sEur,tEur,p2	0.120	0.340	[0.1643 - 0.5832]	[0.021 - 0.880]	0.1721	0.1579	0.071
u.sEur	0.4444	0.2783	[0.151 - 0.398]	[0.0160 - 0.4907]	0.151	0.128	0.065

3031

3032 *Discussion for the admixture history of Boa Vista*

3033 Altogether, our results for the admixture history of Boa Vista born-individuals indicate a largely differ-
 3034 ing admixture history compared to all other islands of the archipelago. First, we find that the admixture
 3035 event at the root of the genetic peopling of the island, although occurring long before the first perennial
 3036 peopling of the island similarly to other islands such as Fogo, Brava, and Maio, is largely biased towards
 3037 European admixture, as opposed to all other islands in the archipelago (**Figure 7D**). Second, we find
 3038 the beginning of a period of recurring admixture from Europe before the mid-16th century, concomitantly
 3039 with the first official settlement of the island, and until its first perennial settlement in the 1650s. Inter-
 3040 estingly, this corresponds to a period when Boa Vista has been used by Cabo Verde as a penitentiary
 3041 island for non-enslaved individuals which may explain the recurring admixture process here identified
 3042 (25–27).

3043 Later-on towards the end of the TAST in the 19th century, Boa Vista experienced an intense pulse
 3044 of African admixture, similarly to Santiago and Saõ Nicolau and probably for similar complex socio-
 3045 cultural reasons (see **Discussion** in the main text). However, overall limited historical records specific
 3046 to this island render speculative the interpretation of our results based on genetics only (**Figure 7-re-**
 3047 **source table 1**).

3048 Finally, the effective size of Boa Vista remained constant and low throughout the history of this
 3049 island (**Figure 7C**), which echoes its' small historical census sizes, mainly due to limited water resources
 3050 on the island, up until today (**Figure 7-resource table 1**). ROH patterns are also consistent with this
 3051 history, with the highest total ROH among the Cabo Verdean islands indicating long term isolation and
 3052 population bottlenecks (**Figures F4** and **Appendix 4-figure 1-2**).

3053 **Admixture history of São Vicente (First official settlement 1570; Perennial settlement:**
3054 **1780)**

3055 *MetHis-ABC inferences detailed results for São Vicente*

3056 For the admixture history of individuals born on São Vicente, we find a recent European admixture
3057 pulse of substantial intensity (median=0.2840, mode=0.2596, 95%CI=[0.0397–0.8044]), having likely
3058 occurred towards the end of the 19th century (generation median=17.4 after founding of Cabo Verde at
3059 generation 0, mode=17.7, 95%CI=[10.6–18.9]); both posterior distributions have relatively narrow
3060 95%CI and clearly depart from their respective priors (**Figure 7, Figure 7-figure supplement 1-3, Ap-**
3061 **pendix 5-table 8).**

3062 This most recent admixture event is preceded by a period of recurrent decreasing African admixture
3063 likely spanning the second half of the most intense period of the TAST starting in the early 18th century
3064 (generation median at the start of the African period of admixture=9.7, mode=12.6, 95%CI=[2.5–16.9]),
3065 and ending during the end of the TAST and the abolition of slavery in the Portuguese Empire in the
3066 mid-19th century (generation median at the end of the African period of admixture=15.8, mode=17.5,
3067 95%CI=[7.4–19.1]), albeit our results are ambiguous for the estimate of the start of this admixture period
3068 as indicated by the large 95%CI. Furthermore, our results are also ambiguous to estimate the intensity
3069 of the African introgression during the period of recurring admixture, as the posterior distributions for
3070 the onset and offset intensities, as well as the shape of the monotonic recurring admixture do not clearly
3071 depart from their respective priors and had large 95%CIs.

3072 We find traces of an older European admixture pulse of substantial intensity (median=0.3403,
3073 mode=0.1772, 95%CI=[0.0149–0.9133]), which likely occurred at the beginning of the 17th century
3074 (generation median =6.4 after founding, mode=2.8, 95%CI=[1.9–15.1]). Our results indicate that this
3075 first admixture event occurred on a root-population that exhibited a large African admixture proportion
3076 (median $s_{\text{Af},0}$ =0.5983, mode=0.8596, 95%CI=[0.0529–0.9835]), albeit this result should be considered
3077 with cautious as CI is overall wide.

3078 Finally, our results clearly indicate a strong effective population expansion since the perennial peo-
3079 pling of the island in the late 18th century, up to 66,715 effective individuals today (median,
3080 mode=85,838, 95%CI=[12,159–98,375]).

3081
3082

3083 **Appendix 5-table 8-São Vicente:**

3084 **NN-ABC posterior parameter estimations for São Vicente island, cross-validation posterior parameter errors, and**
 3085 **cross-validation 95% Credibility Interval accuracies.**

3086 Cross-validation errors and 95% CI accuracies are based on 1,000 NN-ABC posterior parameter inferences using, in turn, each
 3087 one of the 1,000 simulations closest to the observed data used as pseudo-observed data, and the remaining 99,999 simulations
 3088 as the reference table.

3089 Error calculations are based on the mode and, separately, the median point estimate for each 1,000 pseudo-observed simulations
 3090 posterior parameter estimation, compared to the known parameter used for simulation. We considered 11 neurons in the hidden
 3091 layer and a tolerance level of 0.01 (1000 simulations) for all posterior parameter estimation in this analysis as identified in
 3092 **Appendix 1-table 1**. Plotted distributions for posterior parameter estimations can be found in **Figure 7-figure supplement 1-**
 3093 **3**.

3094

3095

SAO VICENTE Afr Rec.-Eur2P scenario parameters	Parameter posterior estimation				1,000 cross-validation errors		
	Mode	Median	50% Credibility Interval	95% Credibility Interval	Mode mean absolute error	Median mean absolute error	95% CI length accuracy
Ne.0	109	262	[115 - 486]	[19 - 918]	288	243	0.061
Ne.20	85838	66715	[42741 - 84818]	[12159 - 98375]	29947	23721	0.048
u.Ne	0.215	0.244	[0.174 - 0.338]	[0.072 - 0.469]	0.094	0.084	0.049
sAfr,0	0.8596	0.5983	[0.3334 - 0.8142]	[0.0529 - 0.9835]	0.3231	0.2499	0.063
tAfr,p1	12.6	9.7	[5.7 - 13.1]	[2.5 - 16.9]	3.9	3.4	0.153
tAfr,p2	17.5	15.8	[13.8 - 17.6]	[7.4 - 19.1]	2.8	2.7	0.235
sAfr,tAfr,p1	0.6796	0.7168	[0.5698 - 0.8525]	[0.2806 - 0.9795]	0.2031	0.1774	0.079
sAfr,tAfr,p2	0.2149	0.2786	[0.1561 - 0.4266]	[0.0256 - 0.7820]	0.1538	0.1457	0.063
u.sAfr	0.072	0.228	[0.111 - 0.360]	[0.015 - 0.484]	0.161	0.126	0.056
tEur,p1	2.8	6.4	[3.1 - 10.0]	[1.9 - 15.1]	4.1	3.3	0.214
sEur,tEur,p1	0.1772	0.3403	[0.1733 - 0.5442]	[0.0149 - 0.9133]	0.2448	0.2126	0.055
tEur,p2	17.7	17.4	[16.3 - 18.0]	[10.6 - 18.9]	2.0	2.1	0.143
sEur,tEur,p2	0.2596	0.2840	[0.1732 - 0.4177]	[0.0397 - 0.8044]	0.1585	0.1498	0.059

3096

3097

3098 *Discussion for the admixture history of São Vicente*

3099 Our results for the admixture history of individuals born on São Vicente indicate a strong European
 3100 admixture event concomitant with the first official peopling of the island occurring at the same time as
 3101 the nearby island of Santo Antão, consistently with historical records (**Figure 7-resource table 1**). How-
 3102 ever, the perennial peopling of this island was difficult due to the very limited water resources, in par-
 3103 ticular compared to the much more hospitable, larger, and nearby Santo Antão. Thus, São Vicente es-
 3104 sentially served as a coal and salt harbor depot during most of its history with a minimal settlement (28),
 3105 which may explain the initial European admixture pulse we identify (**Figure 7**), and our local haplotypic
 3106 shared ancestry results (**Figure 3**).

3107 Later-on and unique in Cabo Verde, our results support a long period of recurring African admix-
 3108 ture occurring during the entire second half of the TAST and ending with the abolition of slavery in the
 3109 Portuguese empire. However, only the final admixture event of this period could be precisely inferred
 3110 to have occurred during the mid-19th century during the abolition of the TAST and of slavery in the
 3111 Portuguese empire (**Figure 7D**). The small haplotypic ancestry shared between São Vicente-born indi-
 3112 viduals and West Central and/or South West Central African population may stem from illegal slave-
 3113 trade known to have surged during this period. Nevertheless, the poor performances of our parameter
 3114 inference for the other parameters of this recurring admixture period may indicate that more complex
 3115 admixture scenarios than the ones considered occurred in this island, thus begging for future work fur-
 3116 ther complexifying admixture histories to be reconstructed with ABC.

3117 Interestingly, historical data show that São Vicente census only very recently started to increase,
3118 with newly available water sources and a protected deep-water harbor in the bay of Mindelo, unique in
3119 Cabo Verde, which favored the massive economic expansion of the island in the late 19th century and
3120 throughout the 20th century (**Figure 7-resource table 1**). Furthermore, the end of the agro-slavery sys-
3121 tem and end of plantation economy in Cabo Verde at the end of the 18th century and beginning of the
3122 19th century are known historically to have triggered emigration from Santo Antão and rural-urban mi-
3123 grations during the 19th and 20th century, essential for São Vicente perennial peopling (28,78). This is
3124 further consistent with extensive familial grand-parental birth-places in Santo Antão and extensive fa-
3125 miliary relationships reported by São Vicente-born individuals in our familial anthropology interviews.

3126 Altogether, these historical, economic, and demographic processes may well explain the onset of
3127 the large reproductive population increase identified in our analyses (**Figure 7C**), as well as haplotypic
3128 local ancestry patterns largely resembling those obtained for Santo Antão (**Figure 3**). Furthermore, they
3129 are consistent with the substantial European admixture pulse identified at the turn of the 19th and 20th
3130 century with our analyses. Reflecting the historical small population size, São Vicente had high total
3131 levels of ROH (**Figure 4**). Interestingly, individuals from this island, on average, show more African
3132 ancestry in ROH compared to the remainder of the genome. This could possibly reflect historical mar-
3133 riage prohibitions or the historically high levels of recurrent African admixture, or both.

3134
3135

3136 **Admixture history of Sal (First official settlement 1529; Perennial settlement: 1841)**

3137 **MetHis-ABC inferences detailed results for Sal**

3138 Finally, the admixture history of individuals born on Sal inferred with NN-ABC is overall ambiguous *a*
 3139 *posteriori* (**Figure 7, Figure 7-figure supplement 1-3, Appendix 5-table 9**). Indeed, while our RF-
 3140 ABC scenario-choice leaned towards a complex admixture history with a period of recurring admixture
 3141 from Europe and two African admixture pulses after the initial founding admixture event for the popu-
 3142 lation of Sal, the duration and intensity of the European admixture period, as well as the first African
 3143 admixture pulse, all showed posterior parameter distributions seldom departing from their priors. Nev-
 3144 ertheless, we clearly identify a recent African admixture pulse of moderate intensity (median=0.2401,
 3145 mode=0.1780, 95%CI=[0.0197–0.6590]), which likely occurred at the end of the 19th century (genera-
 3146 tion median=17.6 after the founding of Cabo Verde at generation 0, mode=17.9, 95%CI=[12.5–19.0]).
 3147 Furthermore, our results indicate a strong and very recent effective size expansion in Sal, up to 63,289
 3148 individuals (median, mode =88,248, 95%CI=[5689–98,181]).

3149

3150 **Appendix 5-table 9-Sal:**

3151 **NN-ABC posterior parameter estimations for Sal island, cross-validation posterior parameter errors, and cross-valida-
 3152 tion 95% Credibility Interval accuracies.**

3153 Cross-validation errors and 95% CI accuracies are based on 1,000 NN-ABC posterior parameter inferences using, in turn, each
 3154 one of the 1,000 simulations closest to the observed data used as pseudo-observed data, and the remaining 99,999 simulations
 3155 as the reference table.

3156 Error calculations are based on the mode and, separately, the median point estimate for each 1,000 pseudo-observed simulations
 3157 posterior parameter estimation, compared to the known parameter used for simulation. We considered 11 neurons in the hidden
 3158 layer and a tolerance level of 0.01 (1000 simulations) for all posterior parameter estimation in this analysis as identified in
 3159 **Appendix 1-table 1**. Plotted distributions for posterior parameter estimations can be found in **Figure 7-figure supplement 1-
 3160 3**.

3161

3162

SAL Afr2P-EurRec. scenario parameters	Parameter posterior estimation				1,000 cross-validation errors		
	Mode	Median	50% Credibility Interval	95% Credibility Interval	Mode mean absolute error	Median mean absolute error	95% CI length accuracy
Ne.0	525	518	[285 - 745]	[41 - 966]	306	250	0.061
Ne.20	88248	63289	[36457 - 82778]	[5689 - 98181]	30007	24554	0.058
u.Ne	0.038	0.076	[0.035 - 0.155]	[0.005 - 0.399]	0.112	0.102	0.056
sAfr,0	0.8853	0.5820	[0.3164 - 0.8077]	[0.0247 - 0.9820]	0.3039	0.2508	0.060
tAfr,p1	3.2	9.0	[4.8 - 13.1]	[1.8 - 16.8]	4.9	4.1	0.122
sAfr,tAfr,p1	0.7261	0.5166	[0.2893 - 0.7374]	[0.0302 - 0.9626]	0.2667	0.2275	0.063
tAfr,p2	17.9	17.6	[16.3 - 18.0]	[12.5 - 19.0]	1.3	1.2	0.212
sAfr,tAfr,p2	0.1780	0.2401	[0.1374 - 0.3655]	[0.0197 - 0.6590]	0.1588	0.1462	0.071
tEur,p1	3.9	9.3	[5.3 - 12.6]	[3.3 - 16.8]	4.2	3.4	0.180
tEur,p2	17.8	16.2	[13.9 - 17.8]	[6.8 - 19.4]	3.7	3.5	0.102
sEur,tEur,p1	0.4931	0.5657	[0.3810 - 0.7810]	[0.1100 - 0.9754]	0.2585	0.2183	0.072
sEur,tEur,p2	0.0730	0.2061	[0.0842 - 0.4034]	[0.0113 - 0.7804]	0.1926	0.1734	0.076
u.sEur	0.137	0.207	[0.102 - 0.346]	[0.011 - 0.486]	0.156	0.128	0.061

3163

3164

3165 **Discussion for the admixture history of Sal**

3166 Sal was among the early Cabo Verdean islands to be officially settled and exploited, in 1529 (**Figure 7-
 3167 resource table 1**), as a source of sea-salt both exported and employed locally in the free-range herding
 3168 meat-production and tannery industry at the historical root of Cabo Verde economy with Europe and
 3169 Africa (26,78). However, its perennial peopling dated only from 1841, the last perennially peopled is-

3170 land of Cabo Verde, as water sources and agricultural surfaces are scarce on this island. This slow de-
3171 mographic expansion is well captured by our inference showing a reduced population size during most
3172 Cabo Verde history on Sal, followed very recently by a strong reproductive size increase (**Figure 7C**).
3173 Furthermore, in this context, our results clearly identifying only a recent admixture pulse of African
3174 origin at the beginning of the 20th century could reflect the recent economic migrations of Western
3175 African populations to this island, during the development of its salt mining activities and its travel and
3176 tourism activities since then. Nevertheless, our scenario-choice results suggested the occurrence of a
3177 period of recurrent European admixture in Sal, which our posterior parameter inference largely failed to
3178 identify. This is possibly due to the complex recent peopling history of Sal that we fail to capture with
3179 genetic data, which will need to be clarified in the future in particular with additional samples from this
3180 island. Nevertheless, reflecting the historical small population size, Sal has high total levels of ROH
3181 (**Figure 4**).
3182

3183 **Appendix 5-table 10-Cabo Verde:**

3184 **NN-ABC posterior parameter estimations for 225 Cabo Verde-born individuals considered as a single random-mating**
 3185 **population, cross-validation posterior parameter errors, and cross-validation 95% Credibility Interval accuracies.**

3186 Cross-validation errors and 95% CI accuracies are based on 1,000 NN-ABC posterior parameter inferences using, in turn, each
 3187 one of the 1,000 simulations closest to the observed data used as pseudo-observed data, and the remaining 99,999 simulations
 3188 as the reference table.

3189 Error calculations are based on the mode and, separately, the median point estimate for each 1,000 pseudo-observed simulations
 3190 posterior parameter estimation, compared to the known parameter used for simulation. We considered 5 neurons in the hidden
 3191 layer and a tolerance level of 0.01 (1000 simulations) for all posterior parameter estimation in this analysis as identified in
 3192 **Appendix 1-table 1**. Plotted distributions for posterior parameter estimations can be found in **Figure 7-figure supplement 1-**
 3193 **3**.
 3194

CABO VERDE Afr2P-Eur2P scenario parameters	Parameter posterior estimation				1,000 cross-validation errors		
	Mode	Median	50% Credibility Interval	95% Credibility Interval	Mode mean absolute error	Median mean absolute error	95% CI length accuracy
Ne.0	343	490	[267 - 726]	[34 - 968]	296	238	0.058
Ne.20	86901	61995	[36958 - 82637]	[8050 - 98176]	26496	23321	0.047
u.Ne	0.469	0.400	[0.310 - 0.463]	[0.172 - 0.497]	0.118	0.107	0.041
sAfr,0	0.5801	0.5015	[0.2560 - 0.7308]	[0.0271 - 0.9794]	0.3000	0.2464	0.057
tAfr,p1	3.1	9.0	[5.0 - 13.0]	[2.0 - 18.0]	5.7	4.2	0.090
sAfr,tAfr,p1	0.4597	0.4831	[0.2575 - 0.7249]	[0.0263 - 0.9644]	0.2556	0.2310	0.049
tAfr,p2	19.2	18.6	[17.2 - 19.3]	[11.9 - 19.3]	1.3	1.2	0.153
sAfr,tAfr,p2	0.7056	0.6224	[0.4317 - 0.7576]	[0.1164 - 0.9303]	0.1483	0.1379	0.037
tEur,p1	2.4	6.1	[3.0 - 9.3]	[2.0 - 16.1]	4.4	3.4	0.146
sEur,tEur,p1	0.1193	0.4300	[0.2038 - 0.7022]	[0.0216 - 0.9718]	0.3006	0.2487	0.056
tEur,p2	18.2	15.1	[11.2 - 17.9]	[4.1 - 19.0]	3.1	2.7	0.086
sEur,tEur,p2	0.1882	0.4150	[0.2029 - 0.6780]	[0.0313 - 0.9647]	0.2471	0.2115	0.051

3195
 3196
 3197

3198 **OTHER RESSOURCE TABLES: in .txt format below and xls format online**

3199

3200

3201 **Figure 1-resource table 1: See .xls file**

3202 **Population table corresponding to the map in Figure 1 and sample inclusion in all analysis.**

3203

3204

3205 **Figure 1-resource table 1: Part – 1 of 3**

Region	Population Code	Population description	N	Latitude	Longitude	Data Reference	Fig.1; Appen dix1-fig.1	Appen dix2-fig.1	Appen dix2-fig.2	Appen dix2-fig.3	Appen dix2-fig.4	Fig.2; Fig.2-fig.sup p.1	Fig.3; Fig.3-fig.sup p.1-2; Appen dix3-fig.1	Fig.4; Fig.4-fig.sup p.1-2; Appen dix4-fig.1-2	Fig.5	Fig.7; Fig.7-fig.sup p1-3;App dix1-fig2-4
	Cabo Verde Kriolu speakers	Born on Santiago	59	15.12	-23.64	This Study & (31)	x	x	x	x	x	x	x	x	x	x
	Cabo Verde Kriolu speakers	Born on Fogo	26	15.12	-23.64	This Study	x	x	x	x	x	x	x	x	x	x
	Cabo Verde Kriolu speakers	Born on Santo Antão	30	15.12	-23.64	This Study	x	x	x	x	x	x	x	x	x	x
	Cabo Verde Kriolu speakers	Born on São Nicolau	25	15.12	-23.64	This Study	x	x	x	x	x	x	x	x	x	x
	Cabo Verde Kriolu speakers	Born on Maio	10	15.12	-23.64	This Study	x	x	x	x	x	x	x	x	x	x
	Cabo Verde Kriolu speakers	Born on Brava	12	15.12	-23.64	This Study	x	x	x	x	x	x	x	x	x	x
	Cabo Verde Kriolu speakers	Born on Bôa Vista	17	15.12	-23.64	This Study	x	x	x	x	x	x	x	x	x	x
	Cabo Verde Kriolu speakers	Born on São Vicente	37	15.12	-23.64	This Study	x	x	x	x	x	x	x	x	x	x
	Cabo Verde Kriolu speakers	Born on Sal	9	15.12	-23.64	This Study	x	x	x	x	x	x	x	x	x	x
	West Western Africa	Cabo Verde Kriolu speakers	Foreign born (Portugal, Mozambic, Angola, France, USA)	8	15.12	-23.64	This Study	x	x	x	x	x	x	-	-	-
Fula		Gambian in Western Division, The Gambia - Fula	74	13.45	-16.58	(16,37,38)	x	x	x	x	-	-	-	-	-	-
GWD		Gambian in Western Division, The Gambia - Mandinka	113	13.45	-16.58	(16,37,38)	x	x	x	x	x	x	Resam ple 50	Resam ple 50	-	-
Jola		Gambian in Western Division, The Gambia - Jola	79	13.45	-16.58	(16,37,38)	x	x	x	x	x	x	Resam ple 50	Resam ple 50	-	-
Mandinka		Gambia	87	13.47	-16.57	(16)	x	x	x	x	x	x	Resam ple 50	Resam ple 50	-	Resam ple 60
Wolof		Gambian in Western Division, The Gambia - Wolof	78	13.45	-16.58	(16,37,38)	x	x	x	x	x	x	Resam ple 50	Resam ple 50	-	-
Central Western Africa	Ahizi	Ivory Coast	18	5.25	-4.61	(29)	x	x	x	x	x	x	-	-	-	-
	MSL	Mende in Sierra Leone	85	8.48	-13.23	(37)	x	x	x	x	x	x	Resam ple 50	Resam ple 50	-	-
	Yacouba	Ivory Coast	17	7.27	-8.17	(39)	x	x	x	x	x	x	-	-	-	-
East Western Africa	Bariba	Benin	20	9.35	2.62	(29)	x	x	x	x	x	x	-	-	-	-
	ESN	Esan in Nigeria	98	9.07	7.48	(37)	x	x	x	x	x	x	Resam ple 50	Resam ple 50	-	-
	Fon	Benin	12	6.35	2.41	(29)	x	x	x	x	x	x	-	-	-	-
	Ga-Adangbe	Ghana	100	8.00	-2.00	(16)	x	x	x	x	x	x	Resam ple 50	Resam ple 50	-	-
	Igbo	Nigeria	99	6.00	7.00	(16)	x	x	x	x	x	x	Resam ple 50	Resam ple 50	-	-
	Yoruba	Benin	20	7.36	2.60	(29)	x	x	x	x	x	x	-	-	-	-
	YRI	Yoruba in Ibadan, Nigeria	108	7.40	3.92	(37)	x	x	x	x	x	x	Resam ple 50	Resam ple 50	-	-

3206

3207

3208 **Figure 1-resource table 1: Part – 2 of 3**

Region	Population Code	Population description	N	Latitude	Longitude	Data Reference	Fig.1; Appen dix1-fig.1	Appen dix2-fig.1	Appen dix2-fig.2	Appen dix2-fig.3	Appen dix2-fig.4	Fig.2; Fig.2-fig.sup p.1	Fig.3; Fig.3-fig.sup p.1-2; Appen dix3-fig.1	Fig.4; Fig.4-fig.sup p.1-2; Appen dix4-fig.1-2	Fig.5	Fig.7; Fig.7-fig.sup p.1-3; Appen dix1-fig.2-4
West Central Africa	Akele	Gabon	37	-0.70	10.22	(29)	x	x	x	x	-	-	-	-	-	-
	Ba.Bongo East	Gabon	27	-2.27	13.58	(29)	x	x	x	-	-	-	-	-	-	-
	Badwee	Cameroon	38	3.56	13.12	(29)	x	x	x	x	-	-	-	-	-	-
	Baka	Cameroon	97	3.08	14.07	(29)	x	x	x	-	-	-	-	-	-	-
	Bakota	Gabon	46	0.57	12.87	(29)	x	x	x	x	-	-	-	-	-	-
	Bakoya	Gabon	20	1.00	14.00	(29)	x	x	x	-	-	-	-	-	-	-
	Bapunu	Gabon	47	-1.87	11.02	(29)	x	x	x	x	-	-	-	-	-	-
	Bateke	Gabon	41	-0.82	12.70	(29)	x	x	x	x	-	-	-	-	-	-
	Bekwil	Gabon	5	1.18	13.22	(29)	x	x	x	x	-	-	-	-	-	-
	Benga	Gabon	38	0.58	9.33	(29)	x	x	x	x	-	-	-	-	-	-
	Bezan	Cameroon	20	5.45	11.36	(29)	x	x	x	-	-	-	-	-	-	-
	Biaka	Aka from CAR	15	4.00	17.00	(29)	x	x	x	-	-	-	-	-	-	-
	Duma	Gabon	39	-0.82	12.70	(29)	x	x	x	x	-	-	-	-	-	-
	Eshira	Gabon	40	-1.22	10.60	(29)	x	x	x	x	-	-	-	-	-	-
	Eviya	Gabon	23	-1.21	10.60	(29)	x	x	x	x	-	-	-	-	-	-
	Fang	Gabon	65	2.08	11.48	(29)	x	x	x	x	-	-	Resam ple 50	Resam ple 50	-	-
	Galoa	Gabon	46	-0.70	10.22	(29)	x	x	x	x	-	-	-	-	-	-
	Makina	Gabon	39	-0.10	11.93	(29)	x	x	x	x	-	-	-	-	-	-
	Ndumu	Gabon	37	-1.63	13.58	(29)	x	x	x	x	-	-	-	-	-	-
	Nzebi	Gabon	61	-1.57	13.20	(29)	x	x	x	x	-	-	Resam ple 50	Resam ple 50	-	-
Obamba	Gabon	45	-0.68	13.78	(29)	x	x	x	x	-	-	-	-	-	-	
Okande	Gabon	7	-0.05	11.62	(29)	x	x	x	x	-	-	-	-	-	-	
Orungu	Gabon	19	-0.72	8.78	(29)	x	x	x	x	-	-	-	-	-	-	
Shake	Gabon	47	-0.82	12.70	(29)	x	x	x	x	-	-	-	-	-	-	
Tsogo	Gabon	60	-1.03	10.67	(29)	x	x	x	x	-	-	Resam ple 50	Resam ple 50	-	-	
Yaounde	Cameroon	39	3.84	11.50	(16)	x	x	x	x	-	-	-	-	-	-	
Sout-West Central Africa	Kimbundu	Angola	17	-8.83	13.22	(29)	x	x	x	x	-	-	x	x	-	-
	Kongo	Angola	10	-8.83	13.22	(29)	x	x	x	x	-	-	x	x	-	-
	Ovimbundu	Angola	12	-8.83	13.22	(29)	x	x	x	x	-	-	x	x	-	-
Umbundo	Angola	5	-8.83	13.22	(29)	x	x	x	x	-	-	x	x	-	-	
South Africa	Sotho	South Africa	86	-29.13	26.26	(16)	x	x	x	x	-	-	Resam ple 50	Resam ple 50	-	-
	Zulu	South Africa	100	-29.00	24.00	(16)	x	x	x	x	-	-	Resam ple 50	Resam ple 50	-	-

3209

3210

3211 **Figure 1-resource table 1: Part 3 of 3**

Region	Population Code	Population description	N	Latitude	Longitude	Data Reference	Fig.1; Appen dix1-fig.1	Appen dix2-fig.1	Appen dix2-fig.2	Appen dix2-fig.3	Appen dix2-fig.4	Fig.2; Fig.2-fig.sup p.1	Fig.3; Fig.3-fig.sup p.1-2; Appen dix3-fig.1	Fig.4; Fig.4-fig.sup p.1-2; Appen dix4-fig.1-2	Fig.5	Fig.7; Fig.7-fig.sup p.1-3; Appen dix1-fig.2-4
East Africa	Baganda	Uganda	99	1.00	32.00	(16)	x	x	x	-	-	-	-	-	-	-
	Banyarwanda	Uganda	96	1.00	32.00	(16)	x	x	x	-	-	-	-	-	-	-
	Barundi	Uganda	93	1.00	32.00	(16)	x	x	x	-	-	-	-	-	-	-
	Ethiopia	Ethiopia	107	8.00	38.00	(16)	x	x	x	-	-	-	-	-	-	-
	Kalenjin	Kenya	100	1.00	38.00	(16)	x	x	x	-	-	-	-	-	-	-
	Kikuyu	Kenya	99	-0.40	36.90	(16)	x	x	x	-	-	-	-	-	-	-
	LWK	Luhya in Webuye, Kenya	97	-1.27	36.61	(37)	x	x	x	-	-	-	-	-	-	-
	Mbuti	DRC	13	1.00	29.00	(29)	x	x	x	-	-	-	-	-	-	-
Europe	Twa	Uganda	2	-0.98	29.62	(39)	x	x	x	-	-	-	-	-	-	-
	FIN	Finnish in Finland	99	60.17	24.93	(37)	x	x	x	x	x	x	Resam ple 50	Resam ple 50	-	-
	GBR	British in England and Scotland	90	52.49	-1.89	(37)	x	x	x	x	x	x	Resam ple 50	Resam ple 50	-	-
	IBS	Iberian populations in Spain	107	40.38	-3.72	(37)	x	x	x	x	x	x	Resam ple 50	Resam ple 50	-	Resam ple 60
	TSI	Toscani in Italy	107	42.10	12.00	(37)	x	x	x	x	x	x	Resam ple 50	Resam ple 50	-	-
South Asia	BEB	Bengali in Bangladesh	86	23.70	90.35	(37)	x	x	-	-	-	-	-	-	-	-
	GIH	Gujarati Indians in Houston, TX	101	22.62	70.69	(37)	x	x	-	-	-	-	-	-	-	-
	ITU	Indian Telugu in the UK	101	17.18	79.79	(37)	x	x	-	-	-	-	-	-	-	-
	PJL	Punjabi in Lahore, Pakistan	94	31.55	74.36	(37)	x	x	-	-	-	-	-	-	-	-
	STU	Sri Lankan Tamil in the UK	99	8.38	80.50	(37)	x	x	-	-	-	-	-	-	-	-
East Asia	CDX	Chinese Dai in Xishuangbanna, China	92	22.00	100.78	(37)	x	x	-	-	-	-	-	-	-	-
	CHB	Han Chinese in Beijing, China	103	39.92	116.38	(37)	x	x	-	-	-	-	Resam ple 50	Resam ple 50	-	-
	CHS	Han Chinese South	104	23.13	113.27	(37)	x	x	-	-	-	-	-	-	-	-
	JPT	Japanese in Tokyo, Japan	104	35.68	139.68	(37)	x	x	-	-	-	-	-	-	-	-
	KHV	Kinh in Ho Chi Minh City, Vietnam	99	10.78	106.68	(37)	x	x	-	-	-	-	-	-	-	-
USA	ASW	African Ancestry in Southwest US	55	35.48	-97.53	(37)	x	x	x	x	x	x	Resam ple 50	Resam ple 50	-	-
	CEU	US Utah residents (CEPH) with Northern and Western European ancestry	99	40.77	-111.89	(37)	x	x	x	x	x	x	Resam ple 50	Resam ple 50	-	-
	MXL	Mexican Ancestry in Los Angeles, California	64	34.05	-118.24	(37)	x	x	-	-	-	-	-	-	-	-
Caribbean	ACB	African Caribbean in Barbados	95	13.10	-59.62	(37)	x	x	x	x	x	x	Resam ple 50	Resam ple 50	-	-
	PUR	Puerto Rican in Puerto Rico	104	18.40	-66.10	(37)	x	x	x	x	x	x	-	-	-	-
South America	CLM	Colombian in Medellin, Colombia	94	4.58	-74.07	(37)	x	x	-	-	-	-	-	-	-	-
	PEL	Peruvian in Lima, Peru	85	-12.04	-77.03	(37)	x	x	-	-	-	-	-	-	-	-

3212

3213

3214 **Figure 4-resource table 1: See .xls file**

3215 **Mean proportion of total length of ROH that are classified as long ($cM \geq 1$) for each Cabo Verdean island of birth.**

3216

Cabo Verdean birth-island	Mean proportion of total length of long-ROH
Brava	0.07973
Fogo	0.13586
Santiago	0.06459
Maio	0.22948
Boa Vista	0.28049
Sal	0.24777
São Nicolau	0.25810
São Vicente	0.18486
Santo Antão	0.25979

3217

3218

3219 **Figure 4-resource table 2: See .xls file**

3220 **Permutation tests' p-values for over/under representation of ancestry in long ROH ($cM \geq 1$) for each Cabo Verdean**
3221 **island of birth.**

3222 As mentioned in the main **Material and Methods 4**, for each individual in each island, we randomly permute the location of
3223 all long ROH (ensuring that no permuted ROH overlap), re-compute the local AFR ancestry proportion falling within these
3224 permuted ROH, and then subtract the global ancestry proportion. We then take the mean of this difference across all individuals
3225 for each island and repeat the process 10,000 times. As there is negligible East Asian ancestry across these individuals, the
3226 AFR and EUR proportions essentially add to 1, and therefore we consider an over/under representation of AFR ancestry in
3227 long ROH to be equivalent to an under/over representation of EUR ancestry in long ROH, respectively. Full permutation
3228 distributions are indicated in **Figure 4-figure supplement 2**.
3229

Cabo Verdean birth-island	AFR over-representation (10,000 permutation p-value)	AFR under-representation (10,000 permutation p-value)
Brava	0.8529	0.1471
Fogo	1	0
Santiago	0.9339	0.0661
Maió	0.9390	0.0610
Boa Vista	0.1562	0.8438
Sal	0.1899	0.8101
São Nicolau	0.1670	0.8330
São Vicente	0	1
Santo Antão	0.0001	0.9999

3230

3231

3232 **Figure 4-resource table 3: See .xls file**

3233 **Mean proportion of total length of long ROH ($cM \geq 1$) that have heterozygous ancestry (AFR and EUR), for each Cabo**
3234 **Verdean island of birth.**

3235

Cabo Verdean birth-island	Mean proportion of total length of long ROH with heterozygous ancestry
Brava	0.00393642
Fogo	0.01171550
Santiago	0.05129846
Maio	0.03436647
Boa Vista	0.01112053
Sal	0.02761951
São Nicolau	0.00143084
São Vicente	0.02112456
Santo Antão	0.02805926

3236

3237

3238 **Table 1-resource table 1: See .xls file**

3239 **Mantel correlations among individual birth-places, residence-places, maternal and paternal birth places, age, and aca-**
 3240 **ademic education duration.**

3241 We considered only the 225 genetically unrelated Cabo Verde-born individuals in these analyses.

3242

3243

Target	Mantel variable	n	Geographic scale	Spearman rho	10000 Mantel two-sided permutation p
abs(Age difference)	log(Birth-loc dist.)	225	within and between islands	<i>0.0046</i>	<i>0.3524</i>
abs(Education duration difference)	log(Birth-loc dist.)	186	within and between islands	0.0553	0.0007
abs(Education duration difference)	log(Residence dist.)	185	within and between islands	0.0809	< 2.10-4
log(Residence dist.)	log(Birth-loc dist.)	224	within and between islands	0.6910	< 2.10-4
log(Father Birth-loc dist.)	log(Birth-loc dist.)	222	within and between islands	0.5967	< 2.10-4
log(Mother Birth-loc dist.)	log(Birth-loc dist.)	224	within and between islands	0.7326	< 2.10-4
abs(Age difference)	log(Birth-loc dist.)	225	within islands only	<i>0.1737</i>	<i>0.0047</i>
abs(Education duration difference)	log(Birth-loc dist.)	186	within islands only	<i>0.0889</i>	<i>0.1310</i>
abs(Education duration difference)	log(Residence dist.)	185	within islands only	<i>0.1632</i>	<i>0.0147</i>
log(Residence dist.)	log(Birth-loc dist.)	224	within islands only	<i>-0.0439</i>	<i>0.2752</i>
log(Father Birth-loc dist.)	log(Birth-loc dist.)	222	within islands only	<i>0.1865</i>	<i>0.0095</i>
log(Mother Birth-loc dist.)	log(Birth-loc dist.)	224	within islands only	0.2356	0.0005

3244

3245

3246

3247

3248

3249

3250

3251

3252 **Figure 7-resource table 1: See .xls file**
 3253 **Historical landmark chronology for the peopling history of Cabo Verde as provided by previous historical work, respectively for each island.**
 3254 See detailed historical references in the table.
 3255
 3256

Part 1 of 6

- First significant indication of permanent settlement
- Administrative information
- Church establishment
- Census

3257

Year	Cabo Verde Unspecified island	SANTIAGO	FOGO	SANTO ANTAO	SAO NICOLAU	BRAVA	MAIO	BOA VISTA	SAO VICENTE	SAL
1460-1466	Discovery of the archipelago	First settlers from Portugal all	First settlers from Portugal all							
1472	Portuguese crown restricting slave-trade out of Cabo Verde. First trade and population movements regulation (All references)									
1480-1493			Remote administration of the island from Santiago, São Filipe church foundation 1. p143							
1495			Royal donation changes island ownership and administration 1. p53							
1504				Royal donation changes island ownership and administration 1. p56			Royal donation changes island ownership and administration 1. p55			
1505							Census* = 225 7. p294			
1507				Extensive livestock farming without permanent peopling, from tax records 3. p135	Extensive livestock farming without permanent peopling, from tax records 3. p135		Extensive livestock farming without permanent peopling, from tax records 3. p135	Extensive livestock farming without permanent peopling, from tax records 3. p135	Extensive livestock farming without permanent peopling, from tax records 3. p135	
1509						Royal donation changes island ownership and administration 1. p57				Royal donation changes island ownership and administration 1. p57
1513	Census* = 3500 1. p147-148	382 slaves imported from "Guinea" 1. p264 4. p135								
1514		1354 slaves imported from "Guinea" 1. p264 4. p135								
1515		1404 slaves imported from "Guinea" 1. p264 4. p135								
1516		26 slaves imported from "Guinea" 4. p135								
1526 1529		Commerce records indicate ~300 slaves sent to Portugal per year during 3 years 1. p97								
1527				Military troops sent from Santiago against Spanish marauders 3. p329	Military troops sent from Santiago against Spanish marauders 3. p329				Military troops sent from Santiago against Spanish marauders 3. p329	

3258

3259 **Figure 7-resource table 1: Part 2 of 6**
 3260

Year	Cabo Verde Unspecified island	SANTIAGO	FOGO	SANTO ANTAO	SAO NICOLAU	BRAVA	MAIO	BOA VISTA	SAO VICENTE	SAL
1528		1404 slaves imported from "Guinea" 1. p267			Fishing watters and boat halt 1. p225				Fishing watters and boat halt 1. p225	
1529							Permanent harbour and salt depot, possible small-size permanent settlement 1. p223-224			Permanent harbour and salt depot, possible small-size permanent settlement 1. p223-224
1532			All trade, administration, and population movements under control by Santiago, except direct trade with Portuguese crown 1. p101-105							
1540						Fogo fishing watters, no mention of permanent settlement 1. p225				
1546 1557	Instances of donations/inheritance of both goods/money and land to the benefit of admixed offsprings 1. p162-164									
1548					Request to Santiago for additional workforce, no trace of the outcome 1. p228				Request to Santiago for additional workforce, no trace of the outcome 1. p228	
1566							Census* = 30, prisoners kept on the island, extensive livestock farming and goat-skin production 5. p275			
1570				Reports of small-size permanent settlement, no census 1. p146		Reports of illegal slave trade 3. p329			Reports of small-size permanent settlement, no census 1. p146	
1572		Census* = 8900, only town residents, no children, no marginalized people 2. p279 1. p231, note	Census* = 1000, in São Filipe 1. p146, note							
1573				Church foundation 1. p146 note						
1580	Census* = 9940 7. p297	Census* = 8000 7. p294	Census* = 1200 7. p294	Census* = 400, Permanent harbor 1. p213 7. p294	Census* = 140, Permanent harbor 1. p213 7. p294	Census* = 100 7. p294	Census* = 50 7. p294	Illegal slave trade of 50 individuals 3. p329 7. p294	Census* = 0 7. p294	Census* = 0 7. p294
1580-1614	Admixed individuals own and/or manage commercial firms 2. p515									
1580-1582			Famine reports (thus implying prior settlement ?) 1. p12-14 6. p106			Famine reports (thus implying prior settlement ?) 1. p12-14 6. p106	Famine reports (thus implying prior settlement ?) 1. p12-14 6. p106			
1582-1731	Second migration wave into Santo Antão and São Nicolau and in the interior of Fogo and Santiago (1. p230; 3. p302; 4. p387; 7. p293)									

3261
 3262

3263
3264

Figure 7-resource table 1: Part 3 of 6

Year	Cabo Verde Unspecified island	SANTIAGO	FOGO	SANTO ANTAO	SAO NICOLAU	BRAVA	MAIO	BOA VISTA	SAO VICENTE	SAL
1582		Census* = 2600 only town residents, no children, no marginalized people, 11700 slaves. Population movements from Ribeira Grande and Praia into the interior of the island until 1731 1. p230 3. p302 4. p387 7. p293	Census* = 260 only town residents, no children, no marginalized people, 2000 slaves. 1. p230 4. p387	Reports of increasing census, no numbers 1. p230	Reports of increasing census, no numbers 1. p230					
1599					Census* = 6 7. p294					
1606							Census* = 10-12, extensive livestock farming 1. p229			
1608							Census* = 10 7. p294			
1613-1639	Admixed individuals own and/or manage commercial firms 2. p515									
1620	Portuguese crown sends boats of women for the peopling of the colony 1. p11									
1623									Census* = 19 7. p294	
1628							Census* = 50 7. p294			
1639									Census* = 0 7. p294	
1650	Census* = 13980 7. p297	Census* = 9500 7. p294	Census* = 2500 7. p294	Census* = 1000 7. p294	Census* = 300 7. p294	Census* = 400 7. p294	Census* = 120 7. p294	Census* = 150 7. p294	Census* = 0 7. p294	Census* = 10 7. p294
1677					Census* = 1000 ?, Permanent clergy 3. p326-327		Permanent clergy 3. p326-327	Permanent clergy 3. p326-327		
1680	Weavery exportations reserved to Portuguese citizen only, Cabo Verdean firms go bankrupt 3. p310		Earthquake and volcano eruption, migration to Brava 1. p12-14	Census* = 500 7. p294		Migration from Fogo 1. p12-14			Census* = 0 7. p294	
1683					Census* = 900 7. p294			Census* = 6 7. p294		
1699							Census* = 230 7. p294			
1700						Census* = 100 7. p294				
1708		400 soldiers sent to repress marooning in the interior regions. Failure of the expedition 3. p306								
1710		Reports of over 600 maroon slaves 3. p306								
1719		Famine 1. p12-14								
1720	Census* = 23130 7. p297	Census* = 12000 7. p294	Census* = 5000 7. p294	Census* = 3000 7. p294	Census* = 650 7. p294	Census* = 1200 7. p294	Census* = 250 7. p294	Census* = 1000 7. p294	Census* = 0 7. p294	Census* = 30 7. p294
1723			Census* = 700 7. p294	Census* = 2500 7. p294	Census* = 1350 7. p294	Census* = 200 7. p294	Census* = 200 7. p294		Census* = 0 7. p294	Census* = 0 7. p294
1727				Census* = 4000, including 502 slaves 3. p295						
1730		Census* = 25000 7. p294	Census* = 13000 7. p294							

3265

3266
3267

Figure 7-resource table 1: Part 4 of 6

Year	Cabo Verde Unspecified island	SANTIAGO	FOGO	SANTO ANTAO	SAO NICOLAU	BRAVA	MAIO	BOA VISTA	SAO VICENTE	SAL
1731		Census* = 17464, ~1800 RibeiraGrande/Praia + ~15664 interior, 16,28% slaves on the whole island 3. p300-302	No census, 25% slaves and highest "white" people proportion among islands 3. p300	No census, 15% slaves ~1600 individuals 3. p296 7. p294	Census* = 360 households ~2600 individuals (7/household), 11% slaves 3. p296	No census, 6% slaves 3. p296	Census* = less than 400 3. p299	Census* = Less than 2% of the total population of Cabo Verde 3. p299		
1750-1780	Third migration wave into all remaining islands: commercial-monopoly shifts on all trades dictate population settlements and movements among Cabo Verde islands. End of the agro-slavery system in Cabo Verde (3. p304)									
1770	Census* = 26000 1. p11									
1772				Census* = 11000 7. p294						
1773			Census* = 5900 1. p12-14							
1774	Census* = 50639 3. p355	Census* = 24358 3. p355	Census* = 5728 3. p355	Census* = 10215 3. p355	Census* = 5000 3. p355	Census* = 3190 3. p355	Census* = 708 3. p355	Census* = 1440 3. p355	Census* = 0 3. p355 7. p294	Census* = 0 3. p355 7. p294
1773-1775	Famine kills 22666 individuals. People sell themselves into slavery to avoid death 1. p12-14 3. p200									
1775	Census* = 28368 3. p355	Census* = 11580 3. p355	Census* = 4225 1. p12-14 3. p355	Census* = 5668 3. p355	Census* = 2920 3. p355	Census* = 2115 3. p355	Census* = 604 3. p355	Census* = 1256 3. p355	Census* = 0 3. p355 7. p294	Census* = 0 3. p355 7. p294
1788									Census* = 0 7. p294	Census* = 0 7. p294
1790	Famine 1. p12-14									
1793										Census* = 0 7. p294
1794									Census* = 100, first settlers 7. p294	
1800	Census* = 56050 7. p294	Census* = 26000 7. p294	Census* = 8000 7. p294	Census* = 12000 7. p294	Census* = 4000 7. p294	Census* = 3000 7. p294	Census* = 700 7. p294	Census* = 2200 7. p294	Census* = 100 7. p294	Census* = 50 7. p294
1803					Census* = 4500 7. p294					
1807	Census* = 58401 7. p294	Census* = 14200 7. p294	Census* = 13150 7. p294	Census* = 13650 7. p294	Census* = 8300 7. p294	Census* = 6950 7. p294	Census* = 451 7. p294	Census* = 1500 7. p294	Census* = 200 7. p294	Census* = 0 7. p294
1814								Famine -> Mig BV -> F et SN 1. Vol1, p12-14		
1819									Census* = 120 7. p294	
1820									Census* = 300 7. p294	
1827	Census* = 74307 7. p297	Census* = 2505 slaves 4. p387	Census* = 1212 slaves 4. p387	Census* = 207 slaves 4. p387	Census* = 171 slaves 4. p387	Census* = 213 slaves 4. p387	Census* = 240 slaves 4. p387	Census* = 489 slaves 4. p387	Census* = 14 slaves 4. p387	Census* = 72 slaves 4. p387
1831	Census* = 88368 7. p294	Census* = 26220 7. p294	Census* = 17000 1. p12-14 7. p294	Census* = 21670 7. p294	Census* = 8530 7. p294	Census* = 9320 7. p294	Census* = 1648 7. p294	Census* = 3860 7. p294	Census* = 250 7. p294	Census* = 0 7. p294
1832	Census* = 60000 7. p294									
1831-1833	Famine kills 30000 1. p12-14		Famine kills 17000 1. p12-14	Famine kills 13000 1. p12-14						
1831	End of the AST in the Portuguese Empire with the official abolition of the AST in Brazil, progressive termination of the AST since the 1815 and AST-abolition in the British Empire (9)									

3268

3269
3270

Figure 7-resource table 1: Part 5 of 6

Year	Cabo Verde Unspecified island	SANTIAGO	FOGO	SANTO ANTAO	SAO NICOLAU	BRAVA	MAIO	BOA VISTA	SAO VICENTE	SAL
1834	Census* = 55833 7. p297	Census* = 21696 7. p294	Census* = 5615 1. p12-14 7. p294	Census* = 13587 7. p294	Census* = 5418 7. p294	Census* = 3990 7. p294	Census* = 1905 7. p294	Census* = 3331 7. p294	Census* = 341 7. p294	Census* = 0 7. p294
1841	Census* = 63000 7. p294	Census* = 19000 7. p294	Census* = 12000 7. p294	Census* = 15000 7. p294	Census* = 7000 7. p294	Census* = 4000 7. p294	Census* = 2000 7. p294	Census* = 3000 7. p294	Census* = 350 7. p294	Census* = 500 7. p294
1844	Census* = 69700 7. p297	Census* = 25000 7. p294	Census* = 7000 7. p294	Census* = 17500 7. p294	Census* = 7200 7. p294	Census* = 4600 7. p294	Census* = 2200 7. p294	Census* = 5200 7. p294	Census* = 400 7. p294	Census* = 600 7. p294
1848									Census* = 553 7. p294	
1850	Census* = 86700 7. p295									
1851	Census* = 101700 7. p295	Census* = 27800 7. p295	Census* = 7500 7. p295	Census* = 30200 7. p295	Census* = 20200 7. p295	Census* = 4300 7. p295	Census* = 4100 7. p295	Census* = 4500 7. p295	Census* = 2100 7. p295	Census* = 1000 7. p295
1854-1855			Cholera kills 800 1. p12-14							
1855	Census* = 120000 7. p295				Census* = 11000 7. p295			Census* = 4000 7. p295		
1856-1878	Abolition of Slavery in the Portuguese Empire									
1856				Census* = 16907 7. p295						
1857	Census* = 100000 7. p295								Census* = 1400 7. p295	
1858	Census* = 85393 7. p295									
1860	Census* = 90000 1. p12-14									
1861	Census* = 89310 7. p297	Census* = 40852 7. p295	Census* = 14341 7. p295	Census* = 14643 7. p295	Census* = 6372 7. p295	Census* = 6557 7. p295	Census* = 1863 7. p295	Census* = 2647 7. p295	Census* = 1141 7. p295	Census* = 894 7. p295
1862	Census* = 97009 7. p295	Census* = 44200 7. p295	Census* = 14426 1. p12-14 7. p295	Census* = 17965 7. p295	Census* = 6731 7. p295	Census* = 6824 7. p295	Census* = 2067 7. p295	Census* = 2621 7. p295	Census* = 1337 7. p295	Census* = 838 7. p295
1864	Census* = 97009 7. p297									
1863-1866	Famine kills 29845 1. p12-14	Famine kills 18000 1. p12-14	Famine forces 7000 individuals into emigration, unknown destinations 1. p12-14						Census increase by 353 individuals (exception) 1. p12-14	
1867	Census* = 67517 7. p297	Census* = 26428 7. p295	Census* = 7431 1. p12-14 7. p295	Census* = 17403 7. p295	Census* = 5522 7. p295	Census* = 5874 7. p295	Census* = 955 7. p295	Census* = 1400 7. p295	Census* = 1690 7. p295	Census* = 814 7. p295
1870	Census* = 76003 1. p12-14 7. p295									
1871	Census* = 76053 7. p297									
1872			Census* = 10000 7. p295			Census* = 8673 7. p295			Census* = 2000 7. p295	
1874	Census* = 90710 7. p297									
1878	Census* = 99311 7. p297	Census* = 41077 7. p295	Census* = 12221 7. p295	Census* = 20507 7. p295	Census* = 8733 7. p295	Census* = 8151 7. p295	Census* = 1600 7. p295	Census* = 2643 7. p295	Census* = 3297 7. p295	Census* = 1082 7. p295
1882	Census* = 103761 7. p295									
1885	Census* = 115461 7. p297	Census* = 45488 7. p295	Census* = 16000 7. p295	Census* = 22000 7. p295	Census* = 11000 7. p295	Census* = 9013 7. p295	Census* = 1000 7. p295	Census* = 4000 7. p295	Census* = 6560 7. p295	Census* = 400 7. p295
1888	Census* = 121127 7. p295									

3271

3272
3273

Figure 7-resource table 1: Part 6 of 6

Year	Cabo Verde Unspecified island	SANTIAGO	FOGO	SANTO ANTAO	SAO NICOLAU	BRAVA	MAIO	BOA VISTA	SAO VICENTE	SAL
1890	Census* = 127390 1. p12-14 7. p297									
1898	Census* = 142537 7. p295									
1899-1900			Famine and smallpox 1. p12-14		Famine and smallpox 1. p12-14					
1900	Census* = 147424 1. p12-14 7. p297									
1901-1902	Famine 1. p12-14		Great poverty 1. p12-14	Great poverty 1. p12-14	Diseases and fevers 1. p12-14	Diseases and fevers 1. p12-14	Great population reduction, no census 1. p12-14			
1903-1904		Famine kills 15000 1. p12-14								
1905	Census* = 135000 1. p12-14									
1910	Census* = 142252 1. p12-14 7. p295						Census* =			
1913	Census* = 147754 7. p295	Census* = 59222 7. p295	Census* = 17800 7. p295	Census* = 33724 7. p295	Census* = 12041 7. p295	Census* = 9207 7. p295	Census* = 1867 7. p295	Census* = 2823 7. p295	Census* = 10491 7. p295	Census* = 579 7. p295
1920	Census* = 160000 1. p12-14									
1930	Census* = 146299 1. p15									
1940	Census* = 181740 1. p16	Census* = 77382 1. p16	Census* = 23022 1. p16	Census* = 35977 1. p16	Census* = 14846 1. p16	Census* = 8528 1. p16	Census* = 2237 1. p16	Census* = 2779 1. p16	Census* = 15848 1. p16	Census* = 1121 1. p16
1942			Census* = 25000 1. p12-14							
1941-1943	Famine 1. p12-14		Famine kills 7500 (31%) 1. p12-14		Famine kills 28%, no census 1. p12-14					
1944			Census* = 17500 1. p12-14							
1946-1948	Great famine kills 65% of the total population 1. p12-14									
1949										
1950	Census* = 149989-148331 1. p16 7. p295	Census* = 59384 1. p16	Census* = 17582 1. p16	Census* = 28379 1. p16	Census* = 10366 1. p16	Census* = 7937 1. p16	Census* = 1942-1044 1. p16 7. p297	Census* = 2985 1. p16	Census* = 19576 1. p16	Census* = 1838 1. p16
1960	Census* = 199902 1. p16	Census* = 88587 1. p16	Census* = 25615 1. p16	Census* = 33953 1. p16	Census* = 13866 1. p16	Census* = 8625 1. p16	Census* = 2680 1. p16	Census* = 3263 1. p16	Census* = 20705 1. p16	Census* = 2608 1. p16
1970	Census* = 270999-272071 1. p16 7. p295	Census* = 128782-129358 1. p16 7. p295	Census* = 29412 1. p16	Census* = 44623 1. p16	Census* = 16308 1. p16	Census* = 7756 1. p16	Census* = 3466 1. p16	Census* = 3569 1. p16	Census* = 31578 1. p16	Census* = 5505 1. p16
1975	Independence of Cabo Verde									
1980	Census* = 295703-320000 1. p16 7. p295	Census* = 145957 1. p16	Census* = 30978 1. p16	Census* = 43321 1. p16	Census* = 13572 1. p16	Census* = 6985 1. p16	Census* = 4098 1. p16	Census* = 3372 1. p16	Census* = 41594 1. p16	Census* = 5826 1. p16
1980-1985	Emigration -2552/year + Diaspora = 405-420K -> 250K USA ; 83-88K West Europe ; 68-76K continental Africa 1. p16									
2015	Census* = 524833 8. p.36	Census* = 294135 8. p.36	Census* = 35837 8. p.36	Census* = 40547 8. p.36	Census* = 12424 8. p.36	Census* = 5698 8. p.36	Census* = 6980 8. p.36	Census* = 14451 8. p.36	Census* = 81014 8. p.36	Census* = 33747 8. p.36

3274
3275

3276 **References in Figure 7-resource table 1**

- 3277 1. Albuquerque, Luís de, and Maria Emília Madeira Santos, eds. 1991. *História geral de Cabo Verde T1*. Vol. 1. 3 vols.
3278 Lisboa : Praia [Cape Verde]: Centro de Estudos de História e Cartografia Antiga, Instituto de Investigação
3279 Científica Tropical ; Instituto Nacional da Cultura de Cabo Verde.
- 3280 2. Albuquerque, Luís de, and Maria Emília Madeira Santos, eds. 1995. *História geral de Cabo Verde T2*. 2. ed. Vol. 2. 3
3281 vols. Lisboa: Centro de Estudos de História e Cartogr. Antiga.
- 3282 3. Albuquerque, Luís de, and Maria Emília Madeira Santos, eds. 2007. *História concisa de Cabo Verde (Resumo da*
3283 *História geral de Cabo Verde T1-3)*. 1 vols. Lisboa: Inst. de Investigação Científica Tropical.
- 3284 4. Carreira, A. 2000. *Cabo Verde: Formação e Extinção de Uma Sociedade Escravocrata (1460-1878)*. 3rd ed. Estudos
3285 e Ensaios. Praia, Cabo Verde: IPC.
- 3286 5. *The voyage of M. George Fenner to Guínea and to the Isles of Capo Verde, An. 1566*. In Hakluyt, Richard. 2014. *The*
3287 *Principal Navigations, Voyages, Traffiques and Discoveries of the English Nation*. Cambridge: Cambridge
3288 University Press. <https://doi.org/10.1017/CBO9781107286306>.
- 3289 6. Brooks, George E. 2006. "Cabo Verde: Gulag of the South Atlantic: Racism, Fishing Prohibitions, and Famines."
3290 *History in Africa* 33: 101–35. <https://doi.org/10.1353/hia.2006.0008>.
- 3291 7. Patterson, K. David. 1988. "Epidemics, Famines, and Population in the Cape Verde Islands, 1580-1900." *The*
3292 *International Journal of African Historical Studies* 21 (2): 291. <https://doi.org/10.2307/219938>.
- 3293 8. Cabo Verde, Statistical Yearbook 2015, Instituto Nacional de Estatística, Praia, Cabo Verde.
3294 https://ine.cv/wp-content/uploads/2017/02/statistical-yearbook-cv-2015_en.pdf.
- 3295 9. Conrad, Robert. 1969. "The Contraband Slave Trade to Brazil, 1831-1845." *Hispanic American Historical Review* 49
3296 (4): 617–38. <https://doi.org/10.1215/00182168-49.4.617>.

3297
3298
3299
3300
3301
3302